

國立高雄師範大學物理系碩士班
碩士論文

Department of Physics

National Kaohsiung Normal University

Master's Thesis

極化氫氘靶的馳豫時間與極化程度量測

Polarized Hydrogen-Deuteride (HD) Target for Strangeness

Production Experiments at SPring-8/LEPS

指導教授：郭榮升博士、章文箴博士

Advisor : Dr. Guo Rung-Sheng, Dr. Chang Wen-Chen

研究生：王素音撰

Graduate : Wang Su-Yin

中 華 民 國 九 十 八 年 六 月

June, 2009

高雄師範大學

博碩士論文全文上網授權書

(提供授權人裝訂於紙本論文書名頁之次頁用)

本授權書所授權之論文為授權人在高雄師範大學
物理學系_____組 97 學年度第二學期取得碩士學位之論
文。

論文題目：極化氫氖靶的馳豫時間與極化程度量測
指導教授：郭榮升, 章文箴

■ 同意

本人具有著作權之論文全文資料，非專屬、無償授予本人畢業學校圖書館，不限地域、時間與次數，以微縮、光碟或數位化等各種方式重製與利用，提供讀者基於著作權法合理使用範圍內之線上檢索、閱覽、下載及列印。

論文全文上載網路公開之範圍及時間：

| | |
|--------|--|
| 校內區域網路 | <input checked="" type="checkbox"/> 立即公開 |
| 校外網際網路 | <input checked="" type="checkbox"/> 立即公開 |

授權人：王素音

簽名：王素音

中華民國 98 年 7 月 7 日

國家圖書館

博碩士論文電子檔案上網授權書

本授權書所授權之論文為授權人在高雄師範大學物理學系 97 學年度第__學期取得碩士學位之論文。

論文題目：極化氫氖靶的馳豫時間與極化程度量測
指導教授：郭榮升,章文箴

茲同意將授權人擁有著作權之上列論文全文（含摘要），非專屬、無償授權國家圖書館，不限地域、時間與次數，以微縮、光碟或其他各種數位化方式將上列論文重製，並得將數位化之上列論文及論文電子檔以上載網路方式，提供讀者基於個人非營利性質之線上檢索、閱覽、下載或列印。

上列論文為授權人向經濟部智慧財產局申請專利之附件或相關文件之一（專利申請案號：_____），請於____年____月____日後再將上列論文公開或上載網路。

因上列論文尚未正式對外發表，請於____年____月____日後再將上列論文公開或上載網路。

授權人：王素音

親筆簽名及蓋章：王素音

民國 98 年 7 月 7 日

國立高雄師範大學碩士班研究生

論文口試審定書

物理學系碩士班 王素音 所提之論文

**Polarized Hydrogen-Deuteride (HD) Target for Strangeness
Production Experiments at SPring-8/LEPS**

經下列委員口試及審議通過，特此證明：

口試委員 柳英輝

黃建文

章文斌

郭芳科

指導教授

郭芳科

章文斌

系主任

何明宗

中華民國九十八年六月十九日

致謝/ Acknowledgments

值此畢業論文完成之際，我謹向所有關心及幫助我的人們表示最誠摯的感謝。

這篇論文是在郭榮升老師與章文箴老師的悉心指導下完成的。他們給了我參與氫氙固態極化靶實驗的機會並總是適時的給予我幫助與指點，也指導了我許多物理概念與實驗的分析方法。

另外也感謝同是參加 LEPS 實驗的前輩，家益學長與伯儒學長，給予我的協助與指導。

I would like to express my gratitude to the whole HD group members, for the helps both on researches and living at Japan, especially for Prof. M. Fujiwara and Prof. M. Yosoi. The very special thanks go out to H. Kohri and T. Ohta, whose expertise, understanding, and patience, added considerably to my graduate experience. I must also acknowledge the young companions, C. Morisaki and K. Ueda, who shared with me in the busy jobs and nice experiences. I would also like to thank T. Kunimatsu, who provided me with technical support of NMR and taken time out from his busy schedule to read my thesis carefully. I would also like to thank my friends in the RCNP for bringing me the nice memory in Japan, particularly Otsuka-san, Takai-san and Tanaka-san.

最後，我要感謝媽媽、建志和親朋好友們，因為你們的支持與陪伴，我才能順利走過了這一段旅程，謝謝你們。

摘要/Abstract

本論文中研發之極化固態氫氦(HD)靶主要是用於研究 ϕ 介子與質子和中子的光致反應。利用高度極化的高能量光子和氫氦靶，可以量測雙極化對稱分佈來研究核子中的奇夸克-反奇夸克成分。本實驗組於 2008 年製作了第一個極化固態氫氦靶。固態氫氦靶置於 17 Tesla 的強磁場，14 mK 的低溫下，經過 53 天的極化過程，氫與氦的極化程度(P)與馳豫時間(T1)分別以核磁共振(NMR)法量測得知。

量測所得的極化程度，遠低於理論所計算在達到熱平衡狀態的期望值。核磁共振訊號的強度與極化程度的非線性關係是造成差異的主要原因。在儲存冷凍器(SC)與傳送冷凍器(TC)的環境下的馳豫時間，證明是足以滿足在運送過程中的需要；同時在照射冷凍器(IBC) 的環境下的馳豫時間是夠長到新的極化固態氫氦靶製作完成。本實驗組計畫將於 2010 年製造第二個新的極化固態氫氦靶，並將其運送到 SPring-8/LEPS 實驗場所，利用圓極化光子束進行整體性能確認。

Abstract

The polarized Hydrogen-Deuteride (HD) target is developed mainly for the study of ϕ meson photoproduction on the proton and neutron. Using the polarized target, one can measure double polarization asymmetries to study $s\bar{s}$ -content in the nucleon. We produced a polarized HD target for the first time in 2008. After the aging time of 53 days at 17 Tesla and at 14 mK, the polarization degree (P) and the relaxation time (T_1) of the hydrogen (H) and deuterium (D) in the HD were measured by using the NMR method as shown in the Table.

| After 53 days aging | P_H | P_D | |
|---------------------|------------|------------|----------------|
| | 41.4±3.1% | 13.1±1.9% | |
| | T_1 of H | T_1 of D | Staying time |
| IBC (0.3K, 1.08T) | 2546±380 | 1741±167.6 | about 3 months |
| SC (1.2K, 1.08T) | 276.6±22.9 | 302.6±28.6 | 3 hours |
| TC (4.2K, 0.15T) | 147.3±3.8 | 47.8±5.5 | 0.5 hours |

The polarization degrees measured are much lower than those expected from the thermal equilibrium state of the aging condition. Non-linear relation between the NMR signal height and the polarization degree is considered to be the main source of the low polarization degree. The relaxation time in the SC and TC condition are found to be long enough for the need of staying time during the transportation of the HD target. The relaxation time in the IBC condition is also long enough to produce the other new polarized HD target for replacement in continuous experiments. We plan to start production of HD and move it to SPring-8/LEPS and carry out a performance check by using circularly polarized photon beams in 2010.

Contents

| | | |
|----------|---|-----------|
| 1 | Introduction | 1 |
| 1.1 | Motivation | 1 |
| 1.1.1 | Strangeness content in the proton and neutron | 1 |
| 1.1.2 | Identification Exchange Particle | 4 |
| 1.2 | HD Target Overview | 4 |
| 1.2.1 | HD Target at Other Laboratories | 4 |
| 1.2.2 | HD target at RCNP | 5 |
| 1.3 | LEPS Experimental Setup | 6 |
| 1.3.1 | SPring-8 | 6 |
| 1.3.2 | Photon Beam | 6 |
| 1.3.3 | Target and Spectrometer | 7 |
| 2 | The PHYDES System | 9 |
| 2.1 | Polarization Mechanism | 9 |
| 2.1.1 | Theoretical Polarization | 9 |
| 2.1.2 | Polarization Method | 10 |
| 2.2 | Polarized Target Production | 12 |
| 2.2.1 | Target Cell | 13 |
| 2.2.2 | Cryogenic and Magnet Systems | 13 |
| 2.3 | NMR Polarimeter | 19 |
| 2.3.1 | NMR Principles | 19 |
| 2.3.2 | NMR Hardware and Software | 20 |
| 2.3.3 | Extracting the Polarization | 22 |
| 2.3.4 | Extracting the Relaxation Time | 22 |
| 3 | Data Taking and Analysis | 25 |
| 3.1 | PHYDES01 Production and Data Taking | 25 |
| 3.2 | Preparation of Analysis | 26 |
| 3.2.1 | Unification of the Signal Amplification | 26 |
| 3.2.2 | Magnetic Field Adjustment | 26 |
| 3.2.3 | Data-Position Shifting | 27 |
| 3.2.4 | Unification of Bin Size | 27 |
| 3.2.5 | Phase correction | 27 |
| 3.2.6 | Background Removing | 28 |
| 3.3 | Relaxation Time Extracting | 29 |
| 3.3.1 | Extracting Signal Area by Histogram Method | 30 |
| 3.3.2 | Extracting Signal Area by Model Method | 33 |
| 3.4 | Polarization Extracting | 35 |
| 3.4.1 | Histogram Method | 38 |
| 3.4.2 | Model Method | 38 |

| | | |
|----------|--|-----------|
| 4 | Result and Discussion | 41 |
| 4.1 | Relaxation Time Extracting | 41 |
| 4.2 | Polarization Extracting | 45 |
| 4.3 | Conclusion | 48 |
| 4.4 | Discussion and the Future | 48 |
| 4.4.1 | Study of Aging Time | 48 |
| 4.4.2 | Lower Polarization | 49 |
| 4.4.3 | NMR Measurement | 50 |
| 4.4.4 | Improvement of D Polarization | 50 |
| 4.4.5 | From Success of Polarized HD Target to Using the Polarized HD Target in LEPS Experiment | 51 |
| 4.5 | Summary | 54 |
| 5 | Summary | 55 |
| A | Distortion of NMR Signals | 59 |
| A.1 | Simple simulation | 61 |
| A.2 | Advanced Simulation | 64 |
| A.3 | Conclusion | 64 |
| B | Detail of Relaxation Time Fitting | 65 |

List of Figures

| | | |
|------|--|----|
| 1.1 | Feynman diagram of ϕ meson photoproduction. | 2 |
| 1.2 | The unpolarized photoproduction cross section $d\sigma/dt$ at $E_\gamma=2.0$ GeV. The solid, dotted,dashed, and dot-dashed lines give the cross section of VDM, OPE, $s\bar{s}$ knockout, and uud knockout with strangeness admixture $B^2=1\%$ and $ a_0 = a_1 = 1/\sqrt{2}$. [9] | 3 |
| 1.3 | The longitudinal asymmetry C_{zz}^{BT} at $E_\gamma=2.0$ GeV with $B^2=0\%$, i.e., the VDM and OPE (solid lines), 0.25% (dashed lines), and 1% (dot-dashed lines) assuming that $\mathbf{a}_0 = \mathbf{a}_1 = 1/\sqrt{2}$. The phases of a_0 and a_1 for (a), (b), (c), and (d) are (+, +), (-, +), (+, -), and (-, -),respectively. [9]. | 3 |
| 1.4 | Feynman diagram of $\Lambda(1520)$ photoproduction. | 4 |
| 1.5 | The relaxation times T_1^H measured at IPN Orsay as a function of the aging [10]. | 5 |
| 1.6 | Standard LEPS magnetic spectrometer. | 6 |
| 1.7 | Standard LEPS magnetic spectrometer. | 7 |
| 2.1 | Energy level of proton. | 9 |
| 2.2 | The polarization could be estimate by Eq. 2.3 and Eq. 2.4. This figure shows the P_H and the P_D at 14mK and 17T. | 11 |
| 2.3 | The equilibrium condition at low temperatures requires the p-H ₂ state with S=0 and L=0. When the o-H ₂ flip to the p-H ₂ , the HD protons can exchange energy with the o-H ₂ spins by means of mutual spin flips. When the o-H ₂ flip to the p-H ₂ , the energy of these two states also generate photon. The photon may flip another p-H ₂ to o-H ₂ , or just generate heat. | 12 |
| 2.4 | The flow chart of target transportation. | 14 |
| 2.5 | Distillator. | 16 |
| 2.6 | Dilution Refrigerator System (DRS) | 16 |
| 2.7 | Storage Cryostat (SC) | 17 |
| 2.8 | The left figure is the perspective drawing of IBC. The right figure is real picture of IBC | 18 |
| 2.9 | The left side of the figure is TC1, which is mainly for moving the target from the DRS to the SC. The right side the figure is TC2, which is mainly for moving the target from the SC to the IBC. | 18 |
| 2.10 | NMR principle | 19 |
| 2.11 | The figure(a) shows diagram of cancellation circuit and the figure(b) shows the picture of cancellation circuit. As shown in figure(c), the x-axis is frequency, the cancellation circuit can cancel signal with selected frequency. | 21 |
| 2.12 | (a) The Kel-F coil supporter with coil, the transmitter and receiver coils are both 50 turns. (b) The Kel-F coil supporter with the target cell. (c) The draft of single coil; the transmitter and receiver coils are both 50 turns in real case. | 21 |
| 2.13 | The signal flow of single coil method. | 22 |
| 2.14 | This figure explain the Eq. 3.4. The blue curve, $P_{thermal_eq}$, is the polarization when HD reach thermal thermal equilibrium. The green curve is the decay function of the polarization in normal case. With taking two curves in account, the final function the violet curve, $P_{target}(t)$ | 23 |
| 3.1 | The original data with the $sensitivity = (1mVrms / -47dBm)$ | 26 |

| | | |
|------|--|----|
| 3.2 | The signal is ten times of original one. We also change the signal shape to positive. | 26 |
| 3.3 | When we choose the time channel, the signal is more clear. But if one choose the time channel, the magnetic field sweep speed or data taking speed should be considered every time. It is inconvenient and inaccurate. | 27 |
| 3.4 | The magnetic field channel signal is more clear by magnetic field adjustment. | 27 |
| 3.5 | Due to the hysteresis from cold finger and aluminum wire ans some unknown reasons, the signal position is shifted. | 28 |
| 3.6 | The highest data point of signal is found, and the signal is shifted horizontally by adjust the point to the theoretical resonance magnetic field. | 28 |
| 3.7 | When the phase is clearly not good, we can adjust it by eyes before data taking. | 29 |
| 3.8 | Before we take an average of all signals, the background should be removed for each signal. The background is assumed to be a first-degree polynomial function. We fit the background in background-only region. | 30 |
| 3.9 | Flow chart of histogram method | 31 |
| 3.10 | Flow chart of error estimation | 32 |
| 3.11 | The area of NMR signals are different between every measurement | 32 |
| 3.12 | The area of NMR signals are also different between average of current increase data ($A_{increase}$, red point) and average of current decrease data ($A_{decrease}$, blue point) | 32 |
| 3.13 | Four models for different shape of NMR signals | 33 |
| 3.14 | Flow chart of model method | 34 |
| 3.15 | These plots show five reference data, and there is no obvious signal. We can not shift the signal position to theoretical resonance position. The noise level of each signal, is around $1 \sim 5 \times 10^{-3}$ | 35 |
| 3.16 | After we averaged some data, a clear signal appeared. Data average can decrease the noise level. Figures show that average of 37 data which measured when current increase and average of 36 data which measured when current decrease. We found the the highest point of the signal, and shifted the the peak position to theoretical resonance position. By this way, one can take an average of 73 data and decrease noise level again. | 36 |
| 3.17 | After we averaged 73 data, a clear peak appeared. The noise level decreased to 2.5×10^{-4} . The signal height is around 2×10^{-3} | 36 |
| 3.18 | Flow chart of polarization estimate | 37 |
| 3.19 | The small peak deviation is included in the signal shape and the signal width is wider than the normal one. The model, which works well in model method of relaxation estimation, not works well now. The small peak deviation should be under consideration. | 39 |
| 3.20 | The new parameter, which is sigma of peak deviation, is added to the fitting. Since four parameters is too many for fitting and the most important is sigma finding, this fitting is done in small range first. After the sigma was got, a new model, under consideration about peak deviation, will be produced | 39 |
| 3.21 | The blue shape is a Gaussian shape with the sigma which is got from fitting. The red shape is original model. If the peak position have a deviation as the Gaussian shape, the black shape will be observe. For easy to imagine, the original model and the new model are ten times of the one we really used. | 39 |
| 3.22 | Use the new model with the deviation, we can do fitting again with signal and background part. | 39 |
| 4.1 | Extracting the relaxation time of D at IBC environment with two methods. | 42 |
| 4.2 | Extracting the relaxation time of D at SC environment with two methods. | 43 |
| 4.3 | Extracting the relaxation time of D at TC environment with two methods. | 43 |
| 4.4 | Extracting the relaxation time of H at SC environment with two methods. | 44 |
| 4.5 | Extracting the relaxation time of H at TC environment with two methods. | 44 |
| 4.6 | Get the background of reference signal from fitting. (Histogram method) | 46 |
| 4.7 | After removing the background, fill a histogram to to estimate the area of reference signal. (Histogram method) | 46 |

4.8 Fit the reference signal by the D signal model where signal deviation is taken into account. Background of this signal is also estimated by this fitting. (Model method) 47

4.9 After fitting by the model to get the background, fill a histogram to estimate the area of reference signal.(Model method) 47

4.10 Add the PHYDES data points into IPN Orsay data. The conversion of aging time of PHYDES data is done by taking account into the concentration of o-H₂. Up to now the results are reasonable. The higher magnetic field or lower temperature causes longer relaxation time. 49

4.11 The time line of SFT from LEPS group [25]. C_1^H is the concentration of o-H₂. In the bottom figure, the H and D polarization are shown as the solid and the dotted curves. 52

A.1 Definition of z axis in superconductor. 60

A.2 The fitting of non-uniformity of the local magnetic field. If the position of cell center is -14 cm, the yellow part is the cell position.The maximum of uniformity of magnetic field, ΔB , is proportioned the B_{center} 60

A.3 Assume that if there is no non-uniformity of the local magnetic field, the D NMR shape is a Lorentzian shape. In case of a simple simulation, we set it to be a Gaussian shape, as shown in the top figure. With taking the non-uniformity of the local magnetic field into account, the D signal is simulated by Eq. A.3. The simulation is shown bottom figure. 62

A.4 The real D signal which got from measurement. The signal area is normalized to be same as the simulation. 62

A.5 Assume that if there is no non-uniformity of the local magnetic field, the H NMR shape is a Lorentzian shape. In case of a simple simulation, we set it to be a Gaussian shape, as shown in the top figure. With taking the non-uniformity of the local magnetic field into account, the H signal is simulated by Eq. A.3. The simulation is shown bottom figure. 63

A.6 The real H signal which got from measurement. The signal area is normalized to be same as the simulation. 63

A.7 This simulation decide the cell position and cell length be fitting the simulation result with the real data 64

B.1 Get the area of D signal at IBC environment with the histogram method. (current-increasing, time = 18 hours.) 66

B.2 Get the area of D signal at IBC environment with the histogram method. (current-decreasing, time = 18 hours.) 67

B.3 Get the area of D signal at IBC environment with the histogram method. (current-increasing, time = 69 hours.) 68

B.4 Get the area of D signal at IBC environment with the histogram method. (current-decreasing, time = 69 hours.) 69

B.5 Get the area of D signal at IBC environment with the histogram method. (current-increasing, time = 266 hours.) 70

B.6 Get the area of D signal at IBC environment with the histogram method. (current-decreasing, time = 266 hours.) 71

B.7 Get the area of D signal at IBC environment with the histogram method. (current-increasing, time = 333 hours.) 72

B.8 Get the area of D signal at IBC environment with the histogram method. (current-decreasing, time = 333 hours.) 73

B.9 Get the area of D signal at IBC environment with the model method. (current-increasing, time = 18 hours.) 74

B.10 Get the area of D signal at IBC environment with the model method. (current-decreasing, time = 18 hours.) 75

B.11 Get the area of D signal at IBC environment with the model method. (current-increasing, time = 69 hours.) 76

| | | |
|------|--|-----|
| B.12 | Get the area of D signal at IBC environment with the model method. (current-decreasing, time = 69 hours.) | 77 |
| B.13 | Get the area of D signal at IBC environment with the model method. (current-increasing, time = 266 hours.) | 78 |
| B.14 | Get the area of D signal at IBC environment with the model method. (current-decreasing, time = 266 hours.) | 79 |
| B.15 | Get the area of D signal at IBC environment with the model method. (current-increasing, time = 333 hours.) | 80 |
| B.16 | Get the area of D signal at IBC environment with the model method. (current-decreasing, time = 333 hours.) | 81 |
| B.17 | Get the area of D signal at SC environment with the histogram method. (current-increasing, time = 22 hours.) | 82 |
| B.18 | Get the area of D signal at SC environment with the histogram method. (current-decreasing, time = 22 hours.) | 83 |
| B.19 | Get the area of D signal at SC environment with the histogram method. (current-increasing, time = 50 hours.) | 84 |
| B.20 | Get the area of D signal at SC environment with the histogram method. (current-decreasing, time = 50 hours.) | 85 |
| B.21 | Get the area of D signal at SC environment with the histogram method. (current-increasing, time = 68 hours.) | 86 |
| B.22 | Get the area of D signal at SC environment with the histogram method. (current-decreasing, time = 68 hours.) | 87 |
| B.23 | Get the area of D signal at SC environment with the model method. (current-increasing, time = 22 hours.) | 88 |
| B.24 | Get the area of D signal at SC environment with the model method. (current-decreasing, time = 22 hours.) | 89 |
| B.25 | Get the area of D signal at SC environment with the model method. (current-increasing, time = 50 hours.) | 90 |
| B.26 | Get the area of D signal at SC environment with the model method. (current-decreasing, time = 50 hours.) | 91 |
| B.27 | Get the area of D signal at SC environment with the model method. (current-increasing, time = 68 hours.) | 92 |
| B.28 | Get the area of D signal at SC environment with the model method. (current-decreasing, time = 68 hours.) | 93 |
| B.29 | Get the area of D signal at TC environment with the histogram method. (current-increasing, time = 7 hours.) | 94 |
| B.30 | Get the area of D signal at TC environment with the histogram method. (current-decreasing, time = 7 hours.) | 95 |
| B.31 | Get the area of D signal at TC environment with the histogram method. (current-increasing, time = 19 hours.) | 96 |
| B.32 | Get the area of D signal at TC environment with the histogram method. (current-decreasing, time = 19 hours.) | 97 |
| B.33 | Get the area of D signal at TC environment with the histogram method. (current-increasing, time = 27 hours.) | 98 |
| B.34 | Get the area of D signal at TC environment with the histogram method. (current-decreasing, time = 27 hours.) | 99 |
| B.35 | Get the area of D signal at TC environment with the histogram method. (current-increasing, time = 46 hours.) | 100 |
| B.36 | Get the area of D signal at TC environment with the histogram method. (current-decreasing, time = 46 hours.) | 101 |
| B.37 | Get the area of D signal at TC environment with the model method. (current-increasing, time = 7 hours.) | 102 |
| B.38 | Get the area of D signal at TC environment with the model method. (current-decreasing, time = 7 hours.) | 103 |
| B.39 | Get the area of D signal at TC environment with the model method. (current-increasing, time = 19 hours.) | 104 |

| | | |
|------|--|-----|
| B.40 | Get the area of D signal at TC environment with the model method. (current-decreasing, time = 19 hours.) | 105 |
| B.41 | Get the area of D signal at TC environment with the model method. (current-increasing, time = 27 hours.) | 106 |
| B.42 | Get the area of D signal at TC environment with the model method. (current-decreasing, time = 27 hours.) | 107 |
| B.43 | Get the area of D signal at TC environment with the model method. (current-increasing, time = 46 hours.) | 108 |
| B.44 | Get the area of D signal at TC environment with the model method. (current-decreasing, time = 46 hours.) | 109 |
| B.45 | Get the area of H signal at SC environment with the histogram method. (current-increasing, time = 0 hours.) | 110 |
| B.46 | Get the area of H signal at SC environment with the histogram method. (current-decreasing, time = 0 hours.) | 111 |
| B.47 | Get the area of H signal at SC environment with the histogram method. (current-increasing, time = 4 hours.) | 112 |
| B.48 | Get the area of H signal at SC environment with the histogram method. (current-decreasing, time = 4 hours.) | 113 |
| B.49 | Get the area of H signal at SC environment with the histogram method. (current-increasing, time = 21 hours.) | 114 |
| B.50 | Get the area of H signal at SC environment with the histogram method. (current-decreasing, time = 21 hours.) | 115 |
| B.51 | Get the area of H signal at SC environment with the histogram method. (current-increasing, time = 47 hours.) | 116 |
| B.52 | Get the area of H signal at SC environment with the histogram method. (current-decreasing, time = 47 hours.) | 117 |
| B.53 | Get the area of H signal at SC environment with the model method. (current-increasing, time = 0 hours.) | 118 |
| B.54 | Get the area of H signal at SC environment with the model method. (current-decreasing, time = 0 hours.) | 119 |
| B.55 | Get the area of H signal at SC environment with the model method. (current-increasing, time = 4 hours.) | 120 |
| B.56 | Get the area of H signal at SC environment with the model method. (current-decreasing, time = 4 hours.) | 121 |
| B.57 | Get the area of H signal at SC environment with the model method. (current-increasing, time = 21 hours.) | 122 |
| B.58 | Get the area of H signal at SC environment with the model method. (current-decreasing, time = 21 hours.) | 123 |
| B.59 | Get the area of H signal at SC environment with the model method. (current-increasing, time = 47 hours.) | 124 |
| B.60 | Get the area of H signal at SC environment with the model method. (current-decreasing, time = 47 hours.) | 125 |
| B.61 | Get the area of H signal at TC environment with the histogram method. (current-increasing, time = 2 hours.) | 126 |
| B.62 | Get the area of H signal at TC environment with the histogram method. (current-decreasing, time = 2 hours.) | 127 |
| B.63 | Get the area of H signal at TC environment with the histogram method. (current-increasing, time = 20 hours.) | 128 |
| B.64 | Get the area of H signal at TC environment with the histogram method. (current-decreasing, time = 20 hours.) | 129 |
| B.65 | Get the area of H signal at TC environment with the histogram method. (current-increasing, time = 47 hours.) | 130 |
| B.66 | Get the area of H signal at TC environment with the histogram method. (current-decreasing, time = 47 hours.) | 131 |
| B.67 | Get the area of H signal at TC environment with the model method. (current-increasing, time = 2 hours.) | 132 |

| | | |
|------|--|-----|
| B.68 | Get the area of H signal at TC environment with the model method. (current-decreasing, time = 2 hours.) | 133 |
| B.69 | Get the area of H signal at TC environment with the model method. (current-increasing, time = 20 hours.) | 134 |
| B.70 | Get the area of H signal at TC environment with the model method. (current-decreasing, time = 20 hours.) | 135 |
| B.71 | Get the area of H signal at TC environment with the model method. (current-increasing, time = 47 hours.) | 136 |
| B.72 | Get the area of H signal at TC environment with the model method. (current-decreasing, time = 47 hours.) | 137 |

List of Tables

| | | |
|-----|---|----|
| 3.1 | The HD target staying time and relaxation time in each refrigerator. | 25 |
| 4.1 | The HD target staying time and relaxation time in each refrigerator. The unit of T_1 is hour. The T_1 of H in IBC condition is cited from Ref. [22]. | 41 |
| 4.2 | When we extracted relaxation time, there are two methods to estimate the signal area. When we extracted polarization degree of D, there are also two methods to estimate the signal area. Therefore, there are four kinds of results of polarization degree. They are consistent. | 45 |
| 4.3 | The HD target staying time and relaxation time in each refrigerator. The unit of T_1 is hour. The T_1 of H in IBC condition is cited from Ref. [22]. | 48 |
| 4.4 | The HD target staying time and relaxation time in each refrigerator. The unit of T_1 is hour. The T_1 of H in IBC condition is cited from Ref [22]. | 54 |

Chapter 1

Introduction

The HD polarized target will be used in the laser-electron photon facility (LEPS) at SPring-8, Japan. At SPring-8 BL33LEP beam-line (LEPS facility), the linearly-polarized photons were produced by Backward-Compton scattering. To introduce a polarized target plays a very crucial role in upgrading the LEPS experiments. The physics motivation for producing HD polarized target is discussed in this chapter.

1.1 Motivation

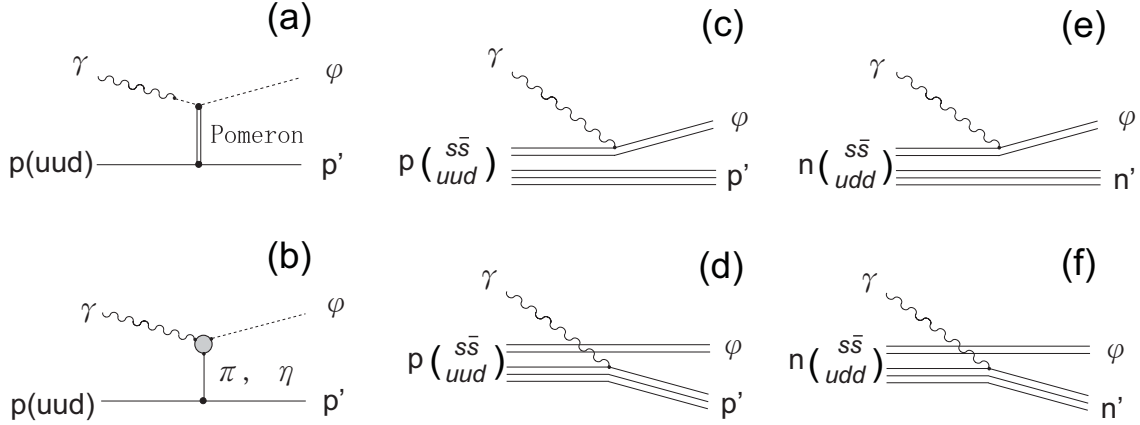
1.1.1 Strangeness content in the proton and neutron

The polarized target enables the measurement of double polarization asymmetries in ϕ meson photoproduction to study the strangeness content in the proton and neutron. It is generally accepted that the low-energy properties of nucleon are well described in terms of three constituent u and d quarks. Therefore, recent experimental results are very surprising. Experiments from the lepton deep inelastic scattering indicate that there may be non-negligible strange quark content in the nucleon and that the strange quarks give 10-20% contributions to the nucleon spin [1, 2]. After these results, there are many experiment [3, 4, 5, 6, 7, 8] which show similar ($\sim 20\%$) or different conclusions ($\sim 0\%$). This problem is actively discussed now. This discrepancy should be solved by revealing new experimental information on the $s\bar{s}$ -quark content of the nucleon.

The ϕ meson photoproduction is dominated by the diffractive production within the vector-meson-dominance model (VDM) through Pomeron exchange as shown in Fig. 1.1(a). Conventional meson exchanges, such as one-pion exchange (OPE), is shown in Fig. 1(b), in the t channel are strongly suppressed by the OZI rule. If the proton has the $s\bar{s}$ -quark content, it's possible that there are the $s\bar{s}$ knockout and uud knockout processes on the ϕ meson photoproduction as shown in Fig. 1.1(c, d). In case of the ϕ meson photoproduction on the neutron, the same processes are possible (Fig. 1.1(e, f)).

The main ingredient of the knockout photoproduction mechanism is the assumption that the constituent quark wave function of proton, in addition to the usual three-quark (uud) component, contains a configuration with explicit $s\bar{s}$ pair. The following wave function is a simple realization of this figure [9].

$$|P\rangle = A|[uud]^{1/2}\rangle + B\{a_0|[uud]^{1/2} \otimes [s\bar{s}]^0]^{1/2}\rangle + a_1|[uud]^{1/2} \otimes [s\bar{s}]^1]^{1/2}\rangle\} \quad (1.1)$$

Figure 1.1: Feynman diagram of ϕ meson photoproduction.

Using this wave function, Titov *et al.* found that the study of cross section in small angle region is not sensitive to the $s\bar{s}$ -quark content in the nucleon. The cross section of VDM is ten times of $s\bar{s}$ knockout, as shown in Fig. 1.2. But the beam-target asymmetry (C_{zz}^{BT}) for the $s\bar{s}$ direct knockout ϕ meson photoproduction (Fig. 1.1(c)) is very sensitive to the $s\bar{s}$ -quark content in the nucleon (Fig. 1.3) [9].

The interference of the vector-meson dominance model amplitude and the knockout amplitude gives distinct contributions to the asymmetry at small ϕ meson angles. The asymmetry C_{zz}^{BT} is defined as

$$C_{zz}^{BT} = \frac{d\sigma(\frac{1}{2}) - d\sigma(\frac{3}{2})}{d\sigma(\frac{1}{2}) + d\sigma(\frac{3}{2})} \quad (1.2)$$

where $d\sigma$ represents $d\sigma/dt$, and $\frac{1}{2}$ and $\frac{3}{2}$ denote the sum of the initial proton and photon helicities.

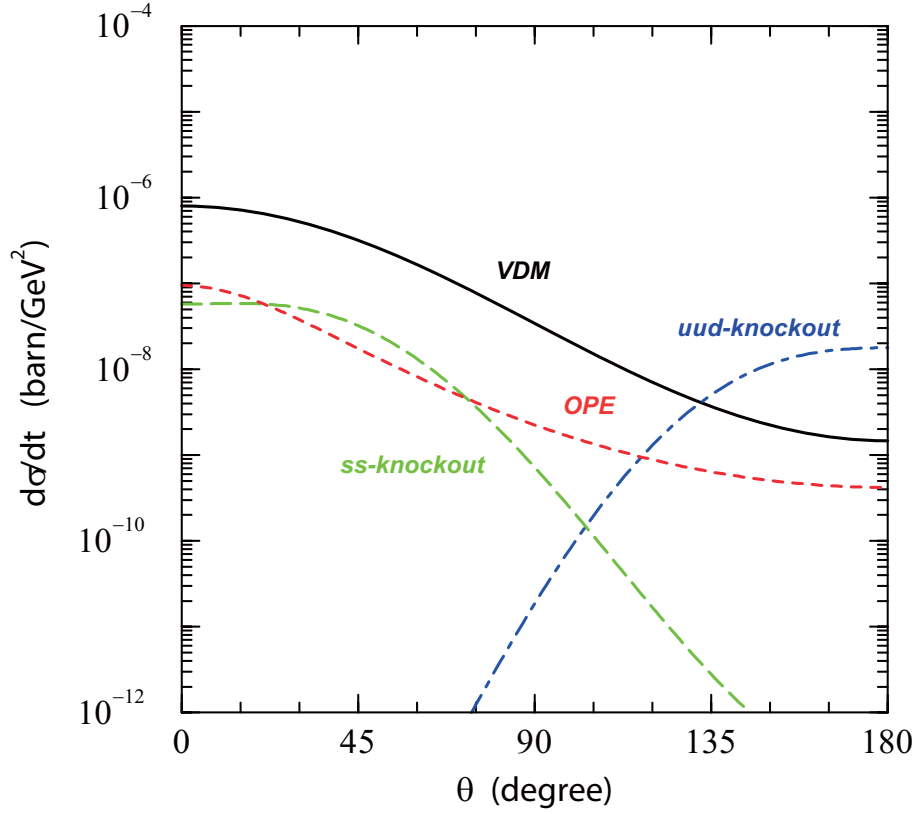


Figure 1.2: The unpolarized photoproduction cross section $d\sigma/dt$ at $E_\gamma=2.0$ GeV. The solid, dotted, dashed, and dot-dashed lines give the cross section of VDM, OPE, $s\bar{s}$ knockout, and uud knockout with strangeness admixture $B^2=1\%$ and $|a_0| = |a_1| = 1/\sqrt{2}$. [9]

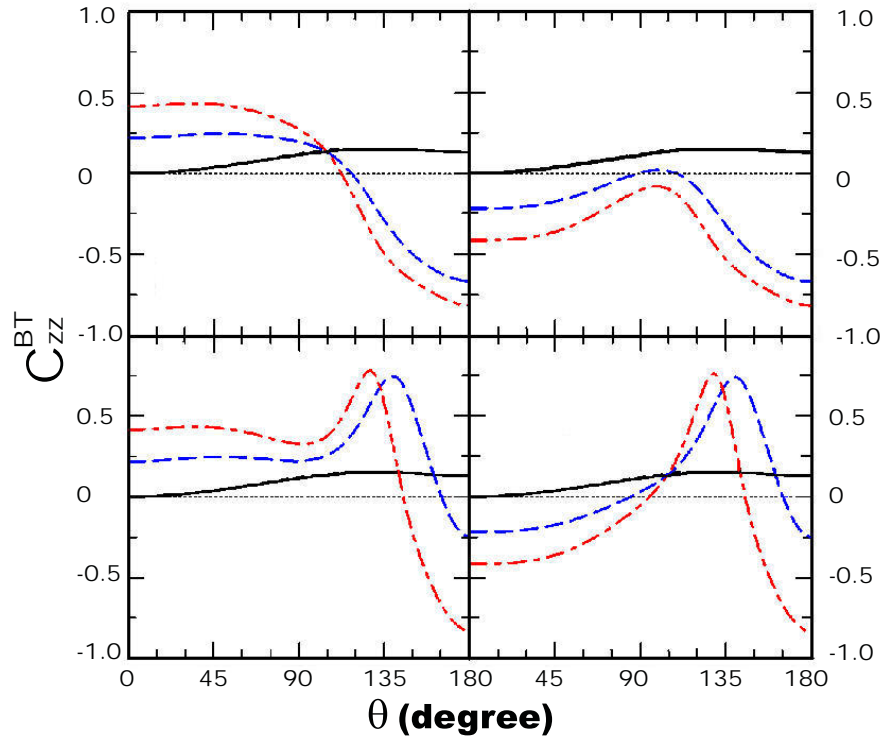


Figure 1.3: The longitudinal asymmetry C_{zz}^{BT} at $E_\gamma=2.0$ GeV with $B^2=0\%$, i.e., the VDM and OPE (solid lines), 0.25% (dashed lines), and 1% (dot-dashed lines) assuming that $\mathbf{a}_0 = \mathbf{a}_1 = 1/\sqrt{2}$. The phases of a_0 and a_1 for (a), (b), (c), and (d) are $(+, +)$, $(-, +)$, $(+, -)$, and $(-, -)$, respectively. [9].

1.1.2 Identification Exchange Particle

With the polarized target and polarized photon beam, we can fix the spin and orientation of initial state particles. It will be a powerful weapon to identify the exchange particle. For example, the t-channel exchange of $\Lambda(1520)$ photoproduction, as shown in Fig. 1.4. In the reaction, it is unclear whether the K^- or K^{*-} is the dominant exchange particle. The spin of spinless kaon, K^- is 0. The spin of vector kaon, K^{*-} is 1. If the spin and orientation of initial state particles are fixed and also the spin and orientation of final state are measured, the exchange particle can be clearly identify.

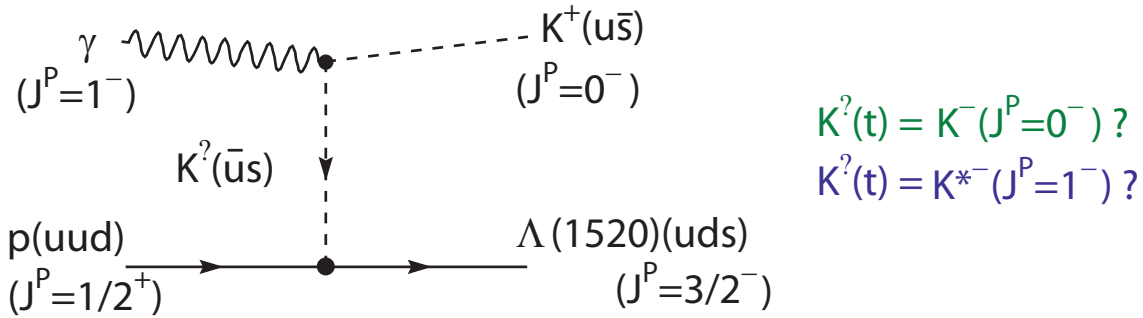


Figure 1.4: Feynman diagram of $\Lambda(1520)$ photoproduction.

1.2 HD Target Overview

For the need of a polarized proton target, solid ortho- H_2 is the most desirable candidate. Unfortunately, the solid ortho- H_2 is unsuitable for dynamic polarization because of its short relaxation time. The next choice, just what we selected, is the solid HD. The HD molecule can be used as both a proton target and a neutron target.

The other of advantages of the HD is that the it does not contain heavy elements, such as C and N. Good dilution factor is very important when we observe reactions with small cross sections using the photon beam.

1.2.1 HD Target at Other Laboratories

At Institut de Physique Nucleaire de Orsay (IPN Orsay), they have developed the static polarization of HD samples using brute force, for HD sample which is purified by double distillation. With commercially available dilution refrigerators (10 mK) and superconducting magnets (15 T), proton polarization (P_H) in excess of 60% and deuteron vector polarization (P_D) higher than 14% have been reached. Fig. 1.5 shows the relaxation times T_1^H measured at IPN Orsay as a function of the aging time. [10].

At the Laser Electron Gamma Source (LEGS) at Brookhaven National Laboratory, the polarized HD target was condensed in a variable temperature cryostat, where the NMR polarization monitoring system was calibrated at 2 K, transferred to a dilution refrigerator for polarization at 15 mK and 15 T, held there for typically

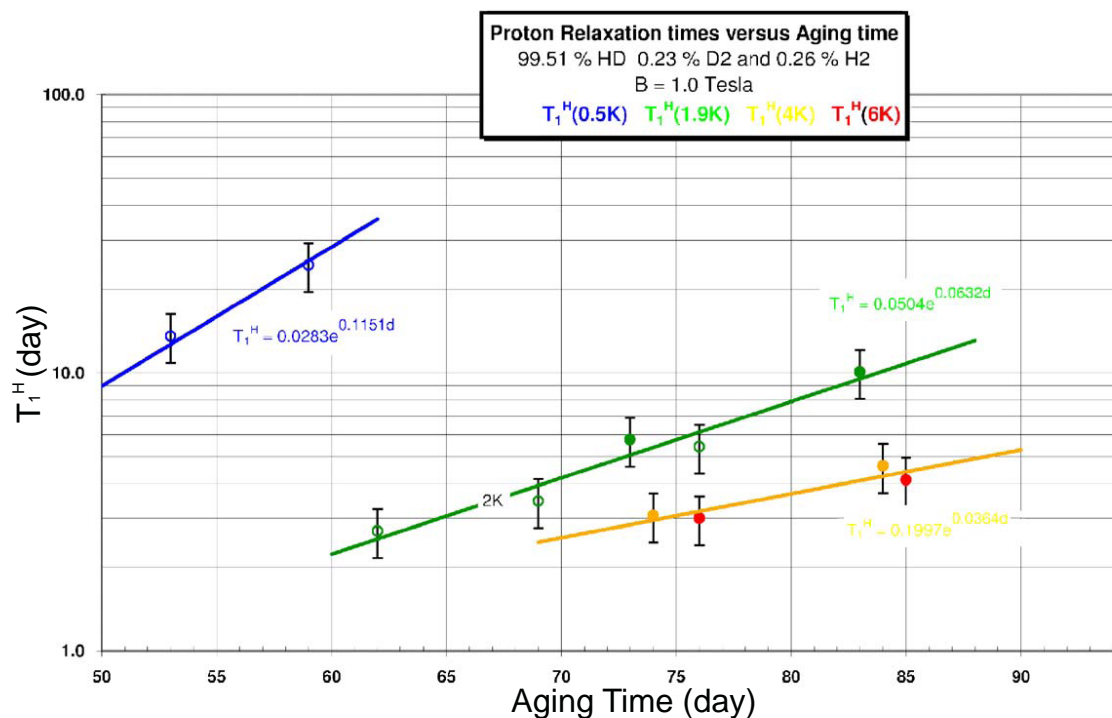


Figure 1.5: The relaxation times T_1^H measured at IPN Orsay as a function of the aging [10].

three months to reach the frozen-spin state, and finally transferred to an In-Beam Cryostat (IBC) operating at 0.3 K, where a thin 0.9 T solenoid maintained the H and D orientations. Data were collected during two periods in Fall 2004 and Spring 2005, the first emphasizing H polarization, with initial P_H 59% and P_D 7%, and the second using increased D polarization following a radio frequency (RF) transfer of spin between H and D, with P_H 32% and P_D 33% [11]. The method which LEGS used to increase D polarization is Saturated Forbidden Transition (SFT), but not Forbidden Adiabatic Fast Passage (FAFP). The $P_D=33\%$ is the maximum value that SFT reach [12].

1.2.2 HD target at RCNP

The HD is an idealistic polarized targets for the LEPS experiments, although thin aluminum wires (20% in weight) is included in the target cell to insure the cooling efficiency. In order to achieve high polarizations of proton and deuteron targets, we employ the static method using “brute force” at low temperature (14 mK) and high magnetic field (17 Tesla). The polarization can exceed 85% for the proton after aging process of 2~3 months. The polarization of 60% for the deuteron can be obtained by transferring the proton polarization to the deuteron by using a method commonly known as “Adiabatic fast passage”. The relaxation time of about one year is achievable by keeping the HD target at low temperature below 300 mK with magnetic field of 1 Tesla during the experiment.

1.3 LEPS Experimental Setup

The HD target will be used in the the laser-electron photon facility (LEPS) at SPring-8, Japan. At SPring-8 BL33LEP beam-line (LEPS facility), the linearly-polarized photon is produced by Backward-Compton scattering. The experimental apparatus of the measurement is described in this chapter.

1.3.1 SPring-8

SPring-8, an acronym of **S**uper **P**hoton **ring-8** GeV facility, is the most powerful third-generation synchrotron radiation facility with 62 beam-lines now. The figure 1.6 shows a schematic view of SPring-8 accelerator complex. The accelerator

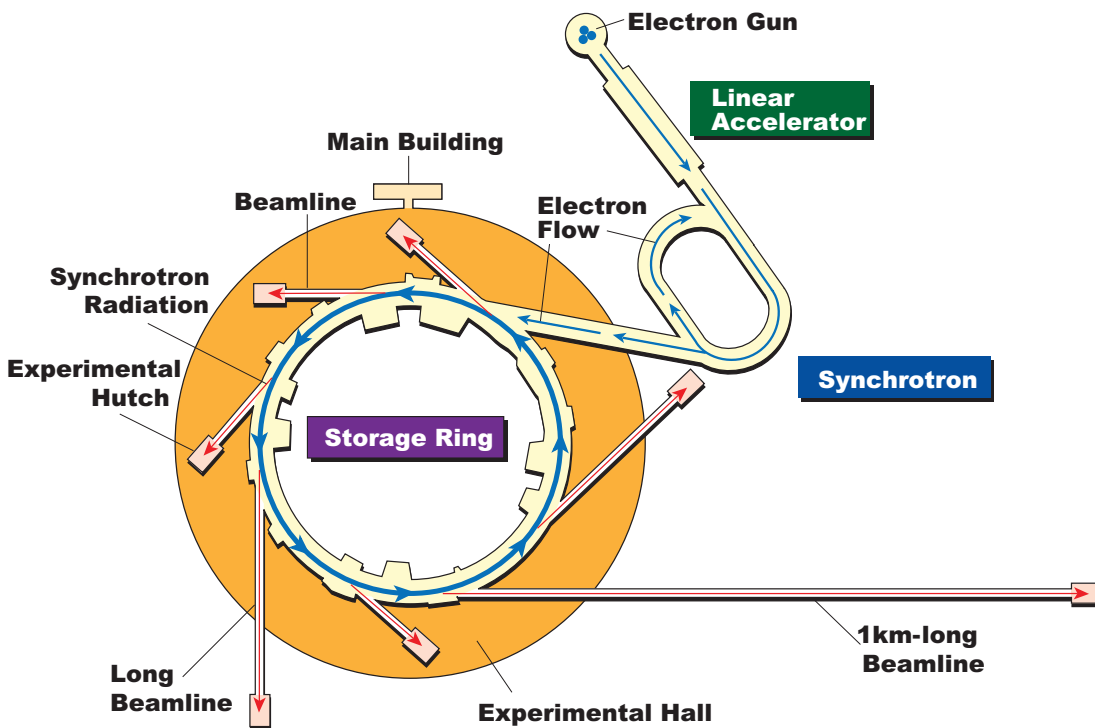


Figure 1.6: Standard LEPS magnetic spectrometer.

complex is composed of an injector linear accelerator, a booster synchrotron and a low emittance storage ring. The linear accelerator generates electrons with an electron gun, and accelerates them to an energy of 1 GeV. The accelerated electron beam is transported to the synchrotron, which then accelerates it to 8 GeV. Next, the beam is injected into the storage ring and stored with the energy of 8 GeV.

1.3.2 Photon Beam

We want to use circularly polarized photon beams with energies of $E=1.5-2.4$ GeV. We expect tagged photon intensity of about 10^6 γ 's/sec.

1.3.3 Target and Spectrometer

The HD target system consists of IBC, gas circulation system, compressor, and control unit. The IBC is installed just in front of the LEPS spectrometer. The gas circulation system and compressor are installed in the BL33LEP hutch. The control unit is placed outside the hutch. When the HD target is transferred from the TC2 to the IBC, the IBC is moved to outside by using the left door. We want to use the standard LEPS spectrometer for investigating trigger rate and hadron S/N ratio. The standard LEPS spectrometer consists of a trigger counter, an aerogel cherenkov counter (AC), a silicon vertex detector (SVTX), three drift chambers (DC1, DC2, and DC3), and a TOF wall as shown in Fig. 1.7.

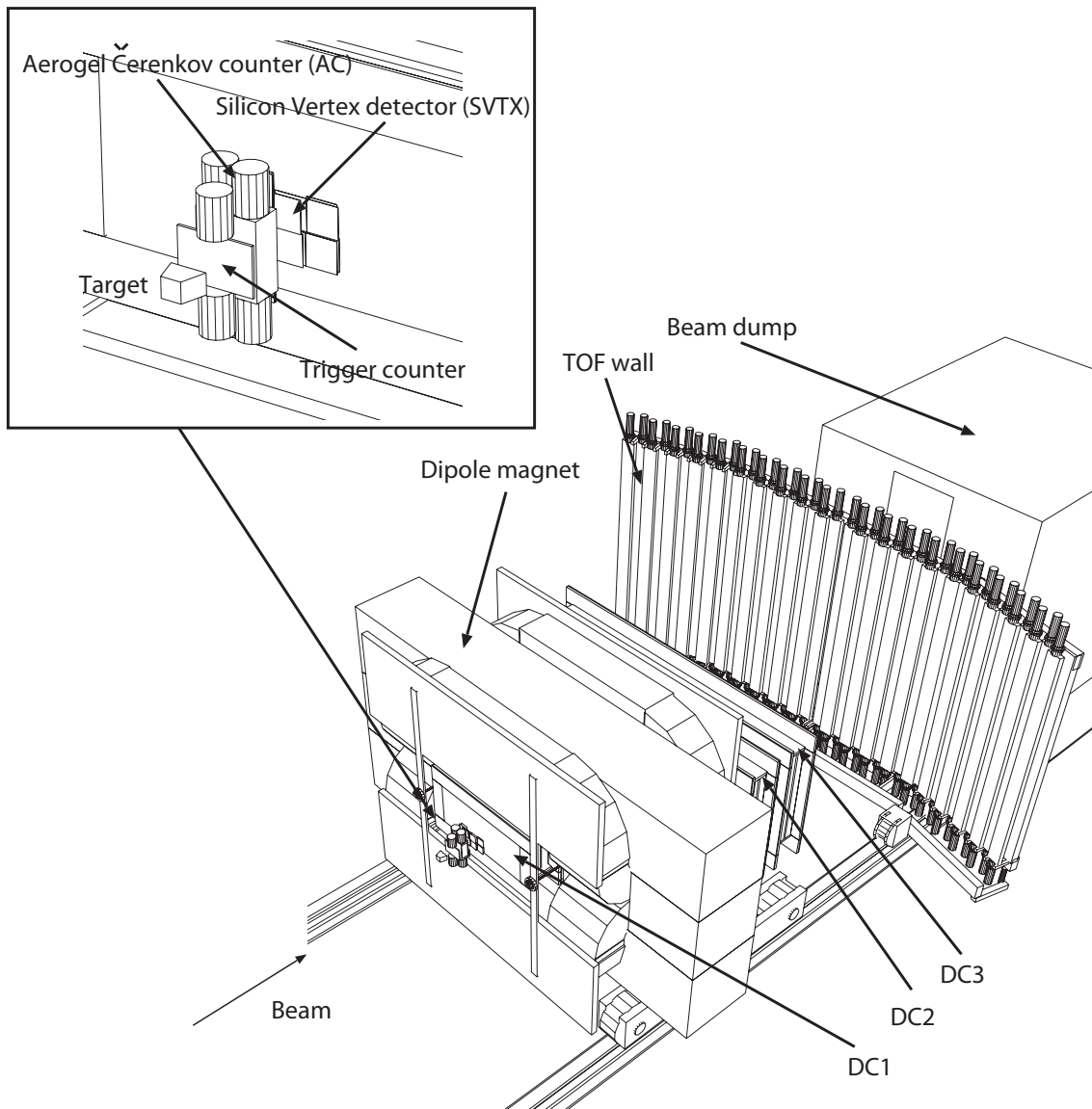


Figure 1.7: Standard LEPS magnetic spectrometer.

Chapter 2

The PHYDES System

The **P**olarized **H**ydrogen-**D**euteride target for **S**trangeness (PHYDES) is designed for the double polarization asymmetries measuring for the ϕ meson photoproduction at SPring-8/LEPS. The PHYDES target system is composed to several distinct sub-systems. This includes the target material, the cryogenic system, a superconducting magnet, and the NMR Polarimeter.

2.1 Polarization Mechanism

2.1.1 Theoretical Polarization

From the Boltzmann law, the polarization only relate to magnetic field and temperature, as shown as the follow equation and figure 2.1.

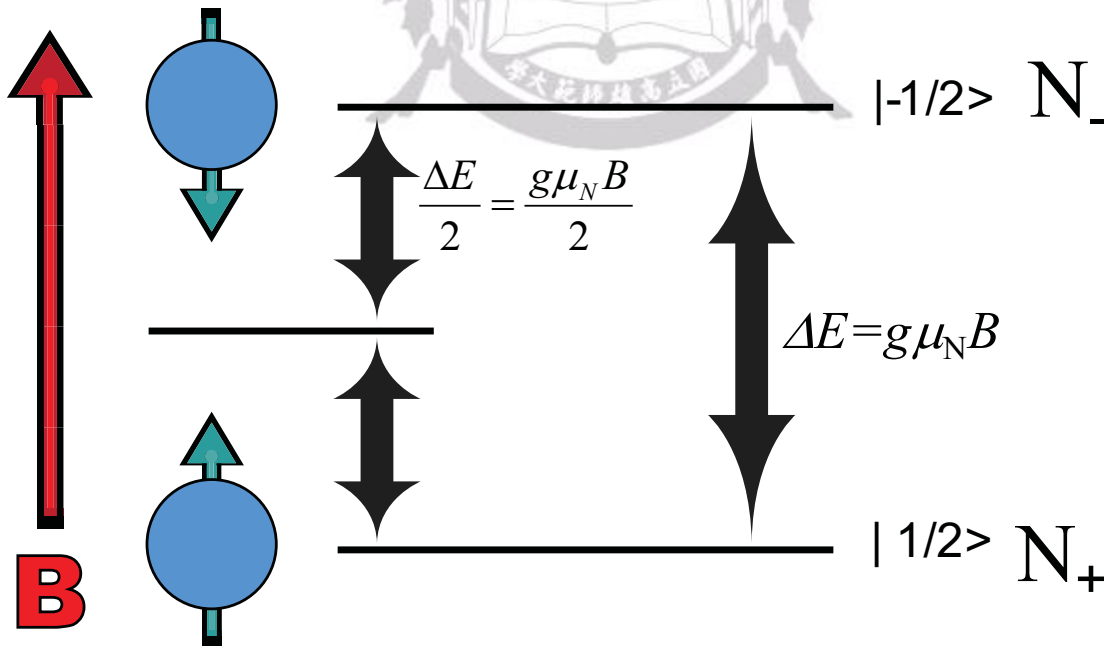


Figure 2.1: Energy level of proton.

$$N_+ = N_{total} \exp\left(\frac{\Delta E}{k_b T}\right); \quad N_- = N_{total} \exp\left(\frac{-\Delta E}{k_b T}\right) \quad (2.1)$$

Where ΔE is

$$\Delta E = g\mu_N B \quad (2.2)$$

Taking the Eq. 2.2 and 2.1 into account, we can get the H polarization as

$$P_H = \frac{N_+ - N_-}{N_+ + N_-} = \frac{\exp(\frac{\Delta E}{k_b T}) - \exp(\frac{-\Delta E}{k_b T})}{\exp(\frac{\Delta E}{k_b T}) + \exp(\frac{-\Delta E}{k_b T})} = \tanh\left(\frac{\Delta E}{k_b T}\right) = \tanh\left(\frac{g\mu_h B}{k_b T}\right) \quad (2.3)$$

and D polarization as

$$P_D = \frac{N_+ - N_-}{N_+ + N_0 + N_-} = \frac{4 \tanh\left(\frac{g\mu_d B}{k_b T}\right)}{\tanh\left(\frac{g\mu_d B}{k_b T}\right)} \quad (2.4)$$

Using above equation, once we know the magnetic field and temperature, we can estimate the polarization in thermal equilibrium state. At $B=17\text{T}$ and $T=14\text{mK}$ in thermal equilibrium state, the H polarization is about 85%, and the D polarization is about 25%, as shown in Fig. 2.2.

2.1.2 Polarization Method

Heteronuclear hydrogen molecules like HD can be polarized and have interesting properties. The proton with spin 1/2 and the deuteron with spin 1 are independently polarized and are independently reversible [13].

The basic symmetry condition imposed on the total wave functions of H_2 (two fermions) and D_2 (two bosons) gives a restriction on the possible nuclear spin orientation at low temperature. For H_2 , the so called ortho state has nuclear spin $S=1$ and molecular orbital angular momentum $L=\text{odd}$ (o- H_2). Since the nuclear spins are aligned, o- H_2 can be polarized. However, the equilibrium condition at low temperatures requires the para-hydrogen (p- H_2) state with $S=0$ and $L=0$. Here, since the nuclear magnetic moments are anti-parallel, the sample cannot be polarized. In the case of deuterium, it is the para-deuterium (p- D_2) combination ($S=1$; $L=\text{odd}$) that disappears at low temperature, leaving the ortho-deuterium (o- D_2) ($S=0,2$; $L=0$). Although 5/6 of the nuclei in this state have their spins parallel ($S=2$), the small magnetic moment of the deuteron makes static polarization of pure deuterium very difficult.

In contrast, the orbital and spin angular momenta of the heteronuclear molecules HD are not limited by symmetry requirements (one fermion and one boson) and hence can be in the molecular rotation state $L=0$ independent of the relative orientation by spin 1/2 and spin 1 species at low temperature. Since the spin-lattice coupling is primarily caused in the process of molecular rotations, the relaxation rates are extraordinary small. Although this long relaxation time is essential for the usage of polarized targets in nuclear physics experiments, it makes the polarization phase equally long. This is a difficulty; we hope to prepare the polarized target in a relatively short time and like to keep the produced polarized target for a long time in experiments. For the polarization of HD, the solution to this difficulty was suggested by Honig in 1967 [14].

Figure 2.3. shows a schematic view of the process of the polarized HD target. The equilibrium condition at low temperatures requires the p- H_2 state with $S=0$

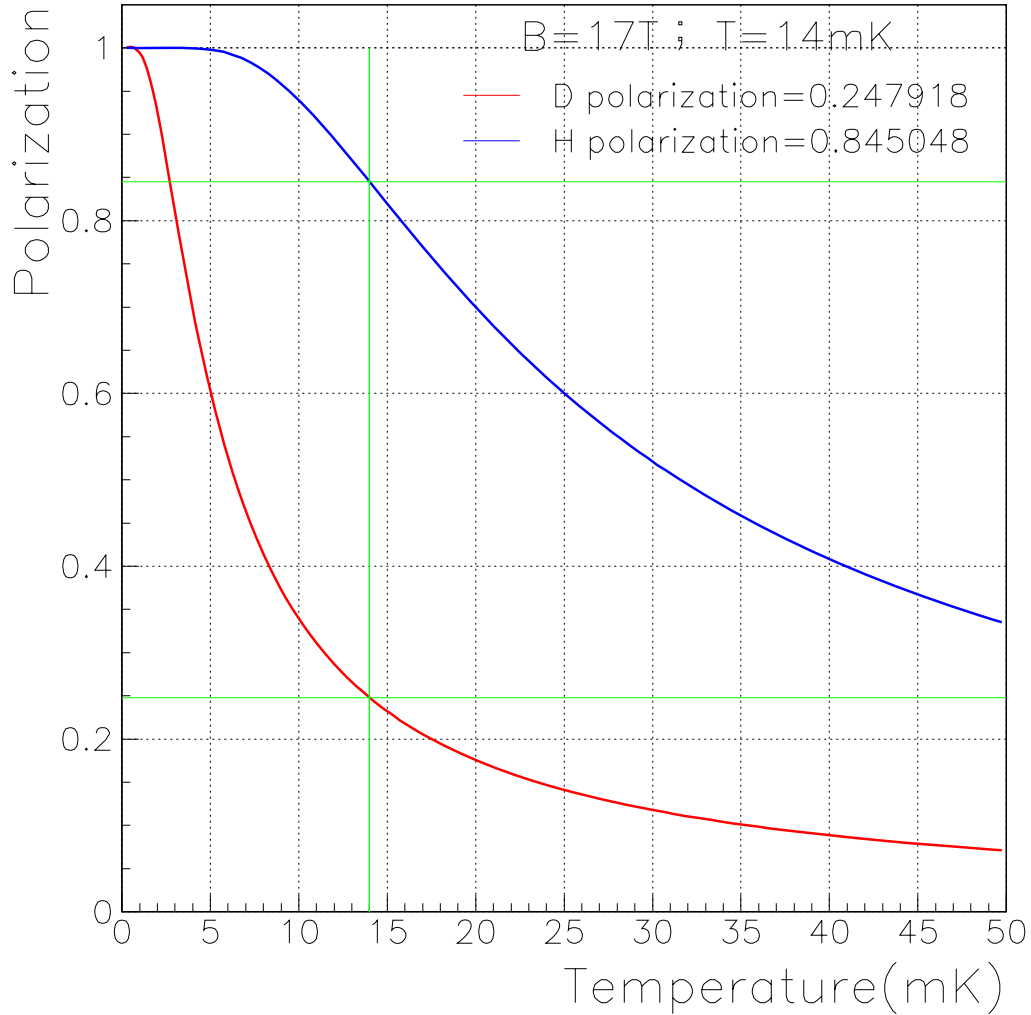
Polarization of HD (when $B=17\text{T}$)

Figure 2.2: The polarization could be estimate by Eq. 2.3 and Eq. 2.4. This figure shows the P_H and the P_D at 14mK and 17T.

and $L=0$. When the $o\text{-H}_2$ flip to the $p\text{-H}_2$, the HD protons can exchange energy with the $o\text{-H}_2$ spins by means of mutual spin flips. When the $o\text{-H}_2$ flip to the $p\text{-H}_2$, the energy of these two states also generate photon. The photon may flip another $p\text{-H}_2$ to $o\text{-H}_2$, or just generate heat.

Therefore, introducing small (approximately the order of 10^{-4}) contamination of $o\text{-H}_2$ and $p\text{-D}_2$, as an impurity, can reduce the relaxation time. The presence of $o\text{-H}_2$ and $p\text{-D}_2$ plays an important role to polarize the target. The molecular orbital angular momentum couples with both the lattice and the nuclear spin. Thus, by doping a small amounts of $o\text{-H}_2$ and $p\text{-D}_2$ into the pure HD, the relaxation times of the H and D in HD are reduced so that the sample can be polarized.

The equilibrium polarizations of 85% for H and 25% (vector) for D can be achieved in this way for HD cooled to 14 mK in a Dilution Refrigerator at the magnetic field of 17 T. The sample must be kept at the temperature of 14 mK and under the field conditions long enough to let the impurities $o\text{-H}_2$ and $p\text{-D}_2$ decay

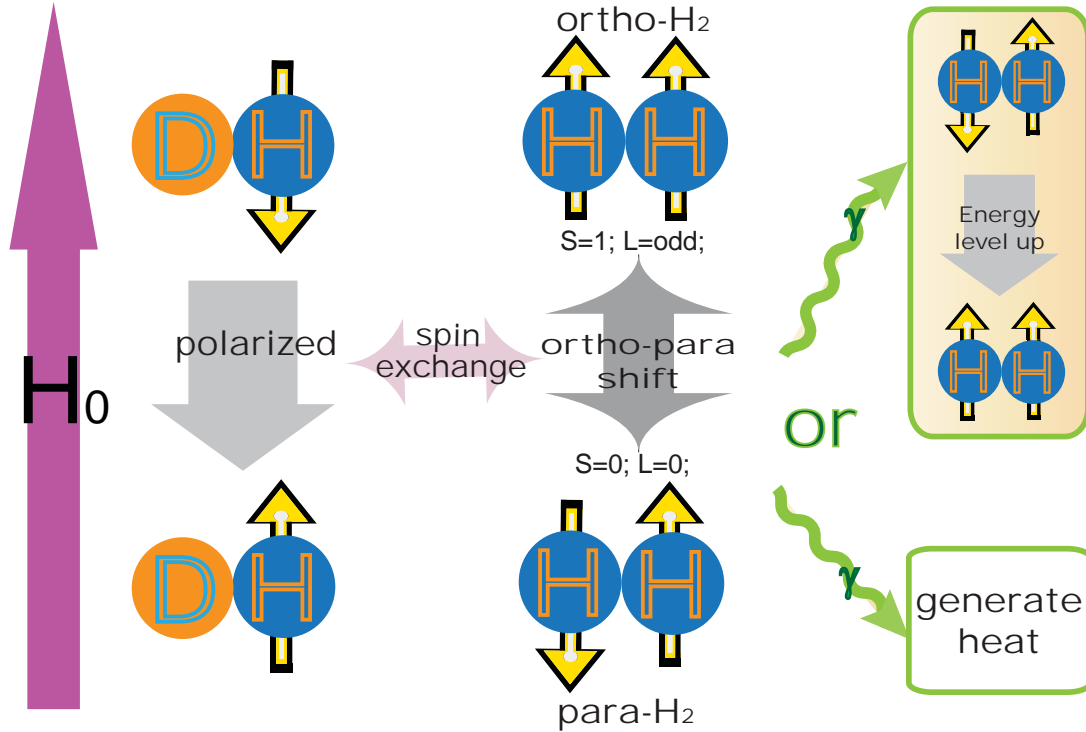


Figure 2.3: The equilibrium condition at low temperatures requires the p-H₂ state with $S=0$ and $L=0$. When the o-H₂ flip to the p-H₂, the HD protons can exchange energy with the o-H₂ spins by means of mutual spin flips. When the o-H₂ flip to the p-H₂, the energy of these two states also generate photon. The photon may flip another p-H₂ to o-H₂, or just generate heat.

to their magnetically-inert ground states, so that the sample spins are effectively frozen. In view of the corresponding decay time constants, this aging process can be very long (40 days to reach H relaxation times longer than a week at 4 K and 0.5 T) and become prohibitive for D. Furthermore, the D polarization is only 20%. Therefore, in the practical cycle which has been used to polarize HD, only o-H₂ doping has been used to polarize H. The D polarization has been obtained by transferring the H polarization to the D, using a method commonly known as Adiabatic Fast Passage [15]. This technique takes advantage of the dipole coupling of H and D nuclei in different HD molecules. In this way, the polarization of deuterium reaches at 60% [16, 17].

2.2 Polarized Target Production

We selected the HD molecule as a polarized nucleon target. The HD molecule can become both a proton target and a neutron target. The HD is an idealistic polarized targets for the LEPS experiments. In order to achieve high polarizations of proton and deuterium targets, we employ the static method using “brute force” at low temperature (14 mK) and high magnetic field (17 Tesla).

2.2.1 Target Cell

The target cell for PHYDES is designed for transport of solid HD in a frozen-spin or equilibrium polarization state from one cryostat to another as well as to transport heat produced in the ortho-para conversion process out from the HD into the cryostat. It must also not generate a large background under hydrogen signal for polarization measurement on the target.

The main components of target cell are the copper target ring, aluminum cooling wires and the Kel-F end-caps. The copper target ring is used to connect the cold finger of the DRS. The copper target ring must be of sufficient purity to provide good thermal conductivity at the millikelvin range of temperatures used to polarize the HD target. The target ring should also be nonmagnetic so that it does not interfere with the NMR line-shape.

The aluminum cooling wires are 50 μm in diameter and 99.999% purity. They are bundled and attached to the target ring. There are approximately 2000 such cooling wires in each target cell. The total mass of the aluminum wires is about 20% of the mass of the HD target material.

The end-caps are made of Kel-F which contains no atomic hydrogen. It won't introduce the additional background to the NMR signals. The majority of the nuclear background is from this material so the parts of the end-caps which will be in the beam are made as thin as possible. The top cap is necessary to reduce the size of hole open to vacuum (or He exchange gas) so that the amount of HD which sublimates from the solid target is negligible. [12].

2.2.2 Cryogenic and Magnet Systems

The polarized HD system include five refrigerators. The procedure of target production is :

1. At RCNP, pure HD gas with the amount of 1 mole is produced by using the HD gas distillator.
2. The HD gas is solidified and the polarization of the reference HD is measured in a ^4He refrigerator (SC).
3. Another ^4He refrigerator (TC1) transfer solid HD from SC to dilution refrigerator system (DRS).
4. The polarization of the solid HD is made and frozen by aging at B=17 Tesla and at T=14 mK in DRS.
5. The polarized HD is transferred from the dilution refrigerator (DRS) to a ^4He refrigerator (SC) by using another ^4He refrigerator (TC1).
6. The polarization of the polarized HD is measured in SC.
7. The SC is transported to SPring-8/LEPS by a truck.
8. At SPring-8/LEPS, the polarized HD is transferred from the SC to a dilution refrigerator(IBC) by using the last ^4He refrigerator (TC2).

All polarization measurements are performed in SC. The flow chart of target transportation is shown in figure 2.4. The IBC provides a magnetic field of 1 Tesla and a temperature of 300 mK during the physics experiment for a few months [13].

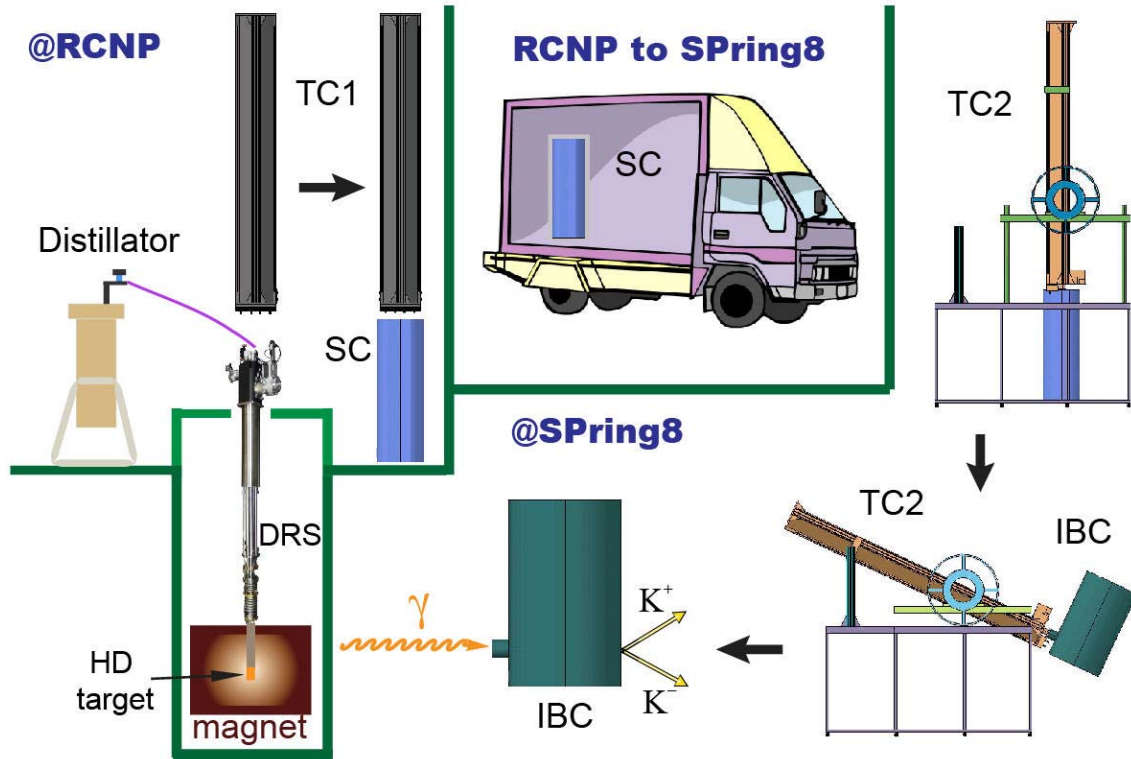


Figure 2.4: The flow chart of target transportation.

Distillator

The purity of commercial HD gas is about 96% and most of contaminations are H_2 (2%) and D_2 (2%). Distillators purify the HD gas up to 99.99% in order to optimize the amount of impurities. There are packings called “Helipack” inside the distiller. Temperature gradient is made by cooling the top and heating the bottom of the distiller. Heat exchange between gas and liquid takes place on the packings. A low-boiling element is vaporized and extracted from the top of the distiller. The difference of the boiling points of HD, H_2 and D_2 enables for the HD gas to be separated from the others. The concentration of H_2 and D_2 is measured by a quadrupole mass spectrometer. [18]

Dilution Refrigerator System (DRS)

The DRS is to polarize the HD target for the first stage at RCNP. We made a hole, where the Dilution Refrigerator (DR) and a dewar were installed, with a depth of 5.5 m and a diameter of 1.6 m. A support frame for the DR and the dewar was constructed to remove vibrations which increase the temperature of the target. We installed the DR, fabricated by Leiden Cryogenics, with a cooling power of 3000W at 120 mK and a lowest temperature of 6 mK. A super-conducting magnet is made by JASTEC company. The magnet has maximum magnetic field at the target center is 17 Tesla (290 A) at 4.2K. Fig. 2.6 shows the DRS picture.

Storage Cryostat (SC)

SC is to keep HD polarization on the way of the transportation from RCNP to Spring8. The SC is transported to SPring-8/LEPS by using a truck. The SC is also used to solidify the HD and measure the polarization of the reference HD. SC is a ^4He refrigerator with superconducting magnet, fabricated by Oxford, with a lowest temperature of 1.2 K and the highest magnetic field of 2.5 Tesla.

In Beam Cryostat (IBC)

IBC is to cool the target during the experiment at SPring-8. The IBC is a ^3He - ^4He dilution refrigerator with superconducting magnet. The lowest temperature of the IBC mixing chamber is 250 mK and the magnetic field to hold the polarization of the HD target is 1 Tesla. Fig. 2.8 shows the perspective drawing of IBC and the real picture of IBC.

Transfer Cryostat (TC)

The 4.2 K transfer cryostats (TC) are provided by France IPN Orsay in 2006. The TC1 is mainly for moving the target from the DRS to the SC. The TC2 is mainly for moving the target from the SC to the IBC (Fig. 2.9). Basically, a left-hand right-hand thread mechanism makes it possible to engage, screw or unscrew a target in or from its cold finger, while a 0.15 T superconducting magnet provides a magnetic field sufficient to hold the target polarization during the period of the cold transfer process of HD from one cryostat to another.



Figure 2.5: Distillator.



Figure 2.6: Dilution Refrigerator System (DRS)



Figure 2.7: Storage Cryostat (SC)

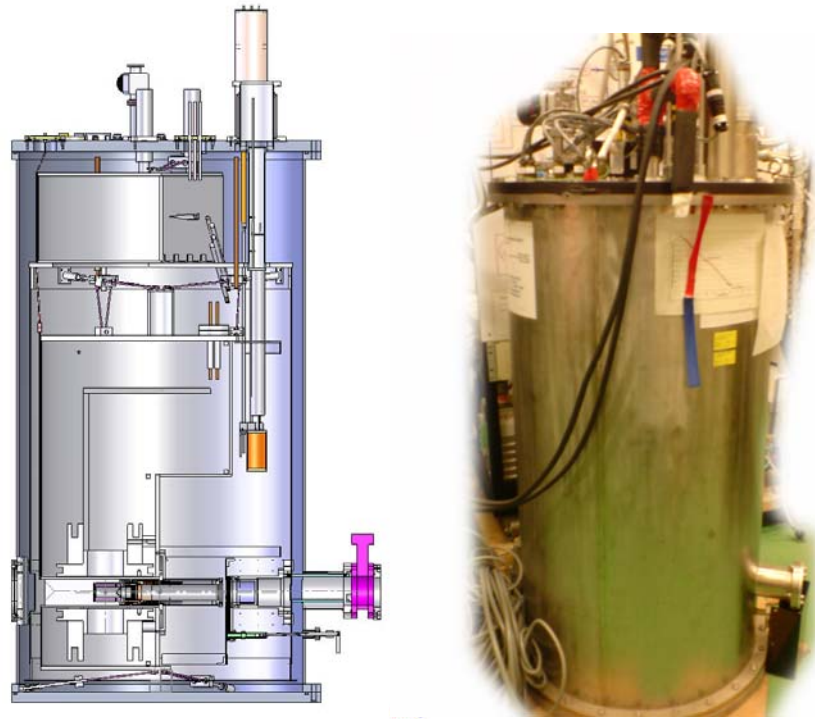


Figure 2.8: The left figure is the perspective drawing of IBC. The right figure is real picture of IBC



Figure 2.9: The left side of the figure is TC1, which is mainly for moving the target from the DRS to the SC. The right side the figure is TC2, which is mainly for moving the target from the SC to the IBC.

2.3 NMR Polarimeter

2.3.1 NMR Principles

What is NMR?

Nuclear magnetic resonance (NMR), is a physical resonance phenomenon involving the observation of specific quantum mechanical magnetic properties of an atomic nucleus in the presence of an applied, external magnetic field. All nuclei that contain odd numbers of nucleons have an intrinsic magnetic moment and angular momentum.

How is NMR Detected?

As the Fig. 2.10, a large static magnetic field breaks the energy degeneracy between the nuclear Zeeman levels so that transitions can be driven by a RF field applied perpendicular to the static magnetic field. The energy absorbed or emitted is proportional to the difference in the populations of the magnetic sub states and hence the polarization of the target material. The RF frequency required, known as the Larmor frequency, is determined by the gyromagnetic ratio of the nuclei of interest and the strength of the static magnetic field. In practice, the frequency response is broadened by small variations in the local magnetic field but, as the term resonance implies, the response is negligible outside of a narrow frequency band centered around the Larmor frequency.

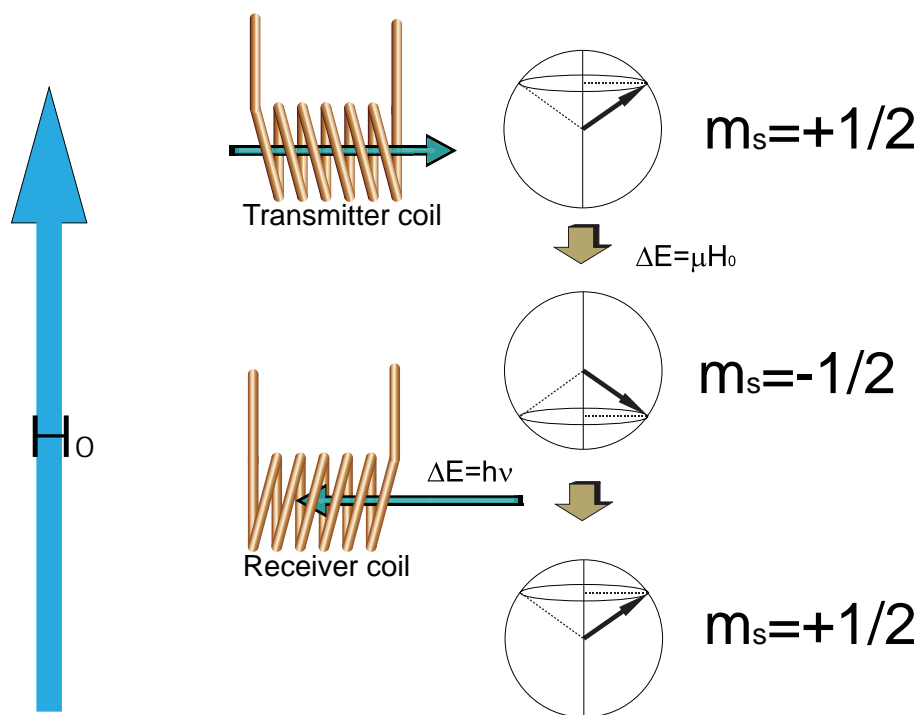


Figure 2.10: NMR principle

How to Get the Polarization by NMR Measurement?

The net absorption or emission of electromagnetic radiation by the nuclear spin system can be modeled macroscopically as the imaginary component of complex magnetic susceptibility, $\chi(\omega) = \chi'(\omega) + i\chi''(\omega)$, where the real part is absorption part and the imaginary part is dispersion part. The vector polarization, P , can be written as

$$P \propto \int_0^{\infty} \chi''(\omega) d\omega \quad (2.5)$$

which forms the basis for the area methods used to determine polarization.

2.3.2 NMR Hardware and Software

The single coil method is selected for PHYDES System. In this method, a single coil is used for both transmitter and receiver coils. When the single coil is used, one should construct an electronic circuit so that an RF signal from a transmitter does not mix with a signal from a receiver. Therefore, we used a cancellation circuit which is proposed by Jefferey and Armstrong [19]. The Fig. 2.11(a) shows diagram of cancellation circuit and the Fig. 2.11(b) shows the picture of cancellation circuit. As shown in Fig. 2.11(c), the x-axis is frequency, the cancellation circuit can cancel signal with selected frequency. When receiver coils receive the signal, the signals come from transmitter but not nuclear magnetic resonance can be canceled easily by cancellation circuit. The cancellation circuit only can cancel signal with selected frequency; therefore during the NMR measurement, the frequency sweeping is out of the question. On the other hand, the whole NMR circuit is related to frequency. Even cancellation circuit is not employed, the frequency sweeping will produce unexpected noise.

The Fig. 2.11(a) shows diagram of cancellation circuit and the Fig. 2.11(b) shows the picture of cancellation circuit, the transmitter and receiver coils are both 1 turns. As shown in Fig. 2.11(c), the x-axis is frequency, the cancellation circuit can cancel signal with selected frequency. The signal coil for PHYDES system is saddle coil, as shown in Fig. 2.12(c). D. M. Ginsberg and Melvin J. Melchner find that the saddle coil with height/diameter=2 and angle 120 degree make most uniform field in the coil [20].

Phase correction is performed by the phase shifter in lock-in amplifier and is to align the phase of the reference signal and measuring signal. In lock-in amplifier, reference and measuring signals are multiplied and integrated. If two signal have same frequency one can get the amplitude of the signal. If two signal have different frequency, signal vanish. So, we can extract the small signal with a fixed frequency embedded in the big noise.

The Fig. 2.13 is diagram of whole circuit for NMR measurement.

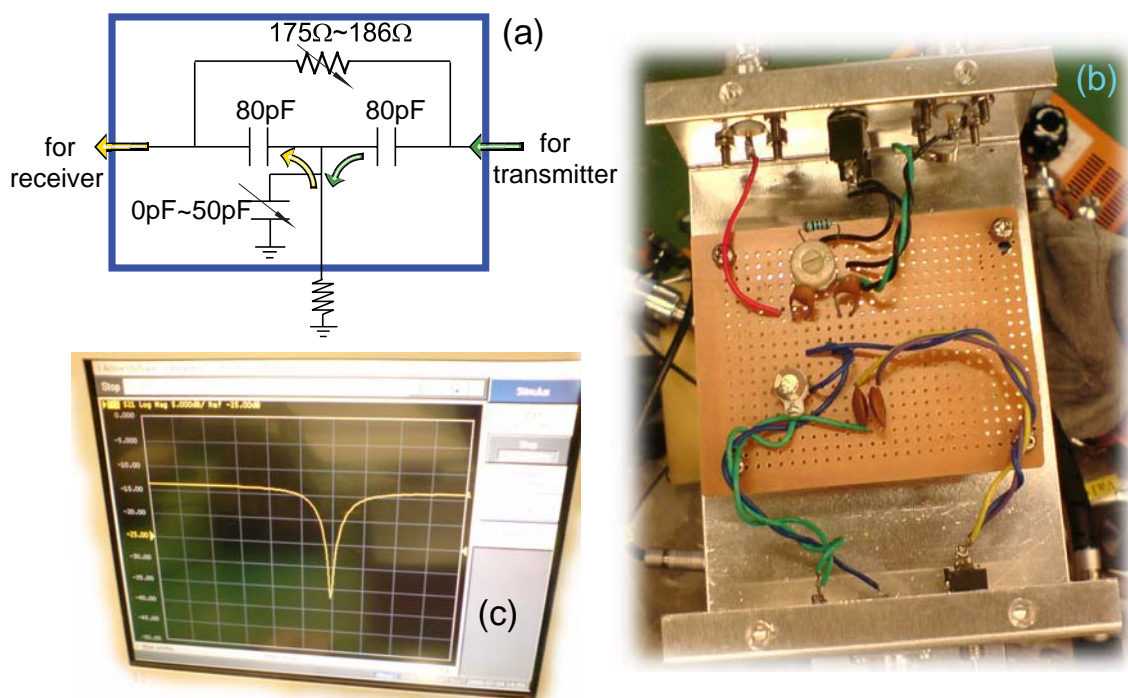


Figure 2.11: The figure(a) shows diagram of cancellation circuit and the figure(b) shows the picture of cancellation circuit. As shown in figure(c), the x-axis is frequency, the cancellation circuit can cancel signal with selected frequency.

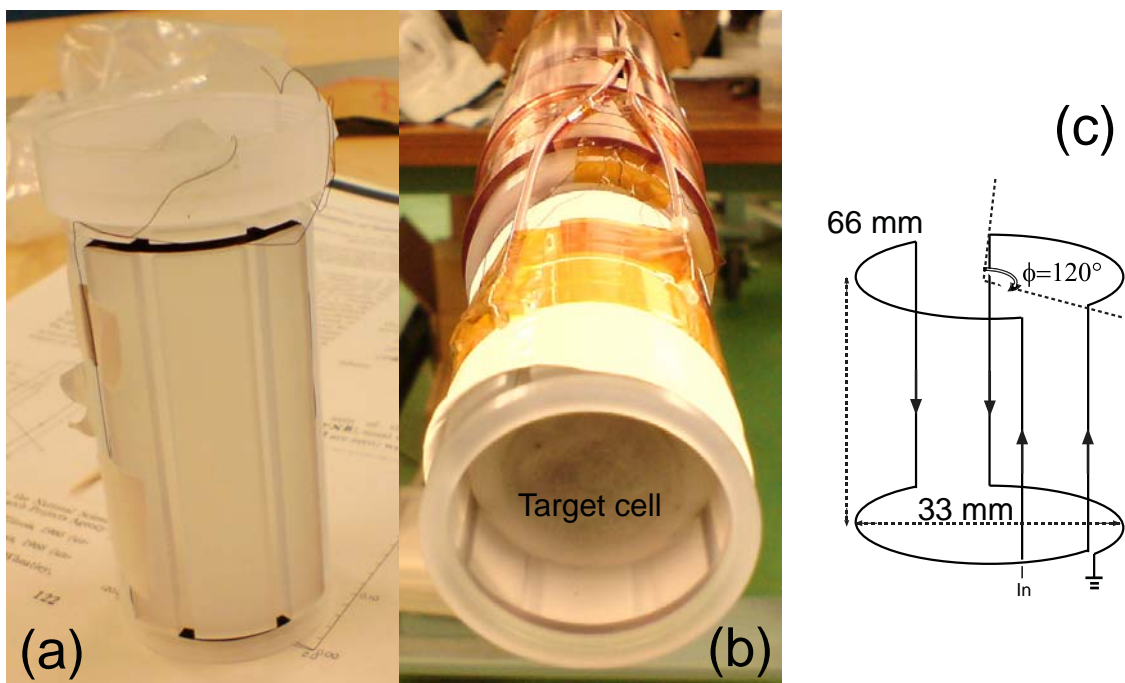


Figure 2.12: (a) The Kel-F coil supporter with coil, the transmitter and receiver coils are both 50 turns. (b) The Kel-F coil supporter with the target cell. (c) The draft of single coil; the transmitter and receiver coils are both 50 turns in real case.

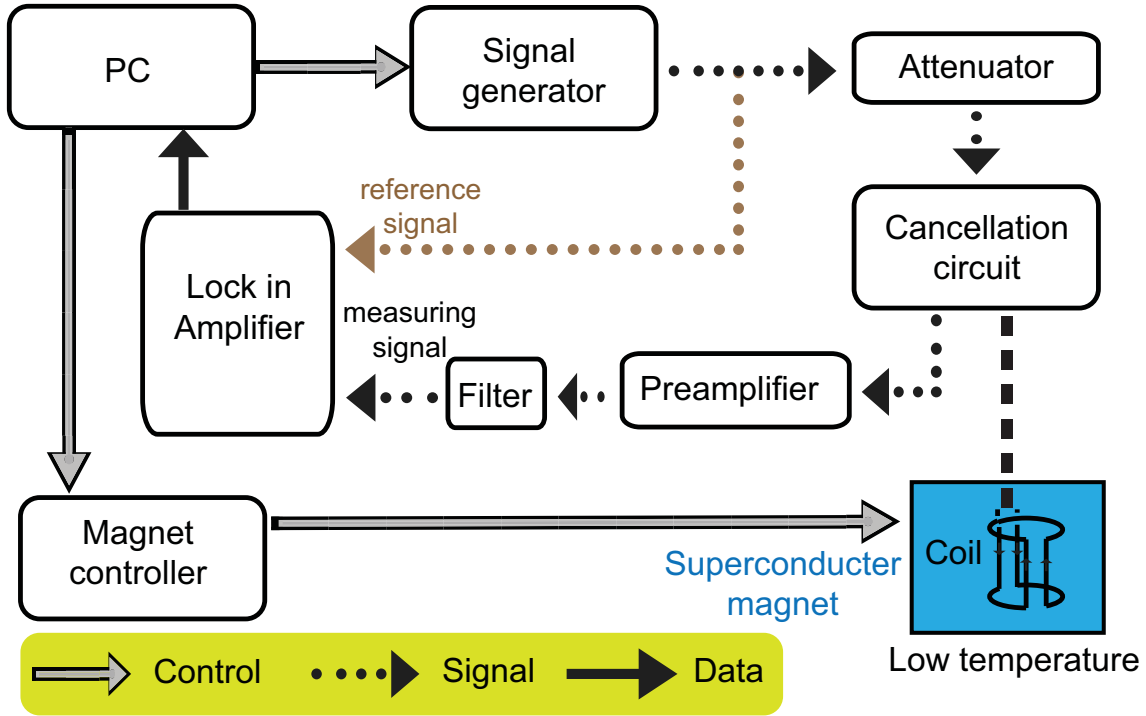


Figure 2.13: The signal flow of single coil method.

2.3.3 Extracting the Polarization

Just like we talked in Section 2.1.1, the polarization is assumed to be proportion to the area of the NMR signals. The main problem is just that we don't know the ratio of area to polarization. There is a easy solution of the problem. From the Boltzmann law (as we talked in section 2.1.1), the polarization is only related to magnetic field and temperature. For getting a reference signal, one can put the target in a stable magnetic field and temperature environment, then wait until thermal equilibrium. Once we measure a target with known polarization by NMR, we can apply the the ratio of area (A) to polarization (P) to estimate the polarization from NMR signal area, as shown in Eq. 2.6. We called this "reference signal".

$$P_{NMR} = \frac{P_{ref} \times A_{NMR}}{A_{ref}} \quad (2.6)$$

2.3.4 Extracting the Relaxation Time

The spin-lattice relaxation time, T_1 is defined as the lifetime in an exponential decay of polarization of the form as follows:

$$P_{target}(t) = P_{target}(0) + (P_{thermal_eq} - P_{target}(0))(1 - \exp(-\frac{t}{T_1})) \quad (2.7)$$

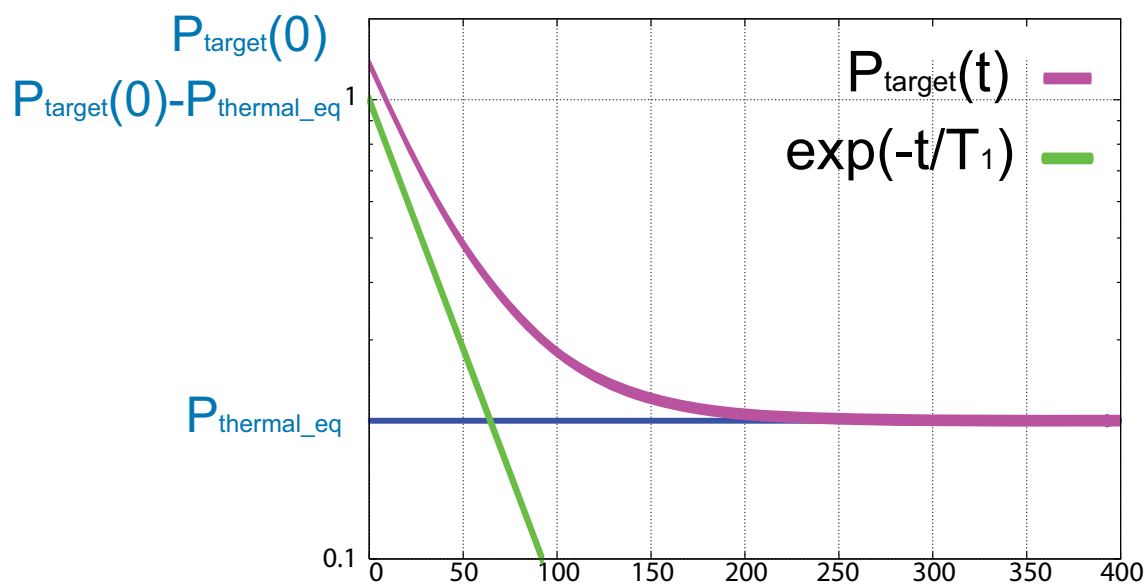


Figure 2.14: This figure explain the Eq. 3.4. The blue curve, $P_{\text{thermal_eq}}$, is the polarization when HD reach thermal thermal equilibrium. The green curve is the decay function of the polarization in normal case. With taking two curves in account, the final function the violet curve, $P_{\text{target}}(t)$.

Chapter 3

Data Taking and Analysis

We produced a polarized HD target for the first time in 2008 and named it PHYDES01. PHYDES01 is made for study of polarization and relaxation time for H and D. In this chapter, the details in data taking and analysis will be shown.

3.1 PHYDES01 Production and Data Taking

We produced a polarized HD target for the first time in 2008. The normal process of PHYDES production was discussed in section. 2.2. The polarized HD system consist of five refrigerators. The TC1 and TC2 did not work in this time; therefore, solidifying HD and measuring polarization were performed at DRS.

Since there were some unexpected accidents, such as damaged of HD gas pipe and the short of pure HD gas, only 0.68 mole HD was solidified for PHYDES01. When HD just was solidified HD in DRS, the H reference signal was measured at $B=1\text{T}$ and $T=4.2\text{K}$. The D reference signal was not measured, because D signal was too small to be observed at $B=1\text{T}$ and $T=4.2\text{K}$. The concentration of H_2 is 1.26% and the concentration of D_2 is 2.07%. So that the concentration of HD is 97.66%.

After the aging time of 53 days at $B=17$ Tesla and at $T=14$ mK, the hydrogen (H) and deuterium (D) in the HD was measured by the NMR system [21]. To make sure that the relaxation time is long enough for the transportation time, we also measured relaxation time in the experimental condition of TC1, SC, and TC2. The details of data taking is summarized in Table 3.1. The details about H reference signal, H polarization and relaxation time in IBC condition are discribed in Morisaki's thesis [22]. Usually, we measured 10 signals for one data group, 5 signals for magnetic field increase, 5 signals for magnetic field decrease. We average the 10 signals to get one data point for relaxation time fitting.

| | reference signal | | IBC | | SC | | TC | |
|---------------------------|------------------|--------|--------|--------|--------|--------|--------|--------|
| Nuclear | H | D | H | D | H | D | H | D |
| Storage Temperature (K) | | 4.2 | | 0.3 | | 1.2 | | 4.2 |
| Storage Magnetic Field(T) | 1.08 | 7.26 | 1.08 | 1.08 | 1.08 | 1.08 | 0.15 | 0.15 |
| Resonance Point (T) | 1.1361 | 7.4044 | 1.1366 | 7.4044 | 1.1366 | 7.4044 | 1.1366 | 7.4044 |
| Radio Frequency(MHz) | 48.373 | | | | 48.395 | | | |
| B Sweep Speed (T/min) | 0.0938 | | | | 0.0938 | | | |
| Sample Rate | 2500 | | | | 500 | | | |

Table 3.1: The HD target staying time and relaxation time in each refrigerator.

3.2 Preparation of Analysis

3.2.1 Unification of the Signal Amplification

Before started aging, we measured the reference signal, and set the sensitivity to $(1mVrms/-47dBm)$. After aging, the signal increase a lot. To prevent the signal overflow, we changed the sensitivity to $(10mVrms/-27dBm)$ to decrease the signal. This change makes the signal size decrease 10% of original one. When we analysis data, just multiplied the signal by ten. With this modification, this signal area is increase ten time. And, of course, this modification is not done on the signals which we got before aging. On the other hand, for convenience, the negative shape is changed to positive. During this modification, the signal area is not changed. These modification are shown in Figure 3.1 and 3.2.

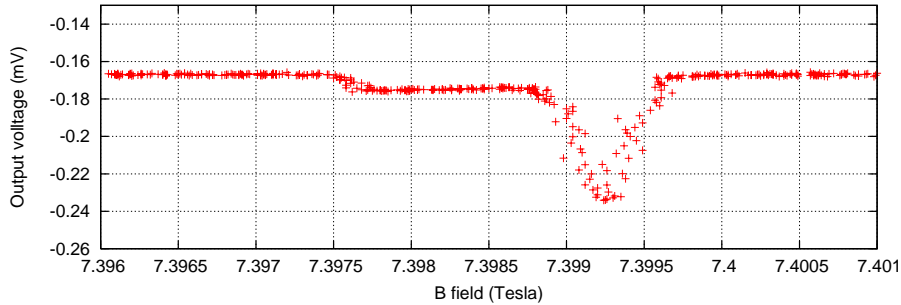


Figure 3.1: The original data with the $sensitivity = (1mVrms/-47dBm)$

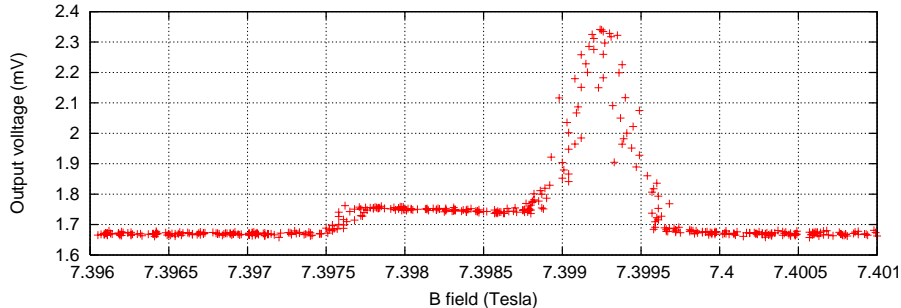


Figure 3.2: The signal is ten times of original one. We also change the signal shape to positive.

3.2.2 Magnetic Field Adjustment

Due to the inaccuracy of measurement, the magnetic field is a little bit messy. Unfortunately, the line width of NMR signal is just very narrow, so that the NMR signal is blurred. Actually, when we sweep the magnetic field, the change of magnetic field is more smooth. We can confirm this by using the time channel, as shown in Fig. 3.3. But if one choose the time channel, the speed of magnetic field sweeping or speed of data taking should be considered each time. It is inconvenient and inaccurate. That is why we choose the magnetic field channel, and do some magnetic field adjustment. We averaged magnetic field of 101 points, and readjusted magnetic field of the center point (the 51th point). The adjusted signal is shown in Figure 3.4.

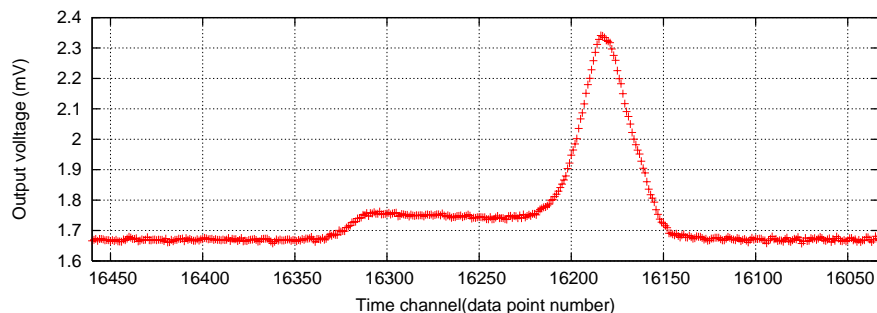


Figure 3.3: When we choose the time channel, the signal is more clear. But if one choose the time channel, the magnetic field sweep speed or data taking speed should be considered every time. It is inconvenient and inaccurate.

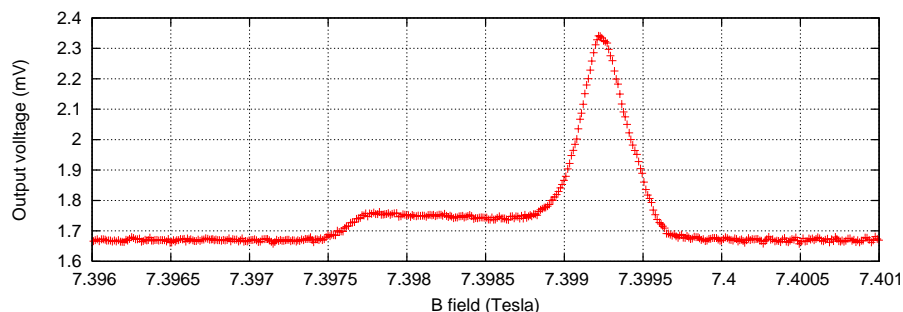


Figure 3.4: The magnetic field channel signal is more clear by magnetic field adjustment.

3.2.3 Data-Position Shifting

Due to the hysteresis from cold finger and aluminum wire and some unknown reasons, the signal position is shifted, as shown in Fig. 3.5

We found the highest data point of signal, and shift the signal horizontally by adjusting the point to the theoretical resonance magnetic field. We also remove the background roughly, in the 3.2.6, the background will be removed more carefully.

3.2.4 Unification of Bin Size

We unify the bin size to 0.0005 T. There is no specific reason for this choice. Just the bin size in all condition should be unified, and this bin size is appropriate for the observation of both small and big signals.

3.2.5 Phase correction

In an ideal NMR experiment there is no phase shift. In practice, during a real NMR experiment a phase correction must be applied to either the time or frequency domain spectra to obtain an absorption spectrum as the real output. As discussed in section 2.3.2, phase correction is performed by the phase shifter in lock-in amplifier and is to align the phase of the reference signal and measured signal. If the phases between the measuring signal and reference signal in lock-in amplifier is different, the value obtained is $RE \cos \phi + IM \sin \phi$ (RE =the real part; IM =the imaginary part;

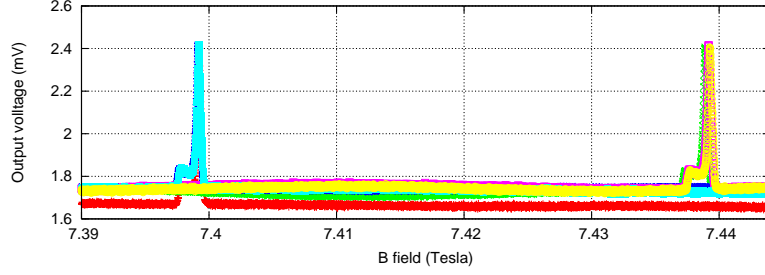


Figure 3.5: Due to the hysteresis from cold finger and aluminum wire and some unknown reasons, the signal position is shifted.

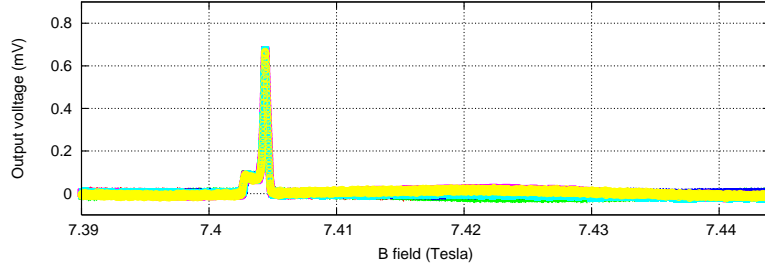


Figure 3.6: The highest data point of signal is found, and the signal is shifted horizontally by adjust the point to the theoretical resonance magnetic field.

ϕ =the difference of the phase). So, to obtain only RE or IM, the phases should be same. This process is equivalent to the coordinate transformation as follow,

$$\begin{pmatrix} RE' \\ IM' \end{pmatrix} = \begin{pmatrix} \cos(\phi) & \sin(\phi) \\ -\sin(\phi) & \cos(\phi) \end{pmatrix} \begin{pmatrix} RE \\ IM \end{pmatrix} \quad (3.1)$$

We adjusted the phase in lock-in amplifier when we just got the signal. But that is just roughly adjusted by eyes. Fig. 3.7 shows the examples of signals with a good phase and bad phase.

After we finished the data taking, one can zoom into the signals by logarithm scale, and adjust phase by Eq.3.1 again.

3.2.6 Background Removing

There is still background included in the signal. That is the residual signal which the cancellation circuit cannot cancel. And by the change of the circuit by the circumstance change (ex. temperature or magnetic field), change the magnitude of the background.

The background is assumed to be a first-degree polynomial function. We fit the background in background-only region. To decide the background region, we pick a group of signals first. For D, we pick up the first data we measured after aging. This group of signal has the highest S/N ratio. For H, after the polarization of empty cell decrease to almost zero (after ten times of relaxation time), we picked a group which with high S/N ratio. The relaxation time of empty cell is around 22 hours [22].

Since the signal shape is different between H and D, we use different background region. We zoom in this signal by logarithm scale and define the flatness region to

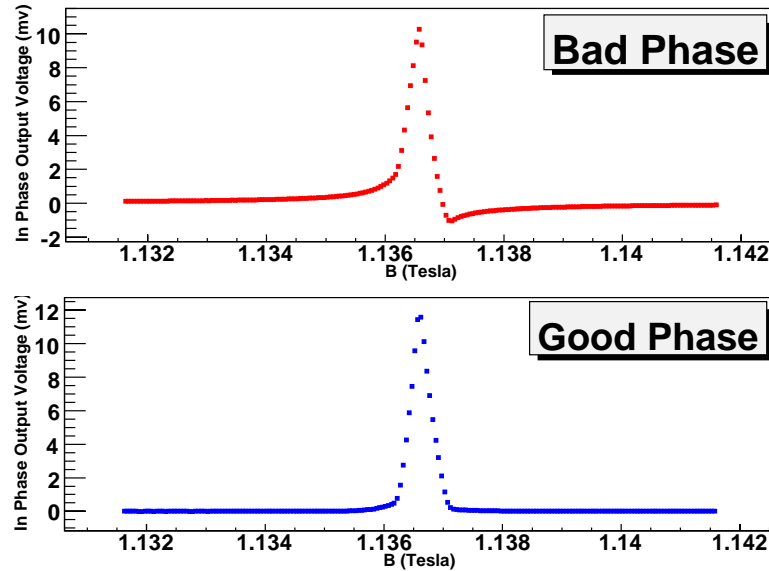


Figure 3.7: When the phase is clearly not good, we can adjust it by eyes before data taking.

be the background region. Some backgrounds are included in the signals. Before we take an average of all signals, the background should be removed for each signal. The background is assumed to be a first-degree polynomial function. The background is only fitted in background-only region, as shown in Fig. 3.8.

3.3 Relaxation Time Extracting

The spin-lattice relaxation time, T_1 is defined as the lifetime in an exponential decay of polarization degree (P) of the form as follow

$$P(t) = P(0) + (P_{thermal_eq} - P(0))(1 - \exp(-\frac{t}{T_1})) \quad (3.2)$$

The polarization degree is assumed to be proportional to the area of the NMR signals (A). The follow equation is used for relaxation time estimation.

$$A(t) = A(0) + (A_{thermal_eq} - A(0))(1 - \exp(-\frac{t}{T_1})) \quad (3.3)$$

At first, we have no idea about the exact value of $A_{thermal_eq}$. The $P_{thermal_eq}$ is clear, but the ratio of area to polarization is unknown. The ratio of area to polarization could be gotten by the study of reference signal. Fortunately, the polarization degree after aging is much higher than the polarization degree of thermal equilibrium state. The $P_{thermal_eq}$ ($A_{thermal_eq}$) can be ignored, in this equation temporarily. After the study of reference signal, we can estimate the $A_{thermal_eq}$ and put it back to this function again.

There are two methods to estimate the area of NMR signals. One is histogram method and another is model method. The results from two methods are consistent.

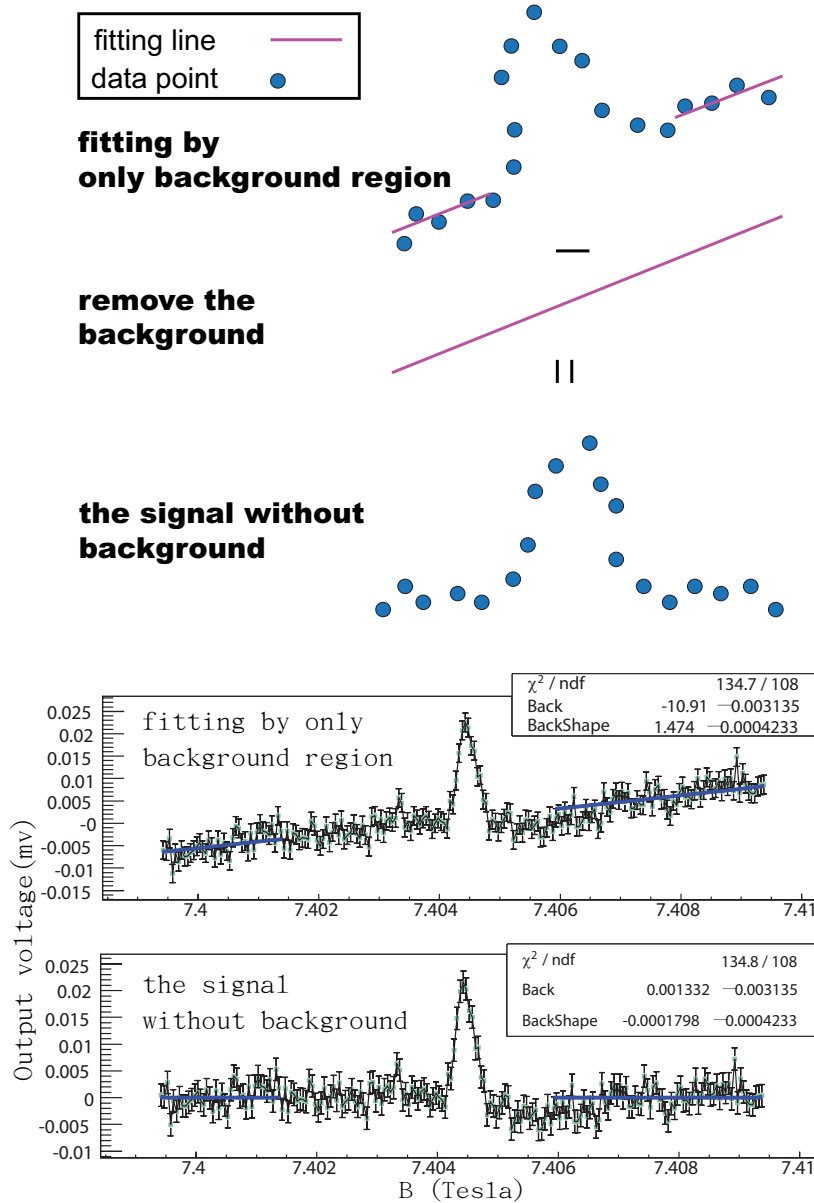


Figure 3.8: Before we take an average of all signals, the background should be removed for each signal. The background is assumed to be a first-degree polynomial function. We fit the background in background-only region.

3.3.1 Extracting Signal Area by Histogram Method

In the histogram method, at first, we fit the background for each signal in background-only region and remove the background, just like the 3.2.6. We average the signals respectively in different sweep direction of magnetic field. After taking average, we fit the background in background-only region to remove the background again. The signal without background is used to fill histogram. The integral of histogram is the signal area. The area obtained is different in two sweep direction of magnetic field. We average them to get the final result of signal area. The flow chart is shown in Figure. 3.9.

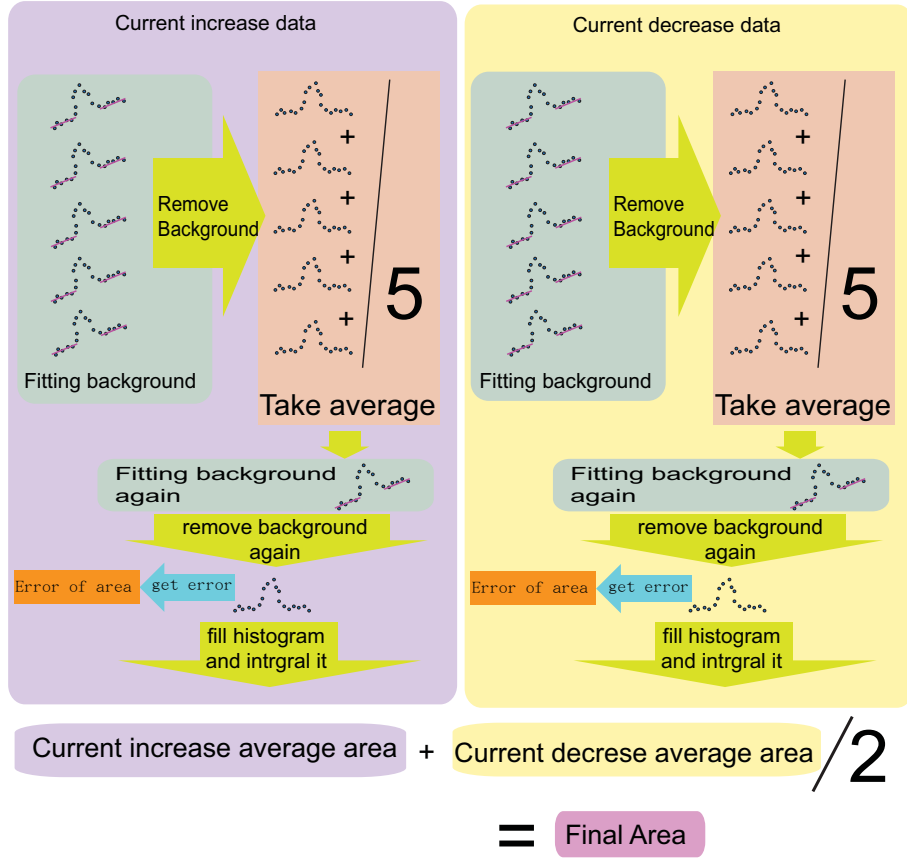


Figure 3.9: Flow chart of histogram method

The error bar is estimated from the data in background side. The signal height of each bin in background part is filled to a new histogram. We use the RMS of the new histogram to be the error bar of each bin. In order to prevent that the difference between the left side and right side of background bring the inaccuracy, the left side and right side of background part are filled to different histogram, respectively. And this estimation shifts the two histograms horizontally by shifting the mean value to zero and then merges two histograms to one histogram. The RMS of final histogram is used to be the final error bar for all bins in the final fitting. The error estimation flow chart is shown in Figure. 3.10. The estimation of the area is done with this error bar. There are 200 bins in the histogram, so that the error of area is 200 times of the error bar of each bin. The above error is the statistical error (E_{stat}).

The systematic error of area of NMR signal is also taken into account. It cause the area of NMR signals to be different between every measurement and also between average of current increase data ($A_{increase}$) and average of current decrease data ($A_{decrease}$), as shown in Fig. 3.11 and Fig. 3.12. The systematic error (E_{sys}) is defined as

$$E_{sys} = \sqrt{(A_{increase} - A_{ave})^2 + (A_{decrease} - A_{ave})^2} \quad (3.4)$$

where the $A_{ave} = (A_{increase} + A_{decrease})/2$. The final error of area of NMR signal (E_{final}) is defined as

$$E_{final} = \sqrt{E_{stat}^2 + E_{sys}^2}. \quad (3.5)$$

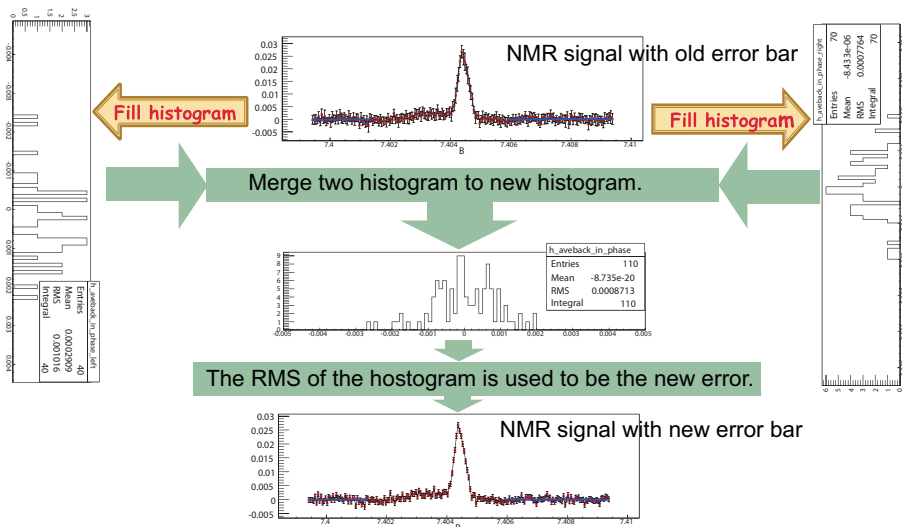


Figure 3.10: Flow chart of error estimation

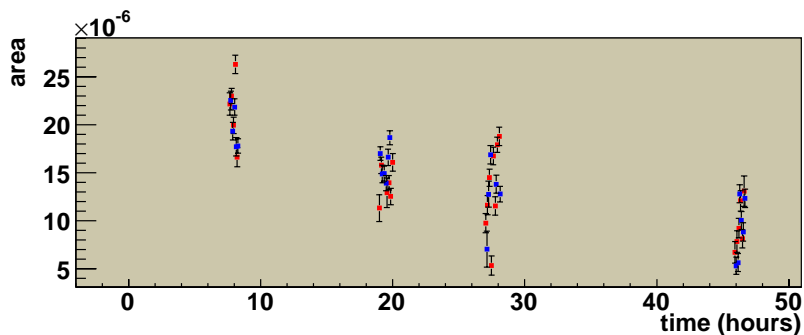
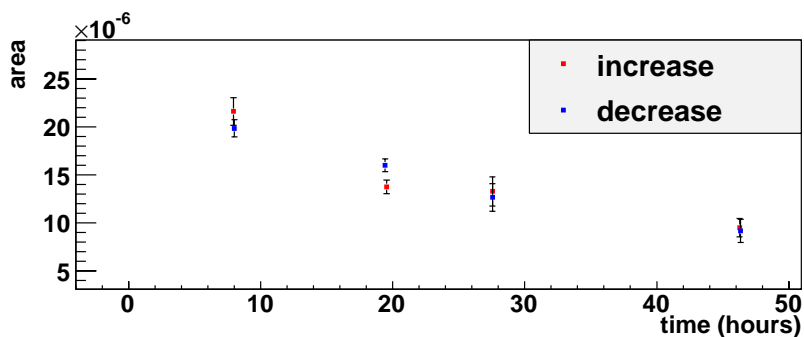


Figure 3.11: The area of NMR signals are different between every measurement

Figure 3.12: The area of NMR signals are also different between average of current increase data ($A_{increase}$, red point) and average of current decrease data ($A_{decrease}$, blue point)

3.3.2 Extracting Signal Area by Model Method

The shapes of NMR signals of H and D do not fit to any given function. Fortunately, even the polarization decreases and the area of NMR signal decreases, the shape of NMR signal is not changed. In other words, when the change of the signal size is due to the change of the polarization, the width of the NMR signal dose not changed. The only change is just the height of signal. We made four models for NMR signals: H signals and D signals in case of increasing and decreasing current, respectively, as shown in Fig. 3.13.

For D, we pick up the first data which we measured after aging. This group of signal has the largest S/N ratio. For H, after the polarization of empty cell decrease to almost zero (after ten times of relaxation time), we picked a group which with high S/N ratio. The relaxation time of empty cell is around 22 hours [22]. After we picked up a group of a NMR signals, we used ‘‘Histogram Method’’, as discussed in 3.3.1, to fill a histogram and made a histogram model. But when we made the model, we made two model for current-increasing and current-decreasing, respectively. After we fill the histogram, the area of histogram is normalized to 1.

The flow chart of model method which is similar to the flow chart of histogram method, is shown in Figure. 3.14. The systematic error is also considered in this method as the Eq. 3.4 and Eq. 3.5.

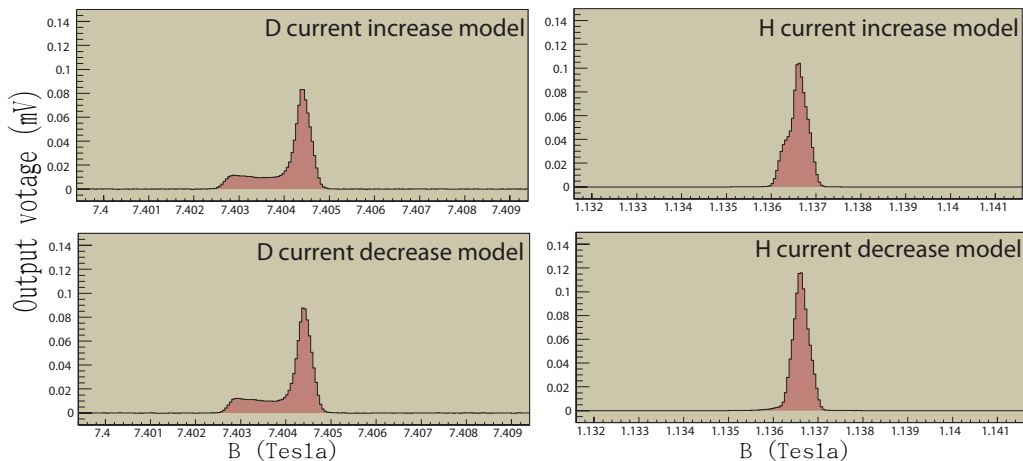


Figure 3.13: Four models for different shape of NMR signals

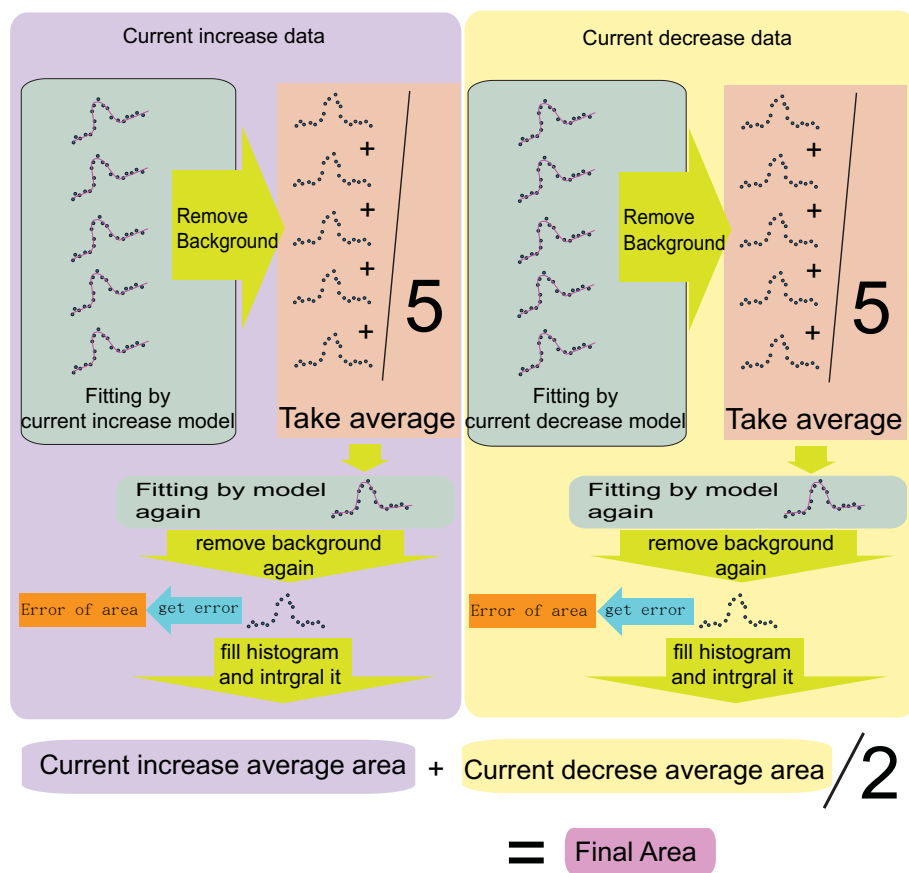


Figure 3.14: Flow chart of model method

3.4 Polarization Extracting

The estimation of H polarization degree is described in Ref. [22]. In this study, we consider the estimation of D polarization degree. The estimation of polarization uses the reference signal to find out the polarization. The reference signal was measured in thermal equilibrium state. The polarization degree can be estimated easily by the Boltzmann law (as we talked in section 2.1.1). When the D reference signal is measured, the HD target is assumed to be at 4.2K and 7.26T in the thermal equilibrium state. The polarization degree of D is 3.6115×10^{-4} . With this information, we can estimate the ratio of polarization to signal area.

The area estimation is similar to that we used in relaxation time estimation. But the reference signal is too small to see the peak in one signal, as shown in Fig. 3.15. To decrease the noise level, one has to average some data to find the peak. Since the signal position varies between current increase and current decrease data, the data average was done, respectively, as shown in Fig. 3.16. After averaging some data, the signal is clear to see. So the signal-position shifting can be done in this moment. We found the highest point of the signal, and shifted the peak position to theoretical resonance position. Based on this move, the data with different direction of current sweep can be averaged. The noise level can be reduced more, as shown in Fig. 3.17. The noise level of original data is $1 \sim 5 \times 10^{-3}$. After we averaged 73 data, the noise level decreased to 2.5×10^{-4} . The signal height is around 2×10^{-3} .

There are still two methods for polarization estimation, histogram method and model method. The flow chart of them is shown in figure 3.18.

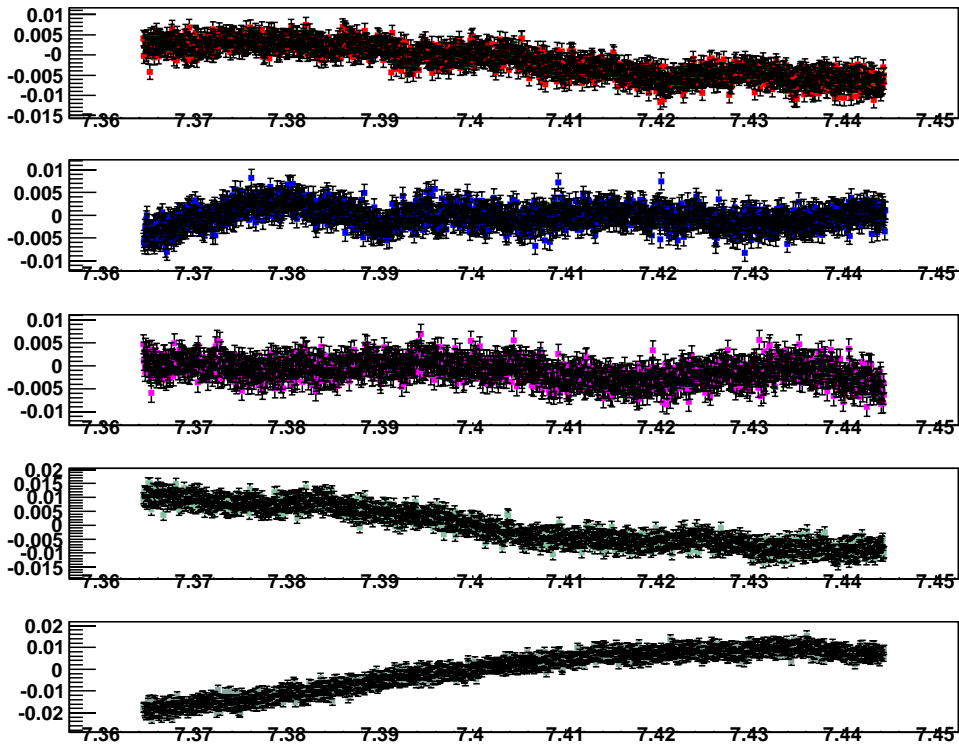


Figure 3.15: These plots show five reference data, and there is no obvious signal. We can not shift the signal position to theoretical resonance position. The noise level of each signal, is around $1 \sim 5 \times 10^{-3}$.

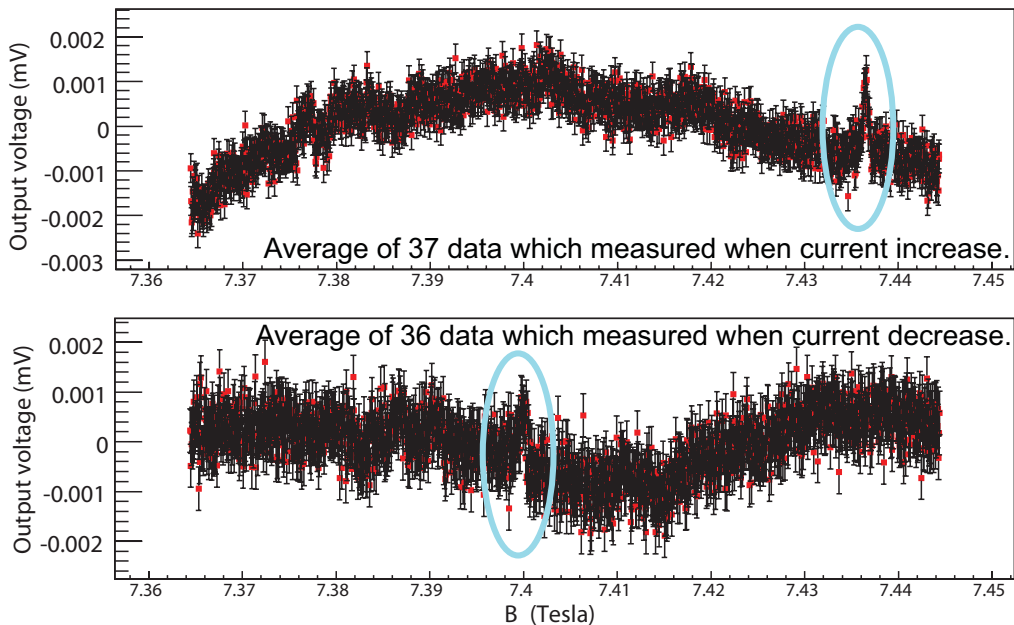


Figure 3.16: After we averaged some data, a clear signal appeared. Data average can decrease the noise level. Figures show that average of 37 data which measured when current increase and average of 36 data which measured when current decrease. We found the the highest point of the signal, and shifted the the peak position to theoretical resonance position. By this way, one can take an average of 73 data and decrease noise level again.

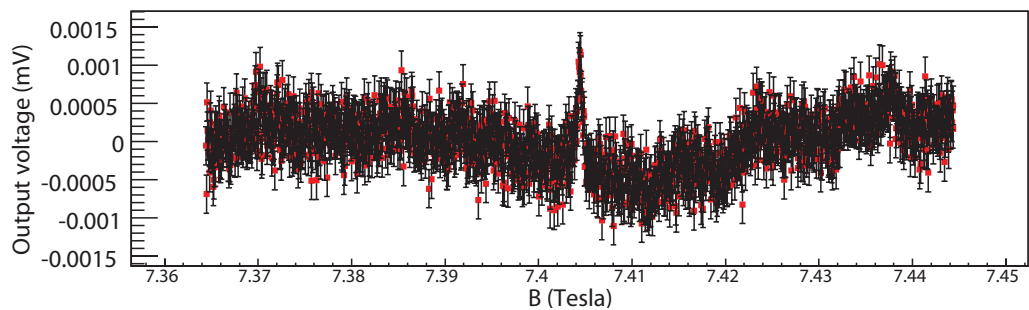


Figure 3.17: After we averaged 73 data, a clear peak appeared. The noise level decreased to 2.5×10^{-4} . The signal height is around 2×10^{-3} .

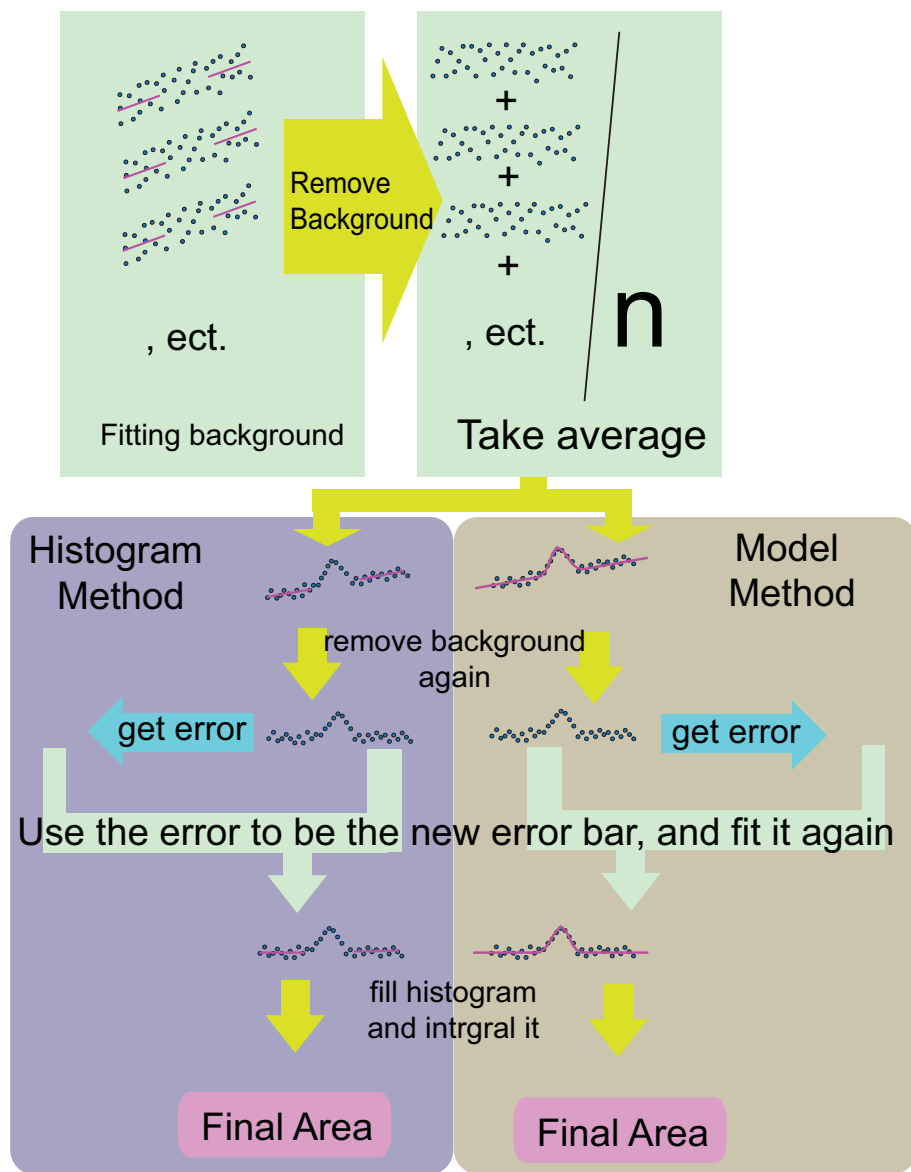


Figure 3.18: Flow chart of polarization estimate

3.4.1 Histogram Method

The histogram method of polarization estimation is almost same as the histogram method of relaxation time estimation, which is shown in 3.3.1. The difference is just the timing of peak-position shifting. Thus the small peak deviation is included in the signal shape and the signal width is wider than the normal one. The background part is same as the background part of histogram method of relaxation time estimation. This choice is a little bit biased, because of the signal width is wider. That is the reason that why we need the model method to confirm the result.

3.4.2 Model Method

The small peak deviation is included in the signal shape and the signal width is wider than the normal one. The model, which works well in model method of relaxation estimation, does not work well now (Figure 3.19). The small peak deviation should be considered. Assuming that the peak deviation is a Gaussian function, a new parameter, which is sigma of peak deviation, is added to the fitting (Figure 3.20). Since four parameters are too many for fitting and the most important is sigma finding, this fitting is done in a small range first. After the sigma was determined, a new model, taking into account peak deviation, is produced. The production diagram of new model is shown in Fig. 3.21. Using the new model with the deviation, we can do fitting again. At this moment, the background part is also under consideration.

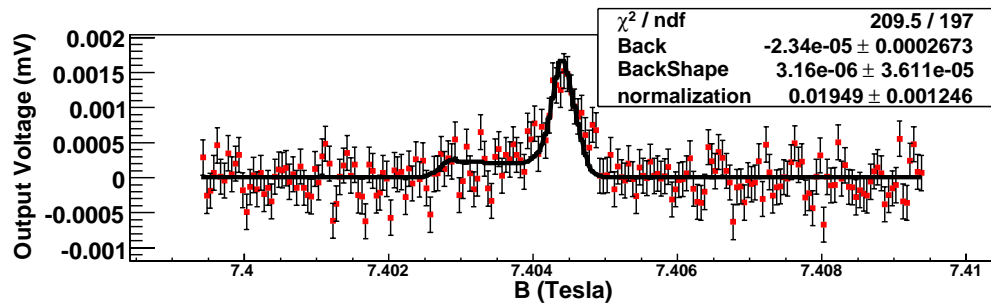


Figure 3.19: The small peak deviation is included in the signal shape and the signal width is wider than the normal one. The model, which works well in model method of relaxation estimation, not works well now. The small peak deviation should be under consideration.

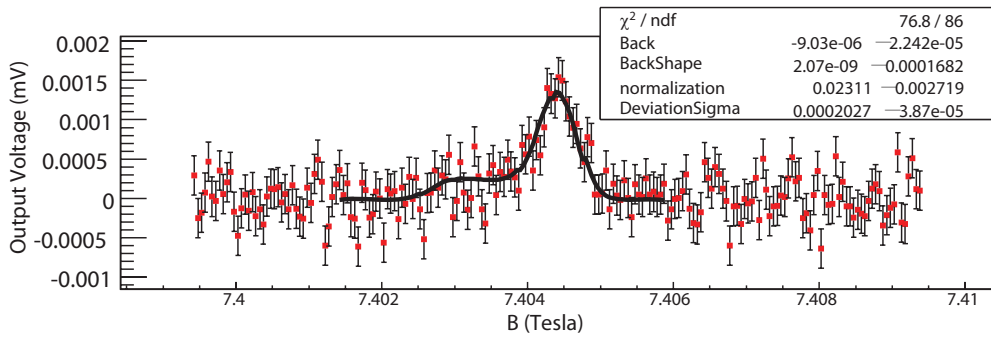


Figure 3.20: The new parameter, which is sigma of peak deviation, is added to the fitting. Since four parameters is too many for fitting and the most important is sigma finding, this fitting is done in small range first. After the sigma was got, a new model, under consideration about peak deviation, will be produced

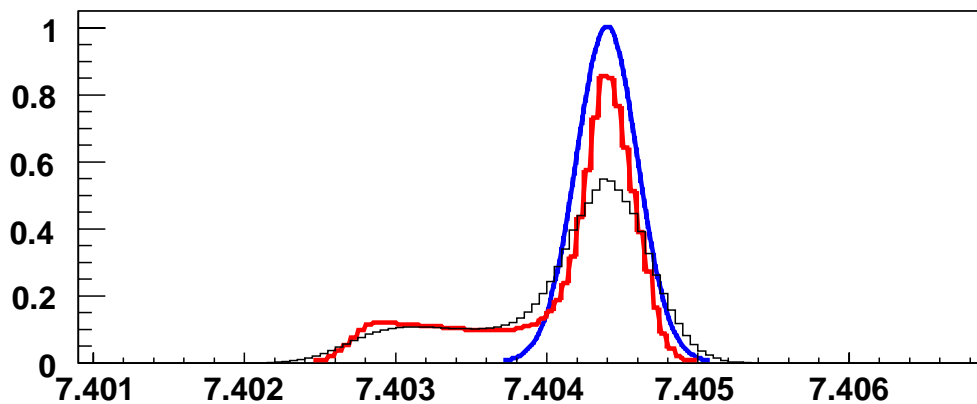


Figure 3.21: The blue shape is a Gaussian shape with the sigma which is got from fitting. The red shape is original model. If the peak position have a deviation as the Gaussian shape, the black shape will be observe. For easy to imagine, the original model and the new model are ten times of the one we really used.

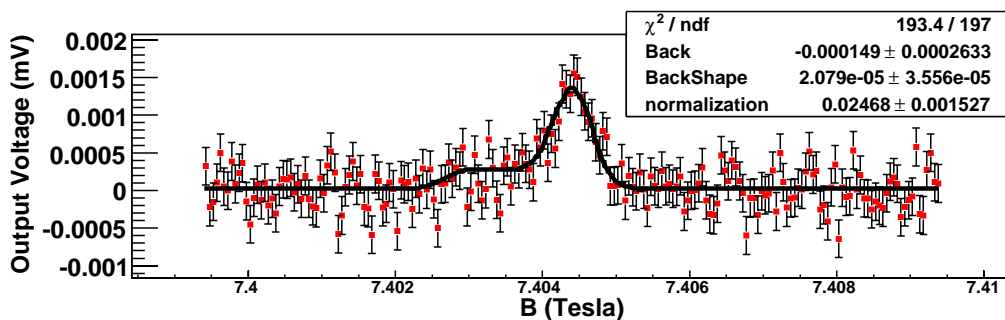


Figure 3.22: Use the new model with the deviation, we can do fitting again with signal and background part.

Chapter 4

Result and Discussion

4.1 Relaxation Time Extracting

As discussed in section 3.3, there are two methods for extracting of relaxation time (T_1). There are three environments of refrigerators that we want to check. These are IBC, SC and TC (included TC1 and TC2). The T_1 is estimate by Eq.3.4. The fitting of all kinds of environments in both methods for H and D are shown in Fig 4.1 ~ Fig 4.5. And the detail about the area of estimation of all the data point is shown in appendix B. All results of T_1 measured are summarized in Table. 4.1.

The result of D shows that two kinds of methods with good consistency. The result of H shows bad consistency. The whole area estimations of relaxation time are placed in the Appendix. B. The model method is not good for big signal. With the model method, compare with the height of the big signal, such like the H signal, the error is too small, so that the chi-square is too large. The fitting can be found not perfect even by eyes, such as Fig. B.71. On the other hand, the H signal shape is not good for model method. There are some unexpected structure included in the H signal shape, such as different direction of current sweeping and background signal from empty cell. Nevertheless, we use histogram method for estimation of signal area. The model method is good for checking the results, especially for the small signals.

| Method | | Histogram Method | | Model Method | |
|-------------------|----------------|------------------|-------------|--------------|-------------|
| Nuclear | Staying time | T_1 of H | T_1 of D | T_1 of H | T_1 of D |
| IBC (0.3K, 1.08T) | about 3 months | 2546±380[22] | 1741±167.6 | 2546±380[22] | 1907± 273.5 |
| SC (1.2K, 1.08T) | 3 hours | 281.2±25.59 | 302.6±28.55 | 237.5±12.75 | 290.1±44.2 |
| TC (4.2K, 0.15T) | 0.5 hours | 147.3±3.8 | 47.8±5.5 | 141.4±2.5 | 44.0±4.6 |

Table 4.1: The HD target staying time and relaxation time in each refrigerator. The unit of T_1 is hour. The T_1 of H in IBC condition is cited from Ref. [22].

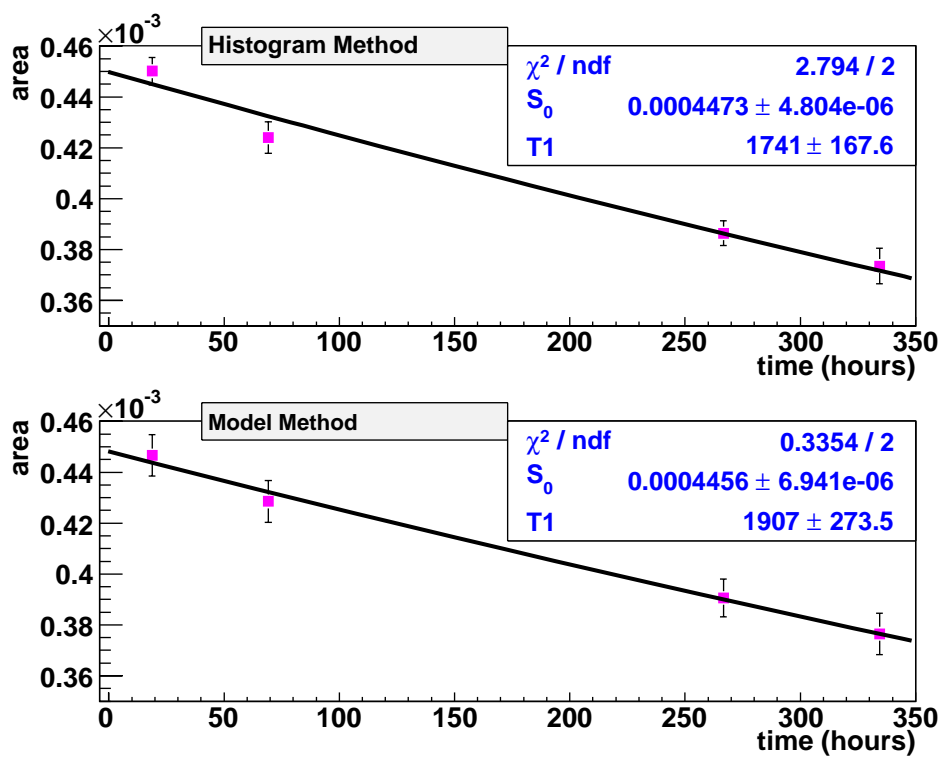


Figure 4.1: Extracting the relaxation time of D at IBC environment with two methods.

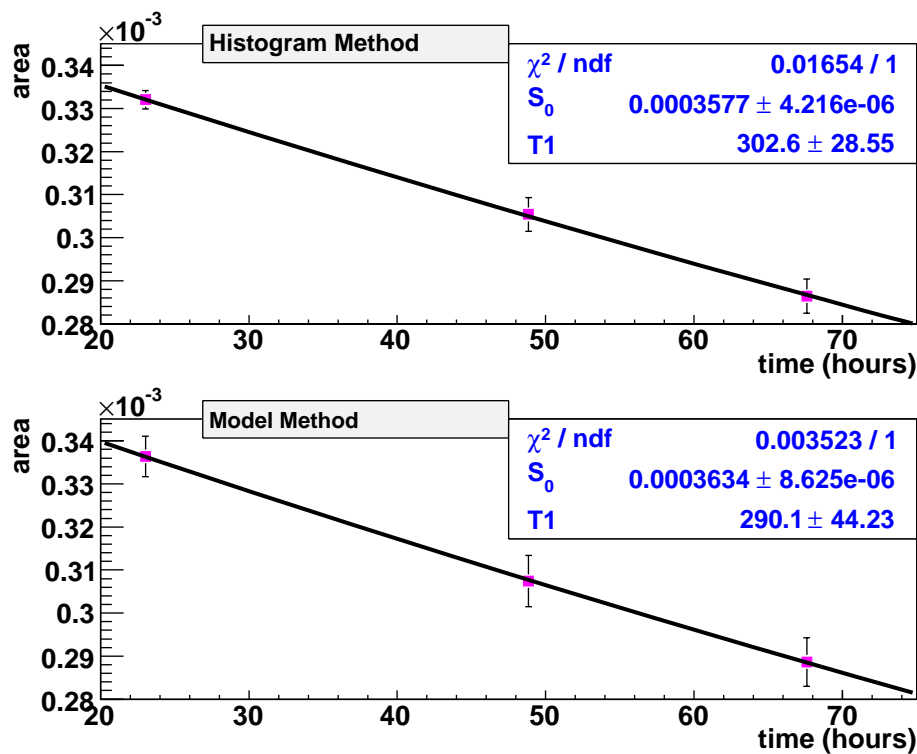


Figure 4.2: Extracting the relaxation time of D at SC environment with two methods.

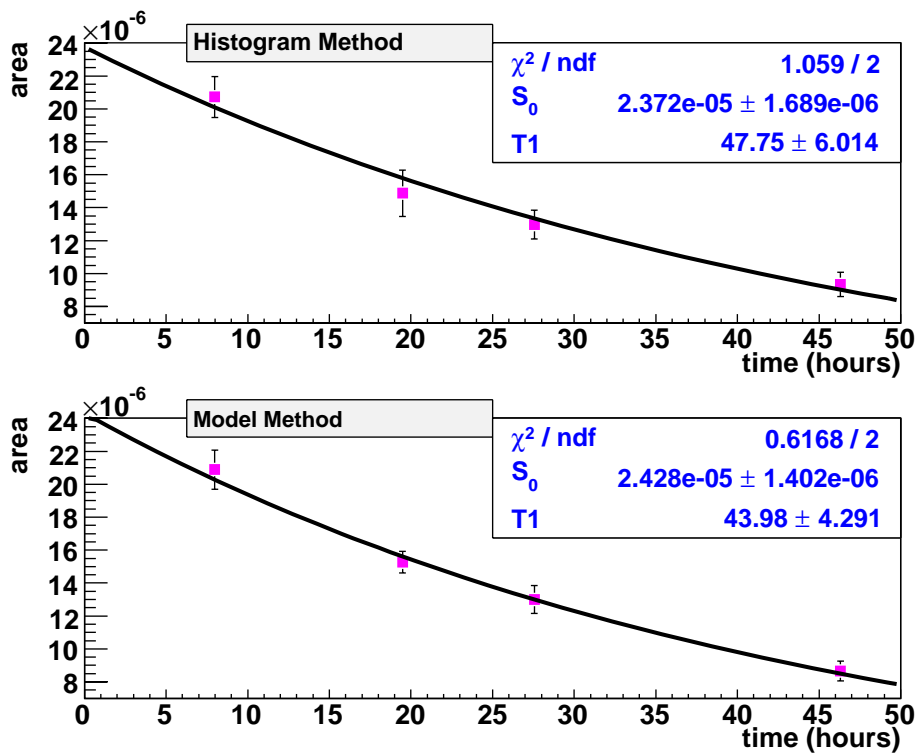


Figure 4.3: Extracting the relaxation time of D at TC environment with two methods.

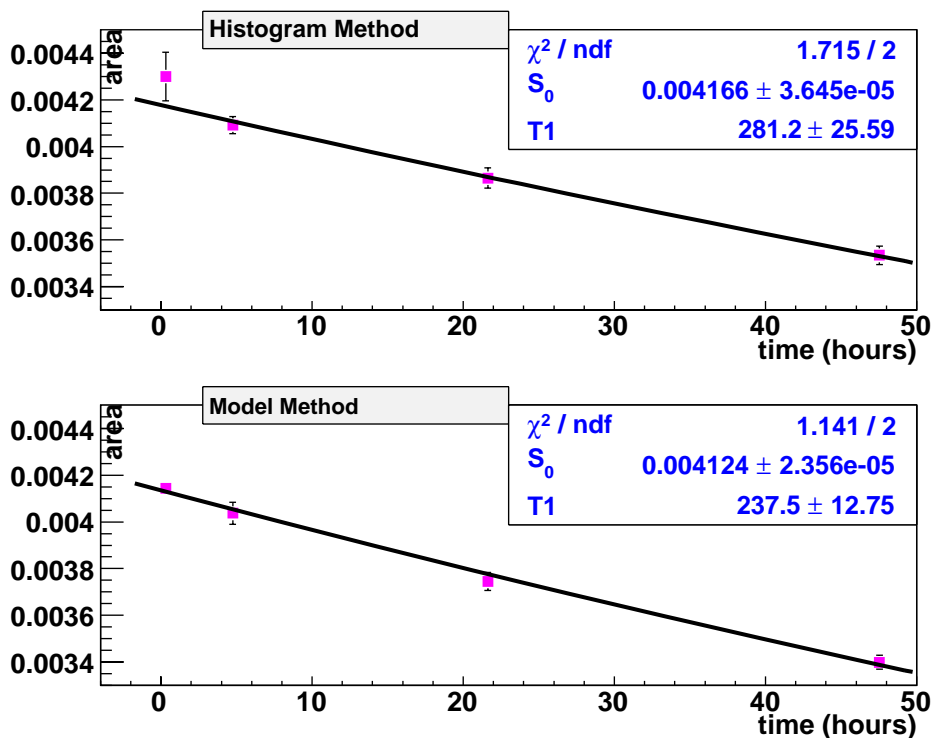


Figure 4.4: Extracting the relaxation time of H at SC environment with two methods.

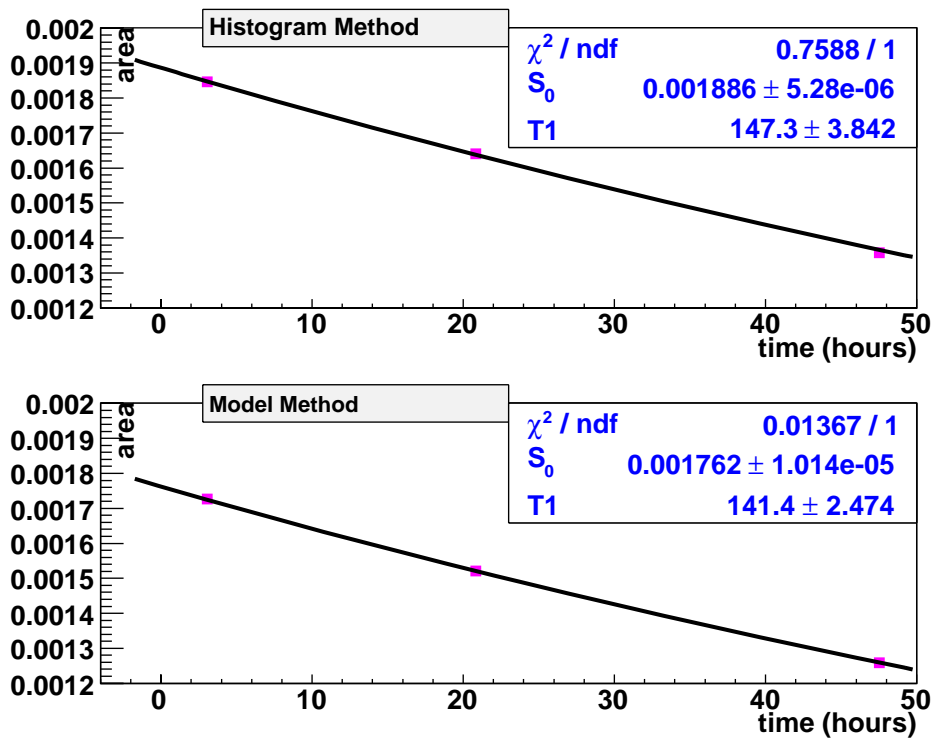


Figure 4.5: Extracting the relaxation time of H at TC environment with two methods.

4.2 Polarization Extracting

As discussed in section 3.4, when we extracted polarization degree of D, there are two methods, histogram method and model method, to estimate the signal area. Fig. 4.6 and Fig. 4.7 show the area estimation of reference signal by histogram method. Fig. 4.8 and Fig. 4.9 show the area estimation of reference signal by model method. The polarization of reference signal can be estimated easily by the Boltzmann law. About the signal area when we just finish the aging, we can figure it out when we estimate the relaxation time, as shown as the S_0 in Fig. 4.1. After the area of reference signal is known, we can estimate the polarization of H and D by the Eq. 4.1. At the same time, the error of the polarization can be estimate by Eq. 4.2. The polarization of H is written in Ref. [22]. This study focuses on the polarization of D.

$$P_{init} = \frac{P_{ref} \times A_{init}}{A_{ref}} \quad (4.1)$$

$$E_{P_{init}} = P_{init} \times \sqrt{\left(\frac{E_{A_{init}}}{A_{init}}\right)^2 + \left(\frac{E_{A_{ref}}}{A_{ref}}\right)^2} \quad (4.2)$$

When we extracted relaxation time (T_1), there are two methods, histogram method and model method, to estimate the signal area. When we extracted polarization degree of D, there are also two method to estimate the signal area. Therefore, there are four kinds of results of polarization degree, as shown in Table. 4.2. They are consistent.

| Ref Method | Histogram | Model |
|----------------------------------|-----------------------------------|----------------------------------|
| A_{ref} | $(1.18 \pm 0.35) \times 10^{-6}$ | $(1.23 \pm 0.18) \times 10^{-6}$ |
| P_{ref} | $(3.6115) \times 10^{-4}$ | |
| A_{init} from Histogram Method | $(4.473 \pm 0.05) \times 10^{-4}$ | |
| A_{init} from Model Method | $(4.456 \pm 0.07) \times 10^{-4}$ | |
| P_{init} from Histogram Method | $13.69 \pm 4.06\%$ | $13.13 \pm 1.93\%$ |
| P_{init} from Model Method | $13.64 \pm 4.07\%$ | $13.08 \pm 1.93\%$ |

Table 4.2: When we extracted relaxation time, there are two methods to estimate the signal area. When we extracted polarization degree of D, there are also two methods to estimate the signal area. Therefore, there are four kinds of results of polarization degree. They are consistent.

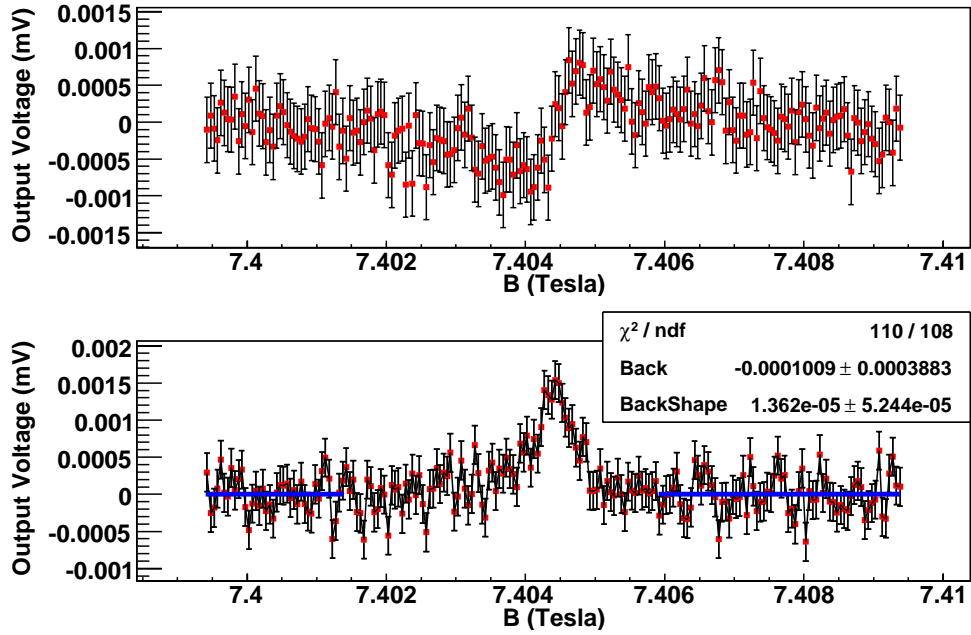


Figure 4.6: Get the background of reference signal from fitting. (Histogram method)

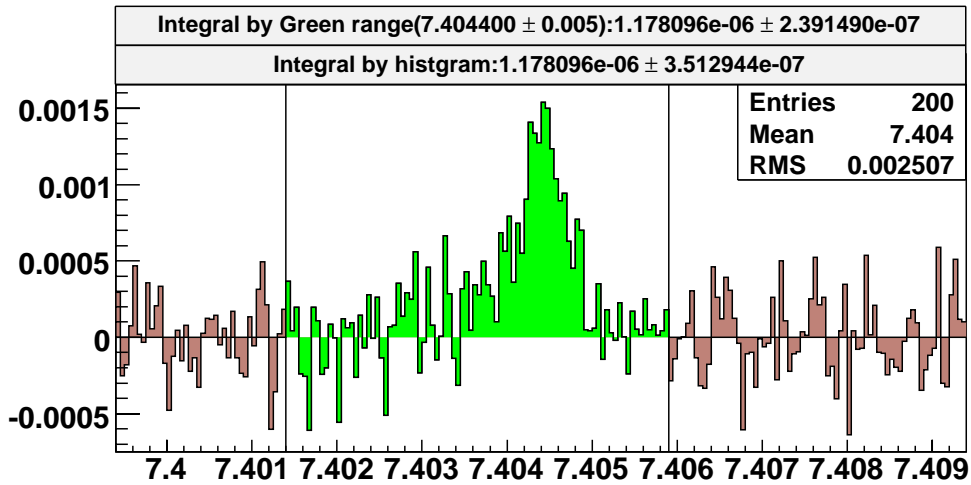


Figure 4.7: After removing the background, fill a histogram to estimate the area of reference signal. (Histogram method)

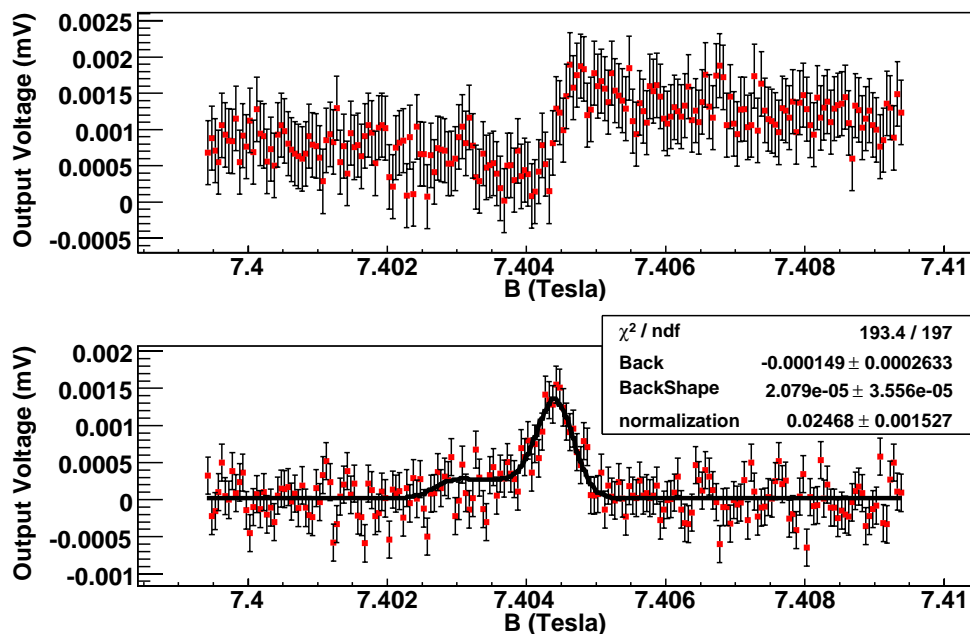


Figure 4.8: Fit the reference signal by the D signal model where signal deviation is taken into account. Background of this signal is also estimated by this fitting. (Model method)

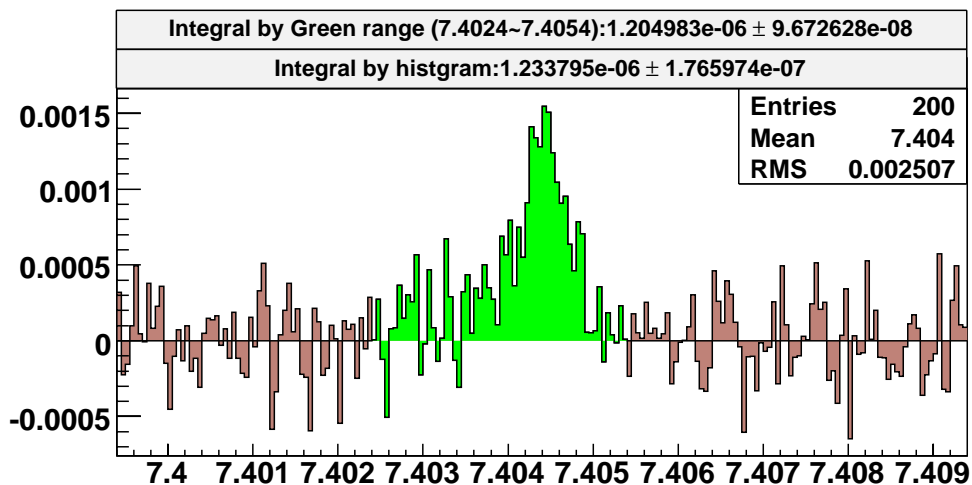


Figure 4.9: After fitting by the model to get the background, fill a histogram to estimate the area of reference signal.(Model method)

4.3 Conclusion

As we talked in section 4.1, the model method is good for small signals. The D signal is not very larger than the error of signal and the chi-square is not so bad. Histogram method and model method are also consistent. Since the most important thing in the histogram method is to design the background part, the histogram method is not good in too small signal with bigger background. When we estimate the area of reference signal, the background is too big. This is also the reason why we take average of many signals to see the peak.

In the estimation of relaxation time, there are both H and D estimation, and there are big signals and small signals, but there is no such a small signal like the reference signal. To unify the estimation of relaxation time, the histogram method is hired. In the estimation of D polarization, the reference signal is too small to use the histogram method, so that the model method is hired.

Just remind reader again, two methods are consistent in D signal. The Table. 4.3 shows the final result.

| After 53 days aging | P_H | P_D | |
|---------------------|--------------|-------------|----------------|
| | 41.4±3.10% | 13.13±1.93% | |
| | T_1 of H | T_1 of D | Staying time |
| IBC (0.3K, 1.08T) | 2546±380[22] | 1741±167.6 | about 3 months |
| SC (1.2K, 1.08T) | 276.6±22.9 | 302.6±28.6 | 3 hours |
| TC (4.2K, 0.15T) | 147.3±3.8 | 47.8±5.5 | 0.5 hours |

Table 4.3: The HD target staying time and relaxation time in each refrigerator. The unit of T_1 is hour. The T_1 of H in IBC condition is cited from Ref. [22].

By taking account of HD target staying time and T_1 in each refrigerator, if the initial polarization is assumed to be 100%, the H polarization becomes 98% and D polarization becomes 97% after moving the HD target from RCNP to SPring-8/LEPS. These results show that the relaxation times are long enough for loss of polarization during transportation. We plan to start a production of HD and move it to SPring-8/LEPS and carry out a performance check by using circularly polarized photon beams in 2010 [23].

4.4 Discussion and the Future

4.4.1 Study of Aging Time

At IPN Orsay, they have studied the relation between concentration of o-H₂ and the relaxation time of H, as shown in Fig. 1.5. Now we just add the PHYDES data points into Fig. 1.5, as shown in Fig. 4.10. The conversion of aging time of PHYDES data is done by taking account into the concentration of o-H₂. For each condition, there is only one point and there is no same condition with IPN Orsay data. It is difficult to say anything of the result. Up to now, the results are reasonable; at least, higher magnetic field or lower temperature causes longer relaxation time. In the future, PHYDES will get more data points to study the relation between concentration of o-H₂ and the relaxation time of H.

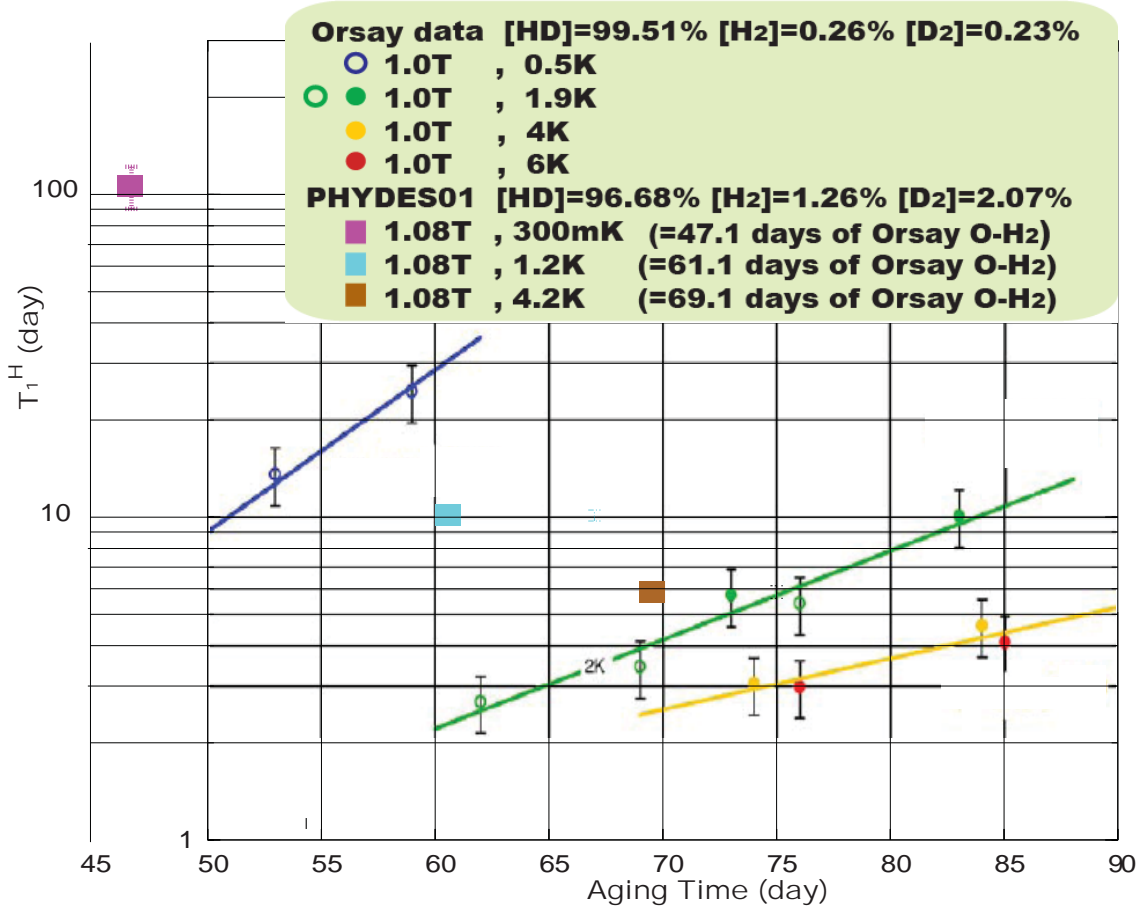


Figure 4.10: Add the PHYDES data points into IPN Orsay data. The conversion of aging time of PHYDES data is done by taking account into the concentration of o-H₂. Up to now the results are reasonable. The higher magnetic field or lower temperature causes longer relaxation time.

4.4.2 Lower Polarization

The polarization degrees measured are much lower than those expected from the thermal equilibrium state of the aging condition.

Bad Linearity of the NMR Signal Height

Non-linear relation between the NMR signal height and the polarization degree is considered to be a main source of the low polarization degree. We assumed the linear relation between the polarization degree and the area of the NMR spectra, and the polarization degree was obtained as about $P_H = 41\%$ and $P_D = 13\%$. Since the polarization degree expected by the aging process is about $P_H = 85\%$ and $P_D = 25\%$, the polarization obtained is much smaller than the expectation. We think that bad linearity of the NMR signal height might cause the small polarization degree and actual polarization degree should be higher than 41%.

Since LEGS collaboration, which also developed the polarized HD target, obtained a polarization degree of about 60%, we expect that we can also achieve at least the same polarization degree after some improvements. We are improving the

NMR system to correctly measure the polarization now [23].

Improvement of Thermal Conduction

That the temperature of the HD target stored in the cell might not be low enough will generate Kapitza resistance between the Al wires and the copper or by contact between the lead cable and the outer shield [24]. We are going to make a new target cell with high purity Al wires.

And also we are developing the single crystal HD target. Single crystal of HD have a structure in which the hexagonal para-hydrogen layers are banked up. The thermal conductivity along the layer is much better than that of polycrystal HD. When the direction of heat conduction from HD to cold stage align along the layer of single crystal HD, we can get good thermal conductivity.

4.4.3 NMR Measurement

Frequency Sweeping or Magnetic Field Sweeping

As discussed in section 2.3.2, the cancellation circuit only can cancel signal with selected frequency; therefore during the NMR measurement, the frequency sweeping is out of the question. On the other hand, the whole NMR circuit is related to frequency. Even cancellation circuit is not employed, the frequency sweeping will produce unexpected noise.

Nevertheless, the magnetic field sweeping will generate heat. Since the gyromagnetic ratio of H is about seven times of gyromagnetic ratio of D. If the Larmor frequency is fixed, the magnetic field for D NMR measurement is about seven times of the magnetic field for H NMR measurement. In case of PHYDES01, the magnetic field for D NMR measurement is about 7T and the magnetic field for H NMR measurement is about 1T. There are three shortcomings of magnetic field sweeping:

- 1:** For sweeping magnetic field, one need to break superconductor-state of magnet, and turn the magnet to drive-state. It waste a lot of liquid helium.
- 2:** If both polarization of D and H are measured, the magnetic field sweep from 1T to 7T will generate a lot of heat and waste a lot of liquid helium.
- 3:** The significant change of magnetic field, makes the polarization of HD unstable.

The shortcoming **1** can not be avoided if the magnetic field sweeping is selected. But the shortcoming **2** and **3** can be avoided easily by designing a new cancellation circuit. If we separate the cancellation circuits of H and D, the significant change of magnetic field can be avoided. We are working on this subject now.

4.4.4 Improvement of D Polarization

Forbidden Adiabatic Fast Passage (FAFP) and Saturated Forbidden Transition (SFT)

The Forbidden Adiabatic Fast Passage (FAFP) and Saturated Forbidden Transition (SFT) are well known methods to reverse nuclear magnetization of a material [16, 17, 12]. One can use an RF transition between H and D to exchange spin. This transition is forbidden in the same molecule, but it is possible between H and D.

The difference between FAFP and SFT is the RF power. The SFT using the small RF power to exchange spin.

The Fig. 4.11 shows the time line of SFP from LEGS group [25]. When the concentration of $o\text{-H}_2$ is still high, the relaxation of H from HD is short. One can increase the polarization of H fast. Once the polarization of H high enough, one can do the SFP to exchange spin. In SFT, the H polarization decrease to same as the D polarization. To take advantage of the still high concentration of $o\text{-H}_2$ (still short relaxation time of H), one can do the second SFP. After the second SFT, the relaxation time of H may be not long enough to do SFT again. Then, one can just start aging, and finally HD target with the both high polarization of H and D. The polarizations of H and D are independent. If polarization of H is the focus, the SFT can be skipped with the aging only. If polarization of D is what is desired, the aging can be skipped with the SFT only.

However, to use FAFP or SFT, there are some difficulty for PHYDES now:

- 1: The concentration of $o\text{-H}_2$ can not be handled easily now.
- 2: The concentration of $p\text{-D}_2$ could decrease the relaxation time of D. If one wants to keep the D polarization after FAFP, the concentration of $p\text{-D}_2$ should be very low. The concentration of $p\text{-D}_2$ can not be handled easily now.
- 3: The amount of heat depends on the amounts of HD and RF power. If the RF power is not high enough, the FAFP efficiency will be bad. In case of 1 mole HD in LEGS group, if they use enough RF power to do FAFP, it generates too much heat, and keeping temperature will be difficult. So that they select the SFT [26].
- 4: The relation between concentration of $o\text{-H}_2$ and the relaxation time of H is not well known enough; therefore it is difficult to select the best timing to do FAFP.

Now we are developing the new distillator to improve purification. A good distillator can help us to control the concentration of $o\text{-H}_2$ and $p\text{-D}_2$ more easily.

About the heat problem, if we are in this situation, we can just use the Saturated Forbidden Transition (SFT). The SFT uses the small RF power to exchange spin.

The work of PHYDES01 helps us to study more about the relation between concentration of $o\text{-H}_2$ and the relaxation time of H. In the future, the new HD target will provide us more information about the relation. All of problems could be solved with more study and preparation, there is no doubt that improvement of D polarization is expected in our next step.

4.4.5 From Success of Polarized HD Target to Using the Polarized HD Target in LEPS Experiment

Even the production of polarized HD target succeeded, before we can start physics experiments using the polarized HD target at SPring-8/LEPS, there are still many subjects to work on:

- 1: The HD target system can be installed in the LEPS experiment hutch.
- 2: The HD target can be safely transferred from RCNP to SPring-8/LEPS.

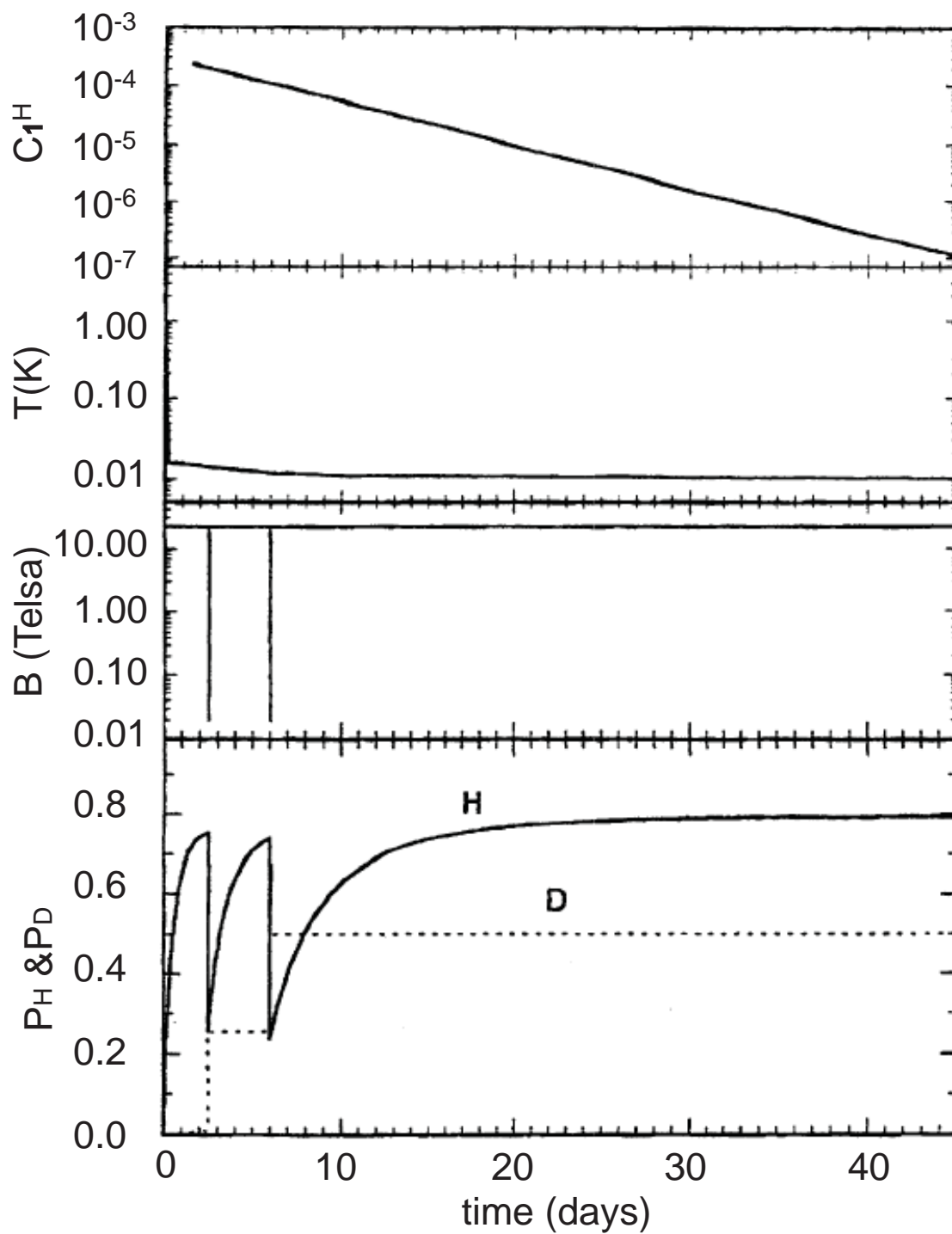


Figure 4.11: The time line of SFT from LEPS group [25]. C_1^H is the concentration of o- H_2 . In the bottom figure, the H and D polarization are shown as the solid and the dotted curves.

- 3:** The polarization of the HD target can be kept when the photon beams of ~ 1 M γ 's/s hit the target.
- 4:** Trigger rate for data taking is acceptable.

We planed to carry out an experiment for 10 days. In the experiment, the performance of the polarized HD target will be checked. Since the relaxation time is expected to be long (more than 100 days after 3 months aging), at least 10 days is needed for proper measurement. [23]

4.5 Summary

The polarized Hydrogen-Deuteride (HD) target is developed mainly for the study of ϕ meson photoproduction on the proton and neutron. Using the polarized target, one can measure double polarization asymmetries to study $s\bar{s}$ -content in the nucleon.

We produced a polarized HD target for the first time in 2008. After the aging time of 53 days at 17 Tesla and at 14 mK, the polarization degree (P) and the relaxation time (T_1) of the hydrogen (H) and deuterium (D) in the HD were measured by using the NMR method as shown in the Table.

| After 53 days aging | P_H | P_D | |
|---------------------|--------------|------------|----------------|
| | 41.4±3.1% | 13.1±1.9% | |
| | T_1 of H | T_1 of D | Staying time |
| IBC (0.3K, 1.08T) | 2546[22]±380 | 1741±167.6 | about 3 months |
| SC (1.2K, 1.08T) | 276.6±22.9 | 302.6±28.6 | 3 hours |
| TC (4.2K, 0.15T) | 147.3±3.8 | 47.8±5.5 | 0.5 hours |

Table 4.4: The HD target staying time and relaxation time in each refrigerator. The unit of T_1 is hour. The T_1 of H in IBC condition is cited from Ref [22].

The polarization degrees measured are much lower than those expected from the thermal equilibrium state of the aging condition. Non-linear relation between the NMR signal height and the polarization degree is considered to be the main source of the low polarization degree. The relaxation time in the SC and TC condition are found to be long enough for the need of staying time during the transportation of the HD target. The relaxation time in the IBC condition is also long enough to produce the other new polarized HD target for replacement in continuous experiments.

We plan to start production of HD and move it to SPring-8/LEPS and carry out a performance check by using circularly polarized photon beams in 2010.

Chapter 5

Summary

A polarized Hydrogen-Deuteride (HD) target has been developed mainly for the study of ϕ meson photoproduction on the proton and neutron. Using the polarized target, one can measure double polarization asymmetries to study $s\bar{s}$ -content in the nucleon.

We produced a polarized HD target for the first time in 2008. The reference data of H (B=1T, T=4.2K) and D (B=7T, T=4.2K) at thermal equilibrium state were measured. The T_1 was obtained by fitting the function, $A(t) = A(0) \exp(-t/T_1)$. After the aging time of 53 days at 17 Tesla and at 14 mK, the polarization degree (P) and the relaxation time (T_1) of the hydrogen (H) and deuterium (D) in the HD were measured.

The polarization degrees measured are much lower than those expected from the thermal equilibrium state of the aging condition. Non-linear relation between the NMR signal height and the polarization degree is considered to be the main source of the low polarization degree.

The relaxation time in the SC and TC condition are found to be long enough for the need of staying time during the transportation of the HD target. The relaxation time in the IBC condition is also long enough to produce the other new polarized HD target for replacement in continuous experiments. The relaxation times of IBC are long enough for loss of polarization during experiment of ϕ meson photoproduction.

We planed to start production of HD and move it to SPring-8/LEPS and carry out an experiment in 2010. In the experiment, the performance of the polarized HD target will be checked.

Bibliography

- [1] D. Adams *et al.*, Phys. Lett. B329, 399 (1994).
- [2] K. Abe *et al.*, Phys. Rev. Lett. 74, 346 (1995).
- [3] L.A. Ahrens *et al.*, Phys. Rev. D 35, 785 (1987).
- [4] J.F. Donoghue and C.R. Nappi, Phys. Lett. B168, 105 (1986).
- [5] A. Bertin *et al.*, Phys. Lett. B388, 450 (1996).
- [6] D.S. Armstrong *et al.*, Phys. Rev. Lett. 95, 092001 (2005).
- [7] A. Acha *et al.*, Phys. Rev. Lett. 98, 032301 (2007).
- [8] A. Airapetian *et al.*, Phys. Rev. Lett. 92, 012005 (2004).
- [9] A.I. Titov, Y. Oh, and S.N. Yang, Phys. Rev. Lett. 79, 1634 (1997).
- [10] M. Bassan, *et al.*, Nucl. Instr. and Meth. 526 (2004) 163.
- [11] S. Hoblit and A. M. Sandorfi *et al.*, Phys. Rev. Lett., 102,172002 (2009).
- [12] Christopher M.Bade, Doctoral dissertation, the College of Arts and Sciences (2006)
- [13] M. Fujiwara *et al.*, Photoproduction Experiment with Polarized HD Target at SPring-8, LEPS/RCNP proposal (2003).
- [14] A. Honig, Phys. Rev. Lett. 19, 1009 (1967).
- [15] A. Honig and H. Mano, Phys. Rev., 14, 1858 (1976).
- [16] A. Honig *et al.*, Nucl. Instr. and Meth. in Phys. Research, 356, 39 (1995).
- [17] A. Honig *et al.*, Spin96, Proceedings of the 12th Int. Symp. on High-Energy Spin Physics, Amsterdam Sept. 1996, edited by C.W. de Jager *et al.*, in World Scientific, p. 365.
- [18] T. Ohta *et al.*, Annual report of RCNP Osaka university (2006).
- [19] K.R. Jefferey and R.L. Armstrong, Rev. Sci. Instr. 38, 634 (1967).
- [20] D. M. Ginsberg and M. J. Melchener, Rev. Sci. Instrum. 41, 122 (1970).
- [21] T. Kunimatsu *et al.*, Annual report of RCNP Osaka university, 9 (2007).
- [22] C. Morisaki, Master thesis of Osaka university (2009).

- [23] H. Kohri *et al.*, Performance check of the polarized HD target, LEPS/RCNP proposal (2009).
- [24] T. Ohta *et al.*, Annual report of RCNP Osaka university (2009).
- [25] D. Babusci *et al.*, LEGS expt. L18/L19 (1994).
- [26] Tsuneo Kageya, Private communication.
- [27] A. V. Minkin and S. L. Tsarevskii, *The Physics of Metals and Metallography*, 2006, Vol. 101, No. 1, pp. 1-6.

Appendix A

Distortion of NMR Signals

The smallest width of the NMR shape can be estimated from the uncertainty principle, as shown in the Eq. A.1 and Eq. A.2. Where the δE means the uncertainty of energy, and the $\delta\omega$ means the uncertainty of frequency.

$$\delta E \cdot \tau = \hbar \quad (\text{A.1})$$

$$\delta\omega = \frac{\delta E}{\hbar} = \frac{1}{\tau} \quad (\text{A.2})$$

In this case, the shape of NMR signal should be a Gaussian shape. But we can find that there is distortion of the NMR signal, especially for the D signal. About distortion of NMR signal, one has to take three important circumstances into account [27]:

- **1:** The uniformity of the line width.
- **2:** The non-uniformity of the local magnetic field in a superconductor.
- **3:** The specific features of the penetration of an ac microwave magnetic field into a superconductor.

The most likely explanation of the distortion of NMR signals in our experiment is the non-uniformity of the local magnetic field in a superconductor. The Z axis profile map is plot in the manual of superconductor. Fig A.1 shows the definition of Z axis.

We reproduced D and H NMR signals shapes by the simulation. This simulation consider only the non-uniformity of the local magnetic field in a superconductor on Z axis. The non-uniformity of x and y axis are not taken into account. This appendix wants to show reader that the non-uniformity of the local magnetic field is strong enough to distort the NMR shape. The most important point is, “if the NMR signal is distorted by the non-uniformity of the local magnetic field, the signal area won’t be changed.”

At the first, the non-uniformity of the local magnetic field fit by Eq. A.3 and the result is shown in Fig. A.2.

$$B_{real} = B_{center} \cdot (P_4x^4 + P_3x^3 + P_2x^2 + P_1x + P_0) \quad (\text{A.3})$$

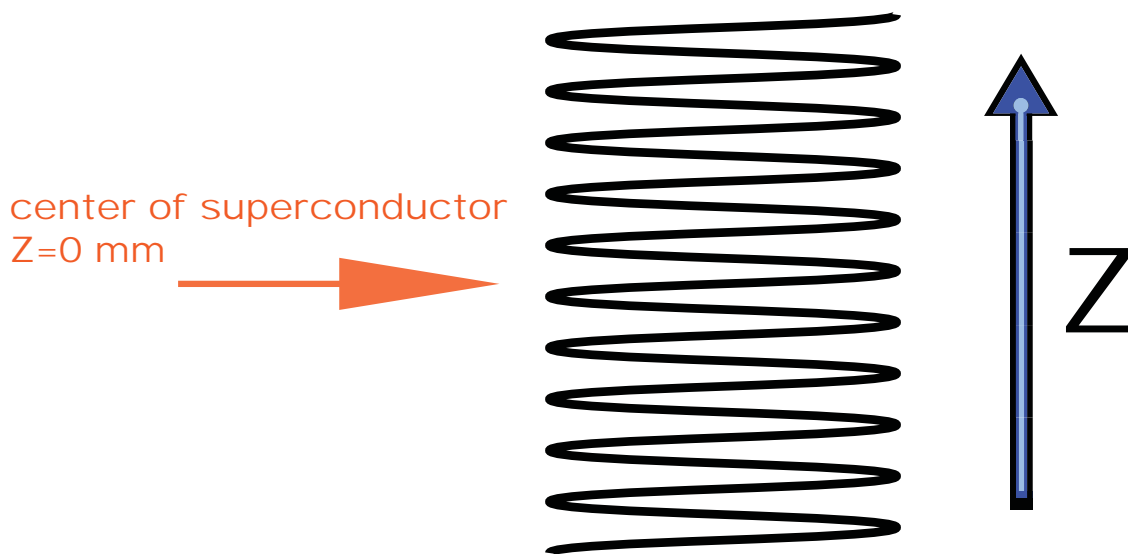


Figure A.1: Definition of z axis in superconductor.

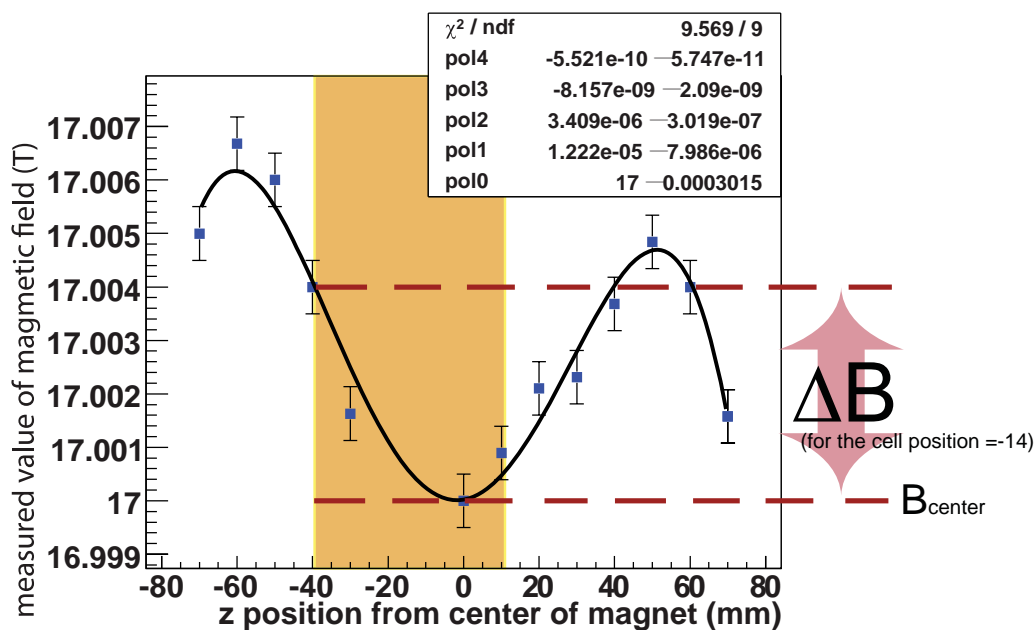


Figure A.2: The fitting of non-uniformity of the local magnetic field. If the position of cell center is -14 cm, the yellow part is the cell position. The maximum of uniformity of magnetic field, ΔB , is proportioned the B_{center} .

When we measure the H signal, we set the superconductor to $B=1.1366\text{T}$. At this moment, the $B_{center}=1.1366\text{T}$. When we measure the D signal, the $B_{center}=7.4044\text{T}$. The maximum of uniformity of magnetic field, ΔB , is proportioned the B_{center} . Therefore the ΔB of D is larger than the ΔB of H. This is the reason why distortion of D is more significant than that of H.

A.1 Simple simulation

Assume that if there is no non-uniformity of the local magnetic field, the NMR shape is a Lorentzian shape. In case of a simple simulation, we set it to be a Gaussian shape, as shown in the top figure in Fig. A.3 and Fig A.5. With taking the non-uniformity of the local magnetic field into account, the D and H signals are simulated by Eq. A.3. The simulations are shown in the bottom figure of Fig A.3 and Fig A.5. The real signals of D and H are shown in Fig A.4 and Fig A.6. In those plots, the signal areas are normalized to be same as the simulation. One can compare the simulation with the real signal. They are not completely same, but the shape and the width is similar.

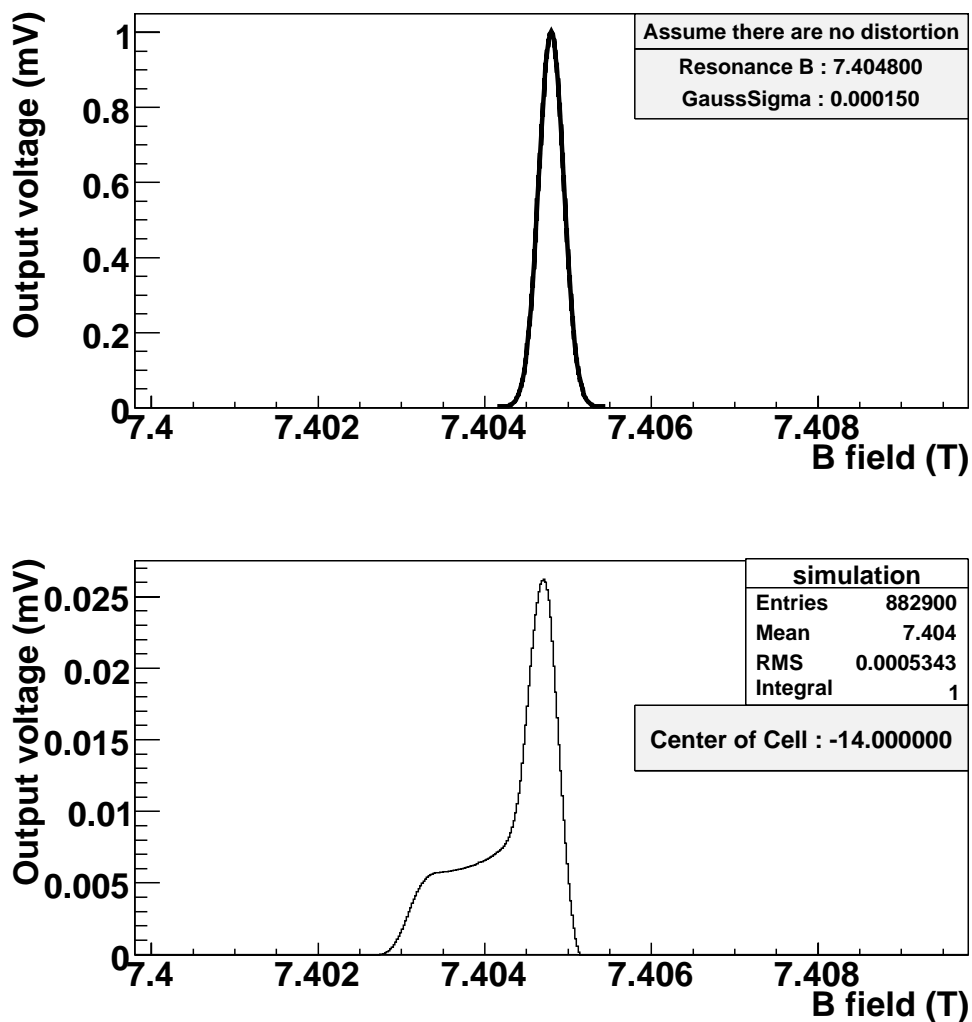


Figure A.3: Assume that if there is no non-uniformity of the local magnetic field, the D NMR shape is a Lorentzian shape. In case of a simple simulation, we set it to be a Gaussian shape, as shown in the top figure. With taking the non-uniformity of the local magnetic field into account, the D signal is simulated by Eq. A.3. The simulation is shown bottom figure.

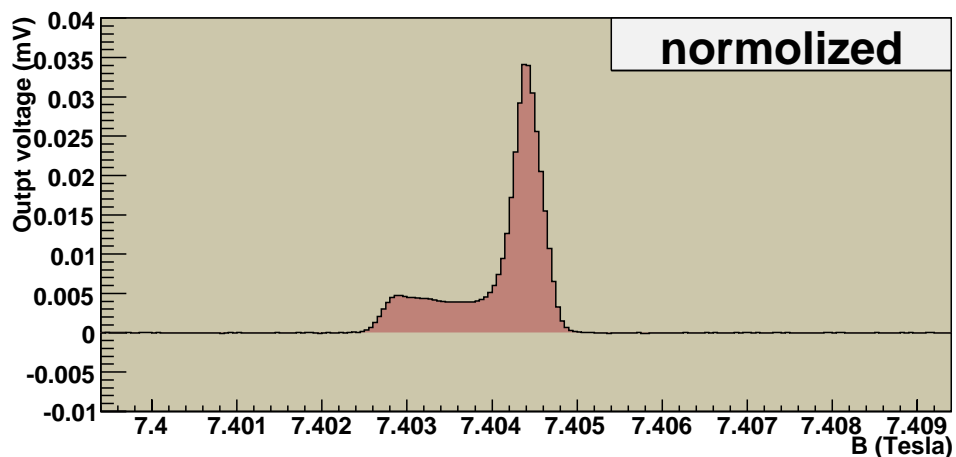


Figure A.4: The real D signal which got from measurement. The signal area is normalized to be same as the simulation.

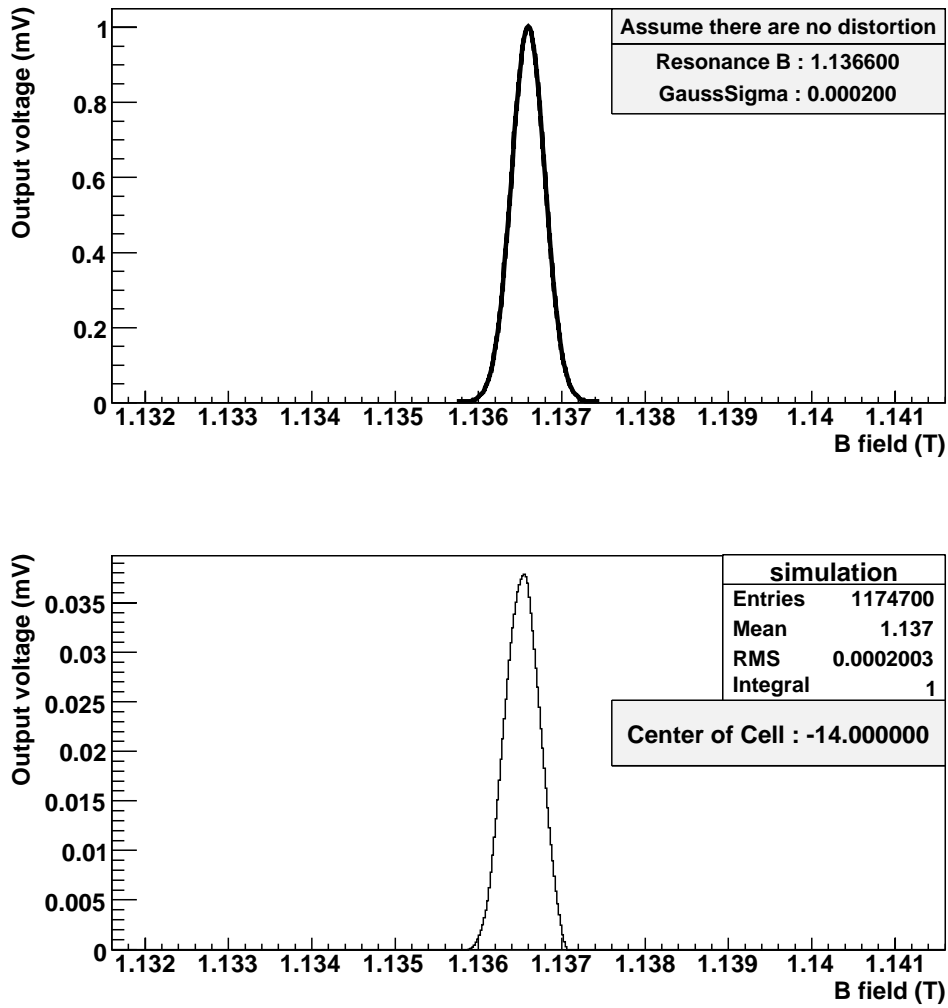


Figure A.5: Assume that if there is no non-uniformity of the local magnetic field, the H NMR shape is a Lorentzian shape. In case of a simple simulation, we set it to be a Gaussian shape, as shown in the top figure. With taking the non-uniformity of the local magnetic field into account, the H signal is simulated by Eq. A.3. The simulation is shown bottom figure.

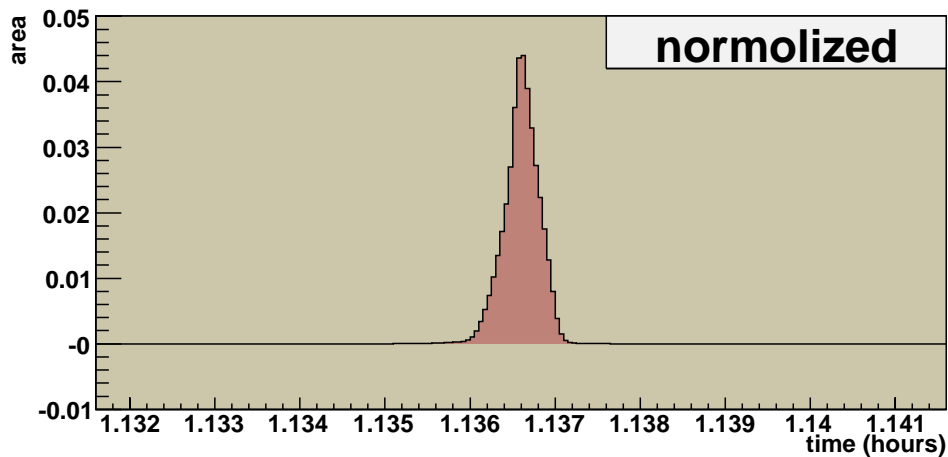


Figure A.6: The real H signal which got from measurement. The signal area is normalized to be same as the simulation.

A.2 Advanced Simulation

There are some questionable points in the simple simulation. First, the target cell length of PHYDES01 may not 50 mm. In normal case, one mole HD is put in empty cell; if the HD filled tight, the cell length is 50 mm. In case of PHYDES01, there is only 0.68 mole HD; therefore the cell length may only 34mm if the HD filled tight. It is also possible that the HD did not filled tight, so that the possible cell length is from 34 mm to 80 mm, where the 80 mm the the length of Al wires. Second, the cell position of -14 cm may be not the best choice. There are a new simulation which decide the cell position and cell length be fitting the simulation result with the real data, as shown in Fig. A.7. This result shows the most likely cell position around -14 cm and cell length around 46 mm. But the simulation result is not very fit to the real signal; therefore the chi-square is large. The “most likely” result is not so trusty.

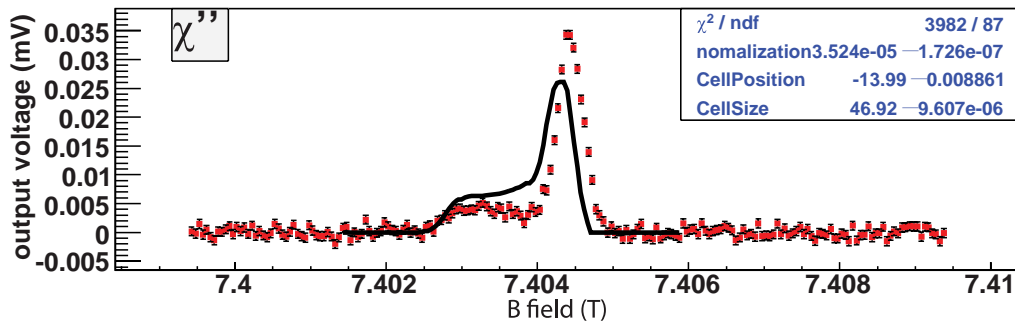


Figure A.7: This simulation decide the cell position and cell length be fitting the simulation result with the real data

A.3 Conclusion

Just reminding reader again, this simulation is rather naive, because it consider only the non-uniformity of the local magnetic field in a superconductor on Z axis. There are still other causes of the distortion, such as the non-uniformity of the local magnetic field in a superconductor on X and Y axis. But this study can help us to understand that even the non-uniformity of the local magnetic field is small ($\sim 10^{-3} Tesla$), it can modify the NMR signal significantly. Fortunately, any distortion from non-uniformity of the magnetic field cannot change the signal area. The signal area is still proportional to the polarization.

Appendix B

Detail of Relaxation Time Fitting

The following pictures show an estimation of the area of D signal at IBC environment with the histogram method. The current-increasing data and current-decreasing data are analyzed, respectively.



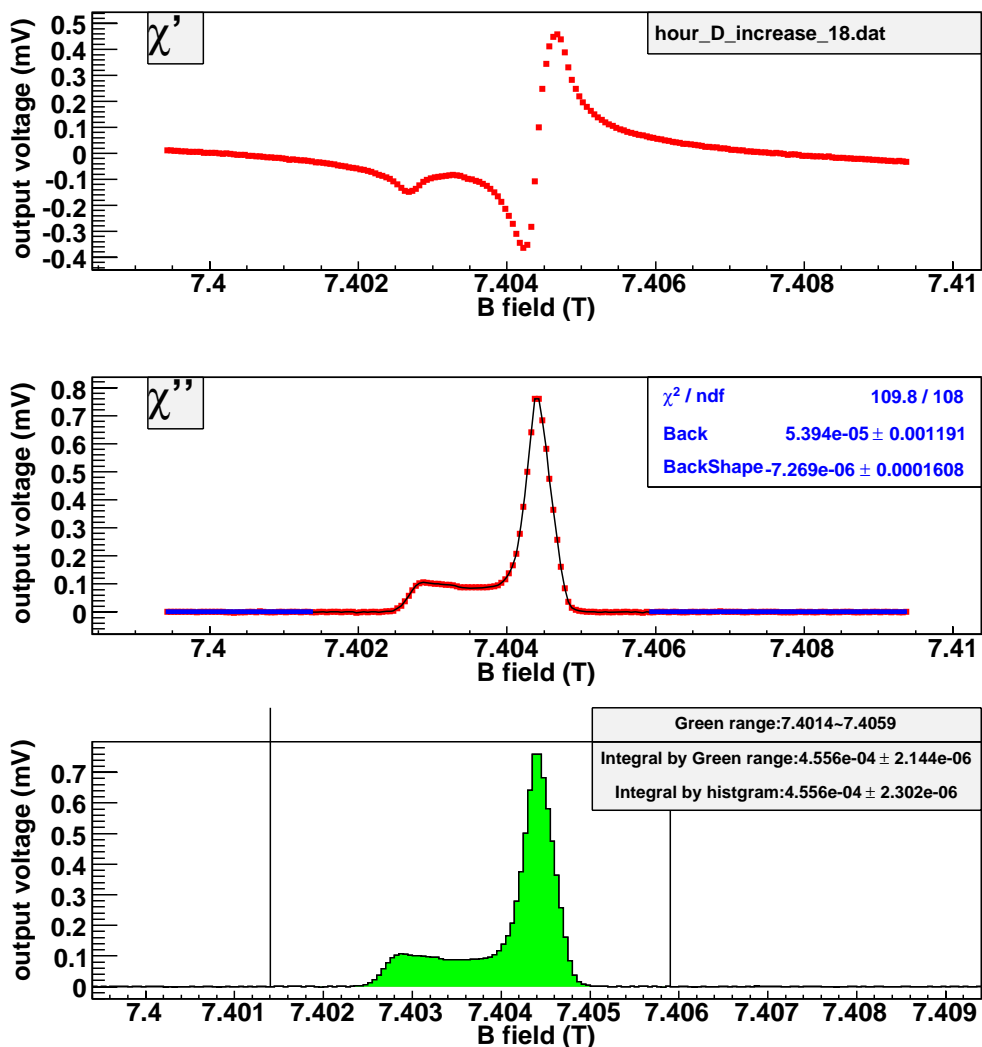


Figure B.1: Get the area of D signal at IBC environment with the histogram method. (current-increasing, time = 18 hours.)

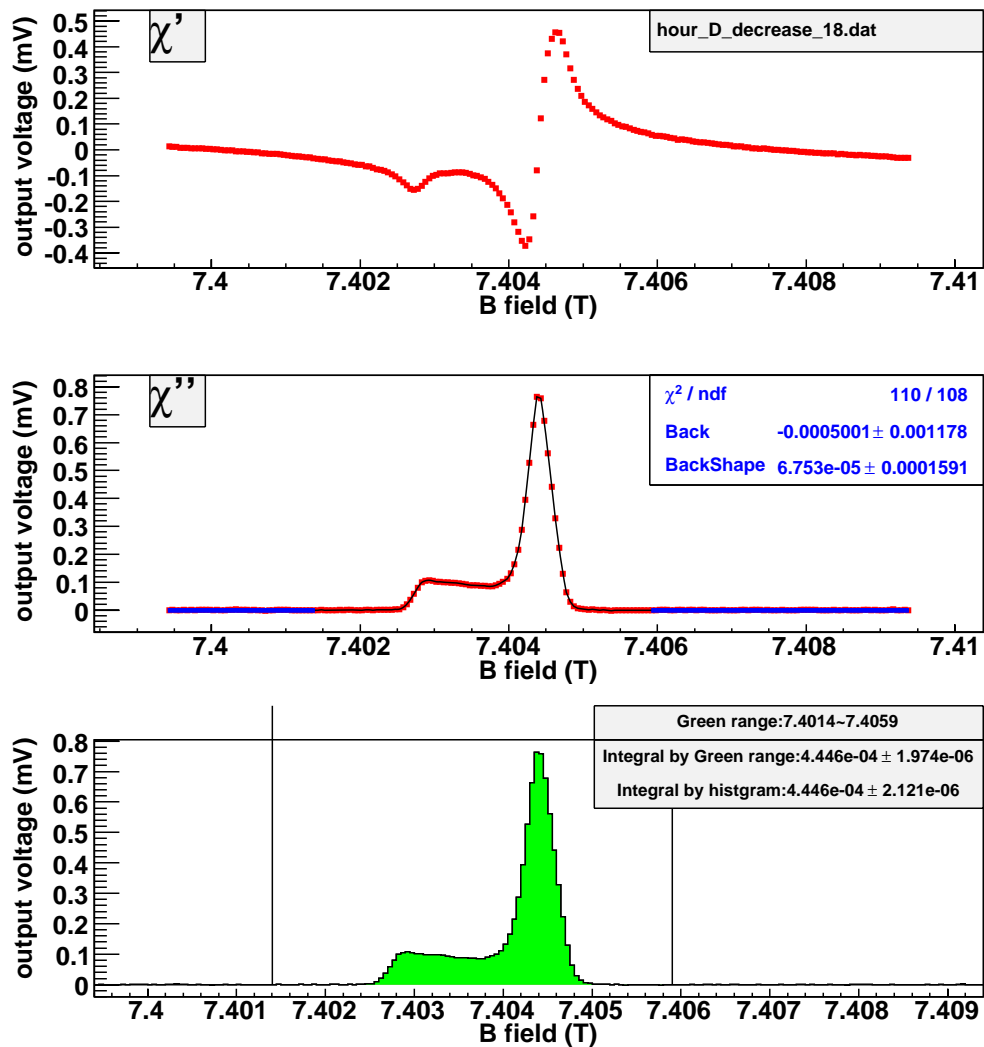


Figure B.2: Get the area of D signal at IBC environment with the histogram method. (current-decreasing, time = 18 hours.)

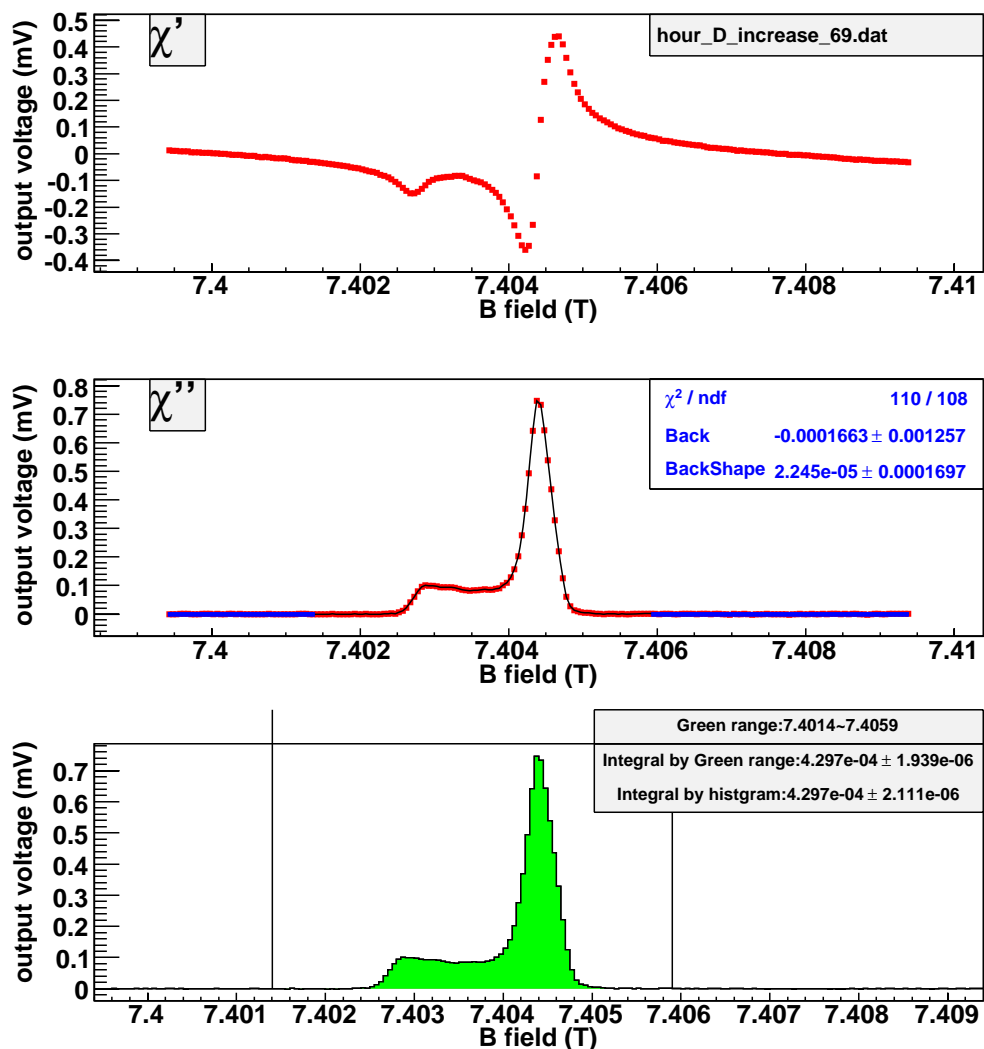


Figure B.3: Get the area of D signal at IBC environment with the histogram method. (current-increasing, time = 69 hours.)

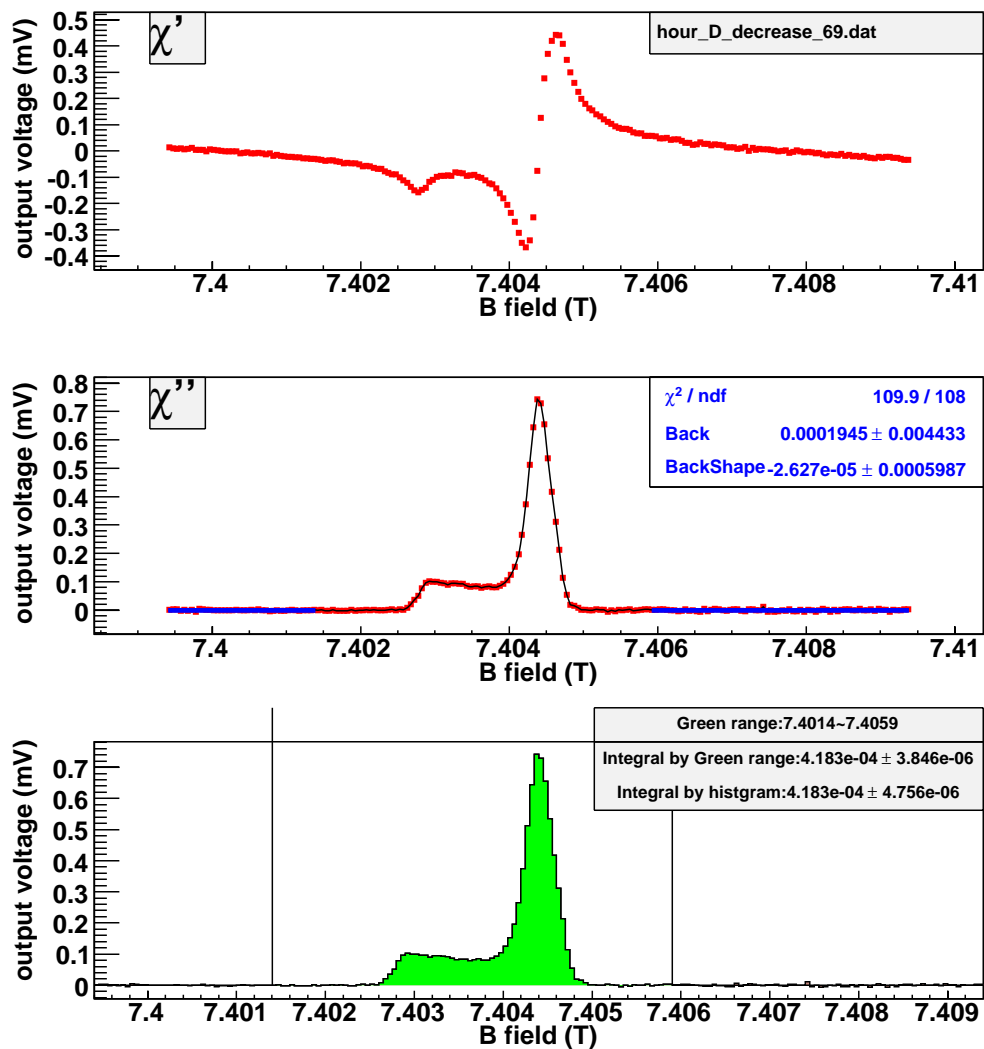


Figure B.4: Get the area of D signal at IBC environment with the histogram method. (current-decreasing, time = 69 hours.)

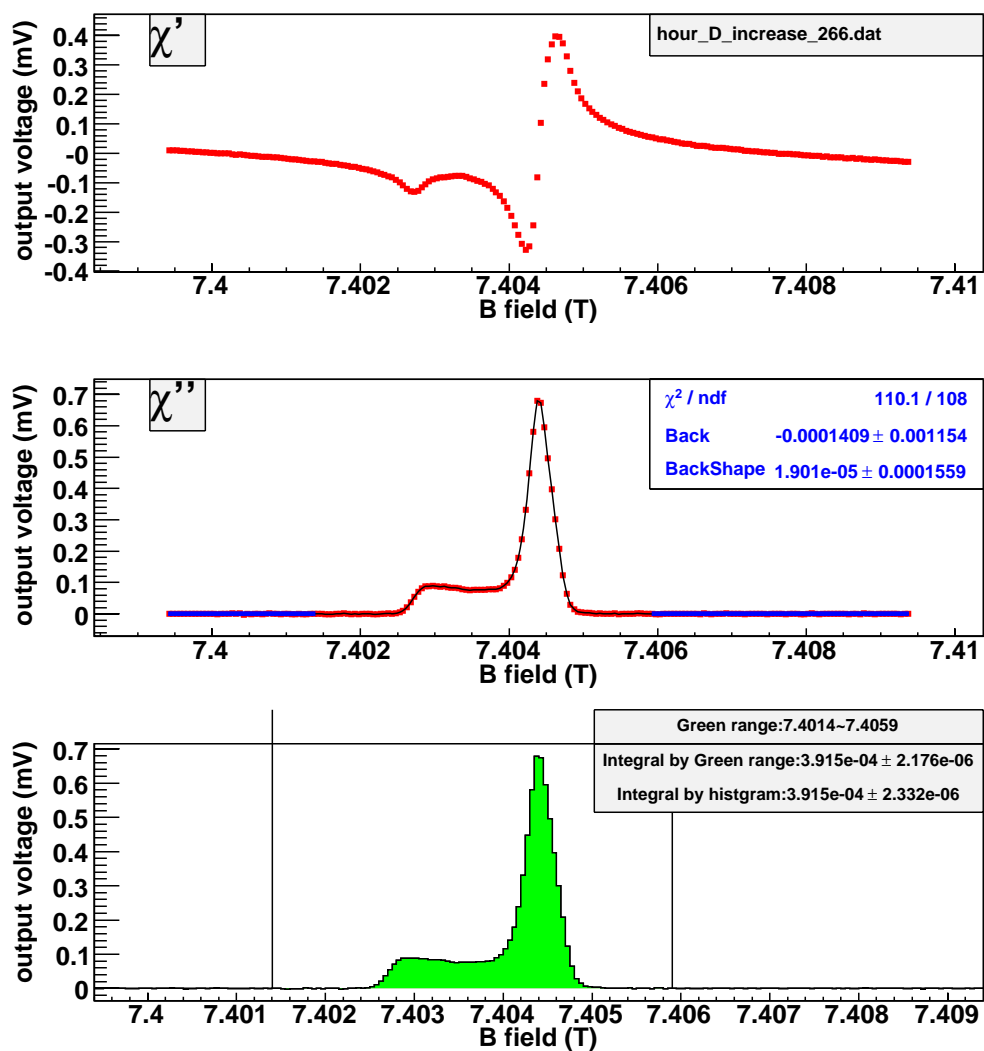


Figure B.5: Get the area of D signal at IBC environment with the histogram method. (current-increasing, time = 266 hours.)

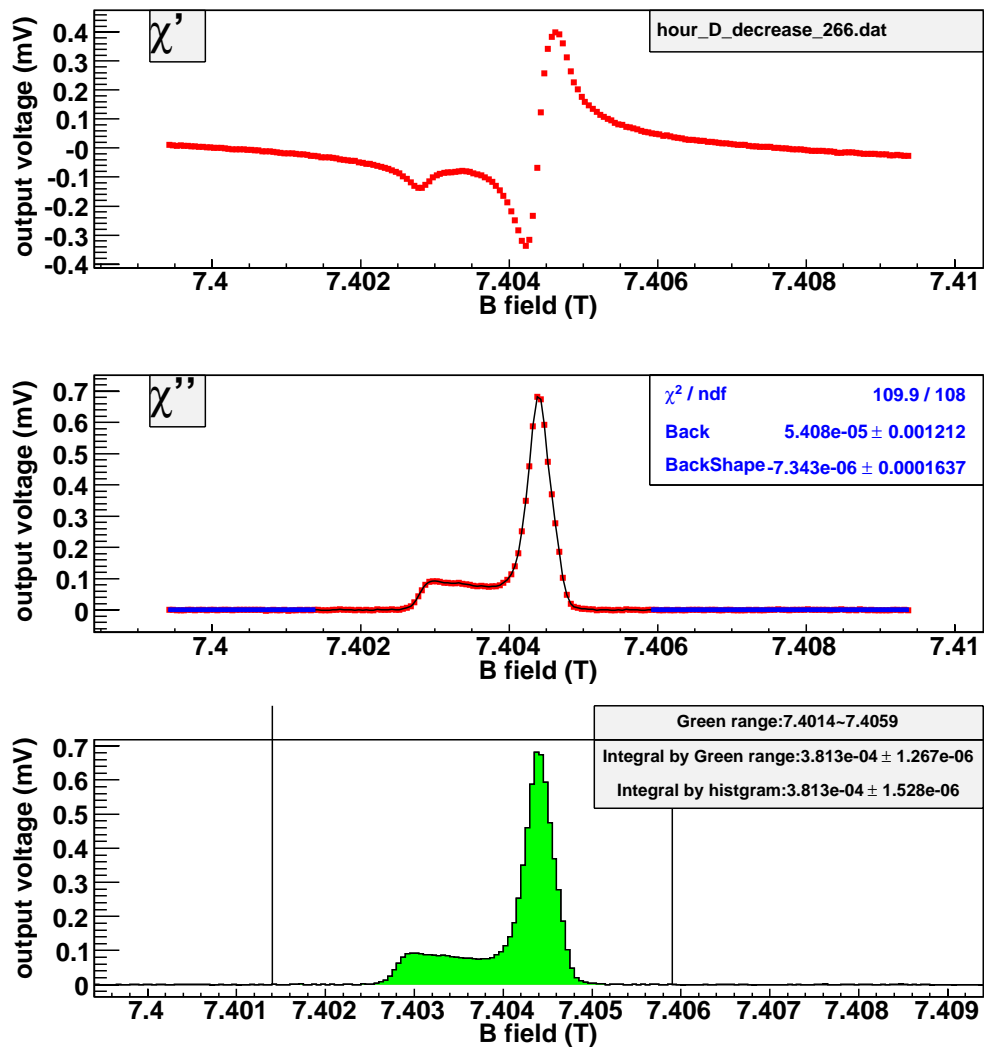


Figure B.6: Get the area of D signal at IBC environment with the histogram method. (current-decreasing, time = 266 hours.)

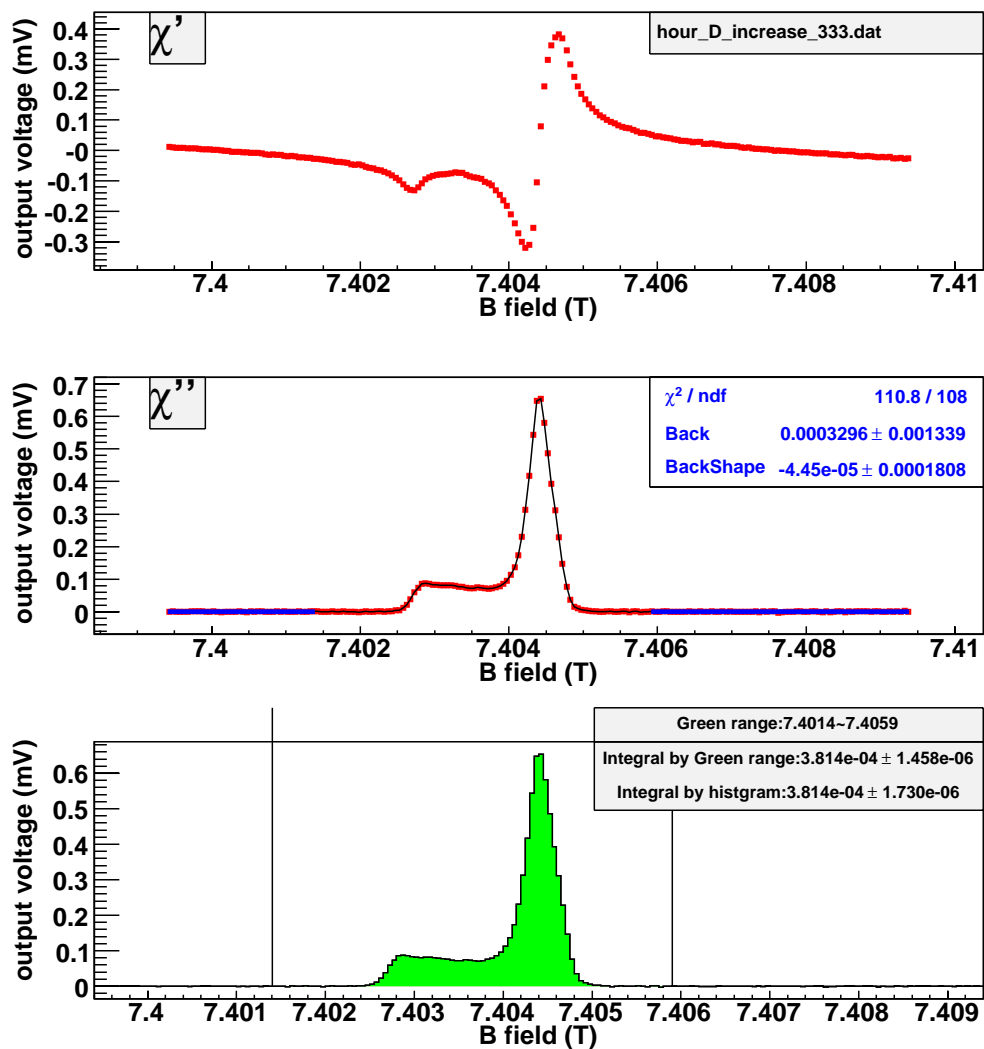


Figure B.7: Get the area of D signal at IBC environment with the histogram method. (current-increasing, time = 333 hours.)

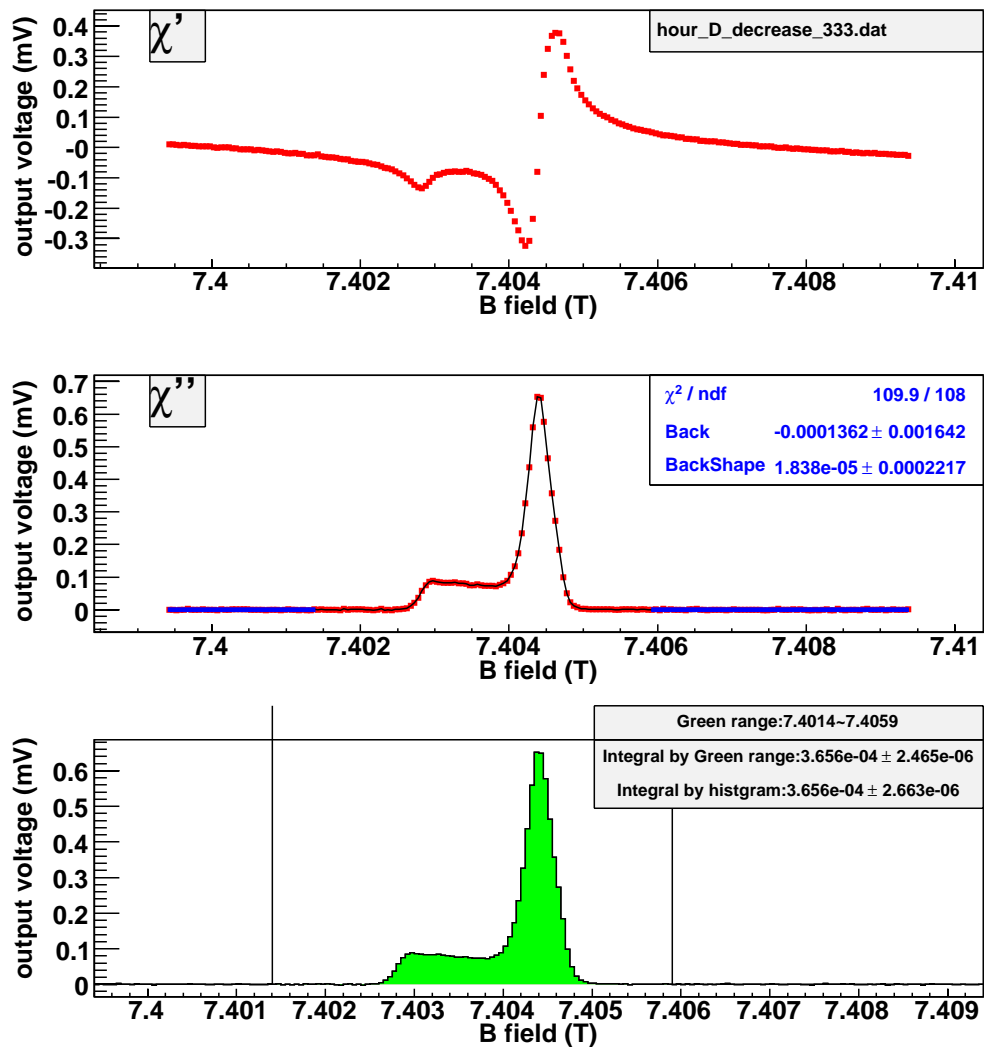


Figure B.8: Get the area of D signal at IBC environment with the histogram method. (current-decreasing, time = 333 hours.)

The following pictures show estimation of the area of D signal at IBC environment with the model method. The current-increasing data and current-decreasing data are analyzed, respectively.

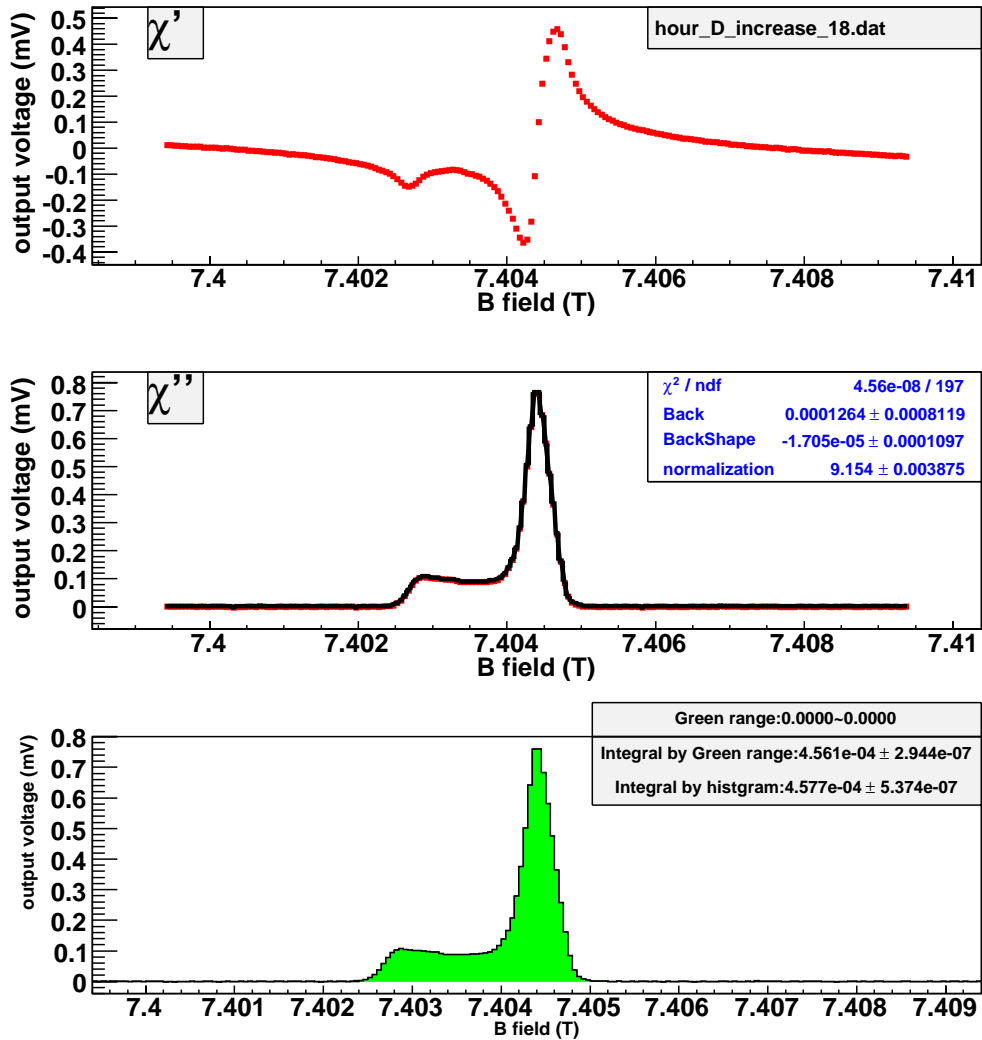


Figure B.9: Get the area of D signal at IBC environment with the model method. (current-increasing, time = 18 hours.)

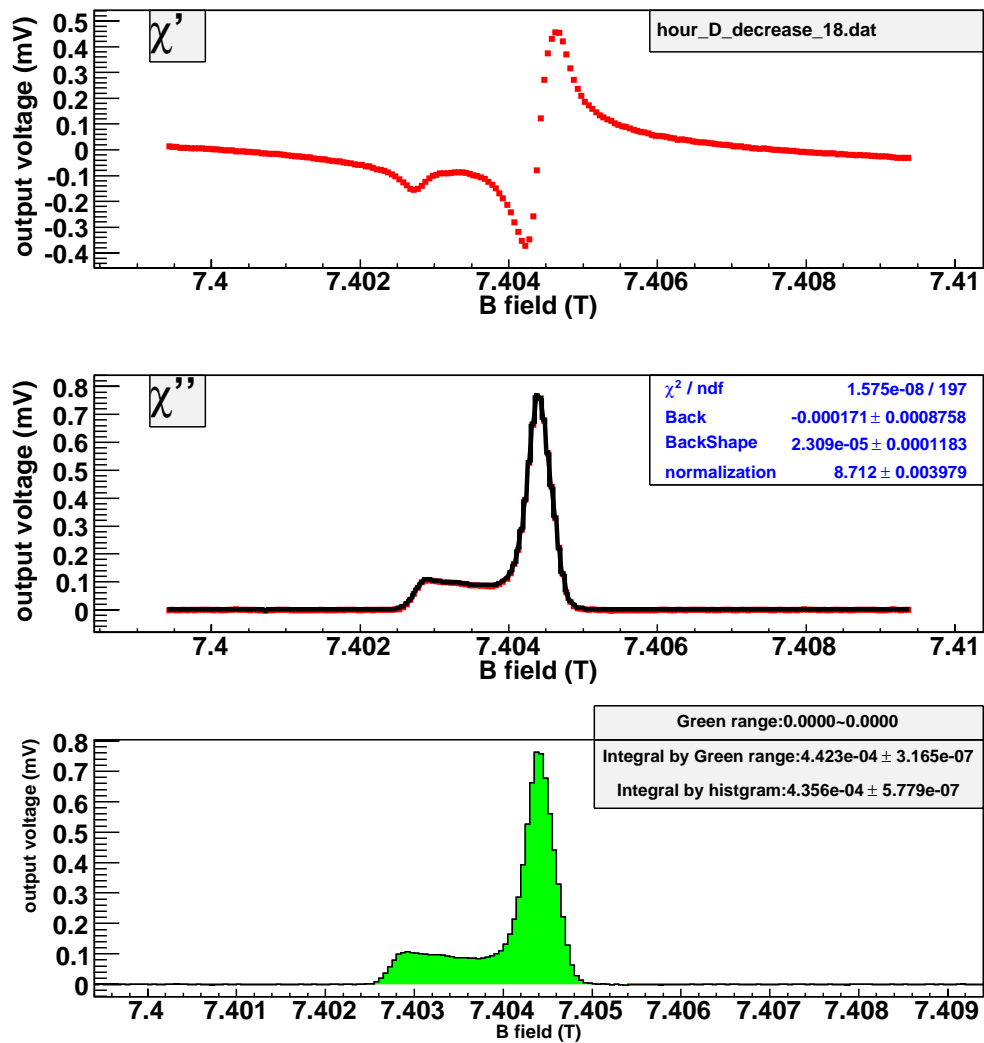


Figure B.10: Get the area of D signal at IBC environment with the model method. (current-decreasing, time = 18 hours.)

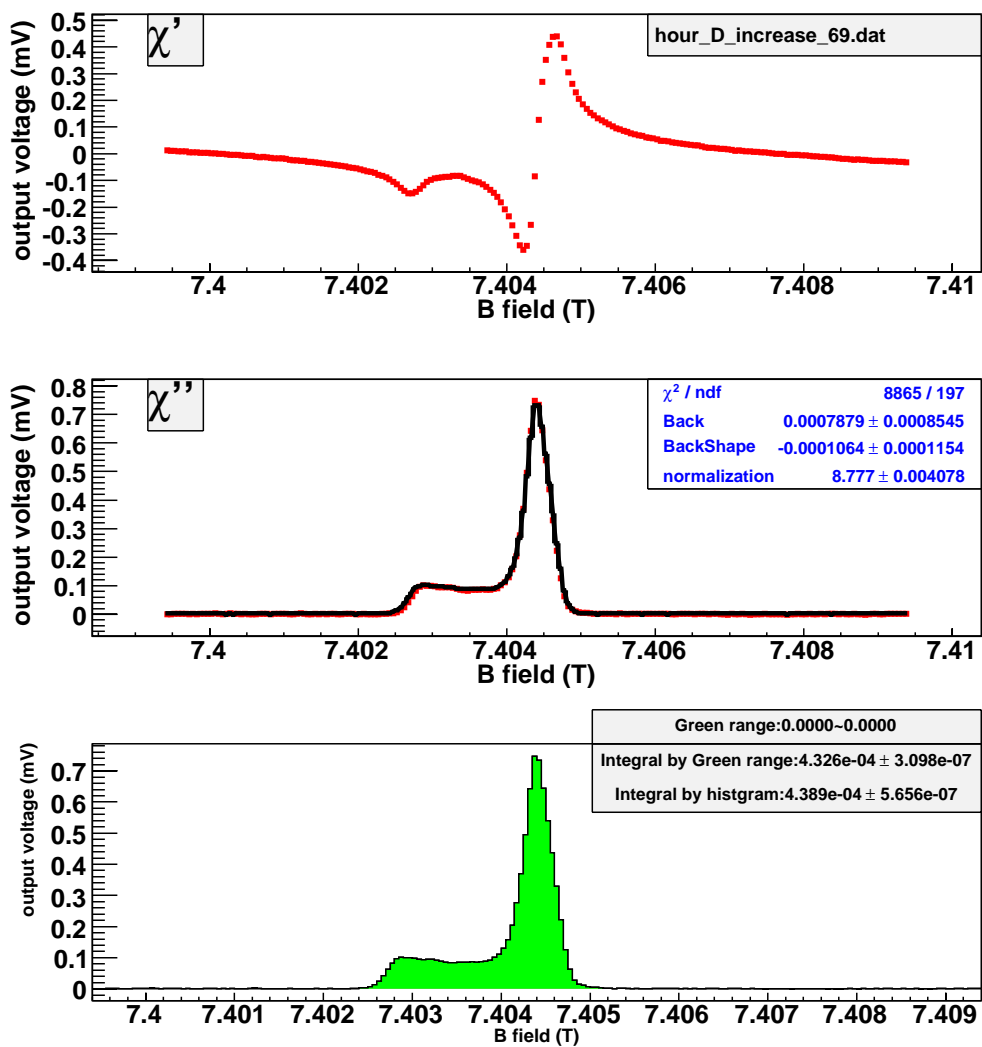


Figure B.11: Get the area of D signal at IBC environment with the model method. (current-increasing, time = 69 hours.)

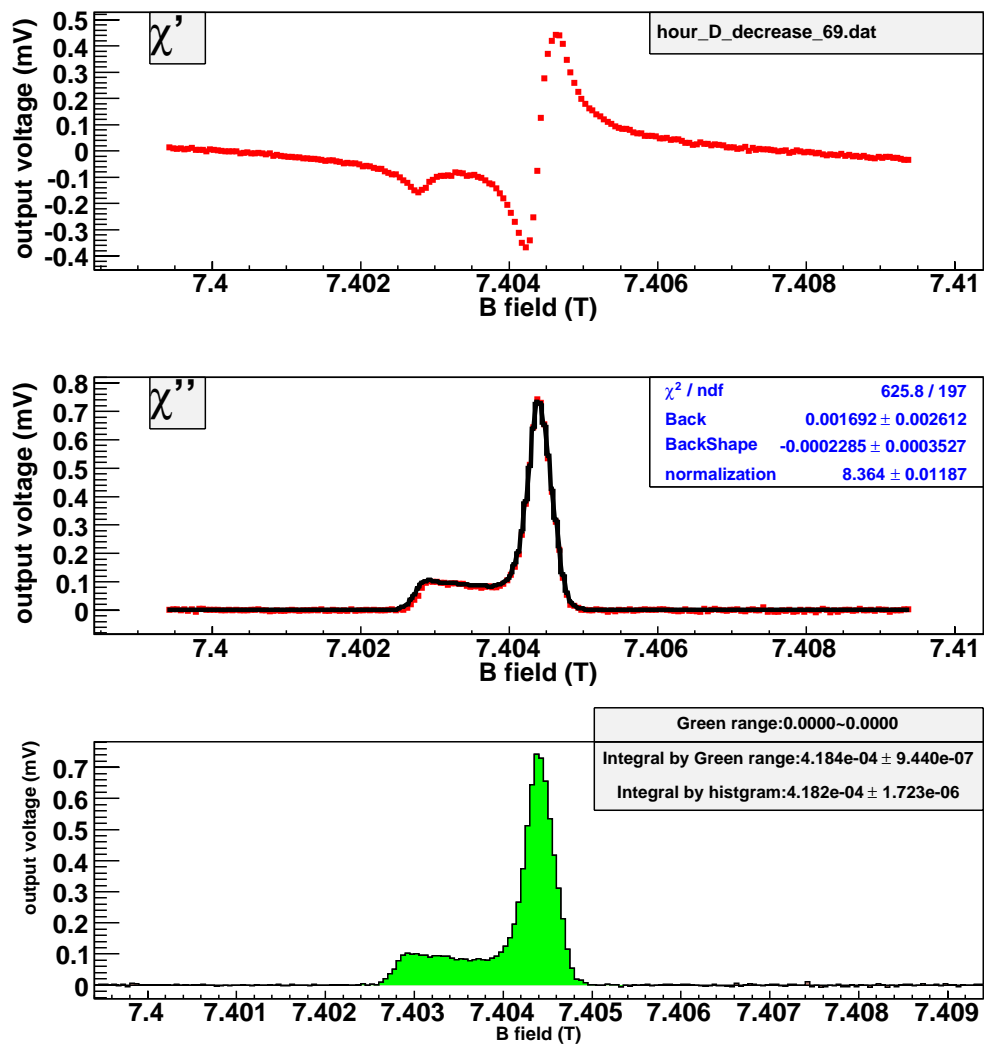


Figure B.12: Get the area of D signal at IBC environment with the model method. (current-decreasing, time = 69 hours.)

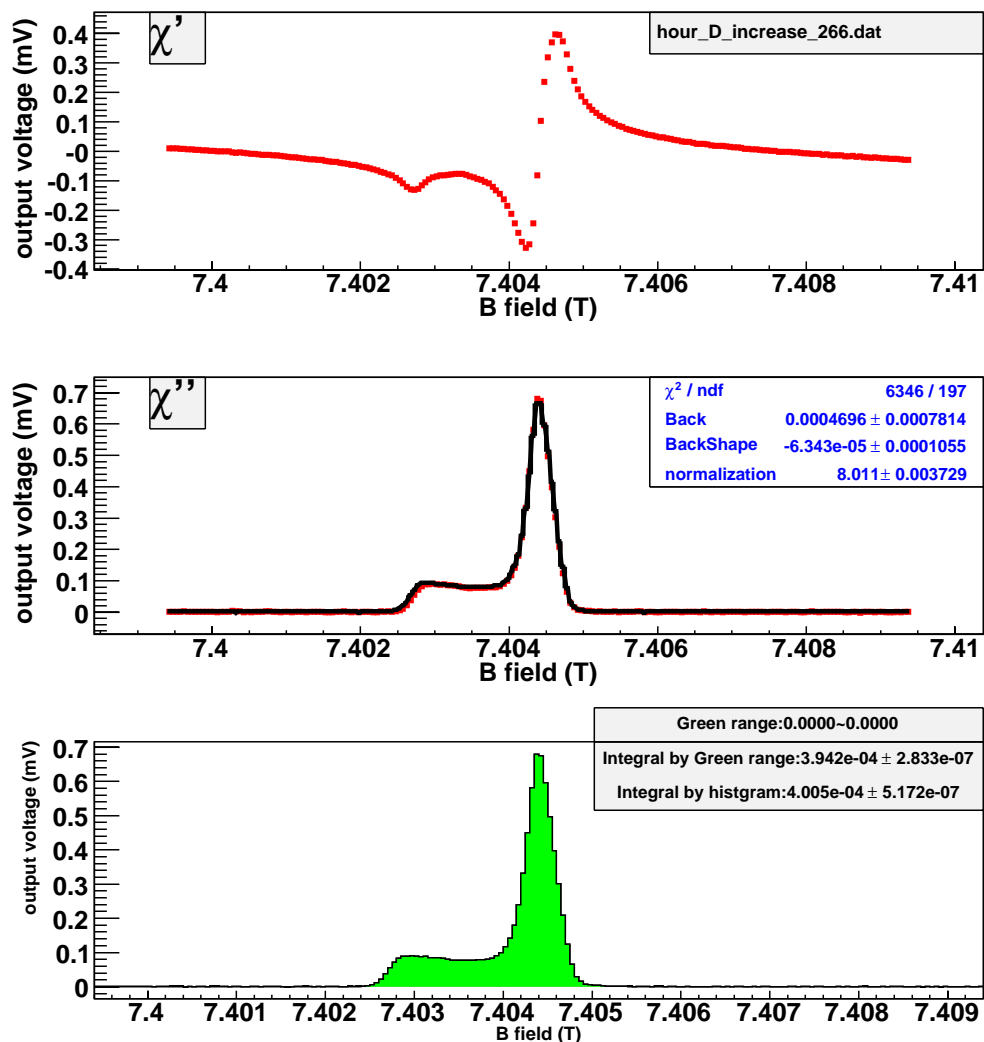


Figure B.13: Get the area of D signal at IBC environment with the model method. (current-increasing, time = 266 hours.)

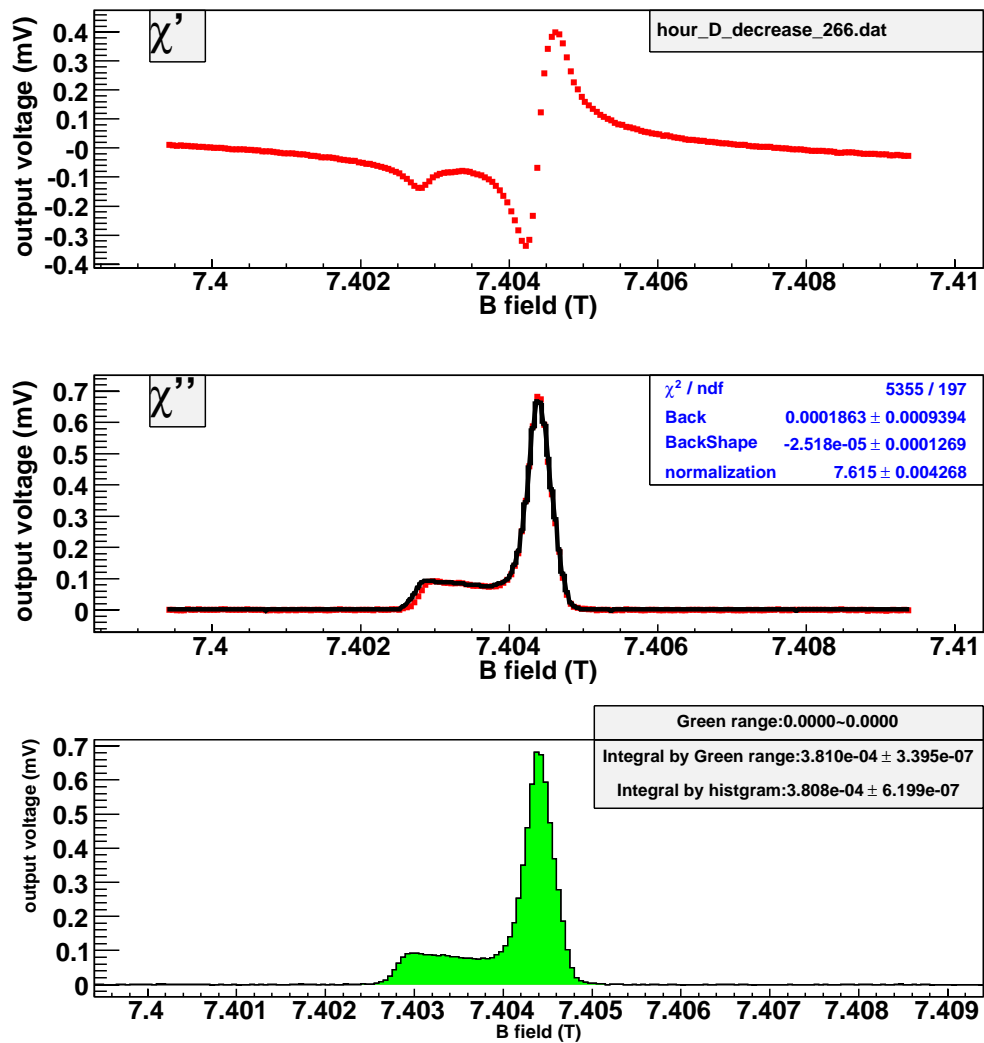


Figure B.14: Get the area of D signal at IBC environment with the model method. (current-decreasing, time = 266 hours.)

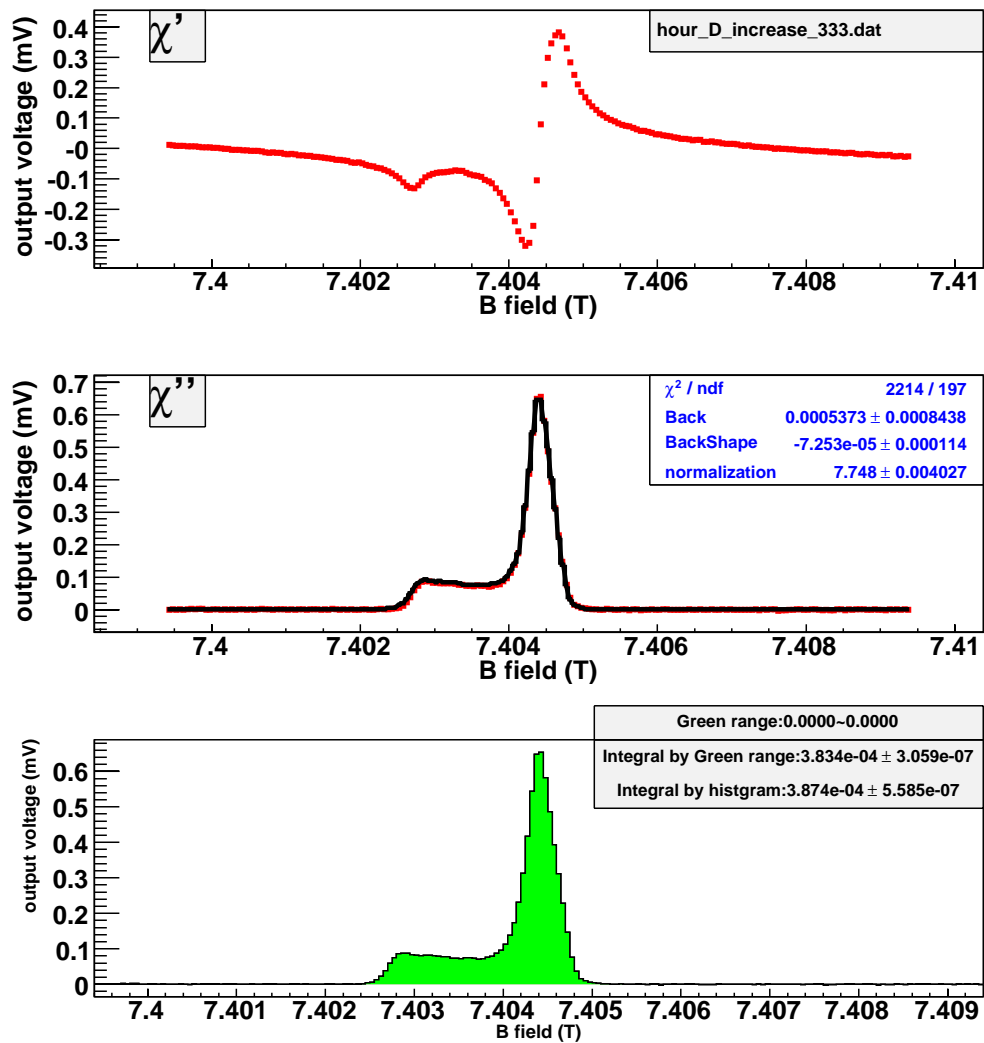


Figure B.15: Get the area of D signal at IBC environment with the model method. (current-increasing, time = 333 hours.)

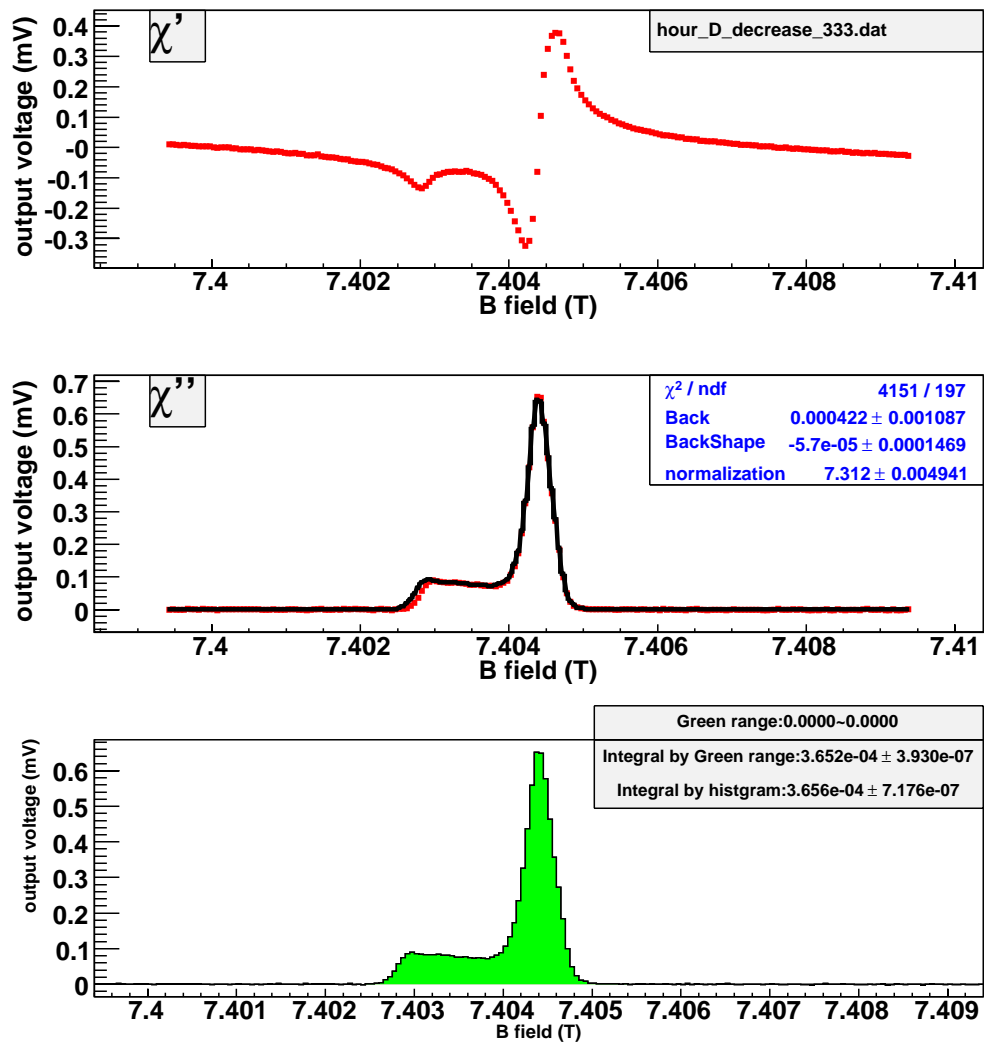


Figure B.16: Get the area of D signal at IBC environment with the model method. (current-decreasing, time = 333 hours.)

The following pictures show estimation of the area of D signal at SC environment with the histogram method. The current-increasing data and current-decreasing data are analyzed, respectively.

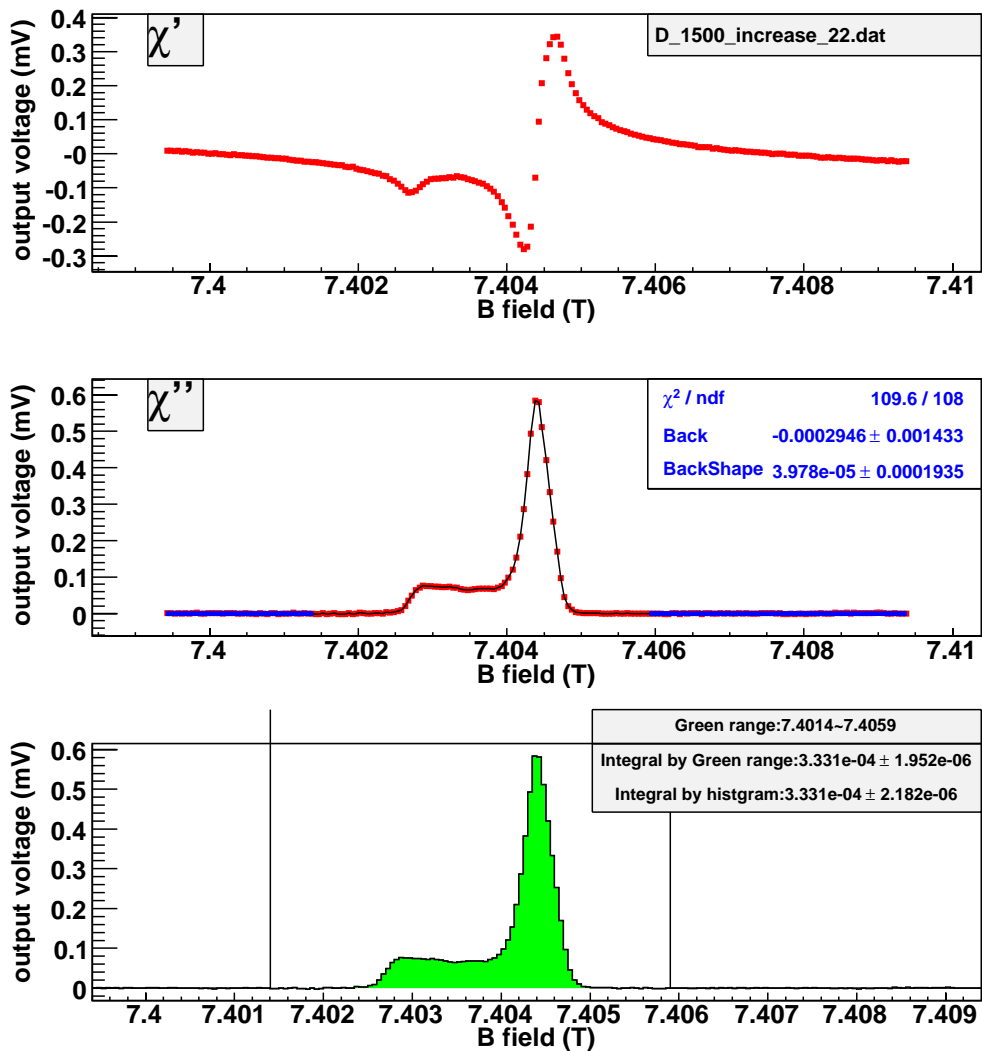


Figure B.17: Get the area of D signal at SC environment with the histogram method. (current-increasing, time = 22 hours.)

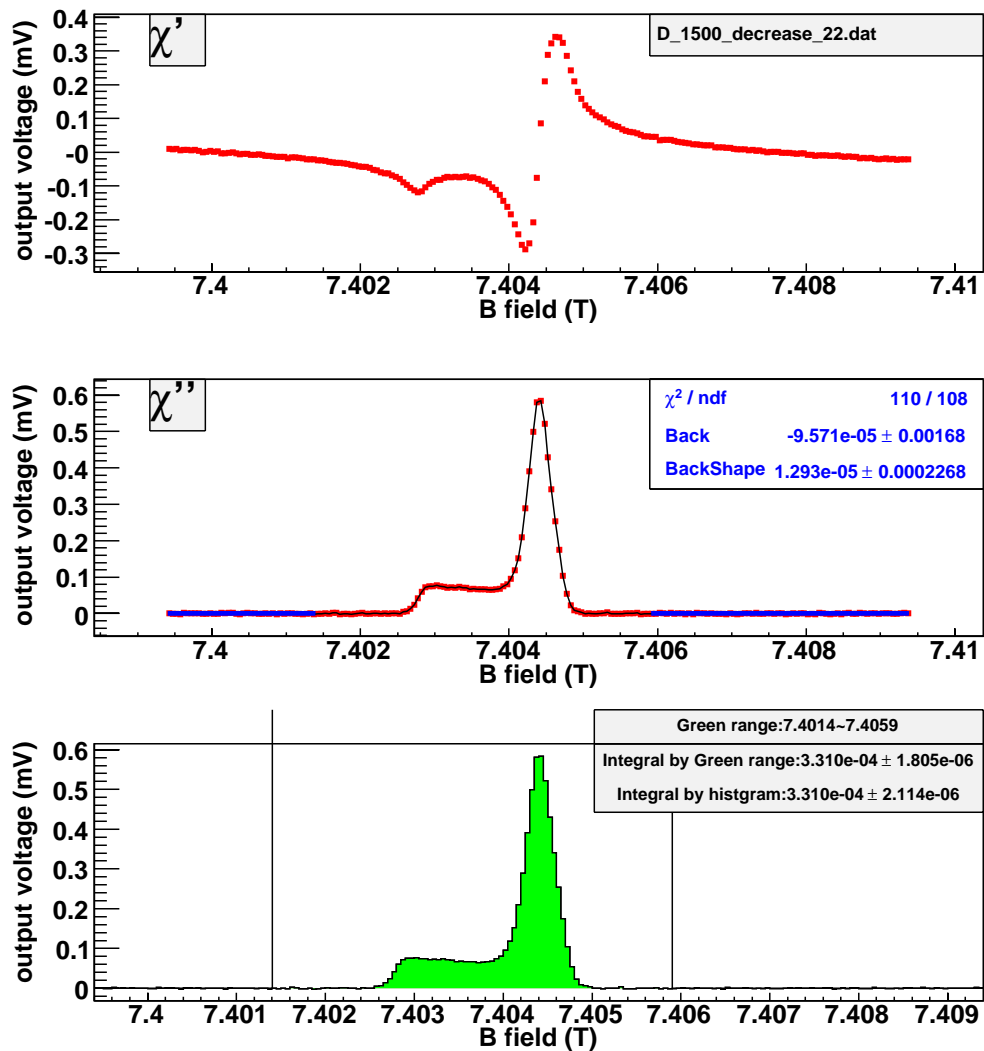


Figure B.18: Get the area of D signal at SC environment with the histogram method. (current-decreasing, time = 22 hours.)

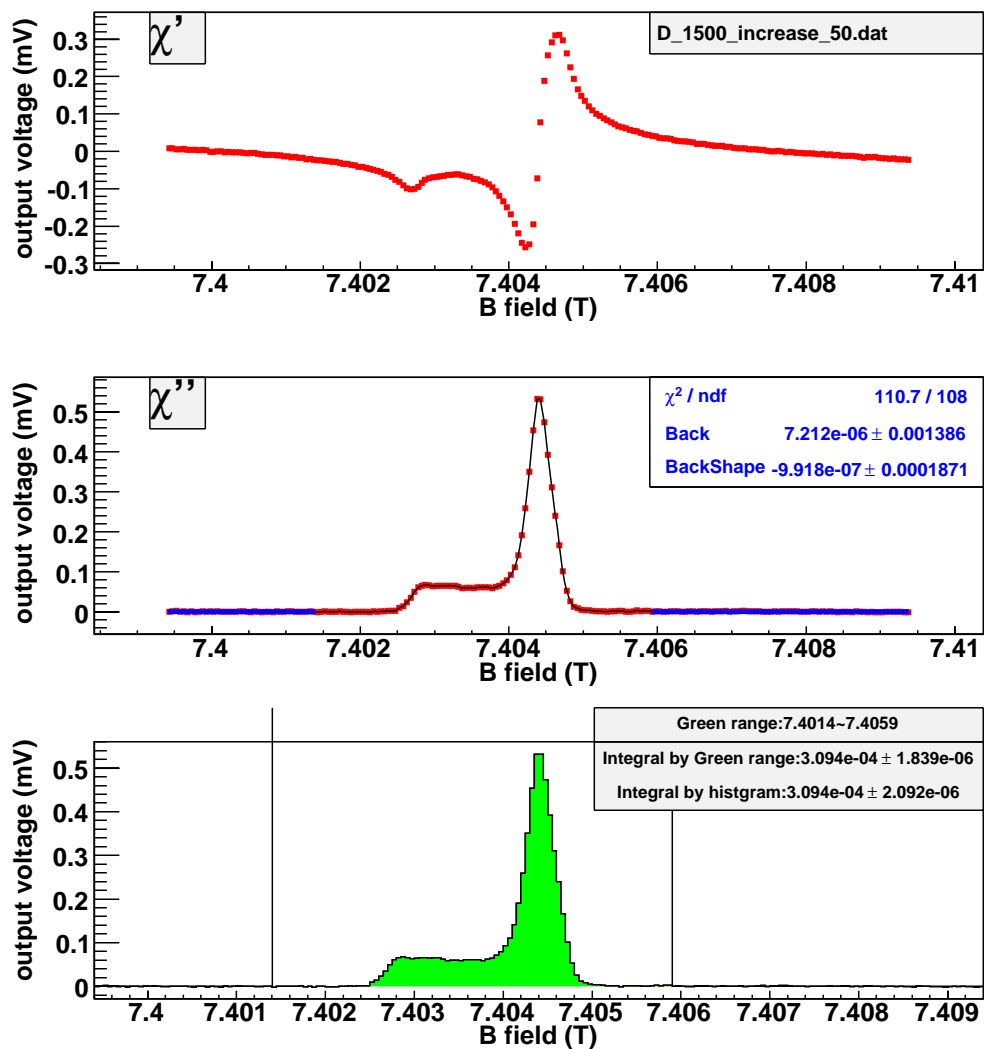


Figure B.19: Get the area of D signal at SC environment with the histogram method. (current-increasing, time = 50 hours.)

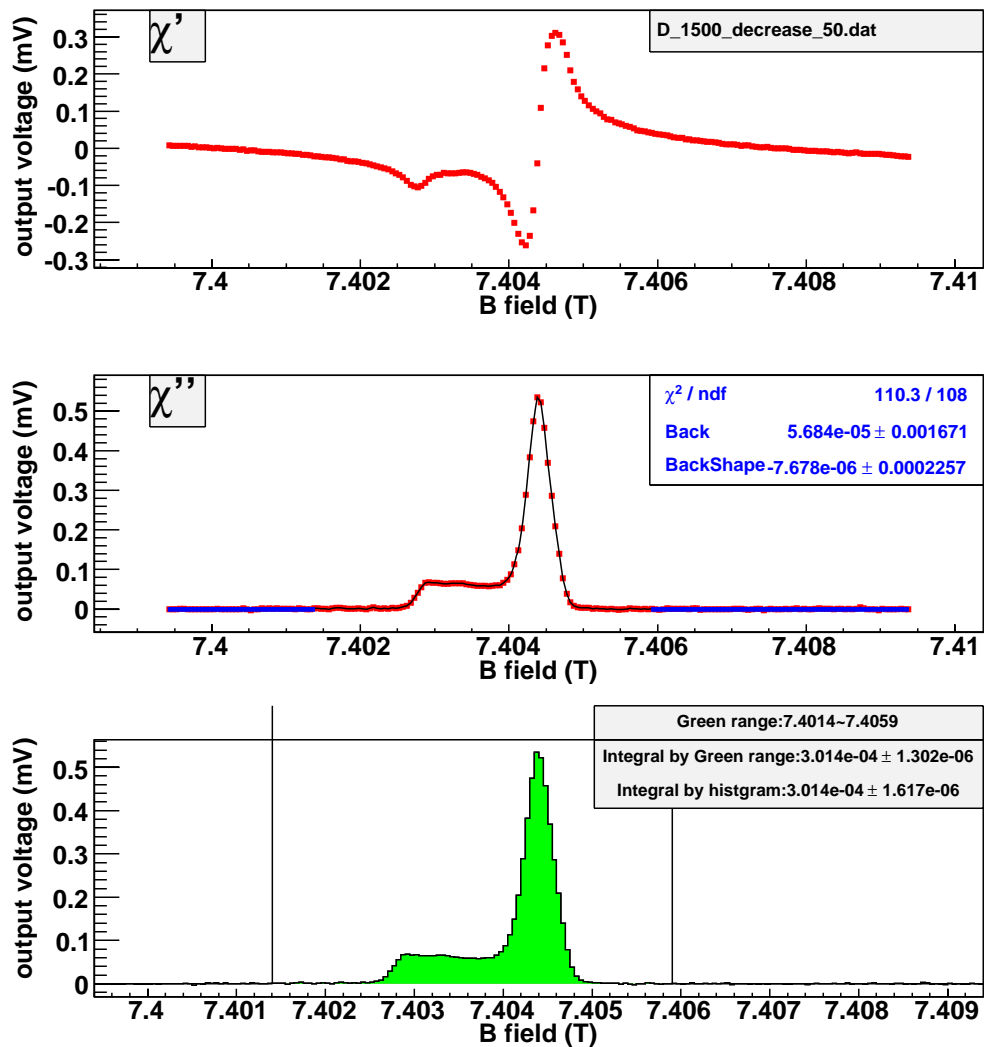


Figure B.20: Get the area of D signal at SC environment with the histogram method. (current-decreasing, time = 50 hours.)

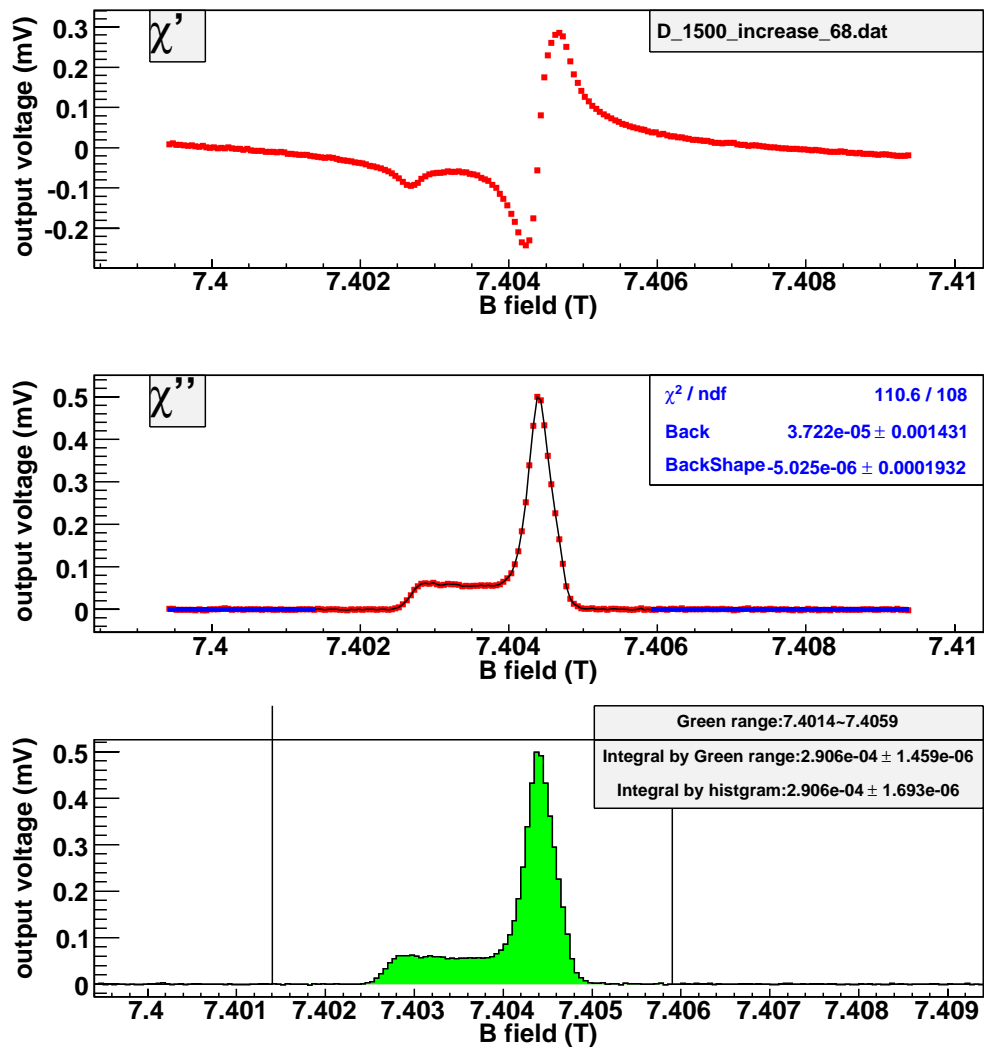


Figure B.21: Get the area of D signal at SC environment with the histogram method. (current-increasing, time = 68 hours.)

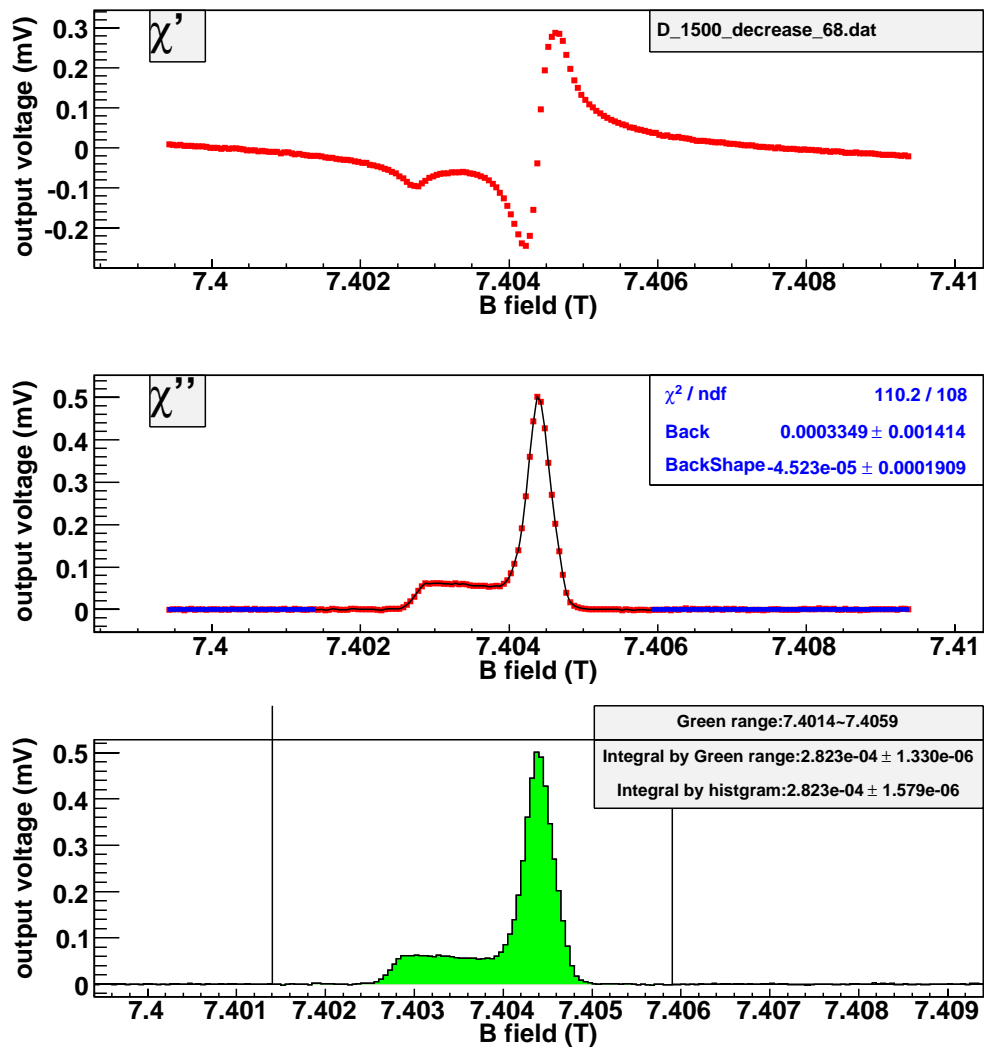


Figure B.22: Get the area of D signal at SC environment with the histogram method. (current-decreasing, time = 68 hours.)

The following pictures show estimation of the area of D signal at SC environment with the model method. The current-increasing data and current-decreasing data are analyzed, respectively.

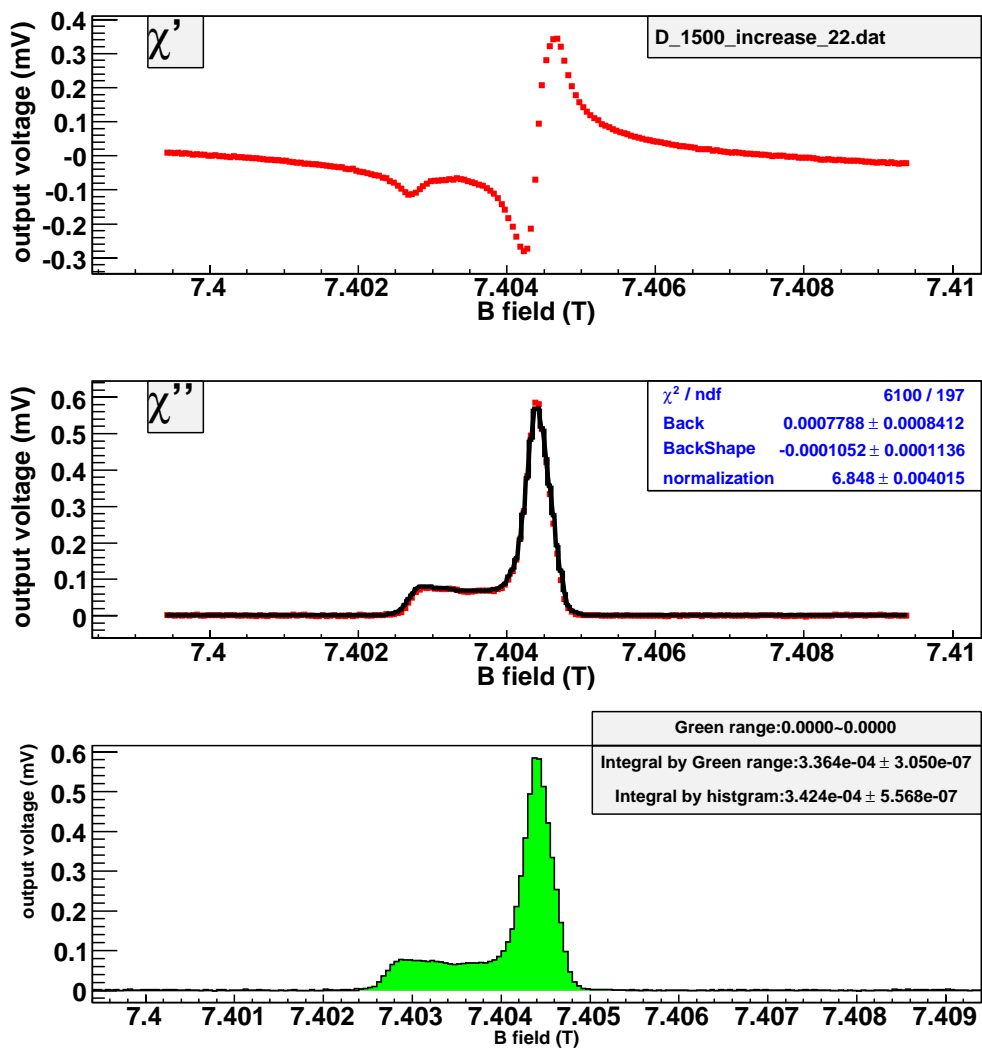


Figure B.23: Get the area of D signal at SC environment with the model method. (current-increasing, time = 22 hours.)

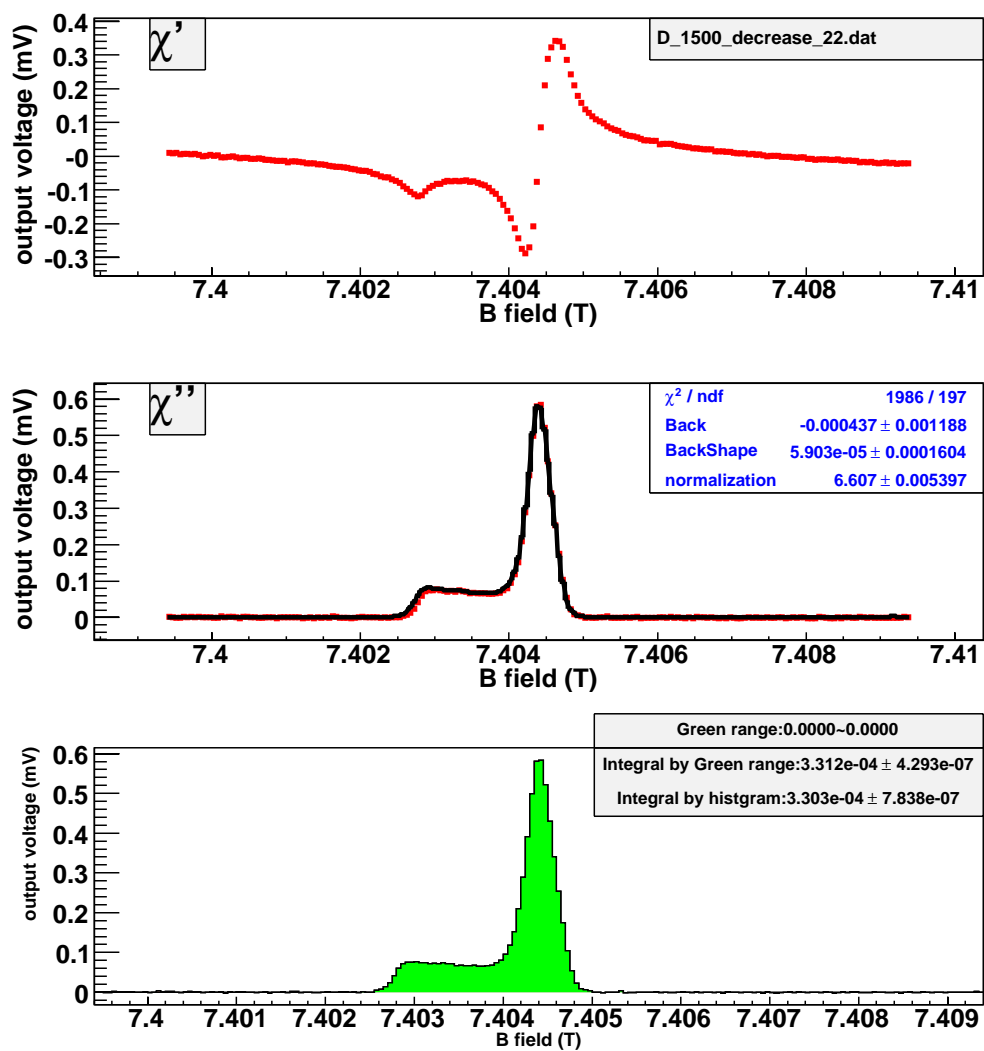


Figure B.24: Get the area of D signal at SC environment with the model method. (current-decreasing, time = 22 hours.)

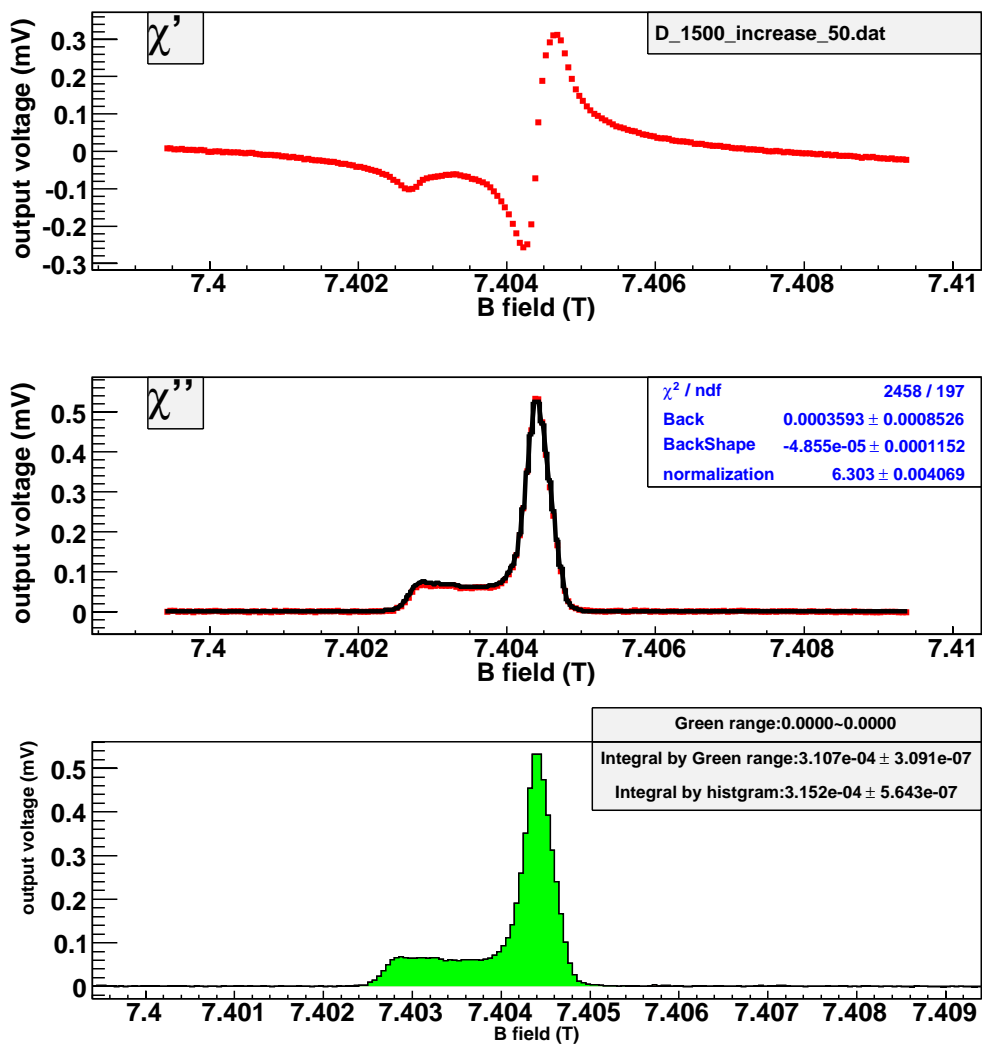


Figure B.25: Get the area of D signal at SC environment with the model method. (current-increasing, time = 50 hours.)

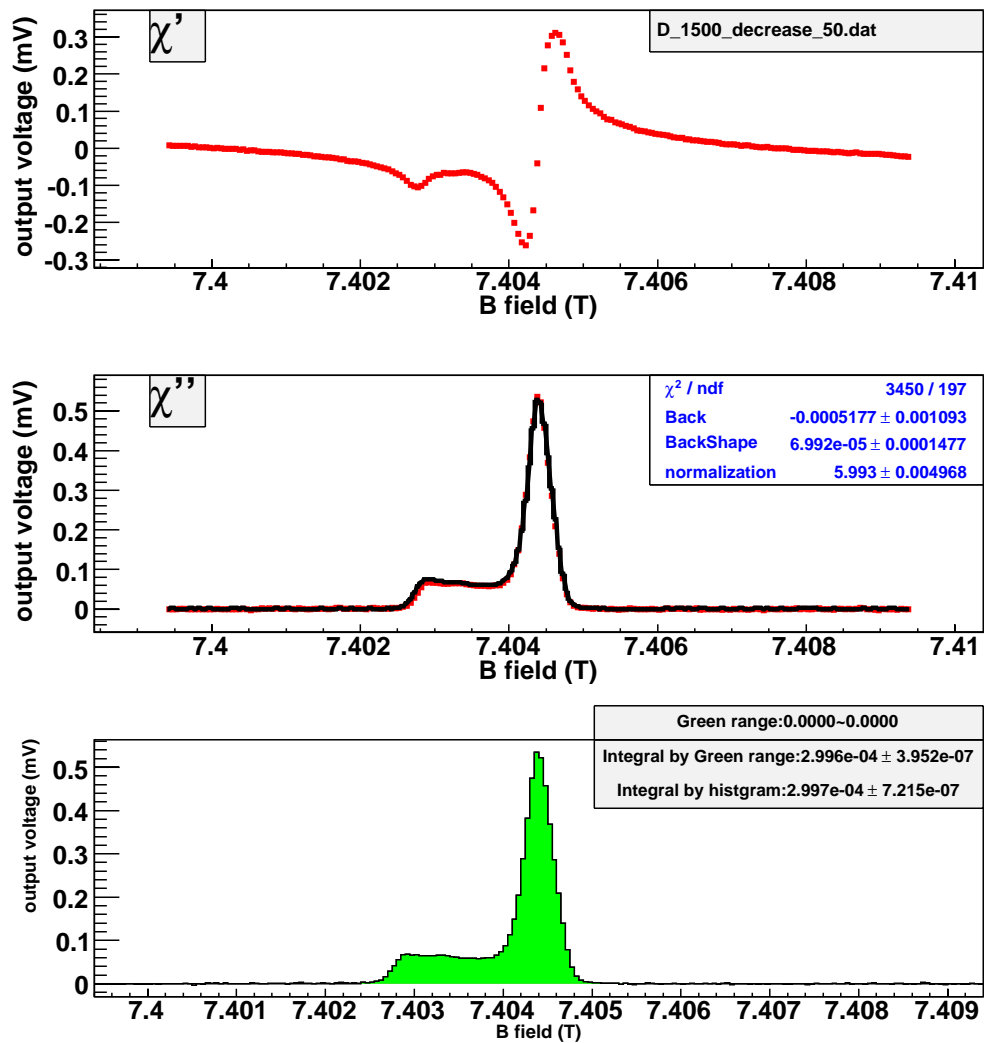


Figure B.26: Get the area of D signal at SC environment with the model method. (current-decreasing, time = 50 hours.)

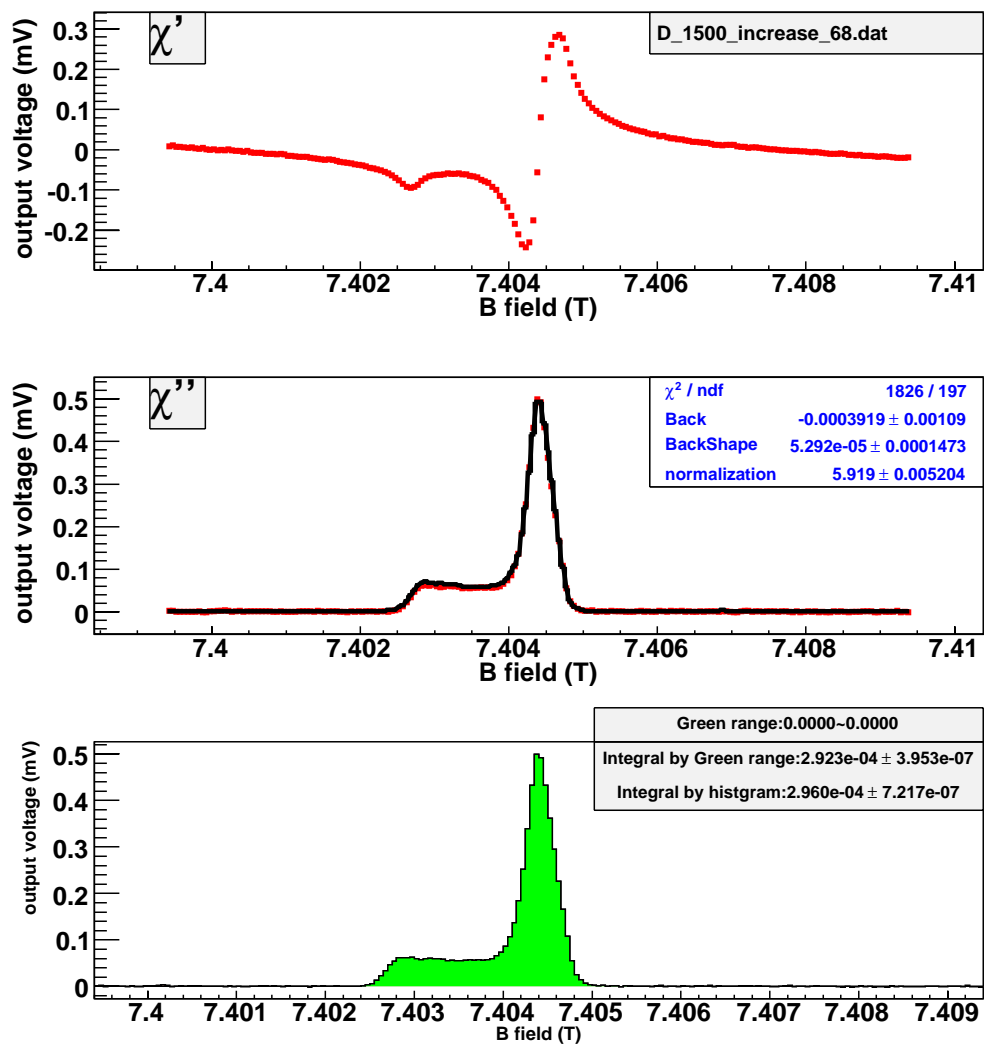


Figure B.27: Get the area of D signal at SC environment with the model method. (current-increasing, time = 68 hours.)

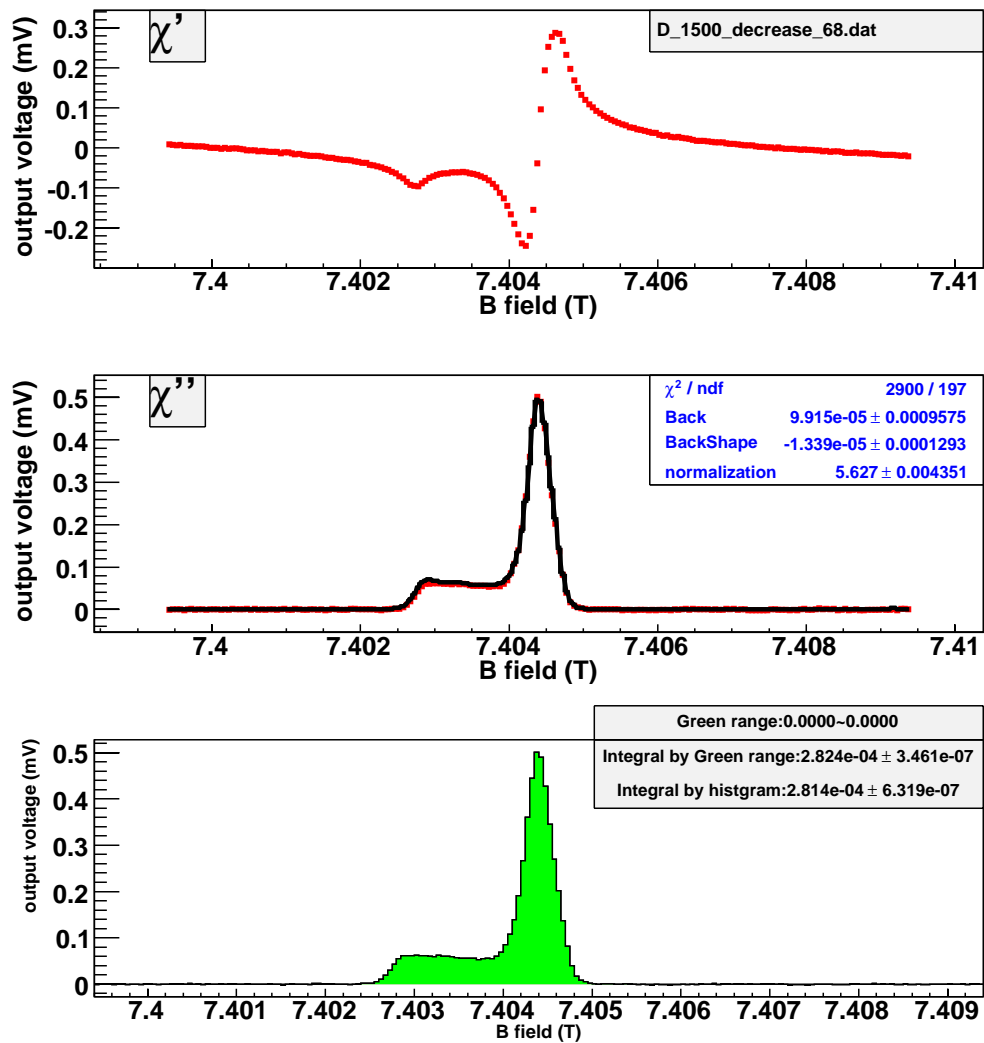


Figure B.28: Get the area of D signal at SC environment with the model method. (current-decreasing, time = 68 hours.)

The following pictures show estimation of the area of D signal at TC environment with the histogram method. The current-increasing data and current-decreasing data are analyzed, respectively.

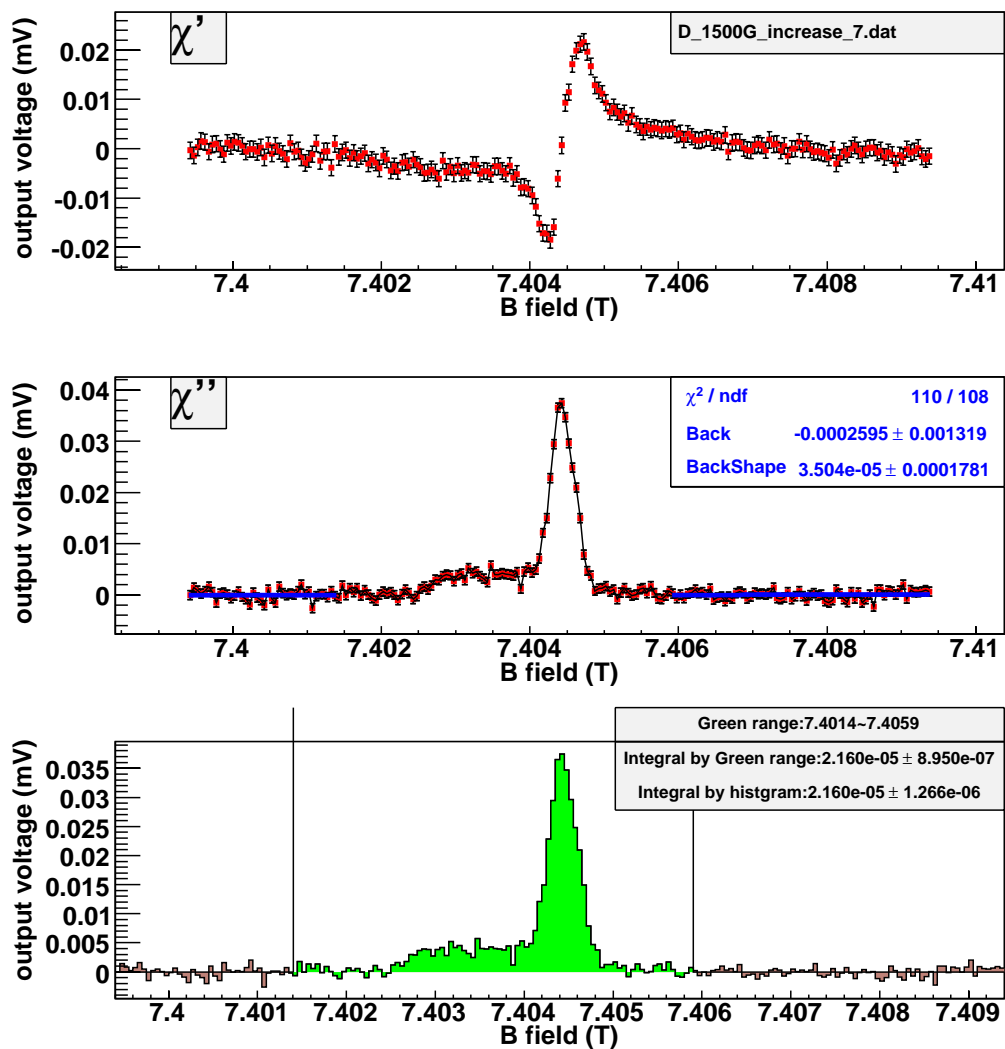


Figure B.29: Get the area of D signal at TC environment with the histogram method. (current-increasing, time = 7 hours.)

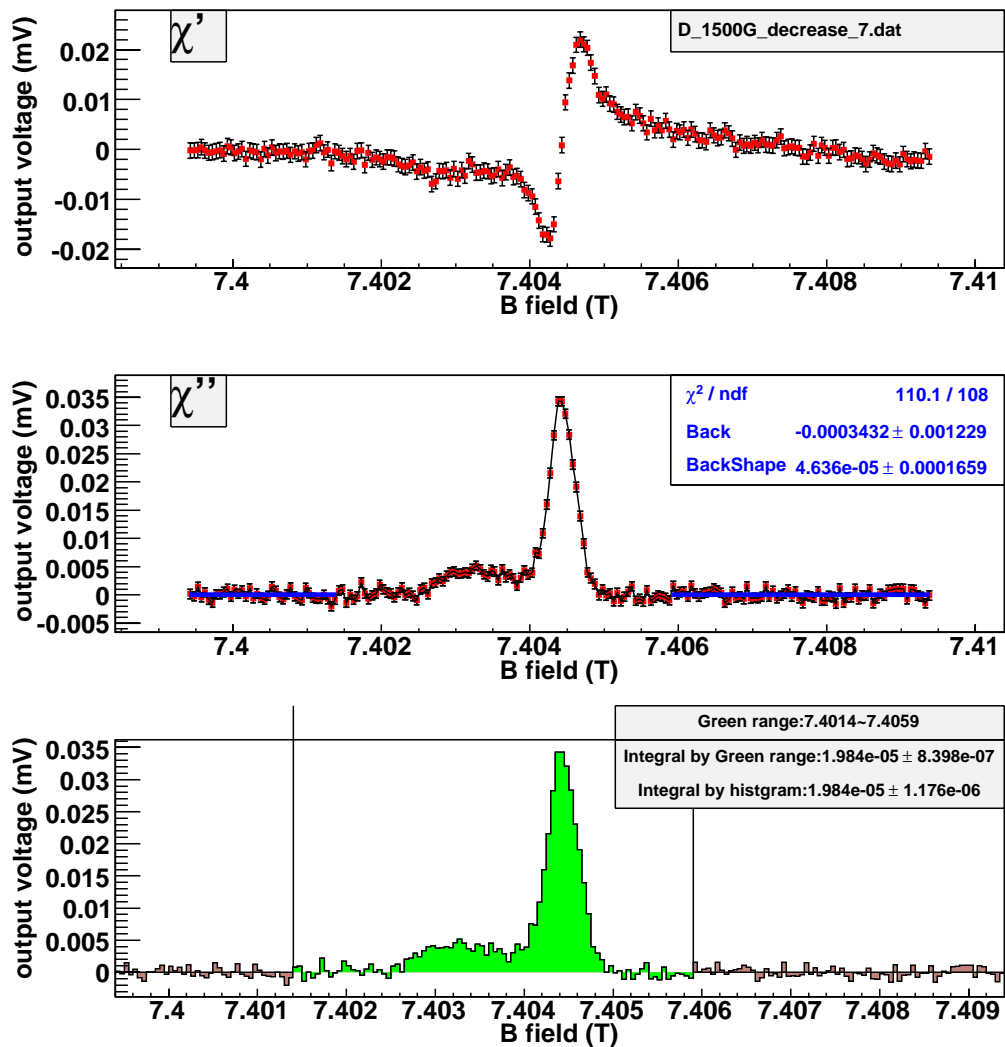


Figure B.30: Get the area of D signal at TC environment with the histogram method. (current-decreasing, time = 7 hours.)

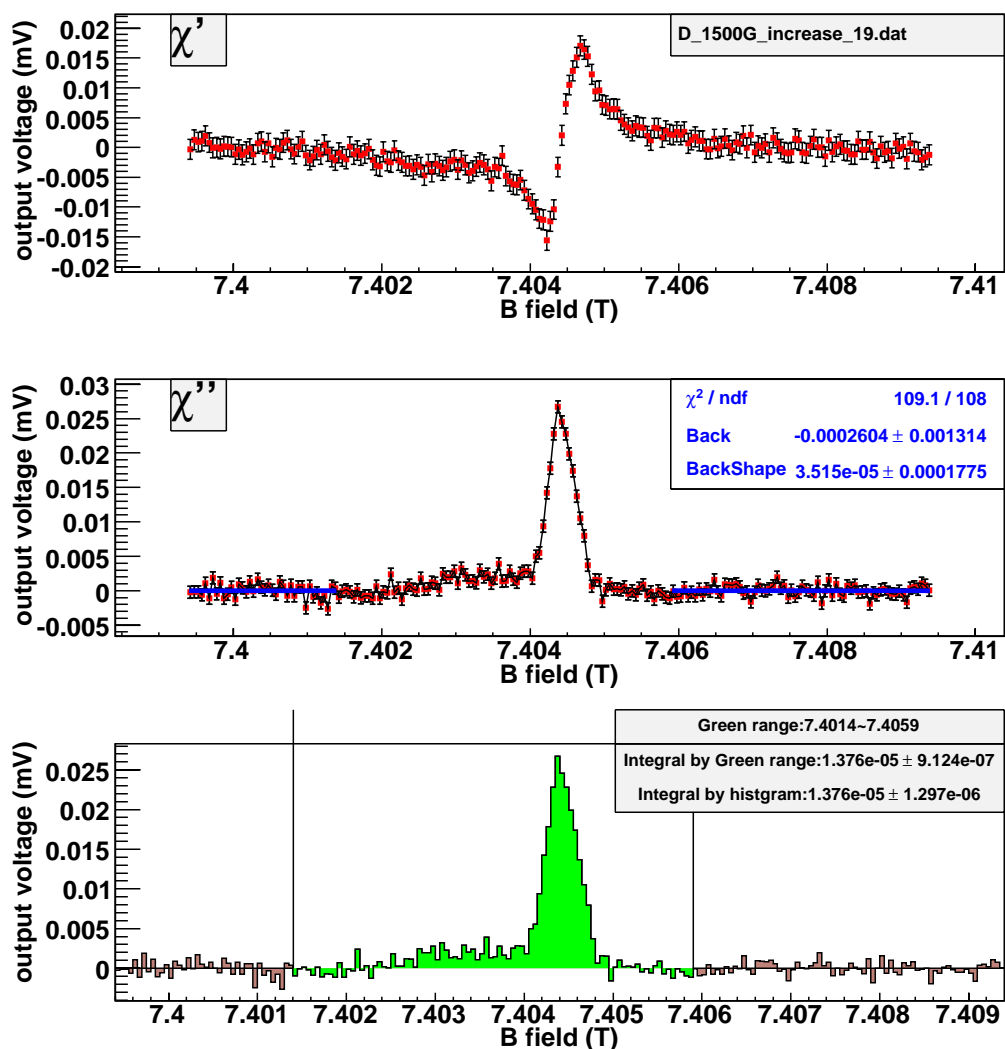


Figure B.31: Get the area of D signal at TC environment with the histogram method. (current-increasing, time = 19 hours.)

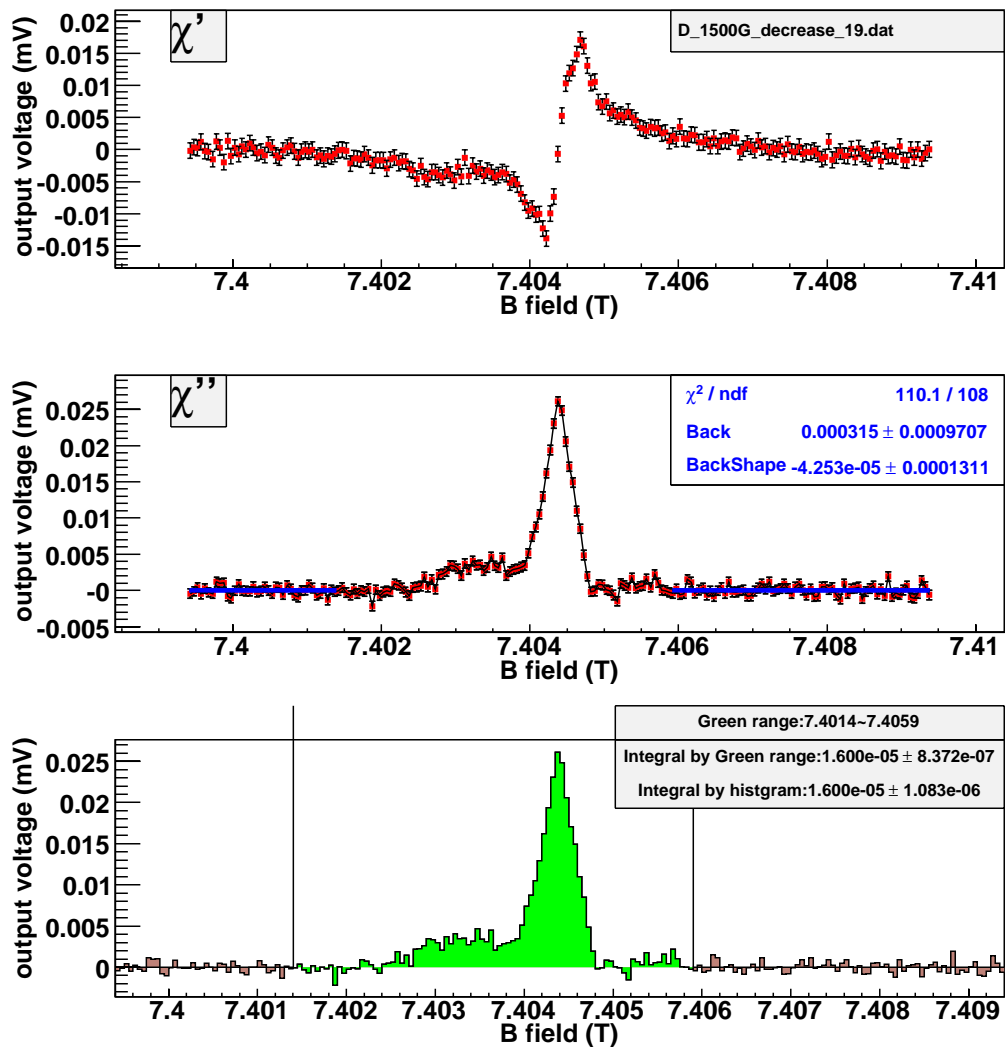


Figure B.32: Get the area of D signal at TC environment with the histogram method. (current-decreasing, time = 19 hours.)

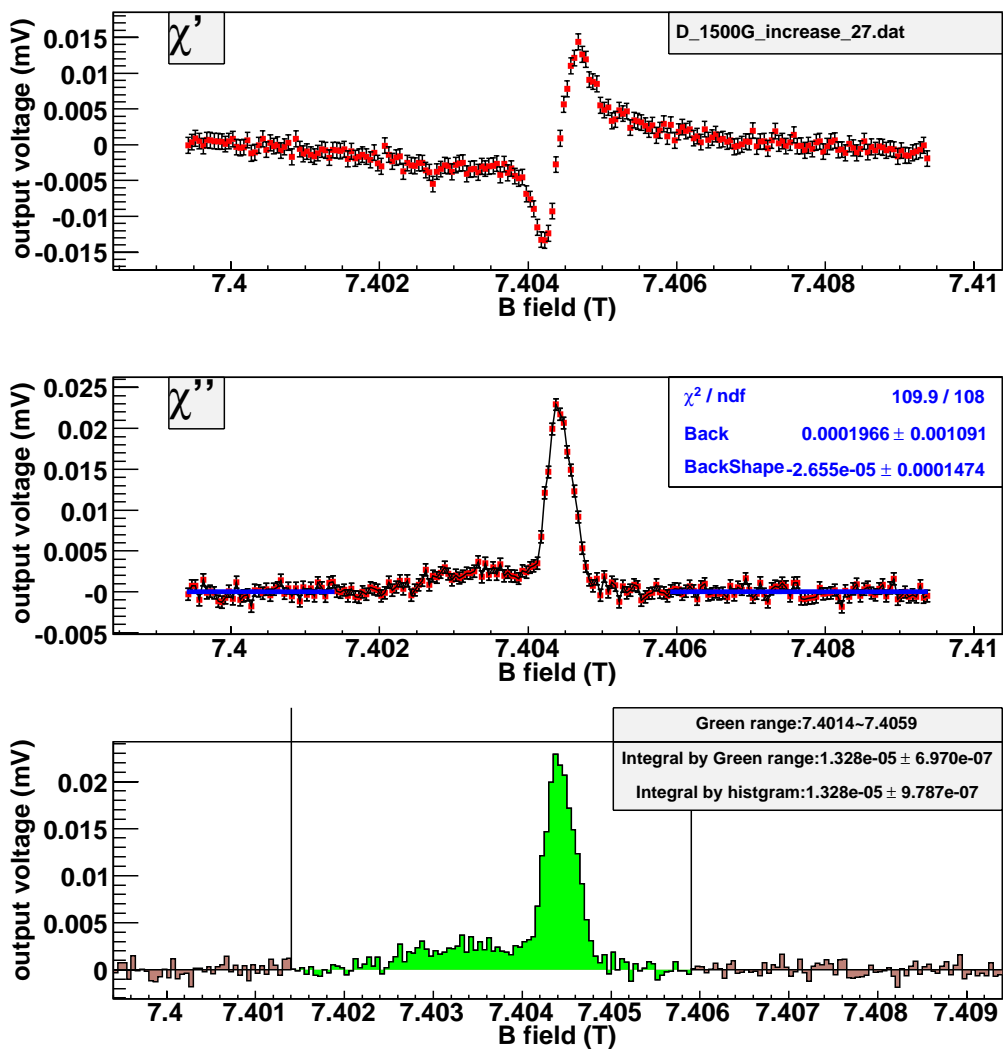


Figure B.33: Get the area of D signal at TC environment with the histogram method. (current-increasing, time = 27 hours.)

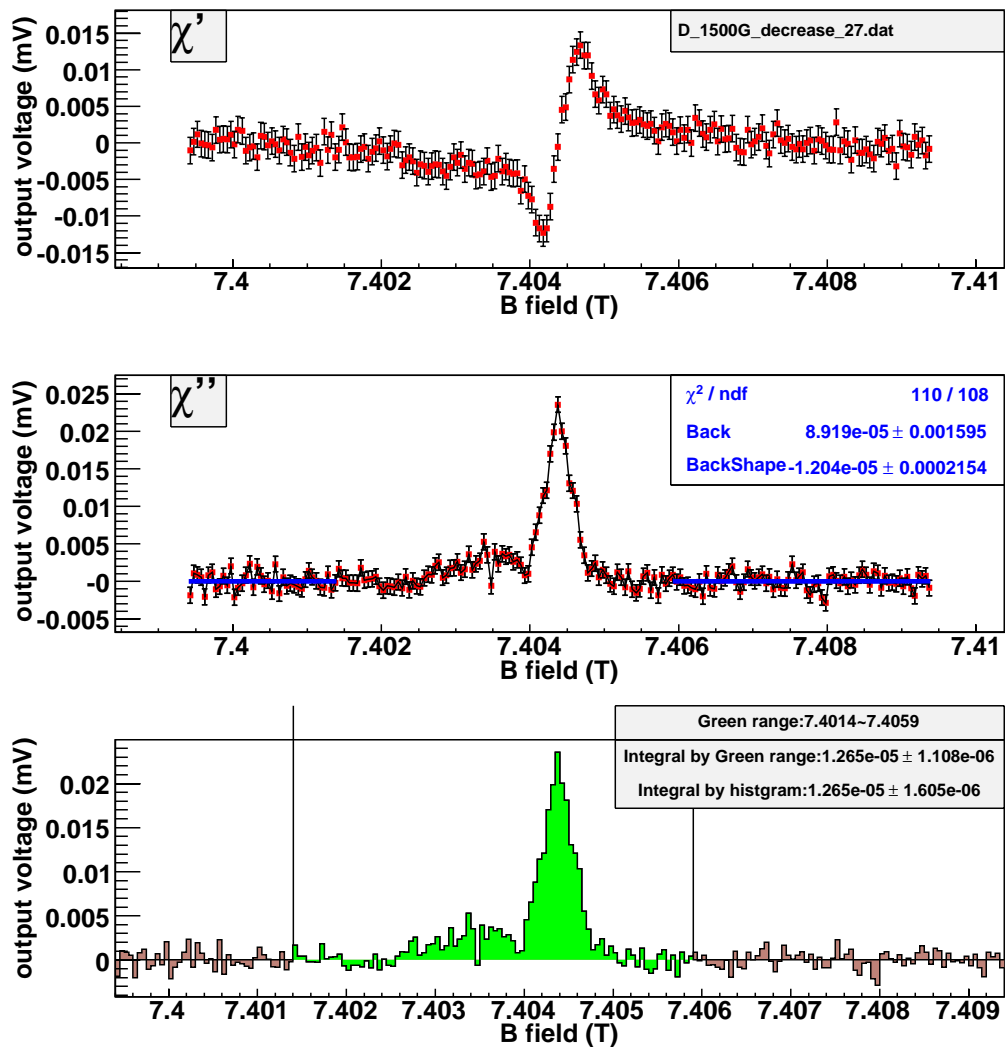


Figure B.34: Get the area of D signal at TC environment with the histogram method. (current-decreasing, time = 27 hours.)

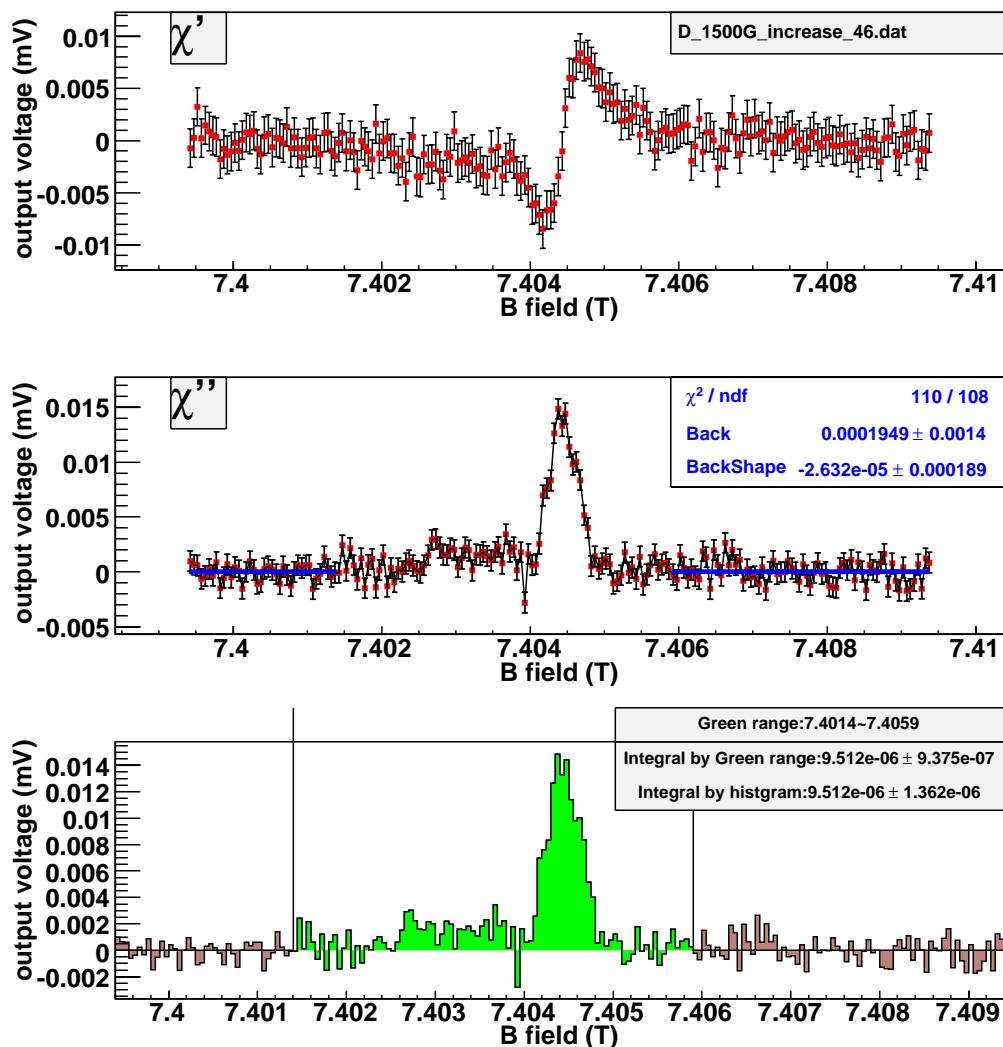


Figure B.35: Get the area of D signal at TC environment with the histogram method. (current-increasing, time = 46 hours.)

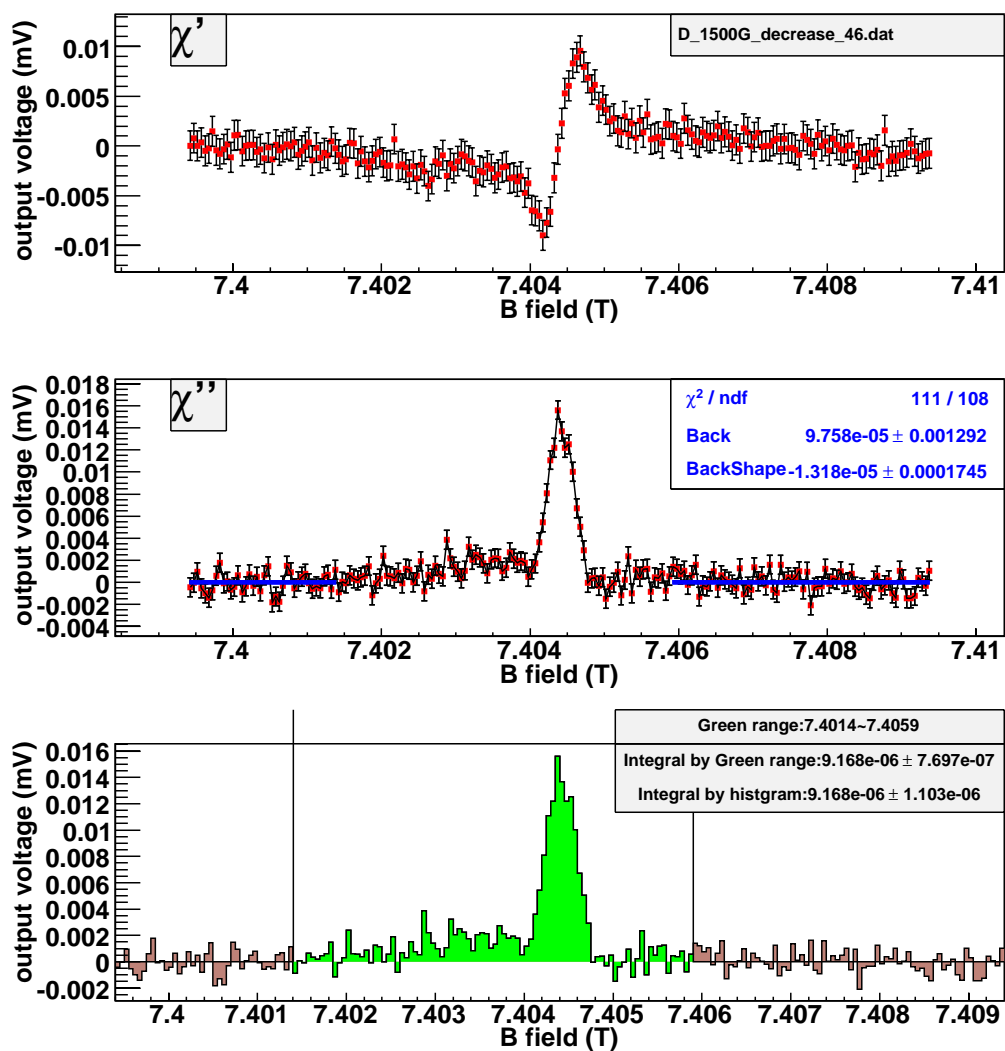


Figure B.36: Get the area of D signal at TC environment with the histogram method. (current-decreasing, time = 46 hours.)

The following pictures show estimation of the area of D signal at TC environment with the model method. The current-increasing data and current-decreasing data are analyzed, respectively.

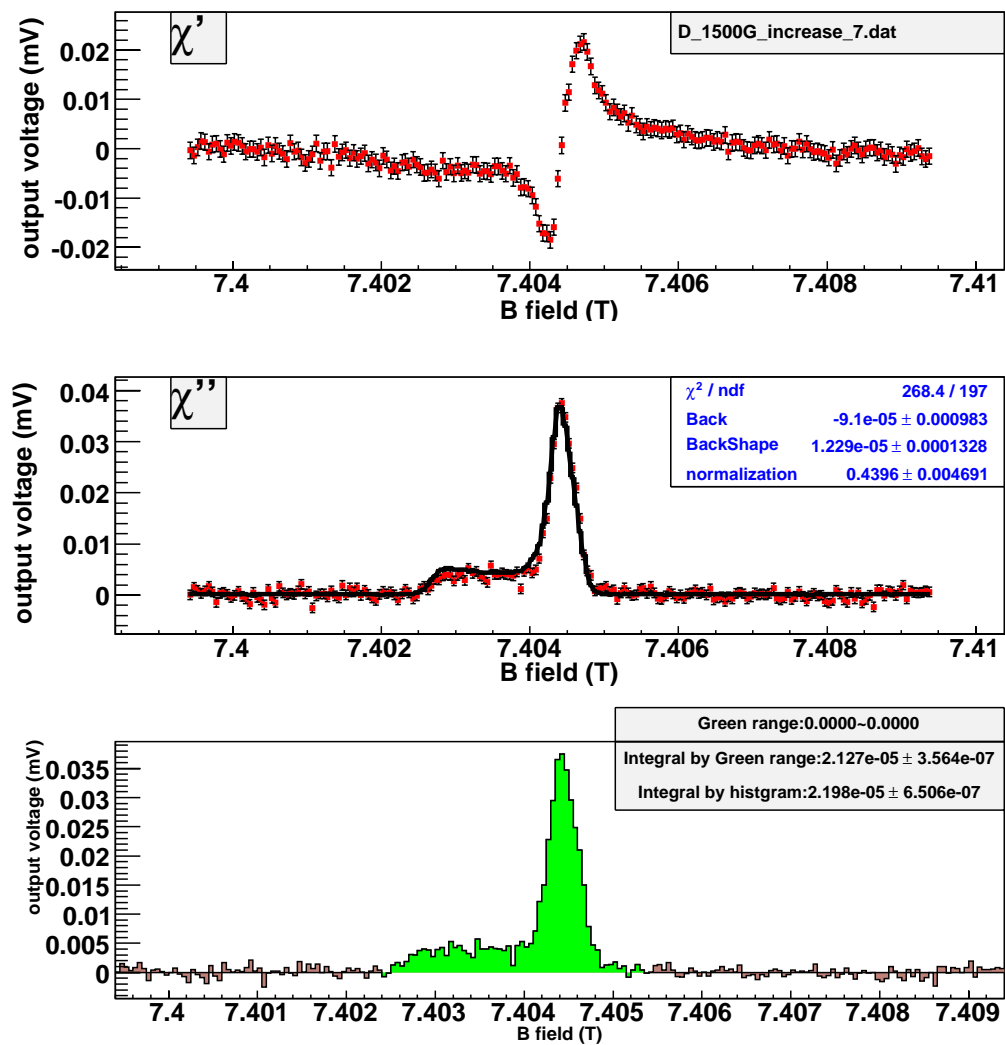


Figure B.37: Get the area of D signal at TC environment with the model method. (current-increasing, time = 7 hours.)

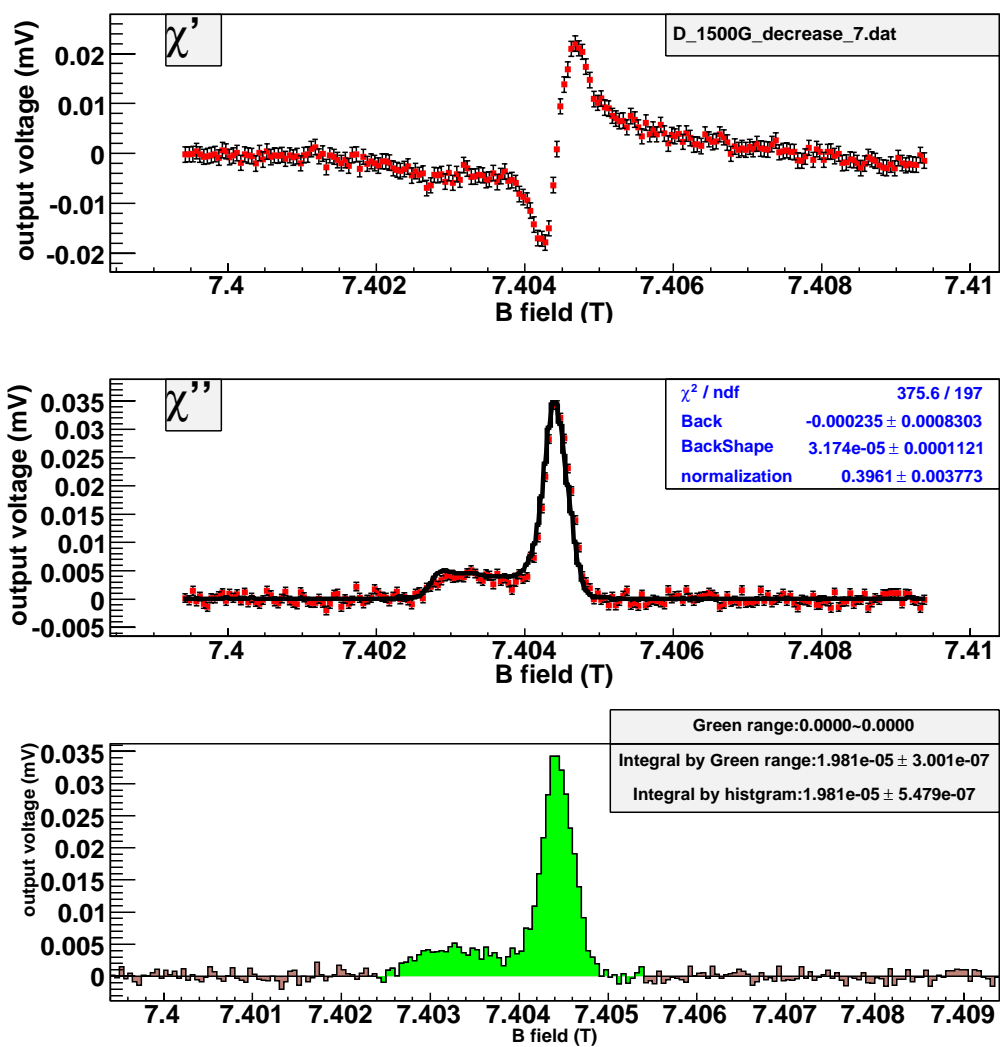


Figure B.38: Get the area of D signal at TC environment with the model method. (current-decreasing, time = 7 hours.)

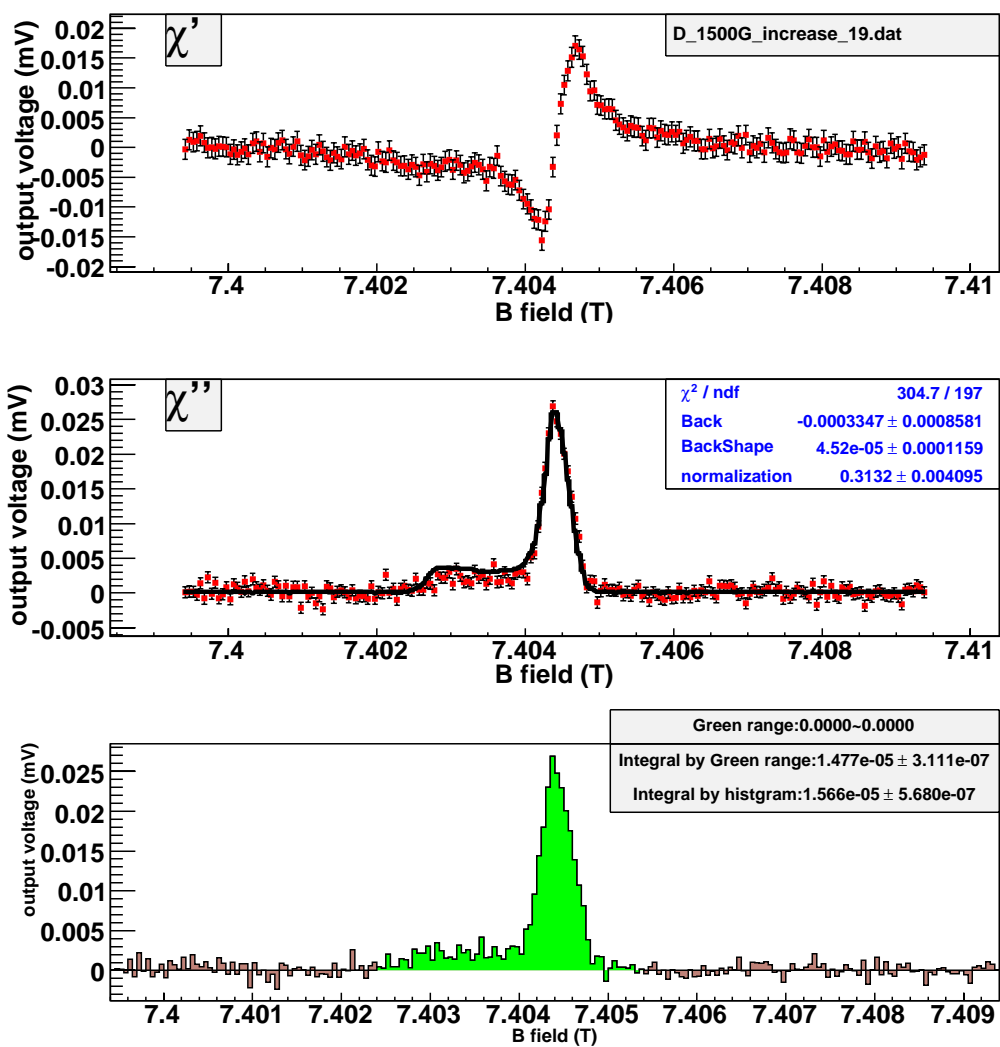


Figure B.39: Get the area of D signal at TC environment with the model method. (current-increasing, time = 19 hours.)

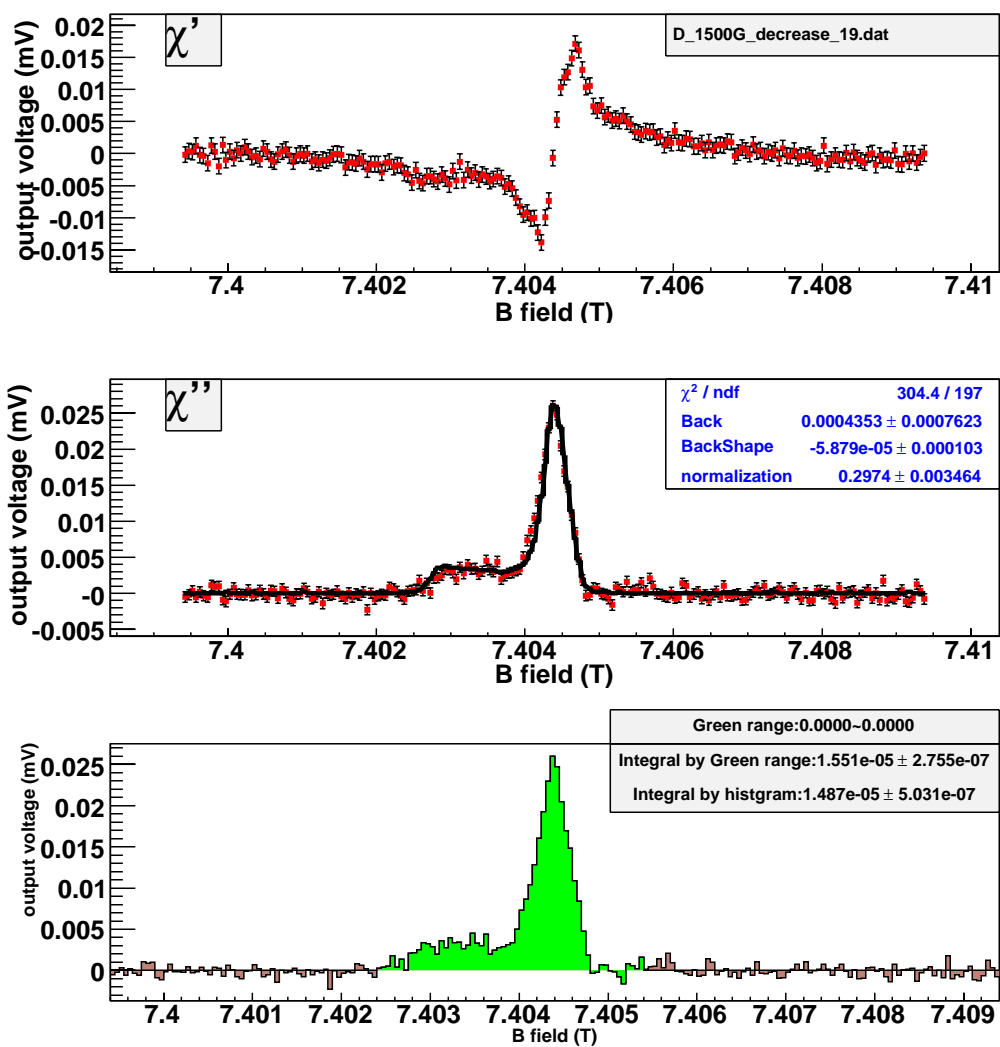


Figure B.40: Get the area of D signal at TC environment with the model method. (current-decreasing, time = 19 hours.)

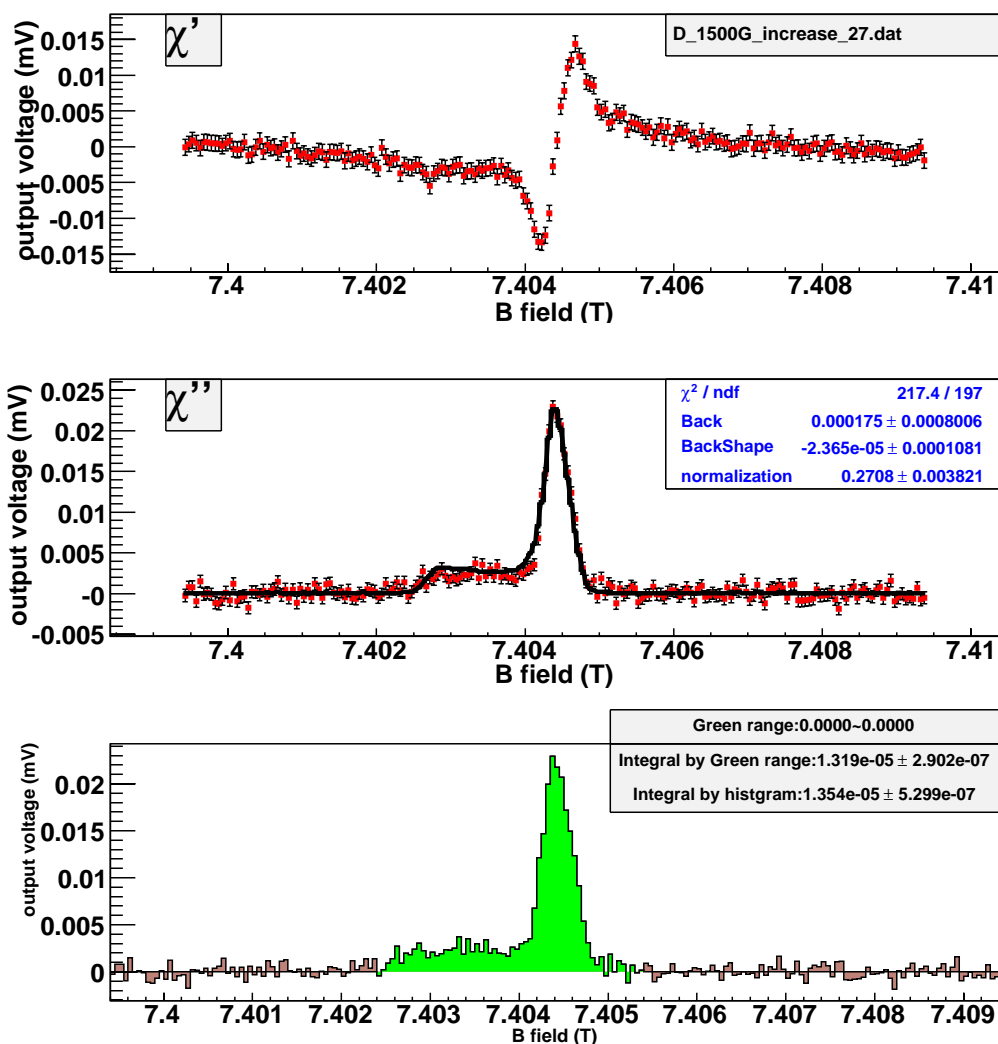


Figure B.41: Get the area of D signal at TC environment with the model method. (current-increasing, time = 27 hours.)

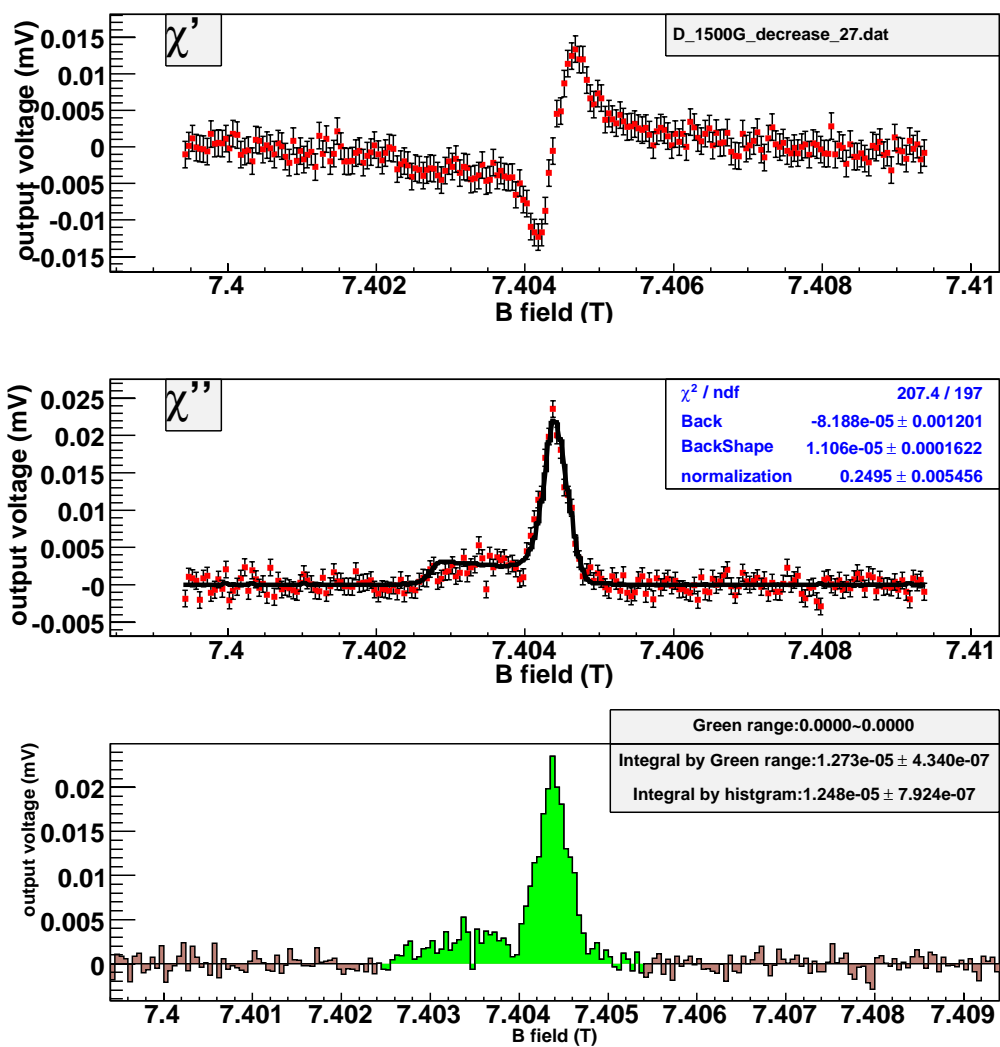


Figure B.42: Get the area of D signal at TC environment with the model method. (current-decreasing, time = 27 hours.)

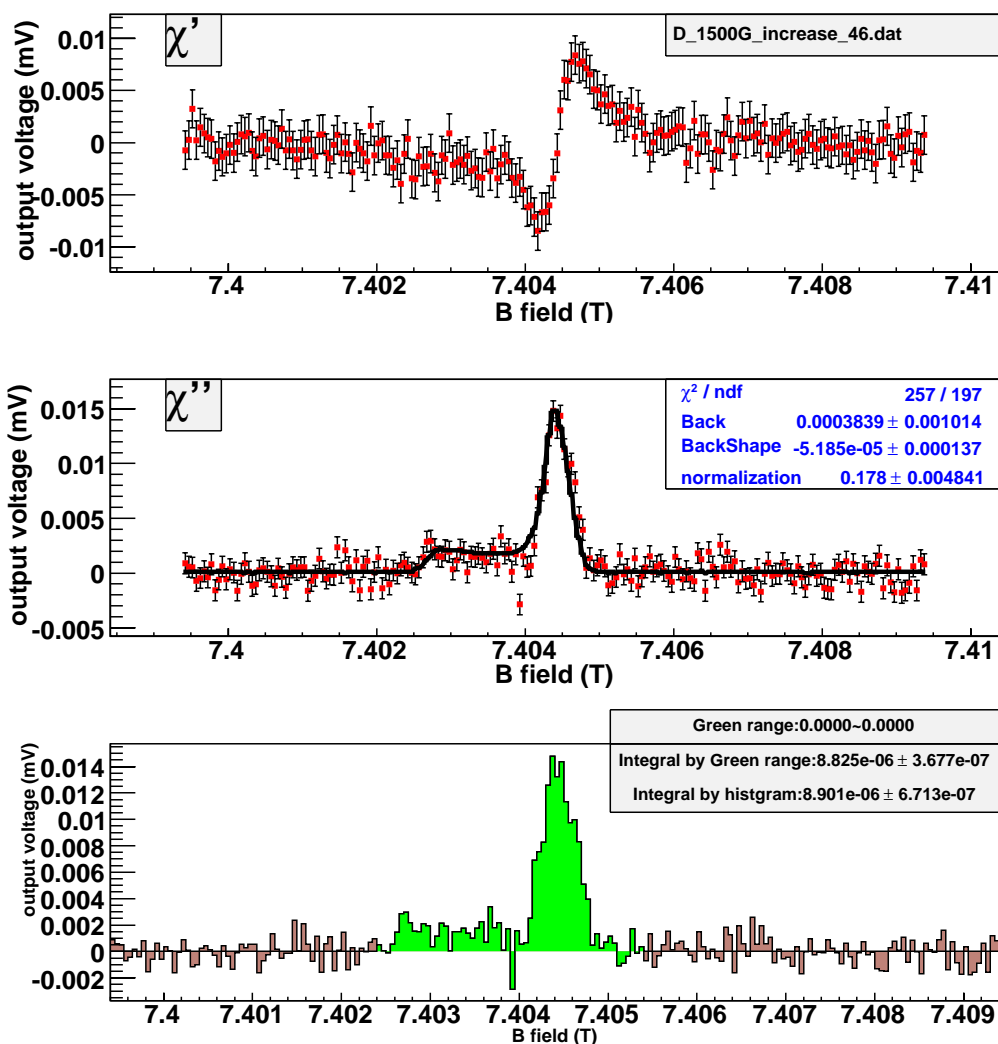


Figure B.43: Get the area of D signal at TC environment with the model method. (current-increasing, time = 46 hours.)

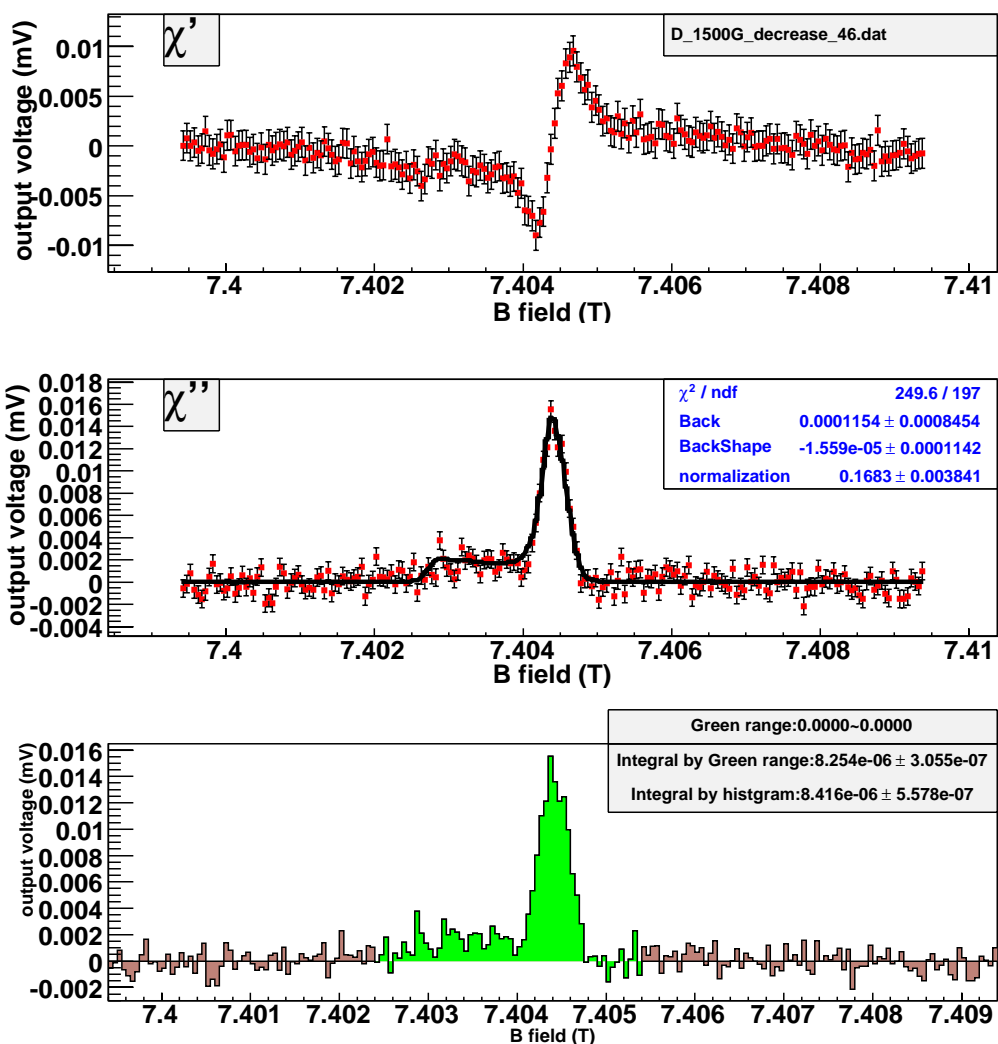


Figure B.44: Get the area of D signal at TC environment with the model method. (current-decreasing, time = 46 hours.)

The following pictures show estimation of the area of H signal at SC environment with the histogram method. The current-increasing data and current-decreasing data are analyzed, respectively.

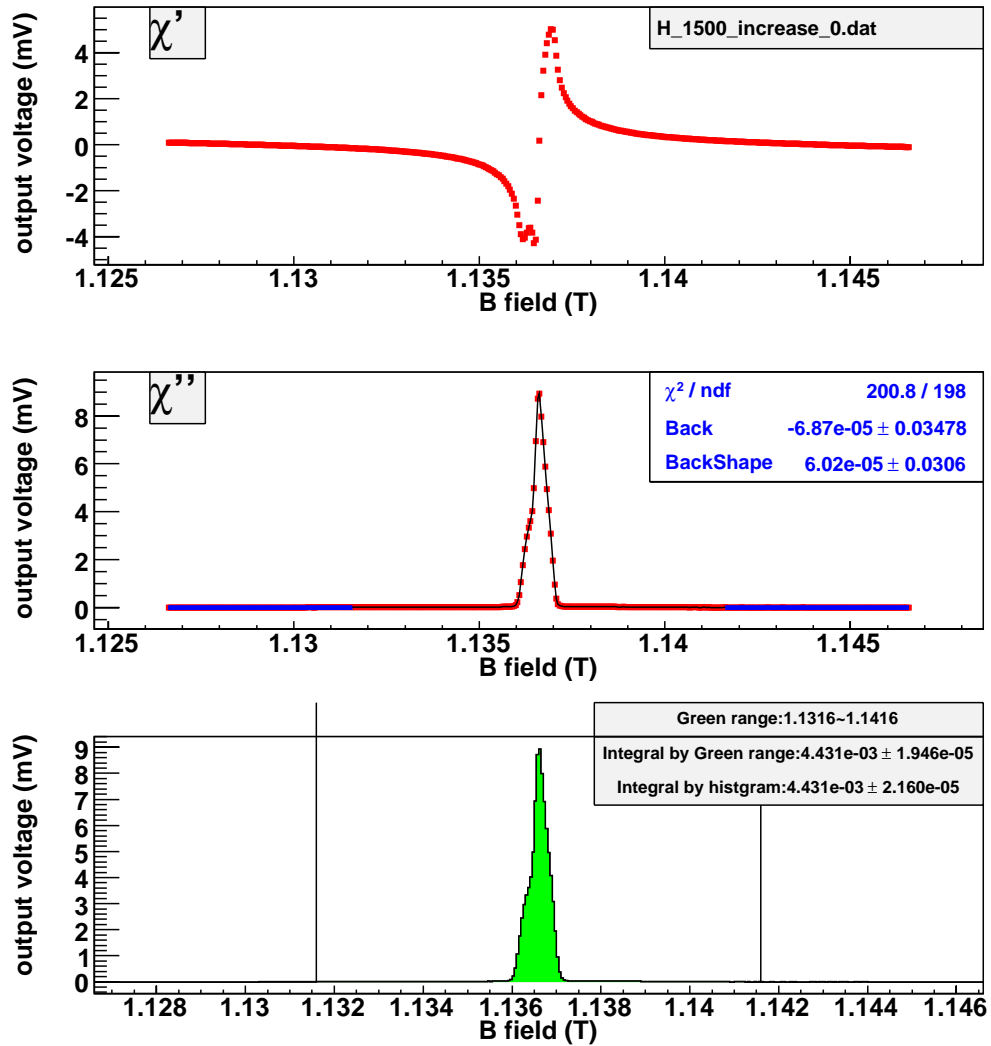


Figure B.45: Get the area of H signal at SC environment with the histogram method. (current-increasing, time = 0 hours.)

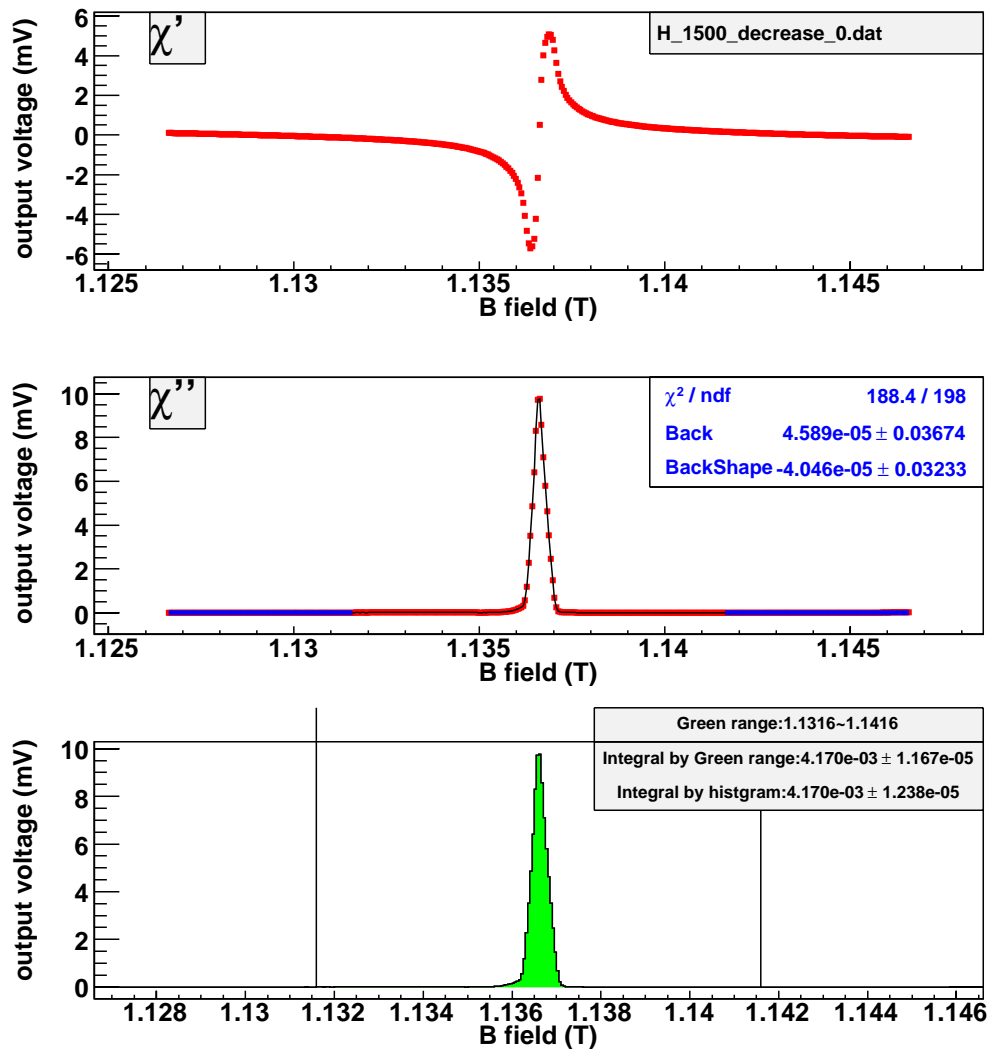


Figure B.46: Get the area of H signal at SC environment with the histogram method. (current-decreasing, time = 0 hours.)

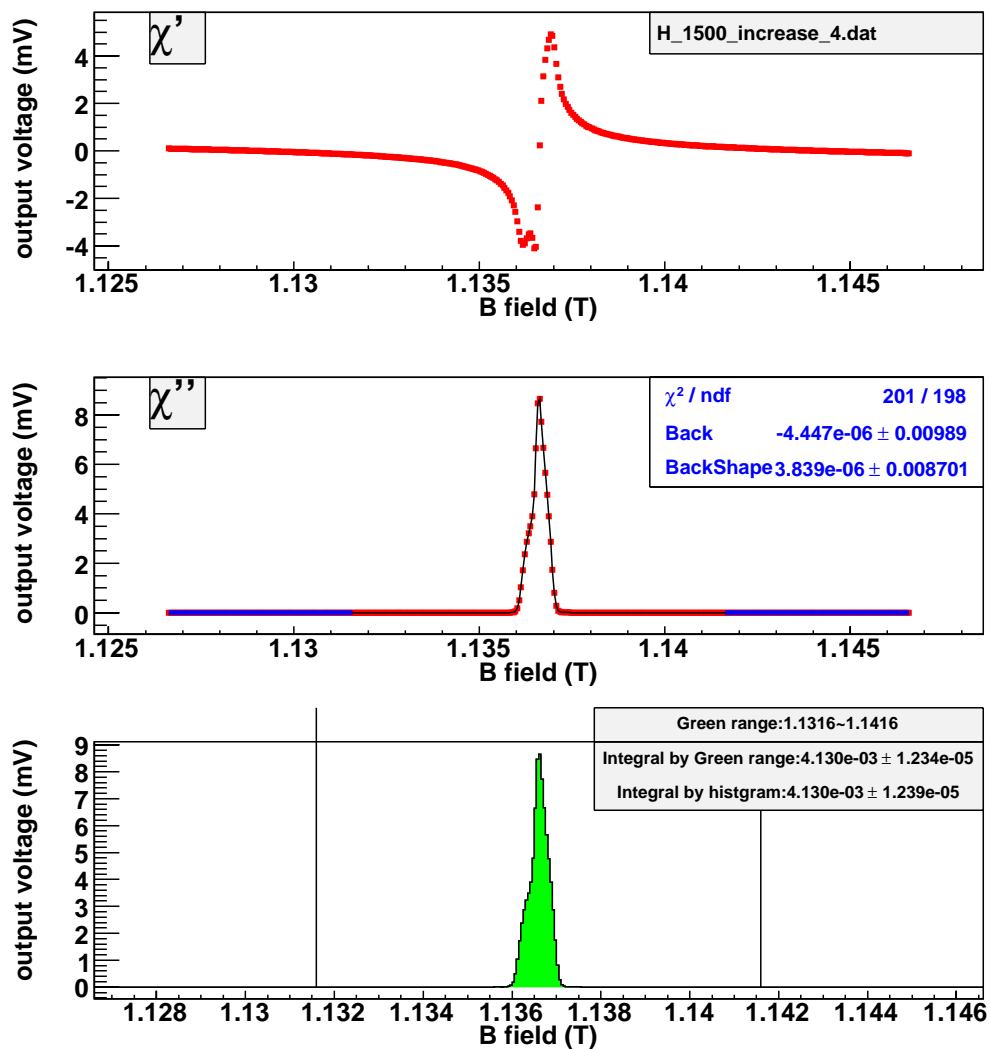


Figure B.47: Get the area of H signal at SC environment with the histogram method. (current-increasing, time = 4 hours.)

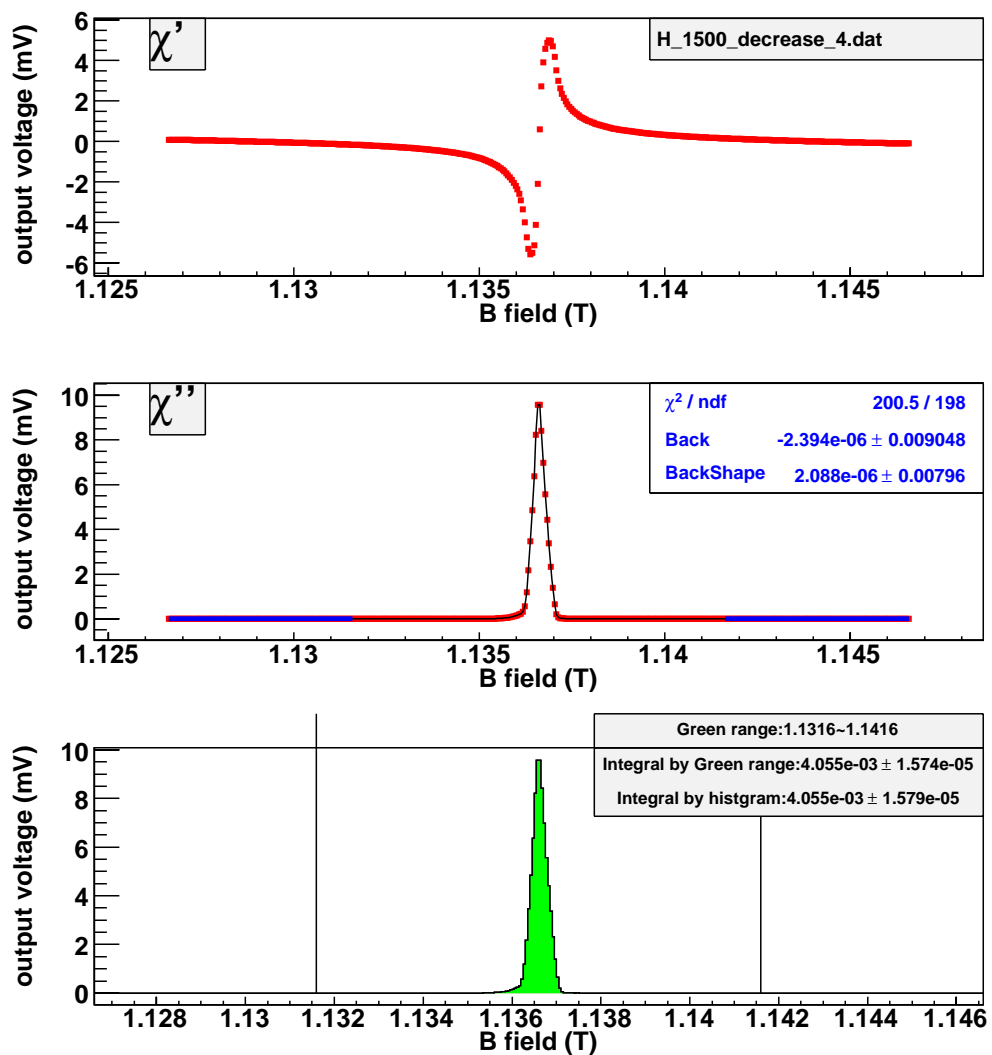


Figure B.48: Get the area of H signal at SC environment with the histogram method. (current-decreasing, time = 4 hours.)

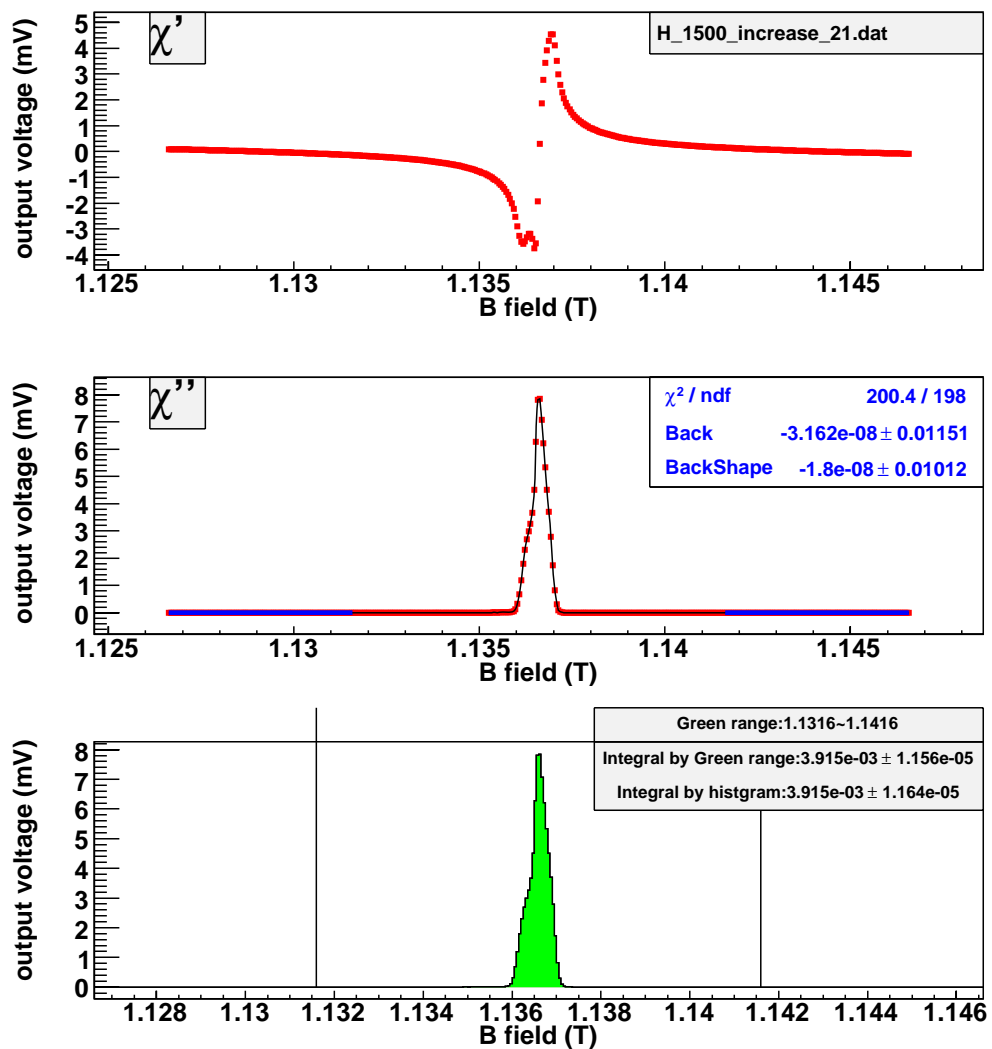


Figure B.49: Get the area of H signal at SC environment with the histogram method. (current-increasing, time = 21 hours.)

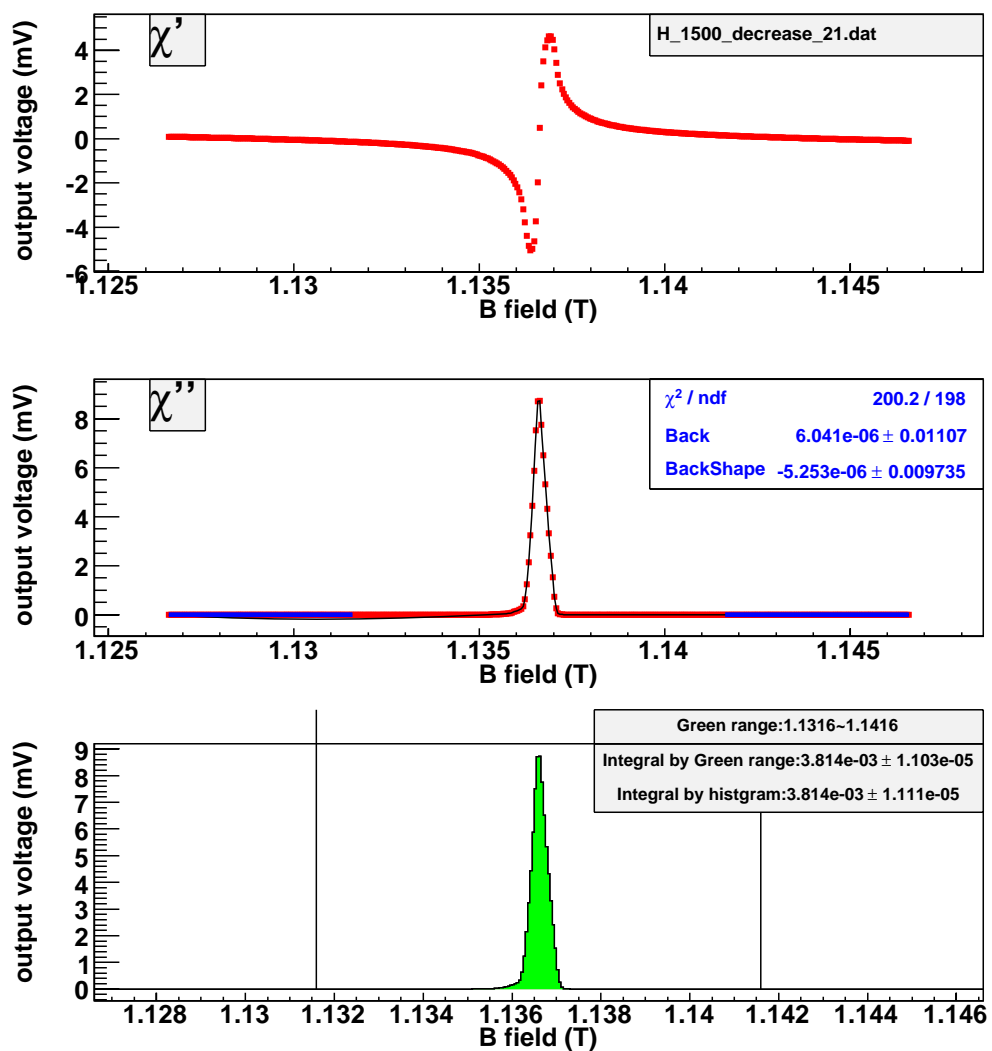


Figure B.50: Get the area of H signal at SC environment with the histogram method. (current-decreasing, time = 21 hours.)

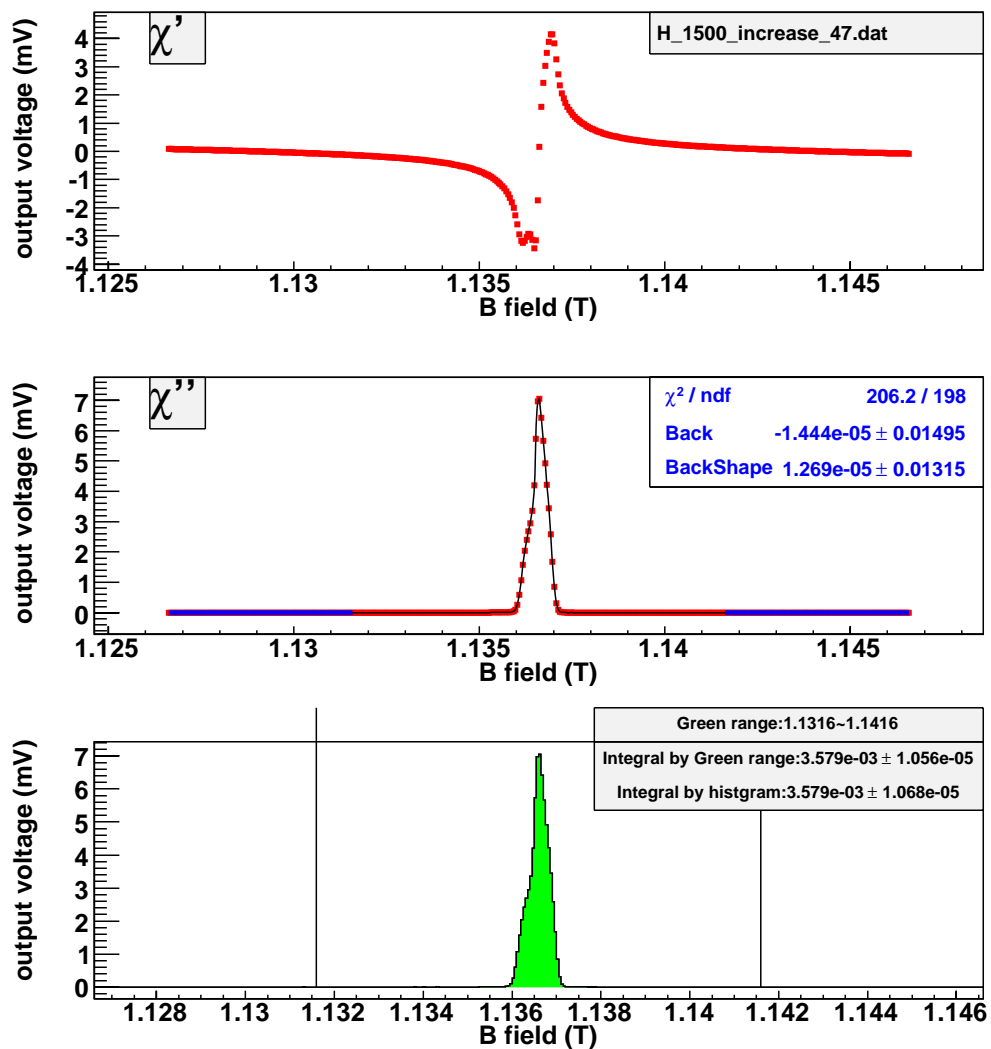


Figure B.51: Get the area of H signal at SC environment with the histogram method. (current-increasing, time = 47 hours.)

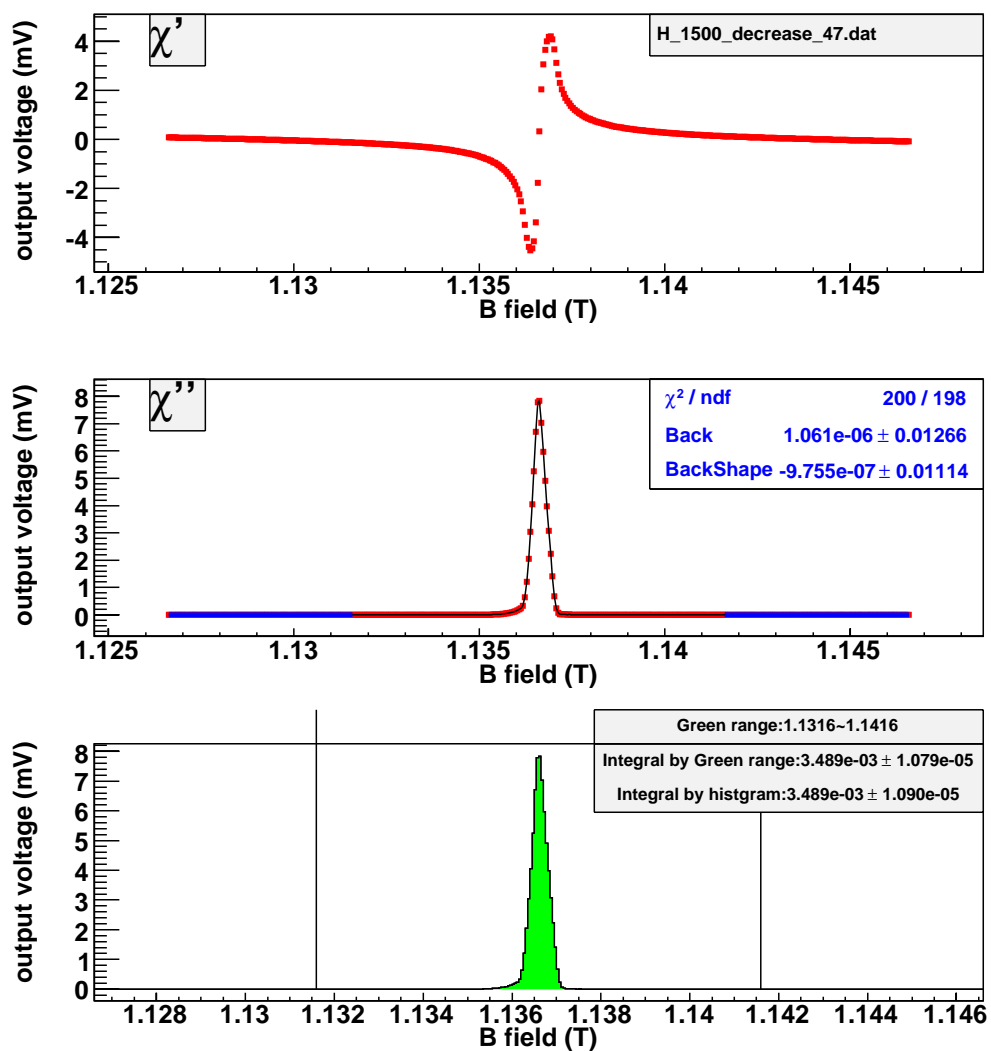


Figure B.52: Get the area of H signal at SC environment with the histogram method. (current-decreasing, time = 47 hours.)

The following pictures show estimation of the area of H signal at SC environment with the model method. The current-increasing data and current-decreasing data are analyzed, respectively.

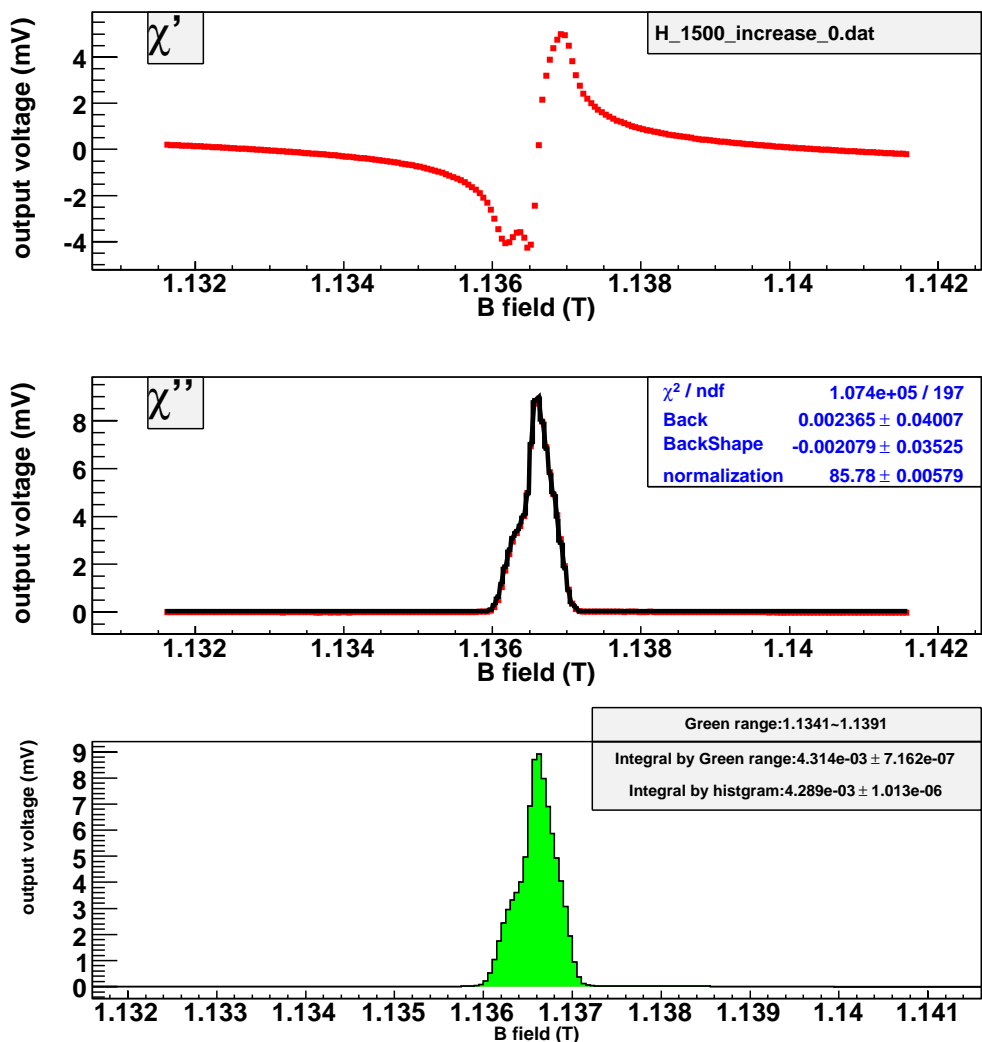


Figure B.53: Get the area of H signal at SC environment with the model method. (current-increasing, time = 0 hours.)

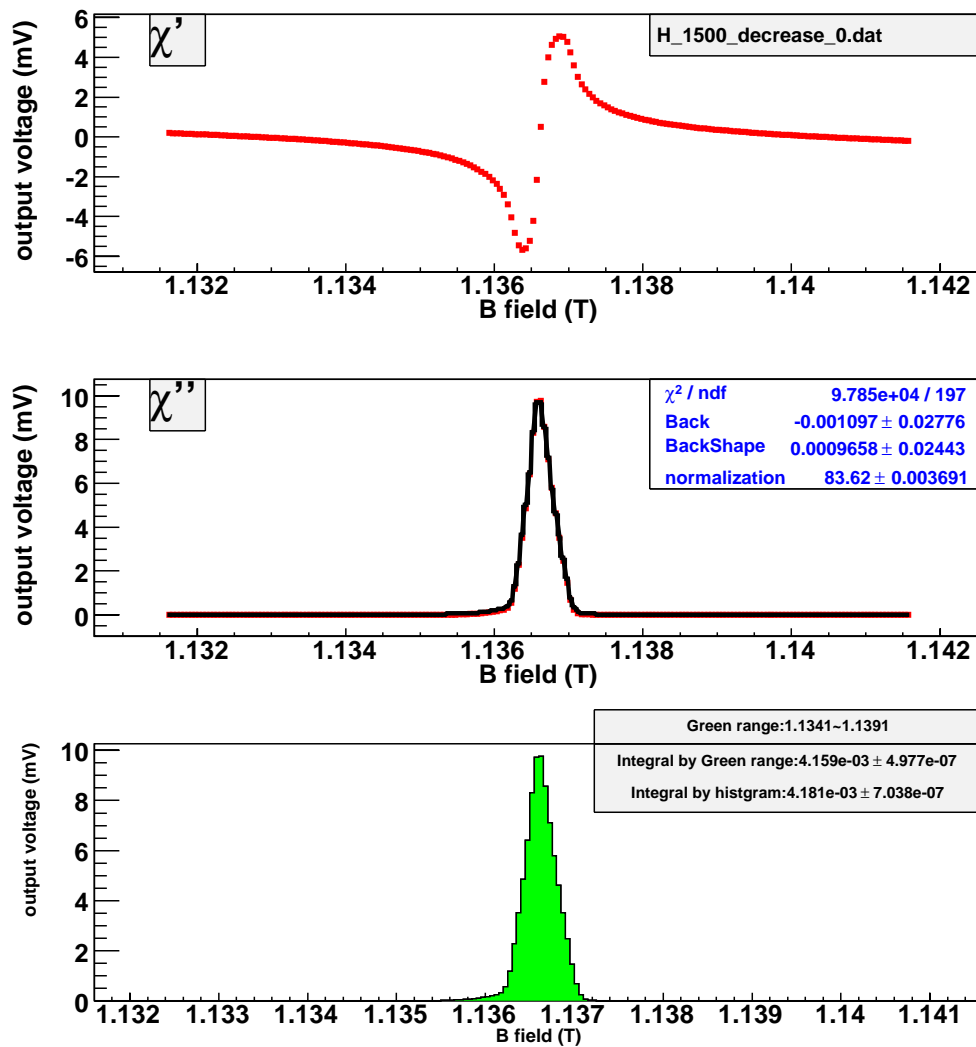


Figure B.54: Get the area of H signal at SC environment with the model method. (current-decreasing, time = 0 hours.)

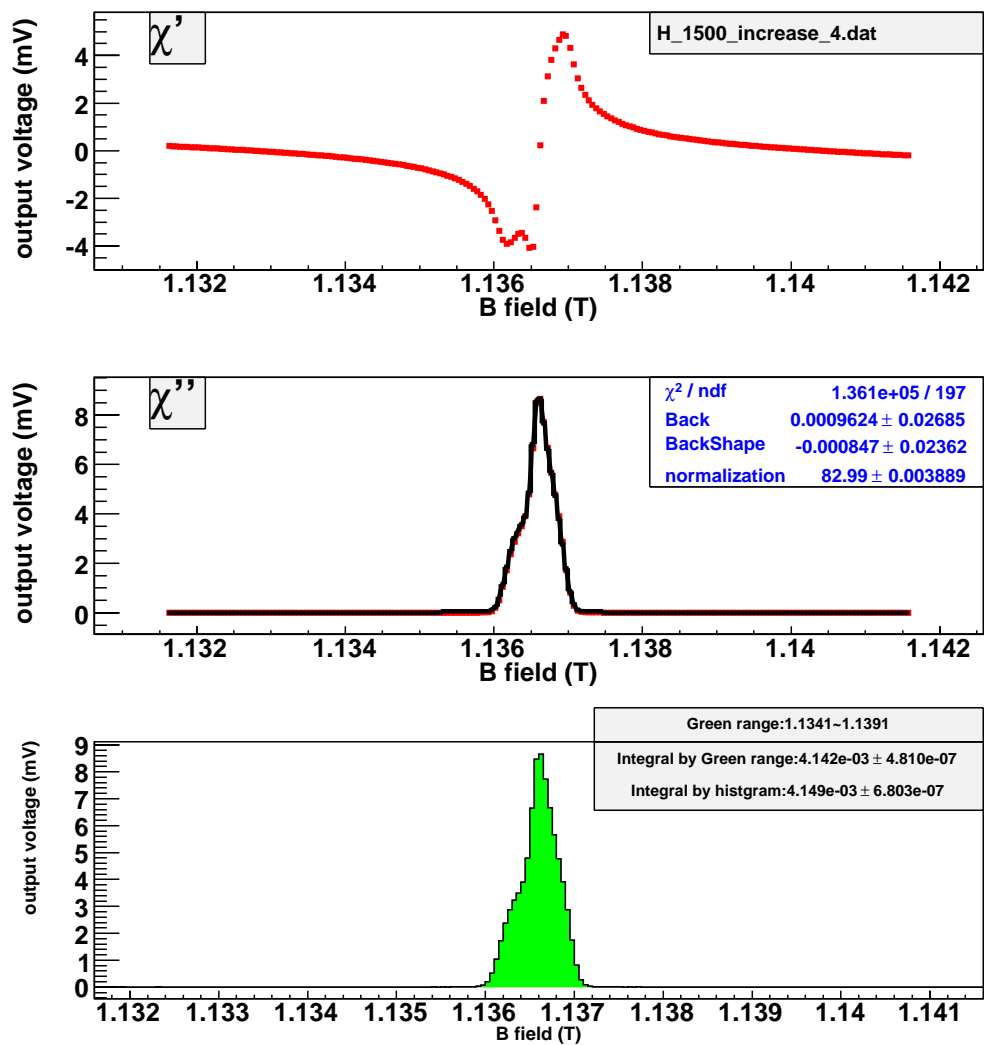


Figure B.55: Get the area of H signal at SC environment with the model method. (current-increasing, time = 4 hours.)

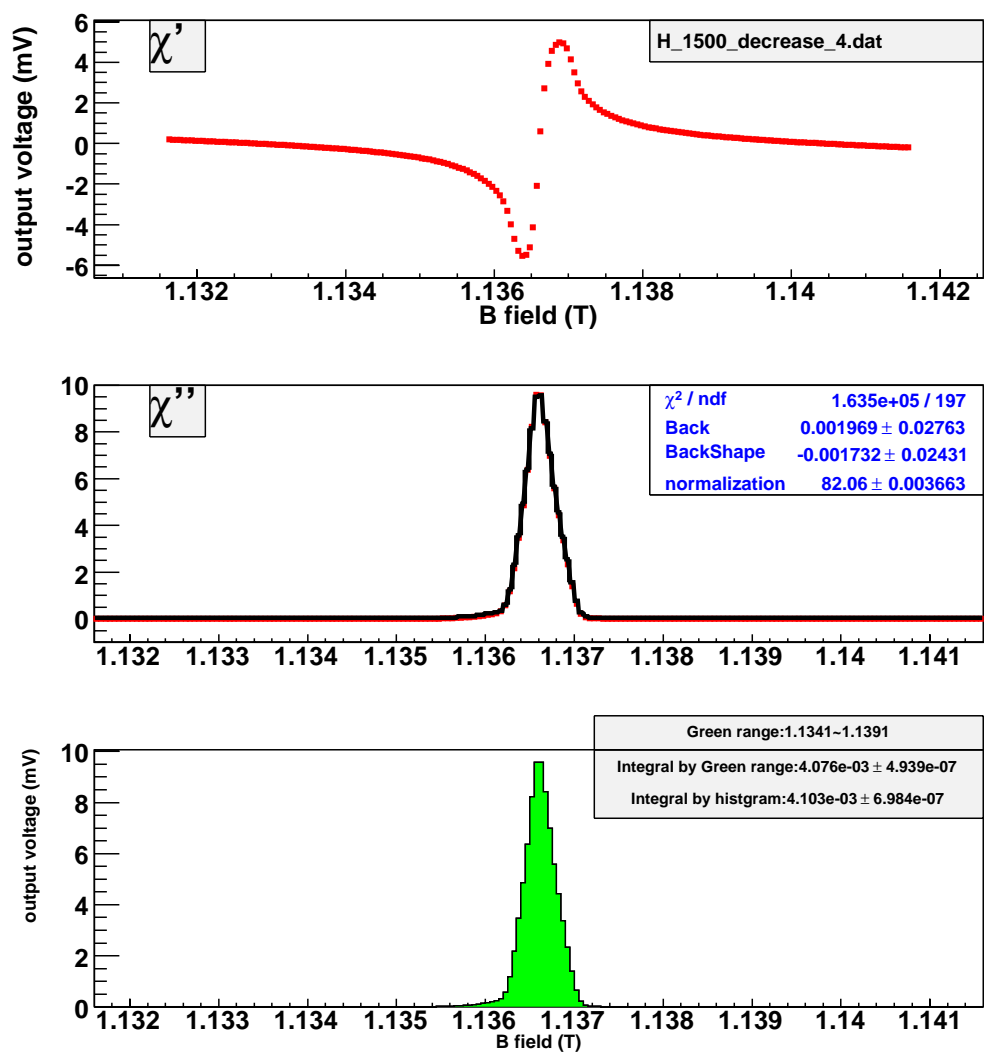


Figure B.56: Get the area of H signal at SC environment with the model method. (current-decreasing, time = 4 hours.)

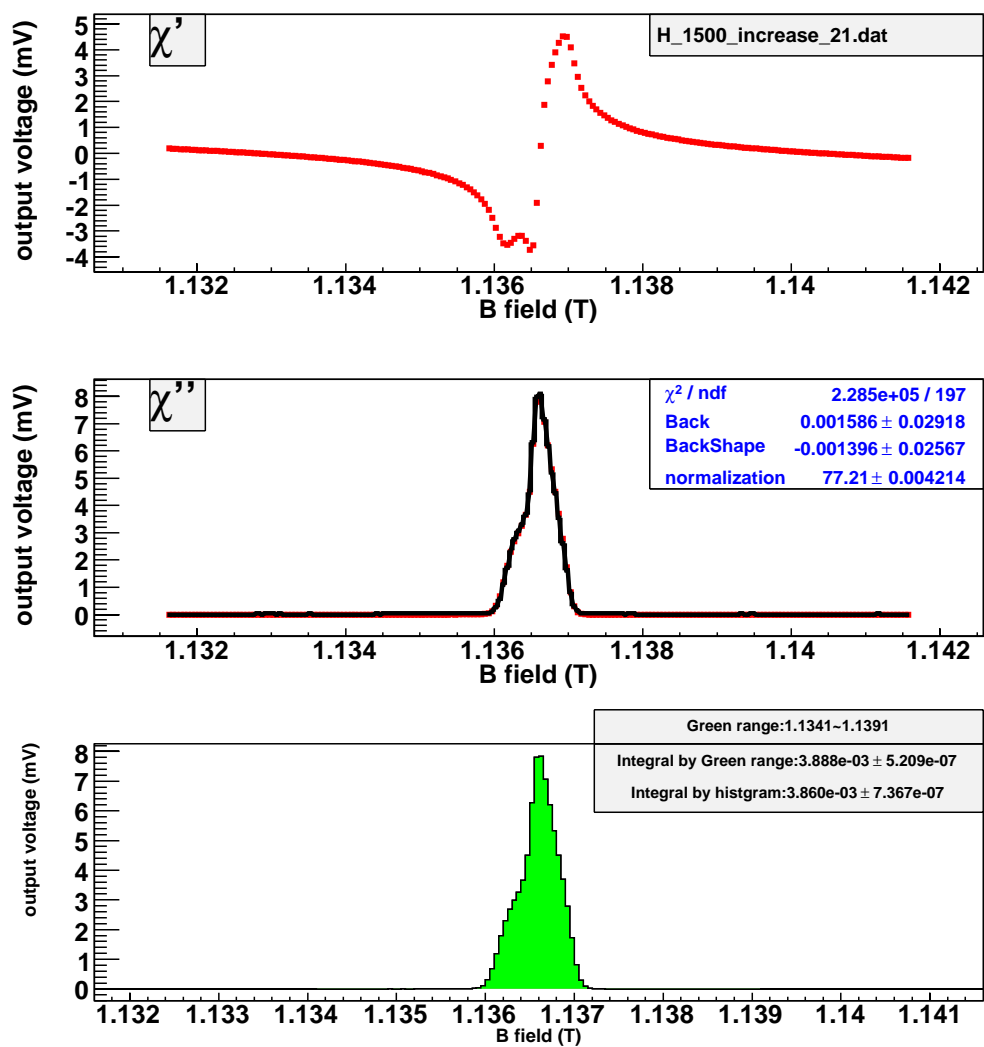


Figure B.57: Get the area of H signal at SC environment with the model method. (current-increasing, time = 21 hours.)

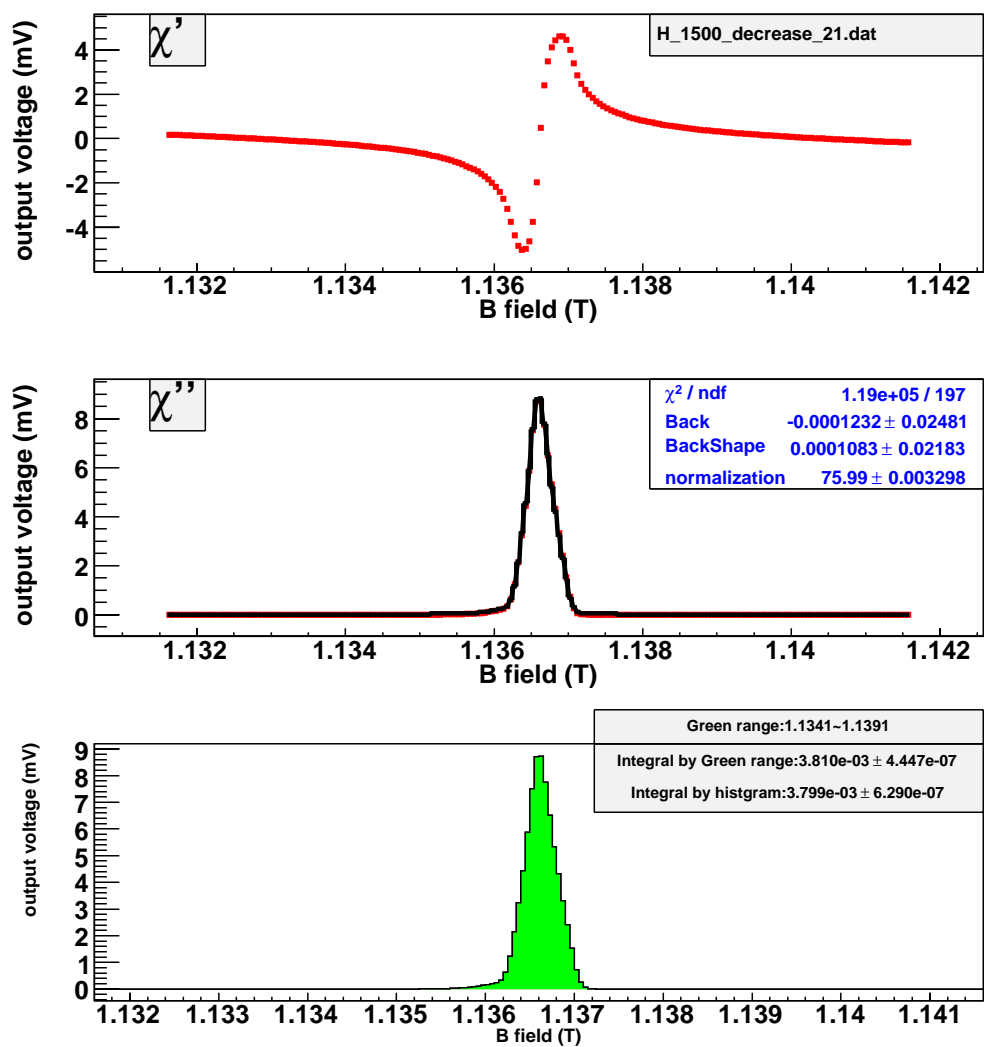


Figure B.58: Get the area of H signal at SC environment with the model method. (current-decreasing, time = 21 hours.)

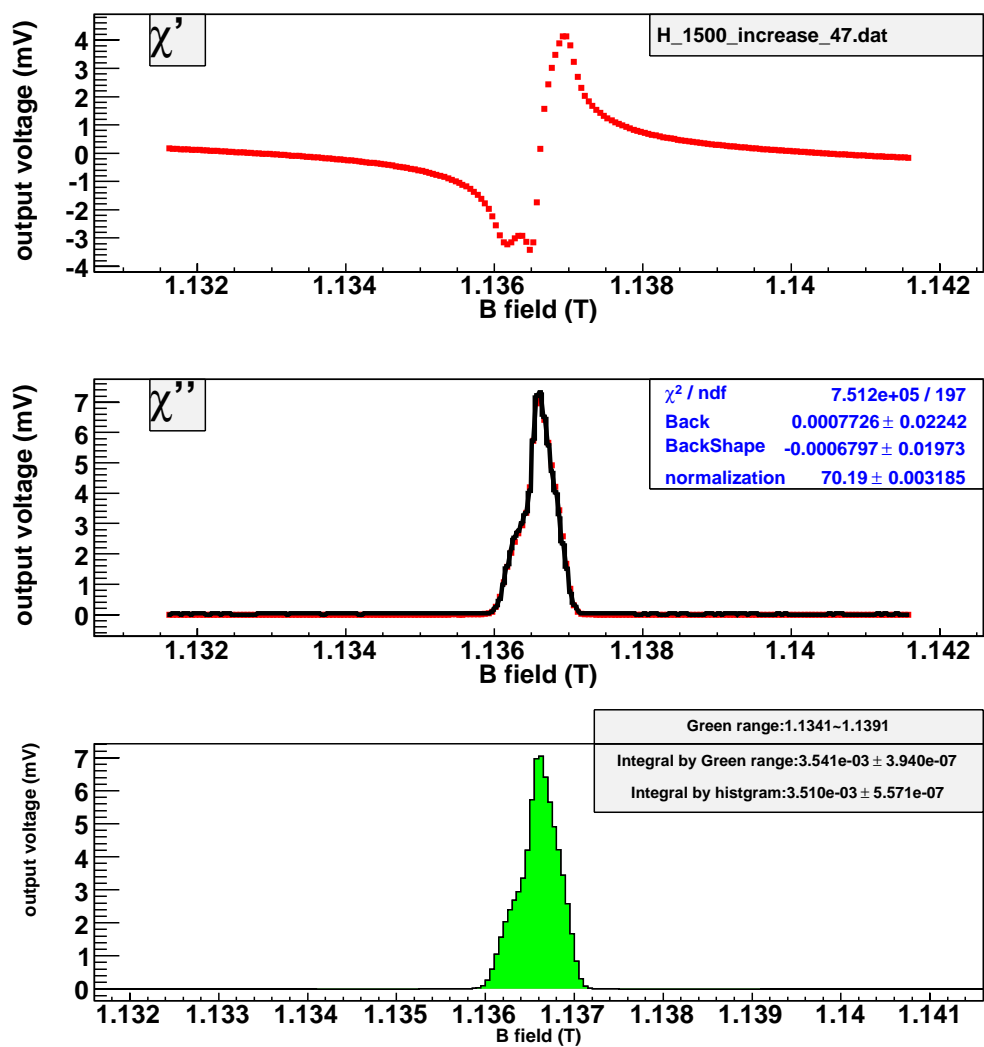


Figure B.59: Get the area of H signal at SC environment with the model method. (current-increasing, time = 47 hours.)

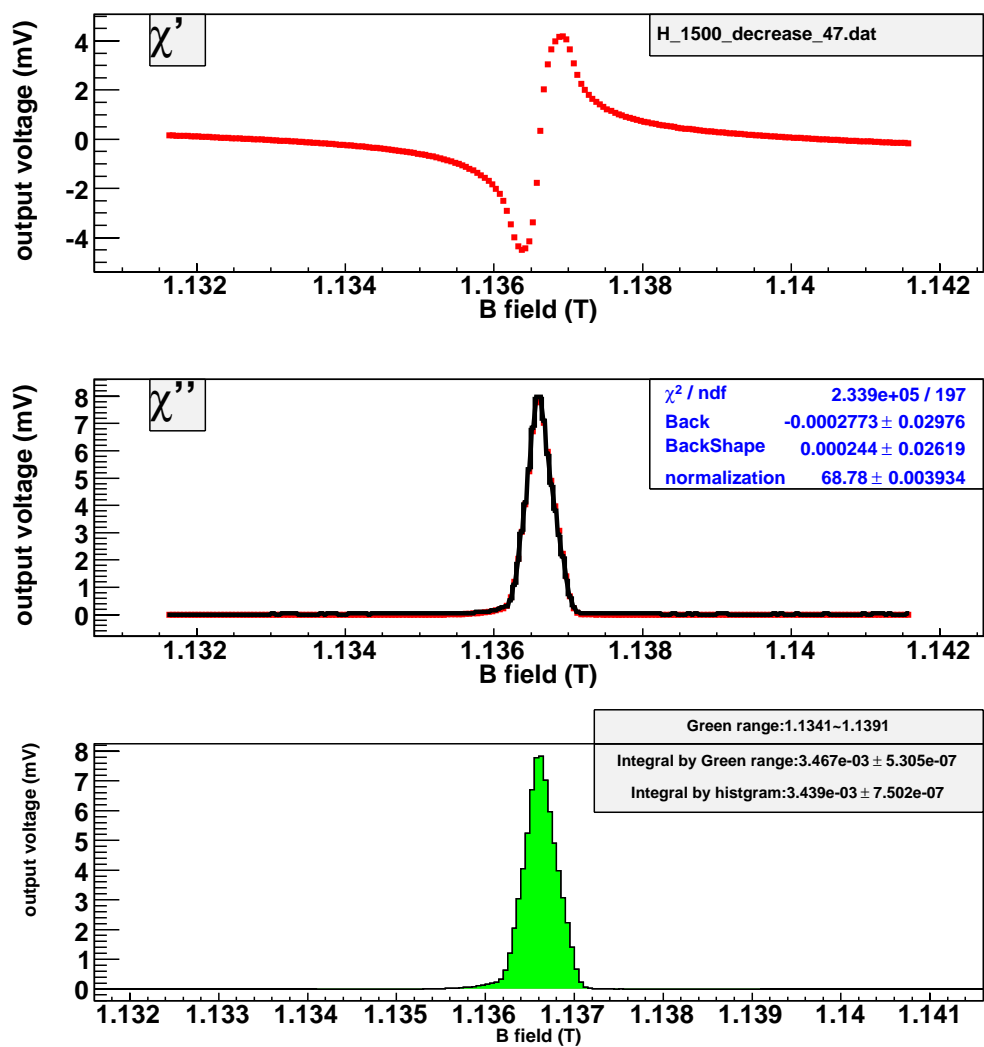


Figure B.60: Get the area of H signal at SC environment with the model method. (current-decreasing, time = 47 hours.)

The following pictures show estimation of the area of H signal at TC environment with the histogram method. The current-increasing data and current-decreasing data are analyzed, respectively.

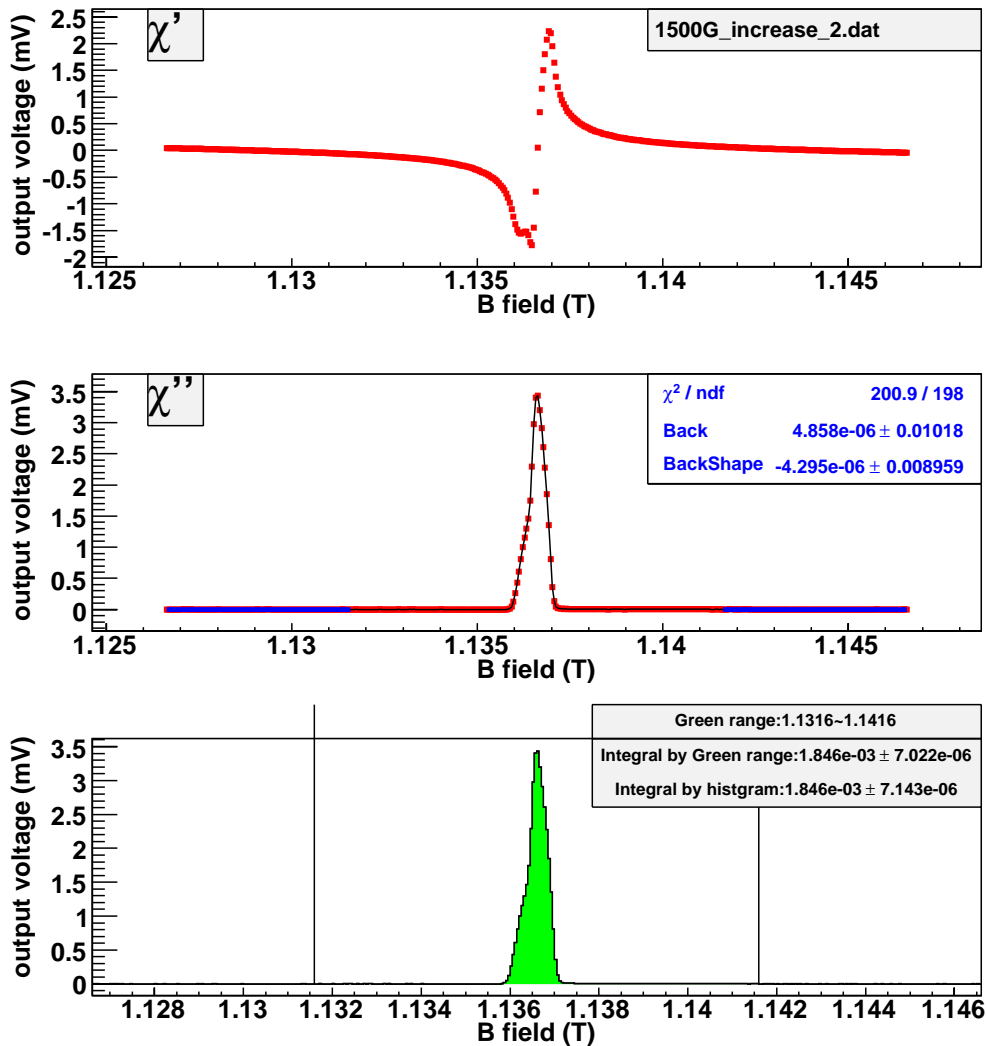


Figure B.61: Get the area of H signal at TC environment with the histogram method. (current-increasing, time = 2 hours.)

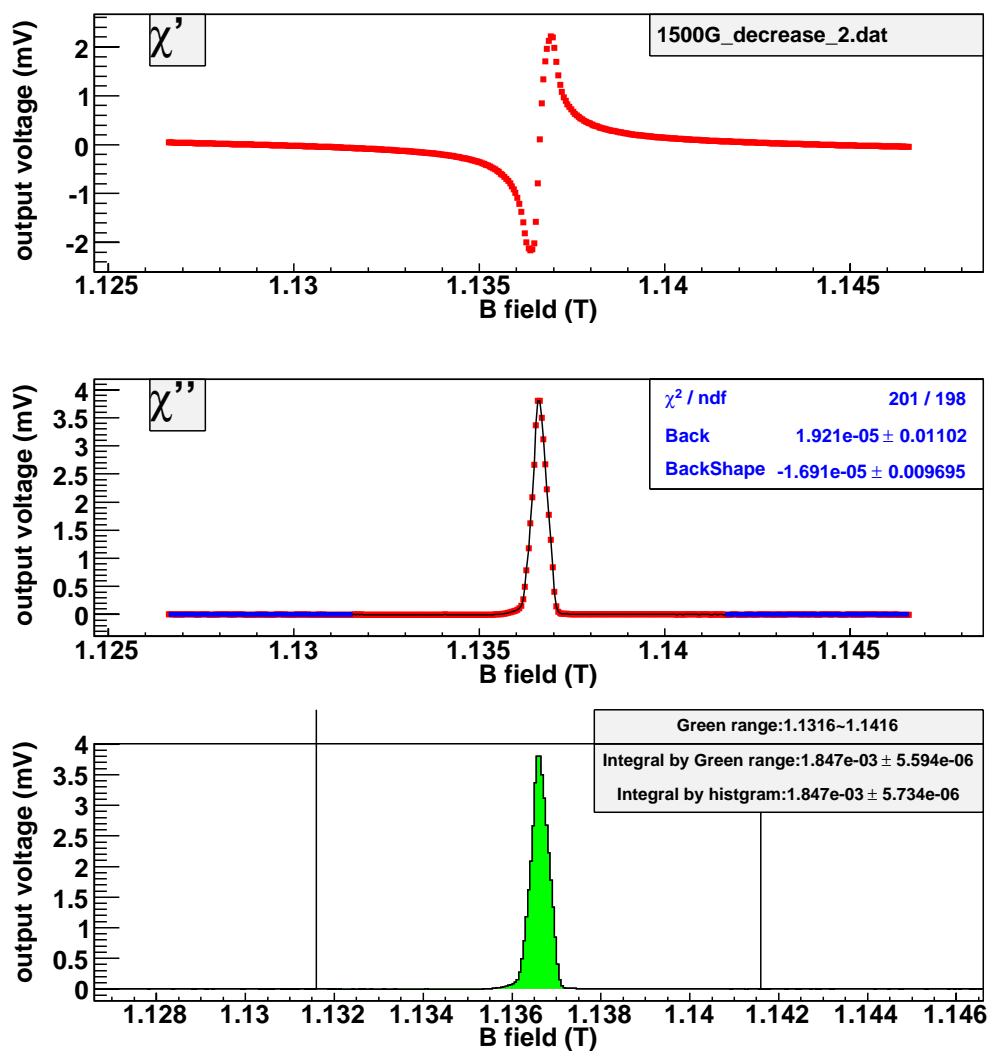


Figure B.62: Get the area of H signal at TC environment with the histogram method. (current-decreasing, time = 2 hours.)

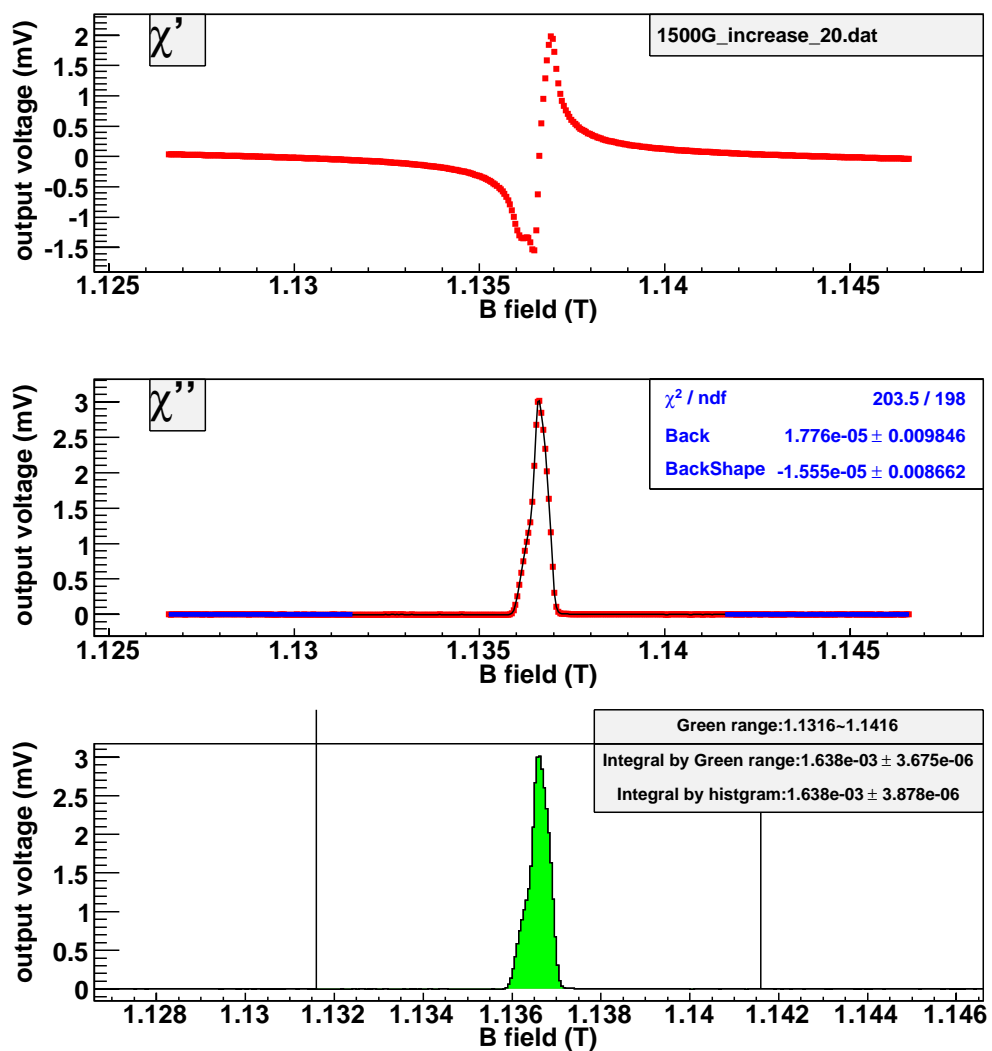


Figure B.63: Get the area of H signal at TC environment with the histogram method. (current-increasing, time = 20 hours.)

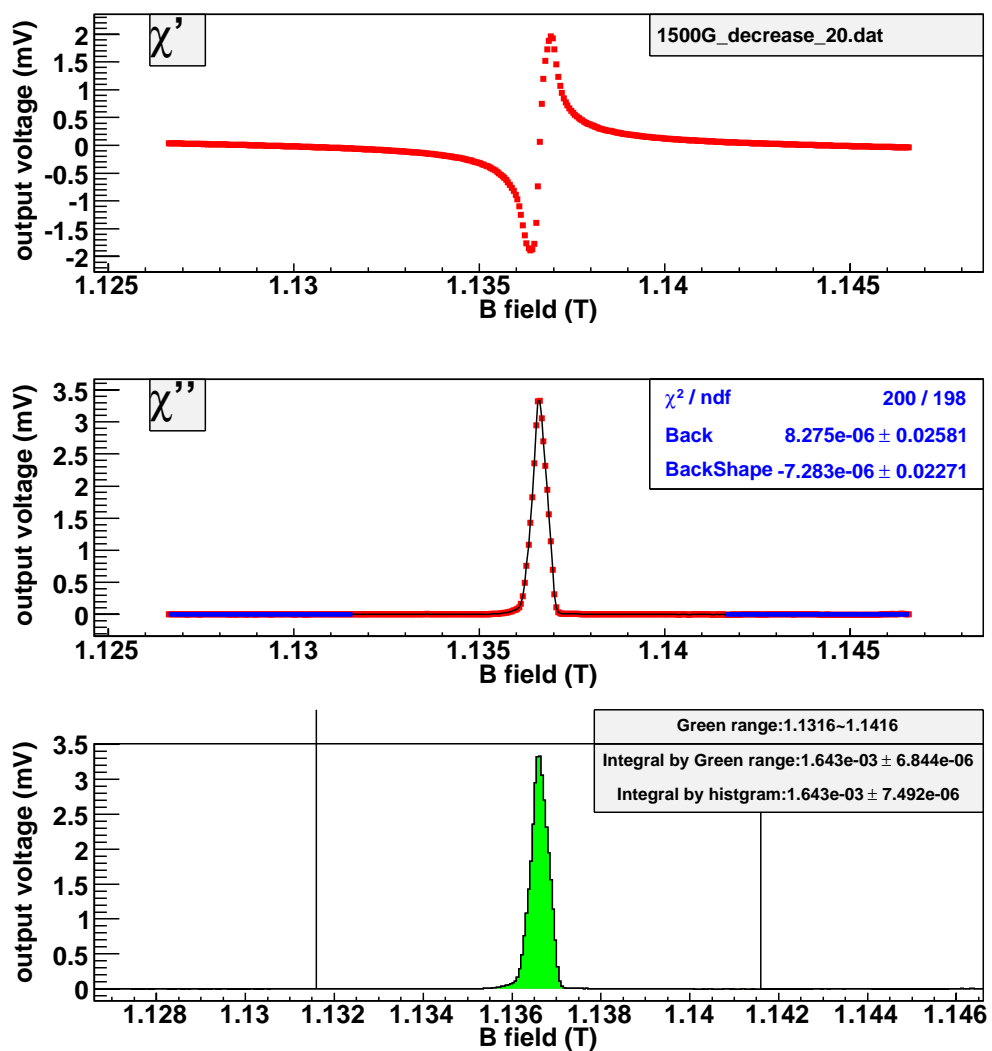


Figure B.64: Get the area of H signal at TC environment with the histogram method. (current-decreasing, time = 20 hours.)

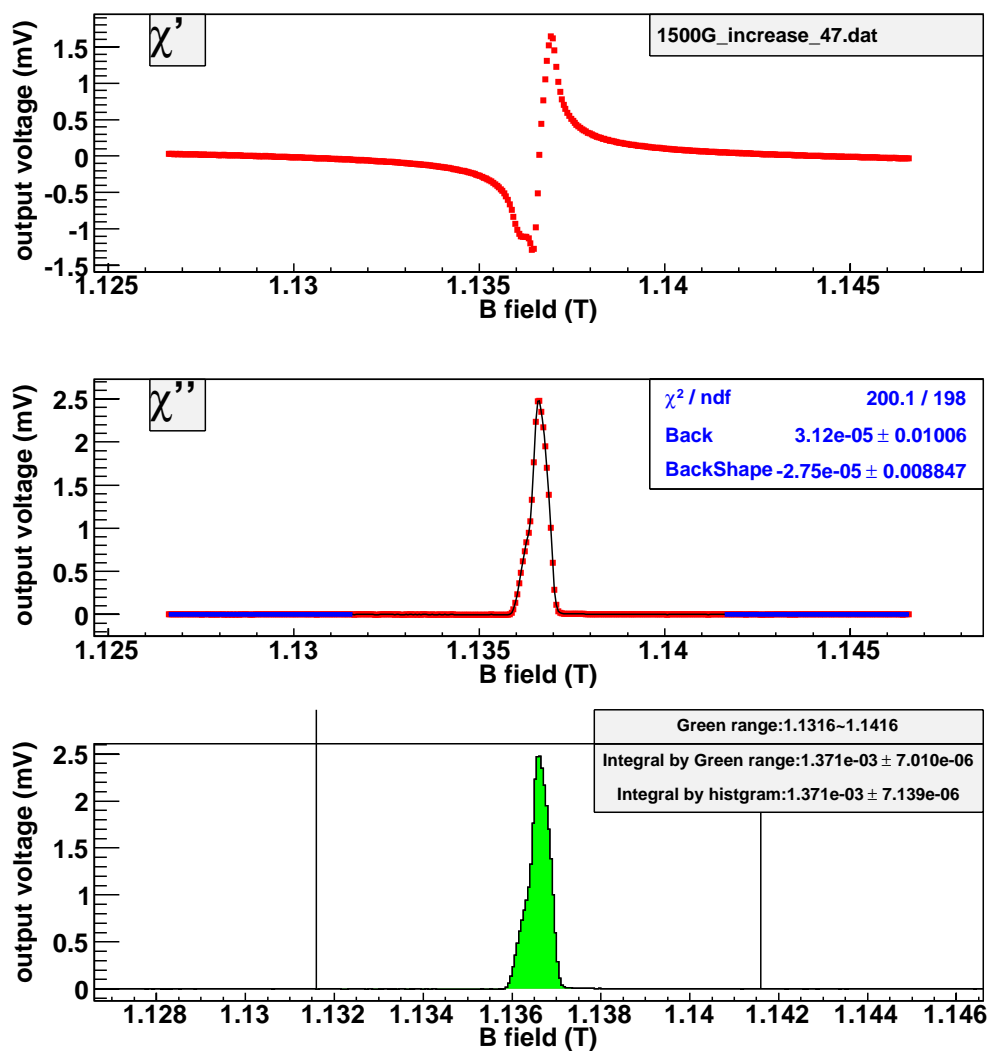


Figure B.65: Get the area of H signal at TC environment with the histogram method. (current-increasing, time = 47 hours.)

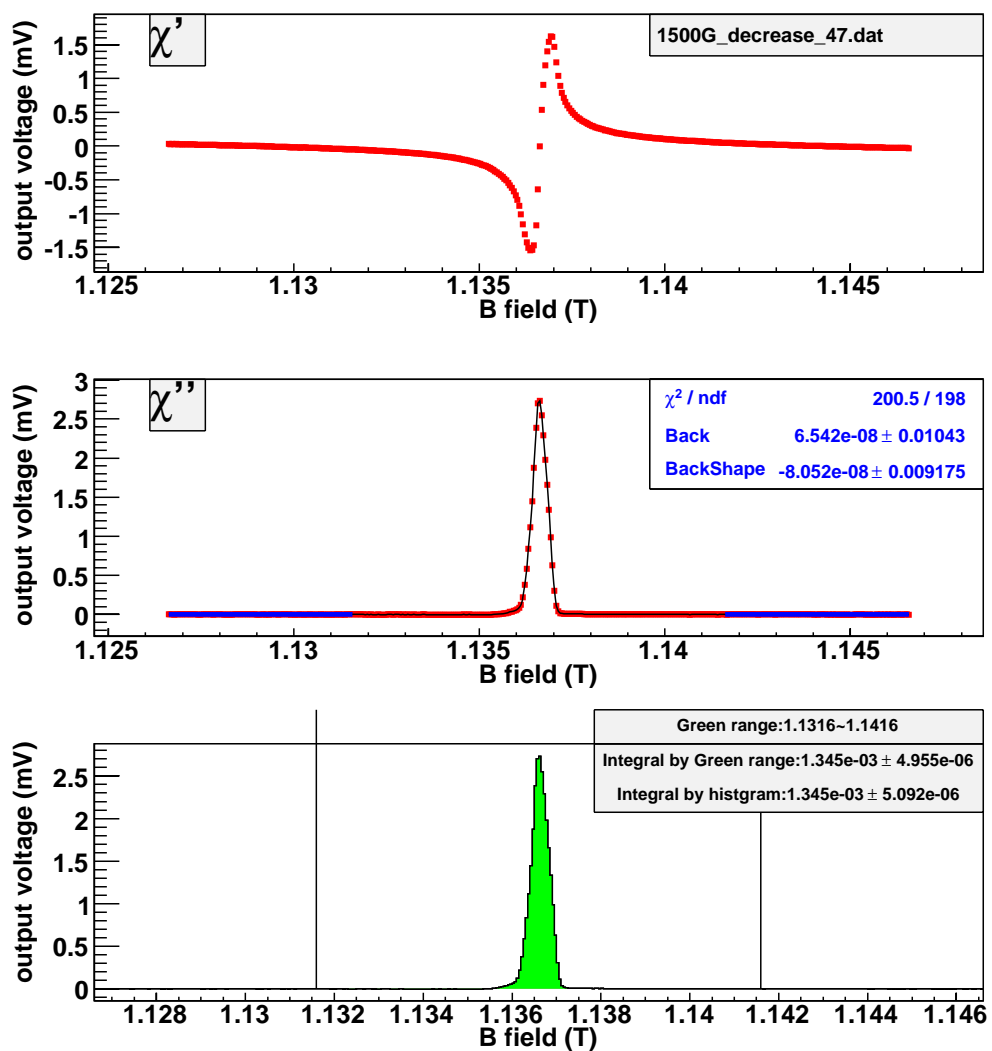


Figure B.66: Get the area of H signal at TC environment with the histogram method. (current-decreasing, time = 47 hours.)

The following pictures show estimation of the area of D signal at TC environment with the model method. The current-increasing data and current-decreasing data are analyzed, respectively.

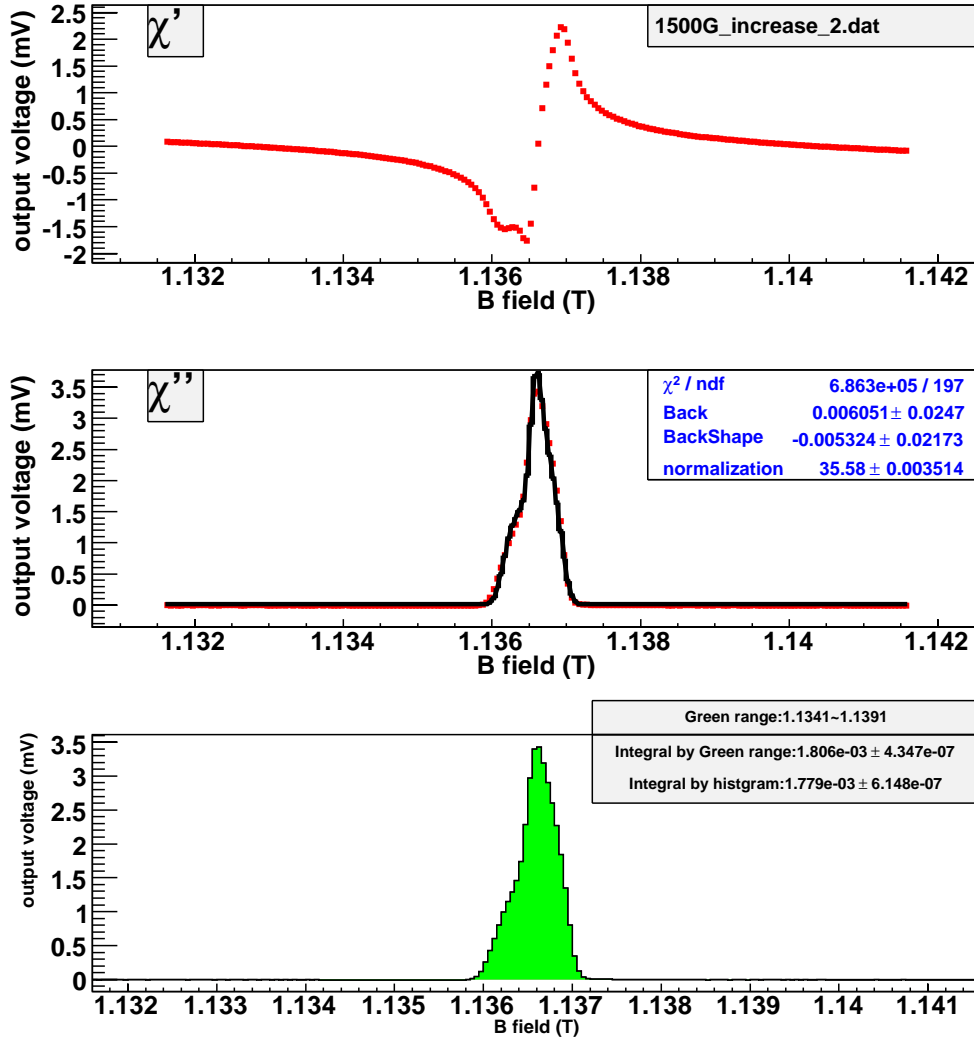


Figure B.67: Get the area of H signal at TC environment with the model method. (current-increasing, time = 2 hours.)

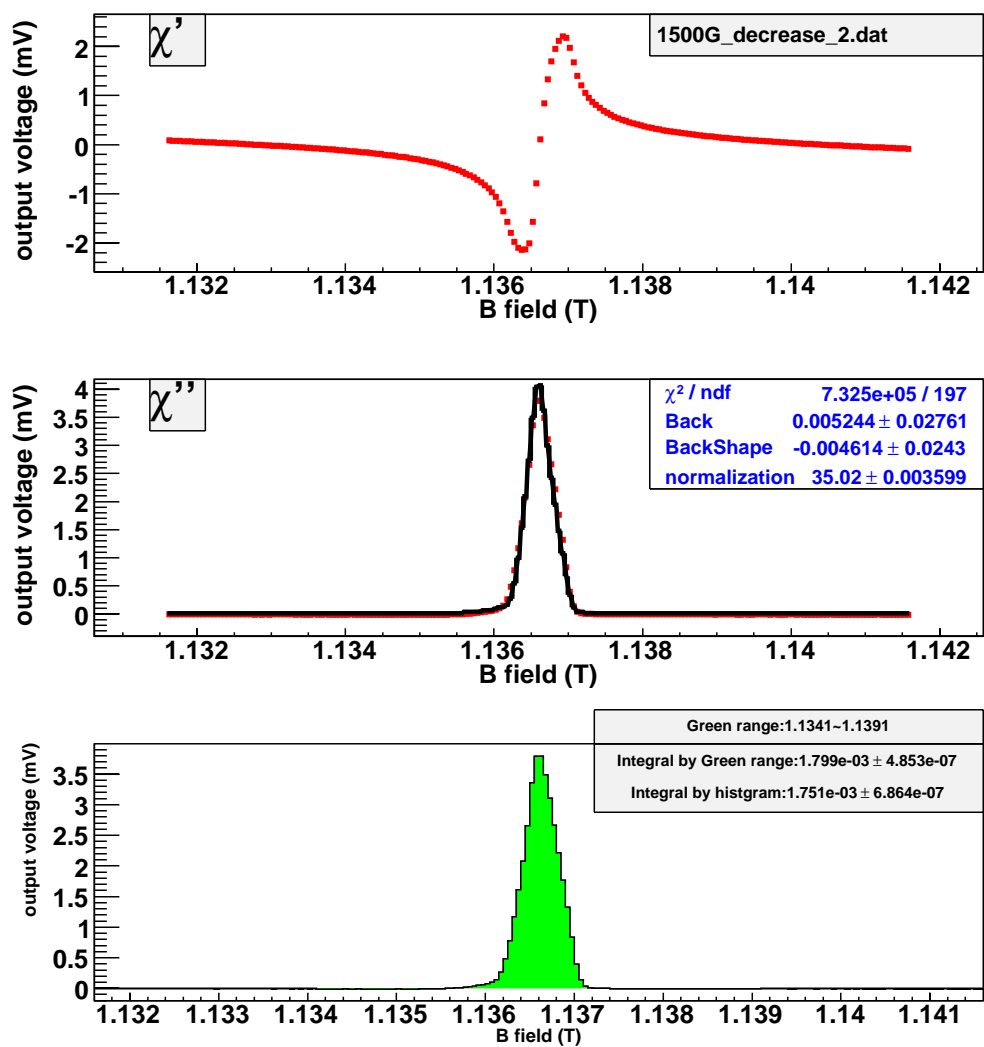


Figure B.68: Get the area of H signal at TC environment with the model method. (current-decreasing, time = 2 hours.)

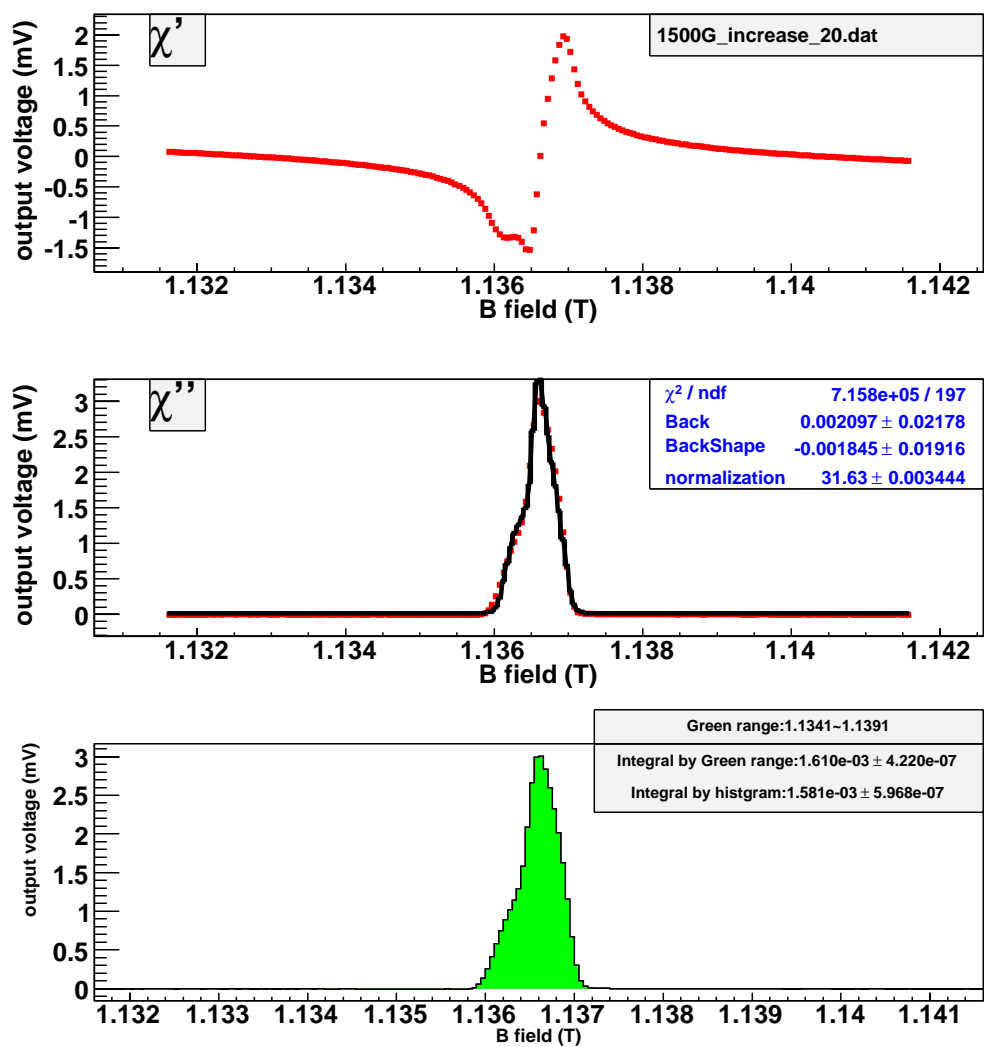


Figure B.69: Get the area of H signal at TC environment with the model method. (current-increasing, time = 20 hours.)

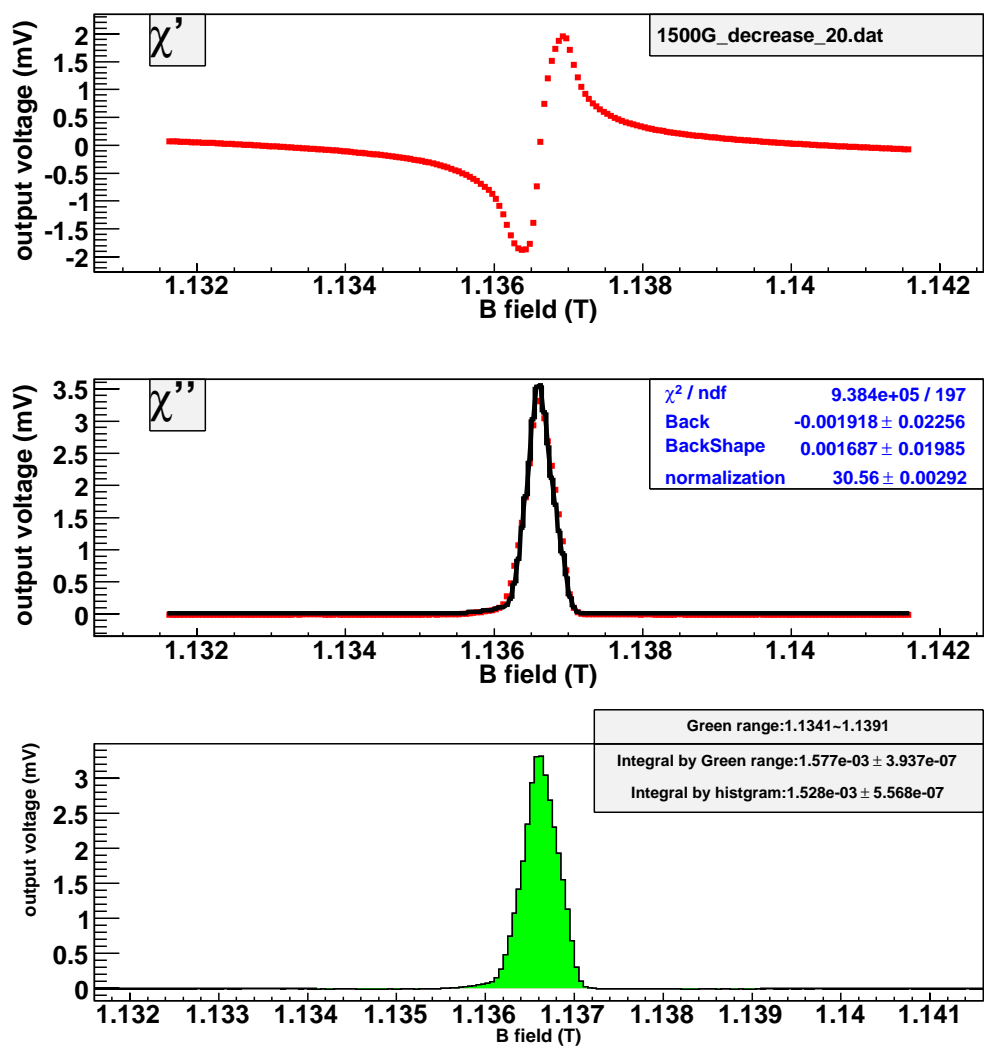


Figure B.70: Get the area of H signal at TC environment with the model method. (current-decreasing, time = 20 hours.)

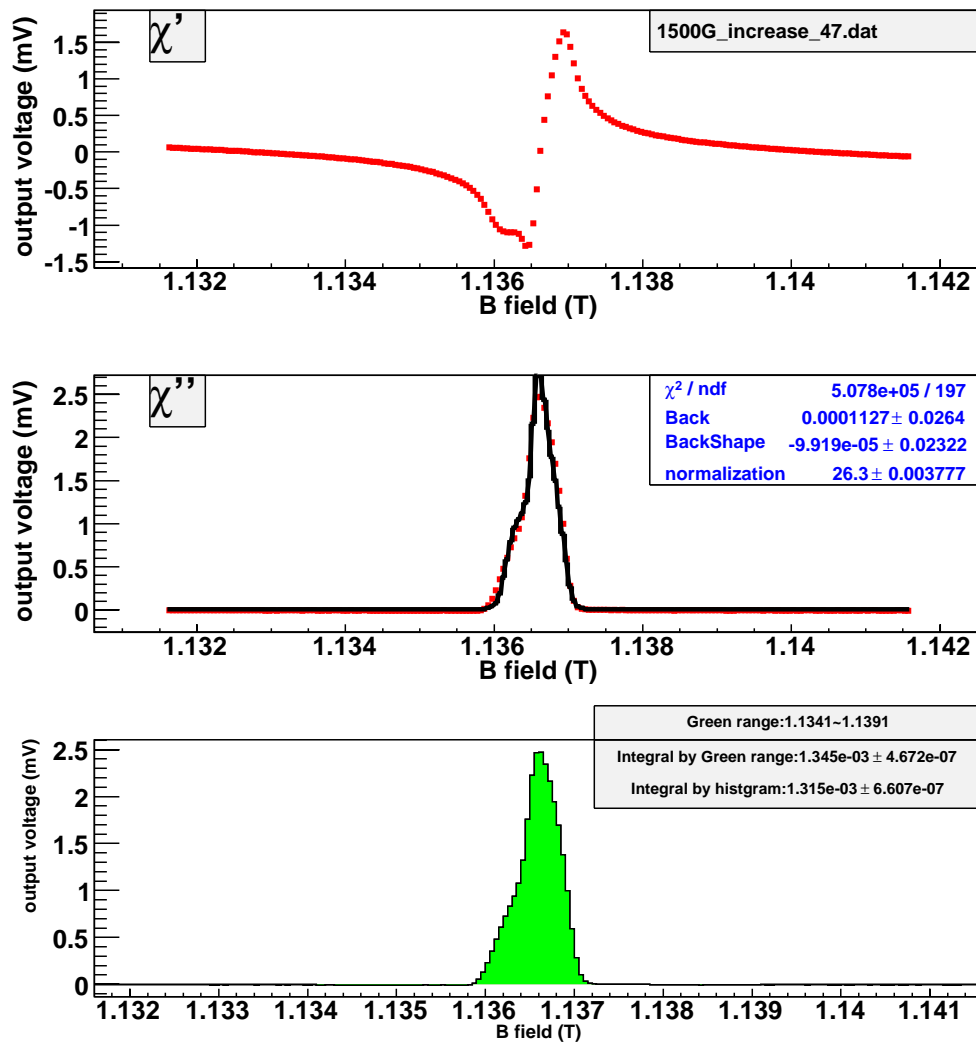


Figure B.71: Get the area of H signal at TC environment with the model method. (current-increasing, time = 47 hours.)

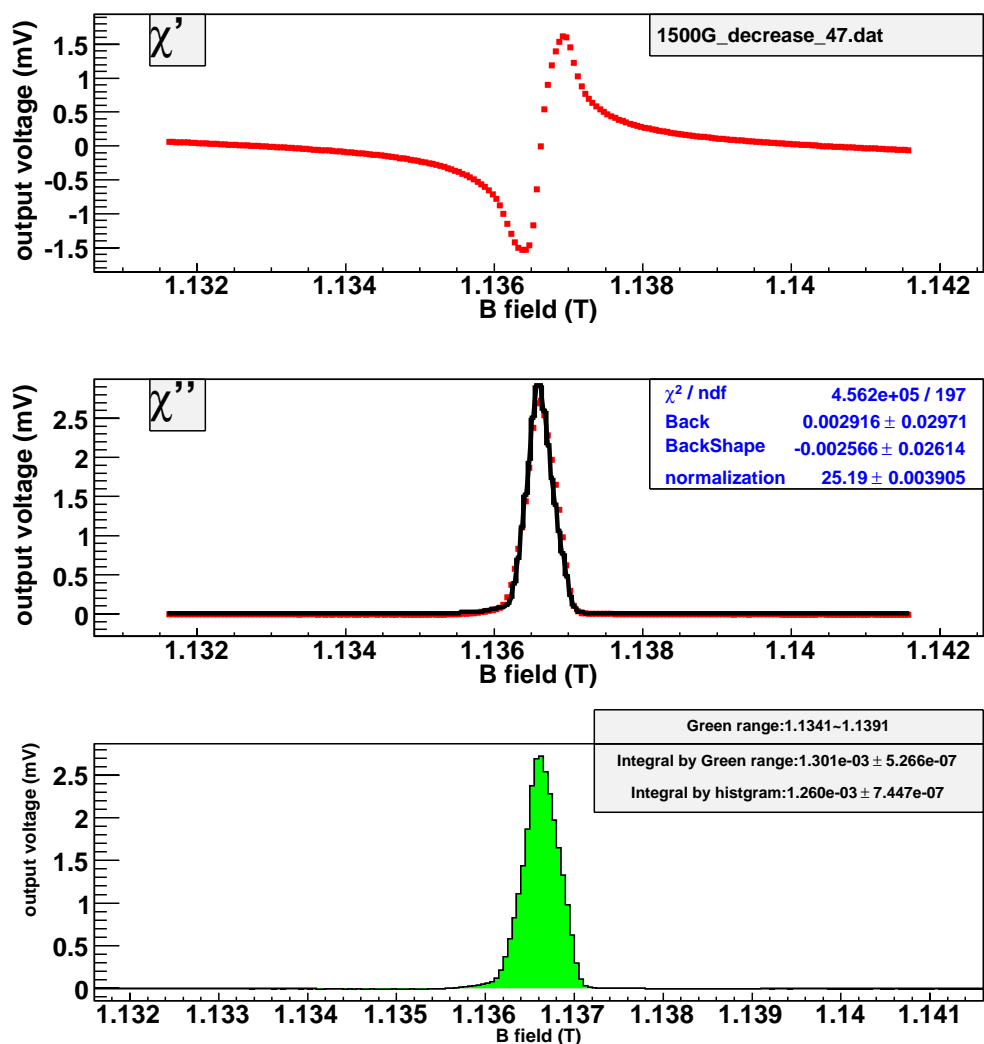


Figure B.72: Get the area of H signal at TC environment with the model method. (current-decreasing, time = 47 hours.)